Light-matter interaction

Collective light scattering in cold atom ensembles

Igor Ferrier-Barbut

cnrs

LABORATOIRE CHARLES FABRY

INSTITUT d'OPTIQUE GRADUATE SCHOOL

université PARIS-SACLAY

anr

erc

Collective light scattering in cold atoms

Do N atoms respond differently w.r.t a single atom?

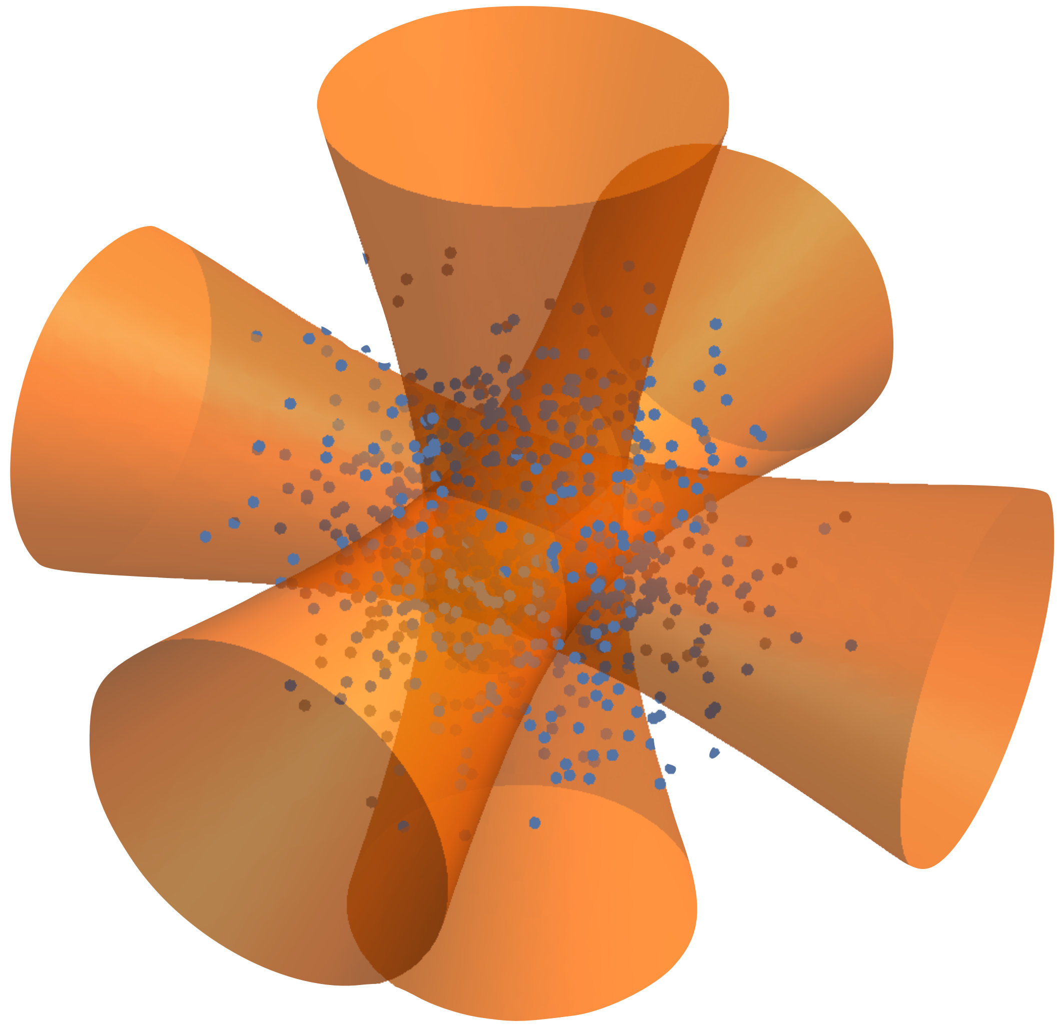

Experimental bias?

- Absorption or fluorescence imaging.
- Optical clocks: shift of the resonance?

Collective light scattering in cold atoms

Do N atoms respond differently w.r.t a single atom?

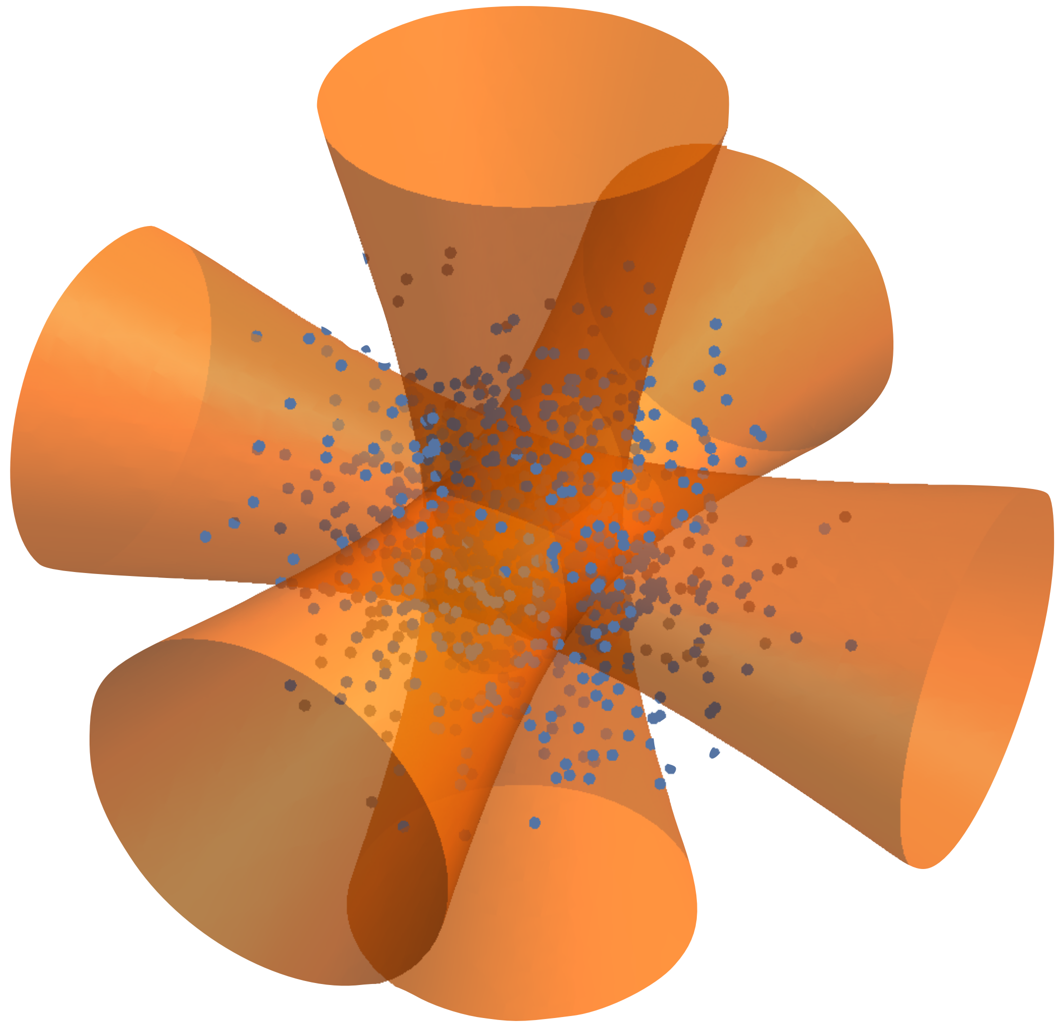

Experimental bias?

- Absorption or fluorescence imaging.
- Optical clocks: shift of the resonance?

Collective enhancement ==> quantum technologies

- One-photon nonlinearities
- Quantum memories
- Improve clock accuracy?

Basic, many-body problem (driven dissipative)

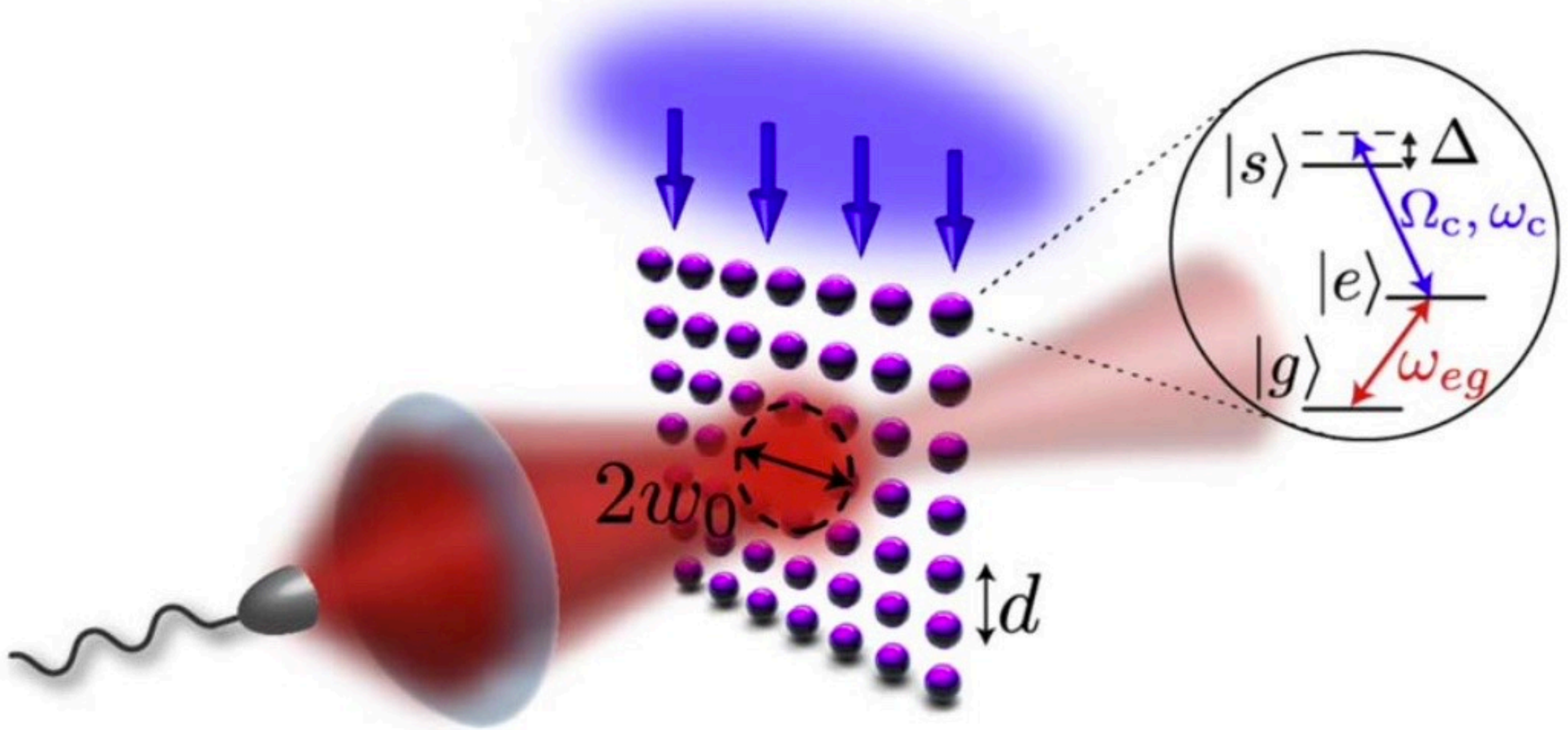

Laser-cooled atoms

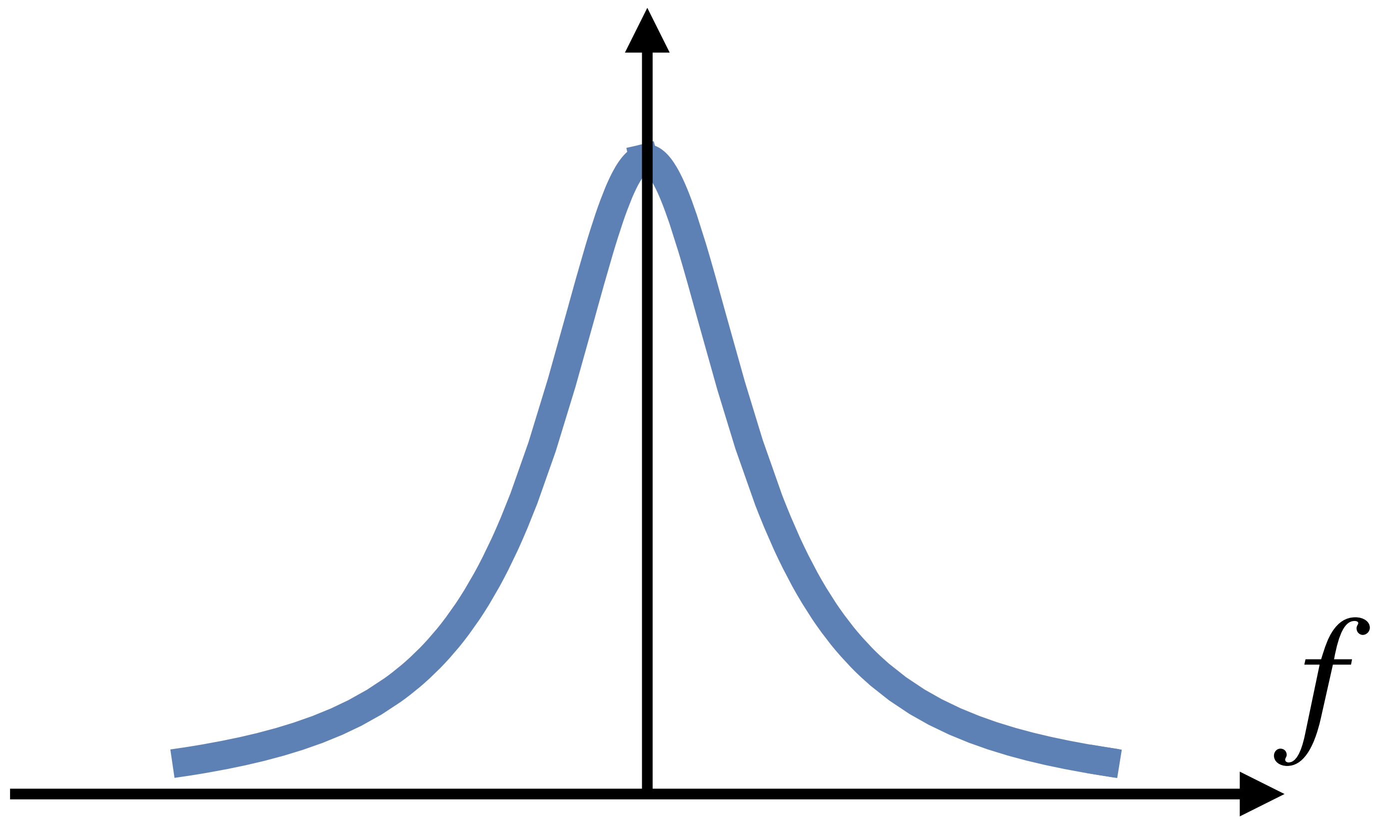

Typical atomic linewidth for alkalis: $\Gamma/2\pi \sim$ MHz

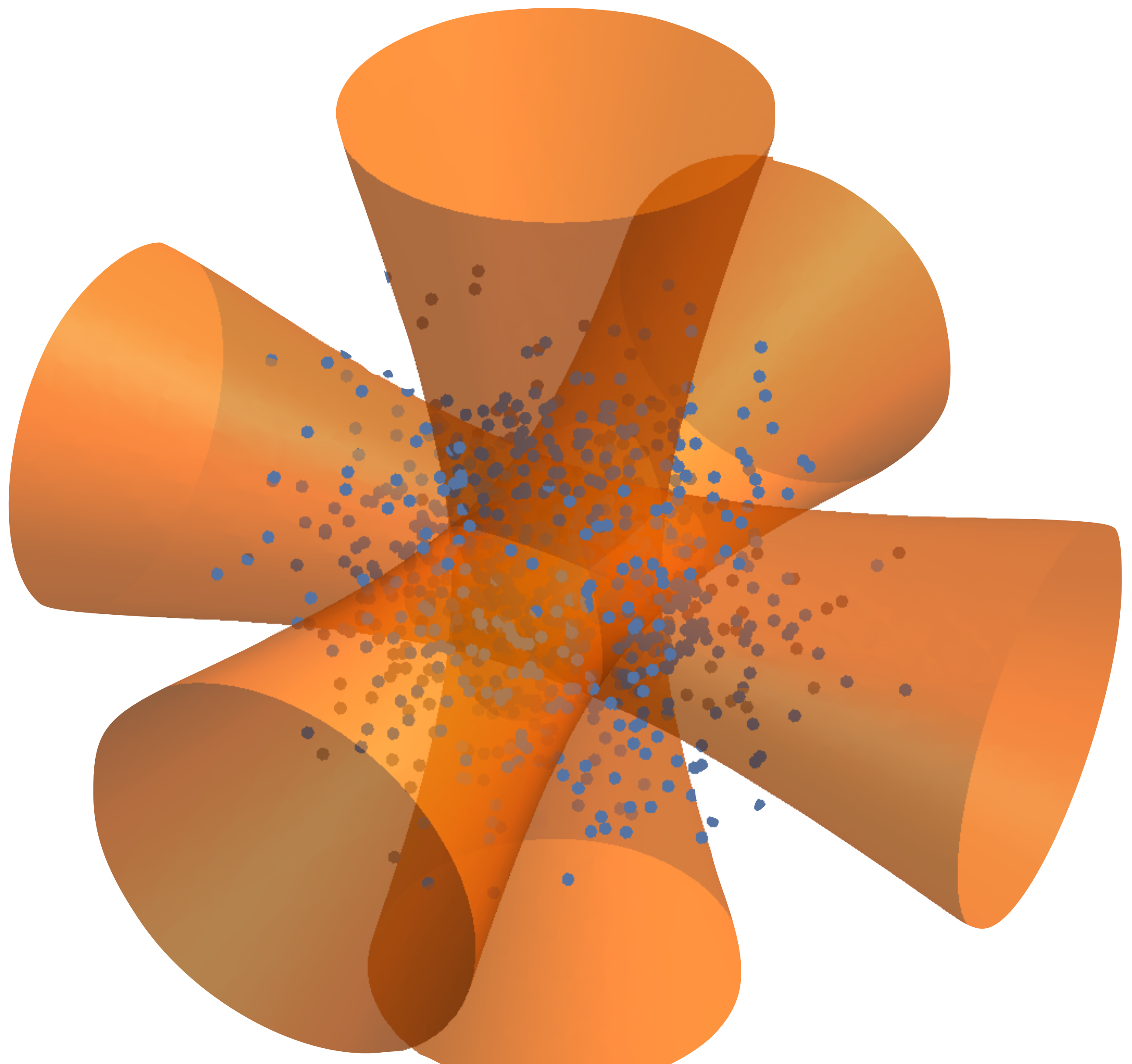

Laser-cooled atoms

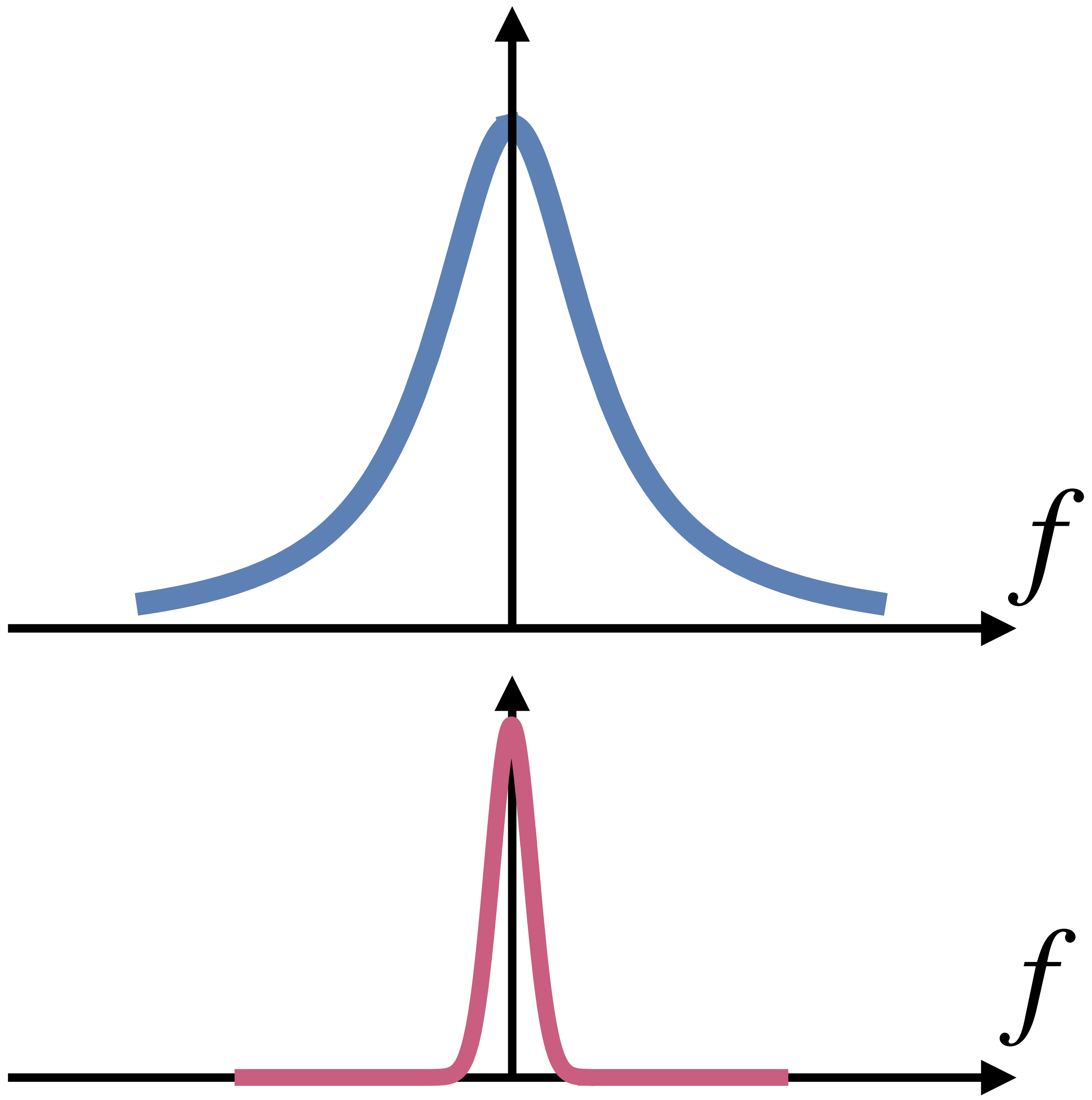

Typical atomic linewidth for alkalis: $\Gamma/2\pi \sim$ MHz

Temperature T~ 1 - 100 μK

Typical Doppler broadening: $\Delta\omega = k\Delta v,\ \Delta\omega_{\mathrm{D}}/2\pi \sim 10^4 - 10^5$ Hz

Typical collision rate: $\lesssim$ 10 kHz: no dephasing

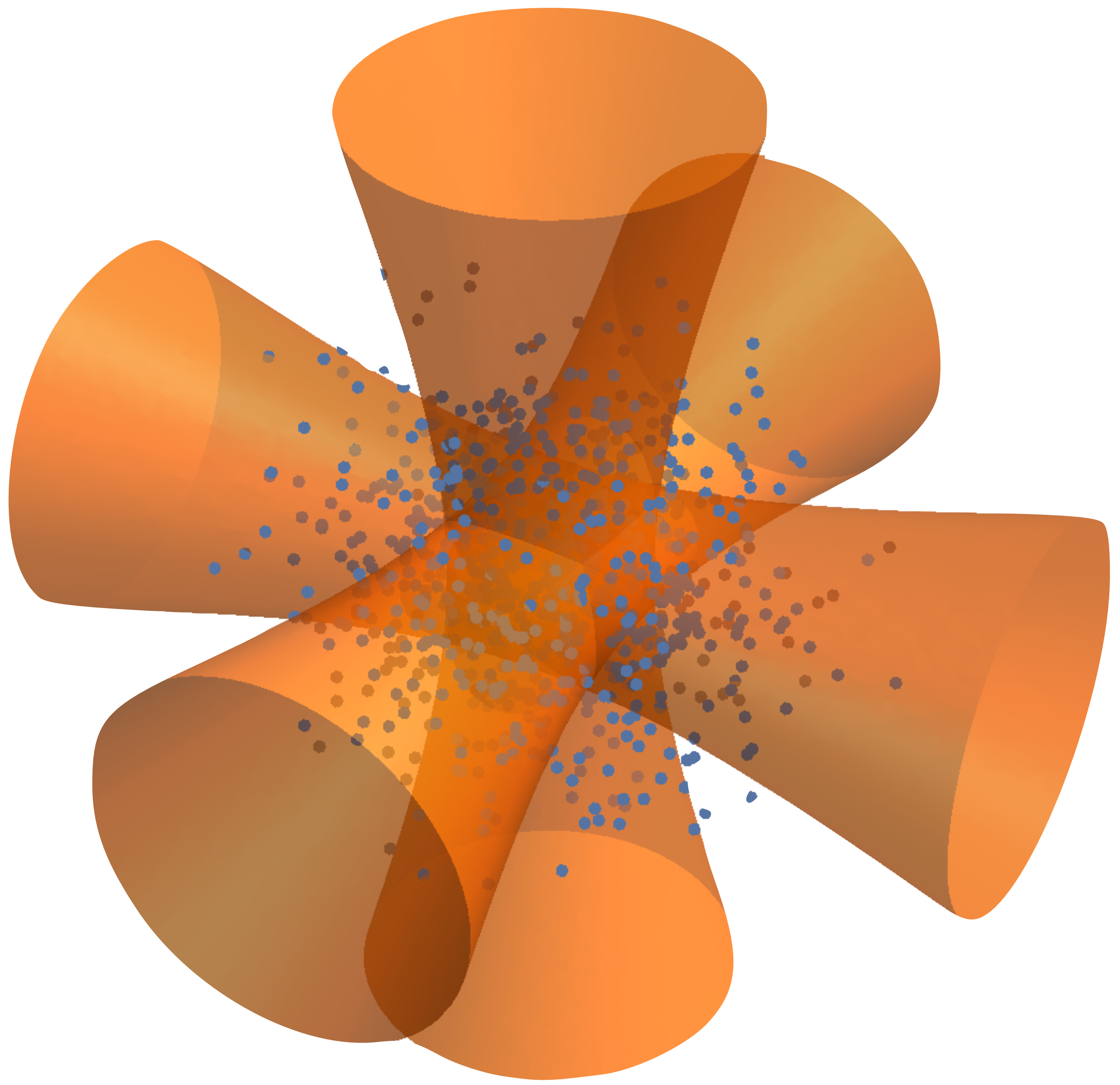

Laser-cooled atoms

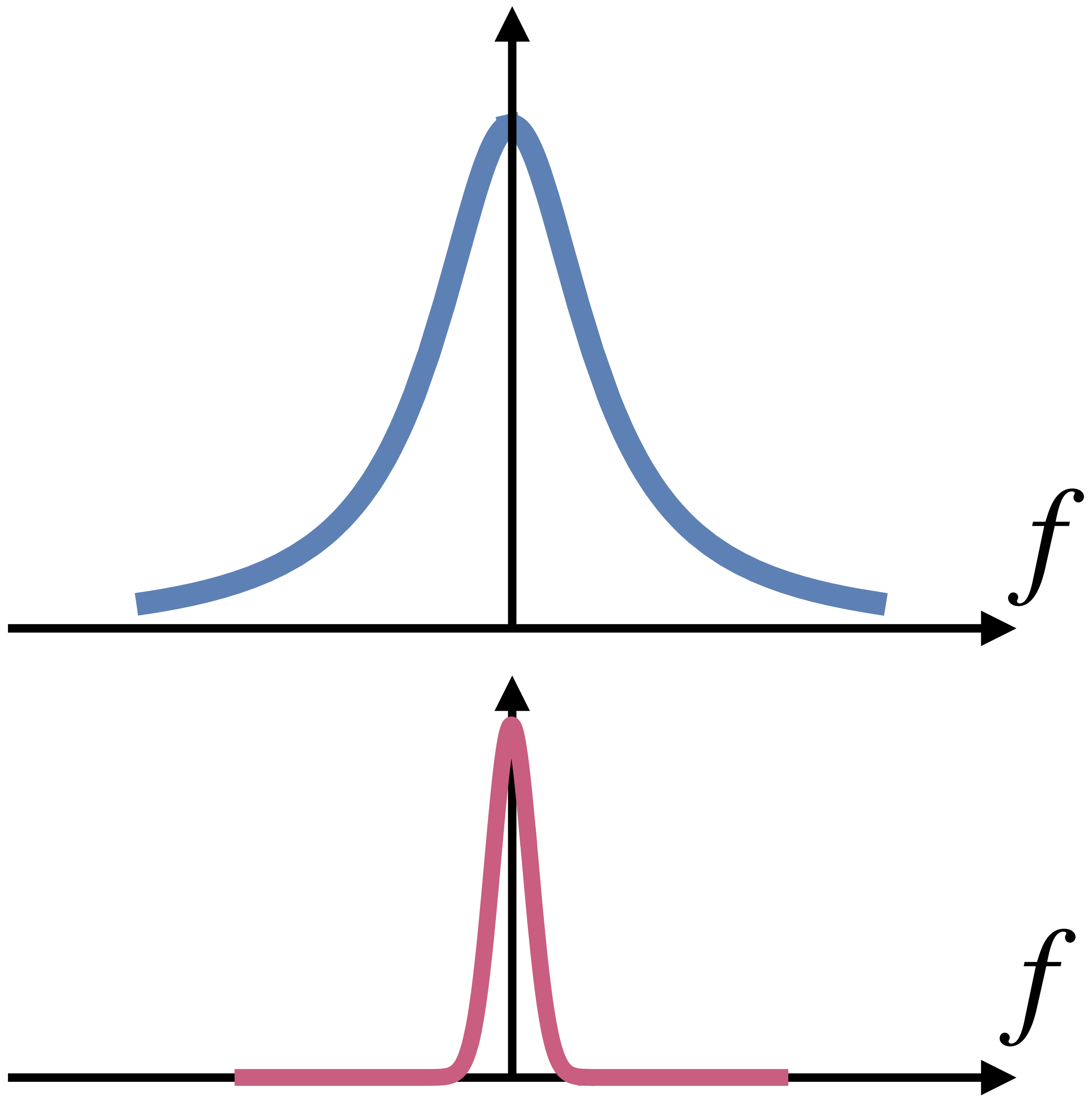

Typical atomic linewidth for alkalis: $\Gamma/2\pi \sim$ MHz

Temperature T~ 1 - 100 μK

Typical Doppler broadening: $\Delta\omega = k\Delta v, \;\; \Delta\omega_{\mathrm{D}}/2\pi \sim 10^4 - 10^5$ Hz

Typical collision rate: $\lesssim$ 10 kHz: no dephasing

No inhomogeneous broadening $\Gamma \gg \Delta\omega$: **atoms are identical**

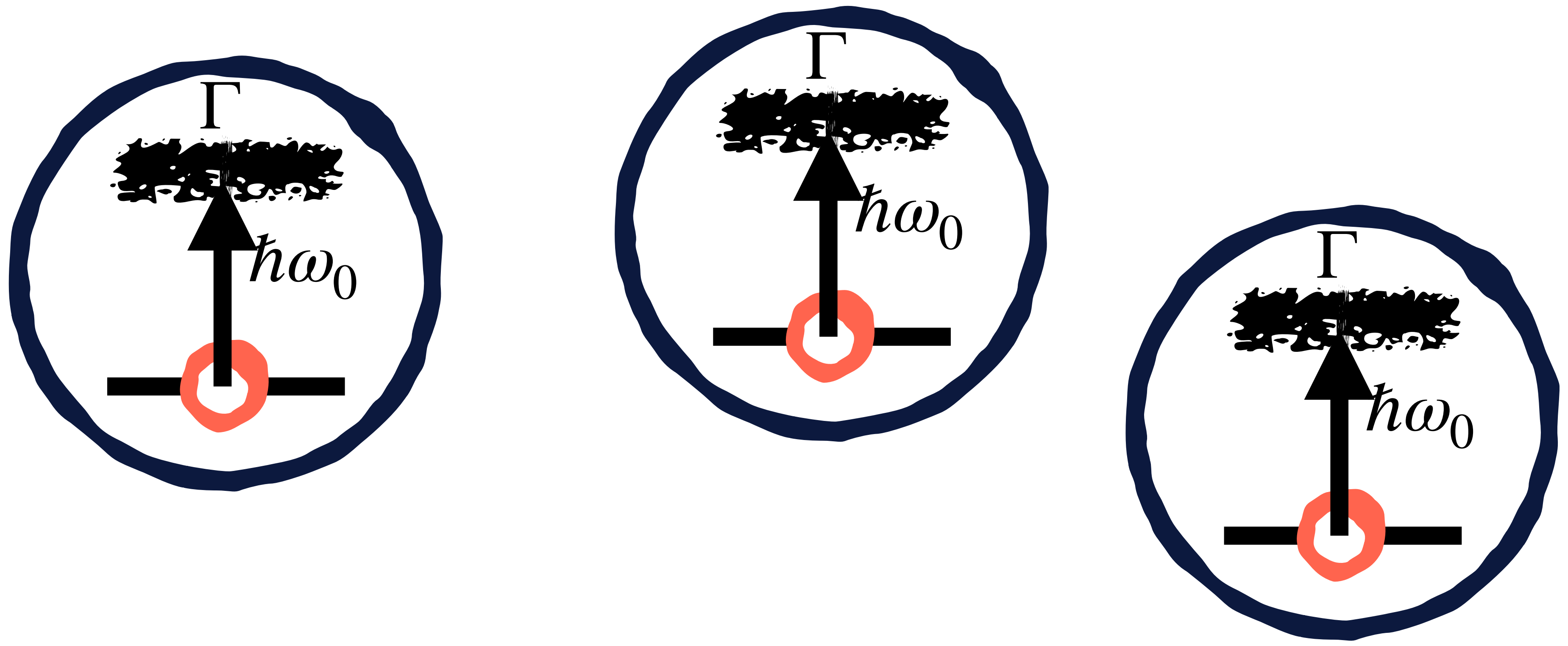

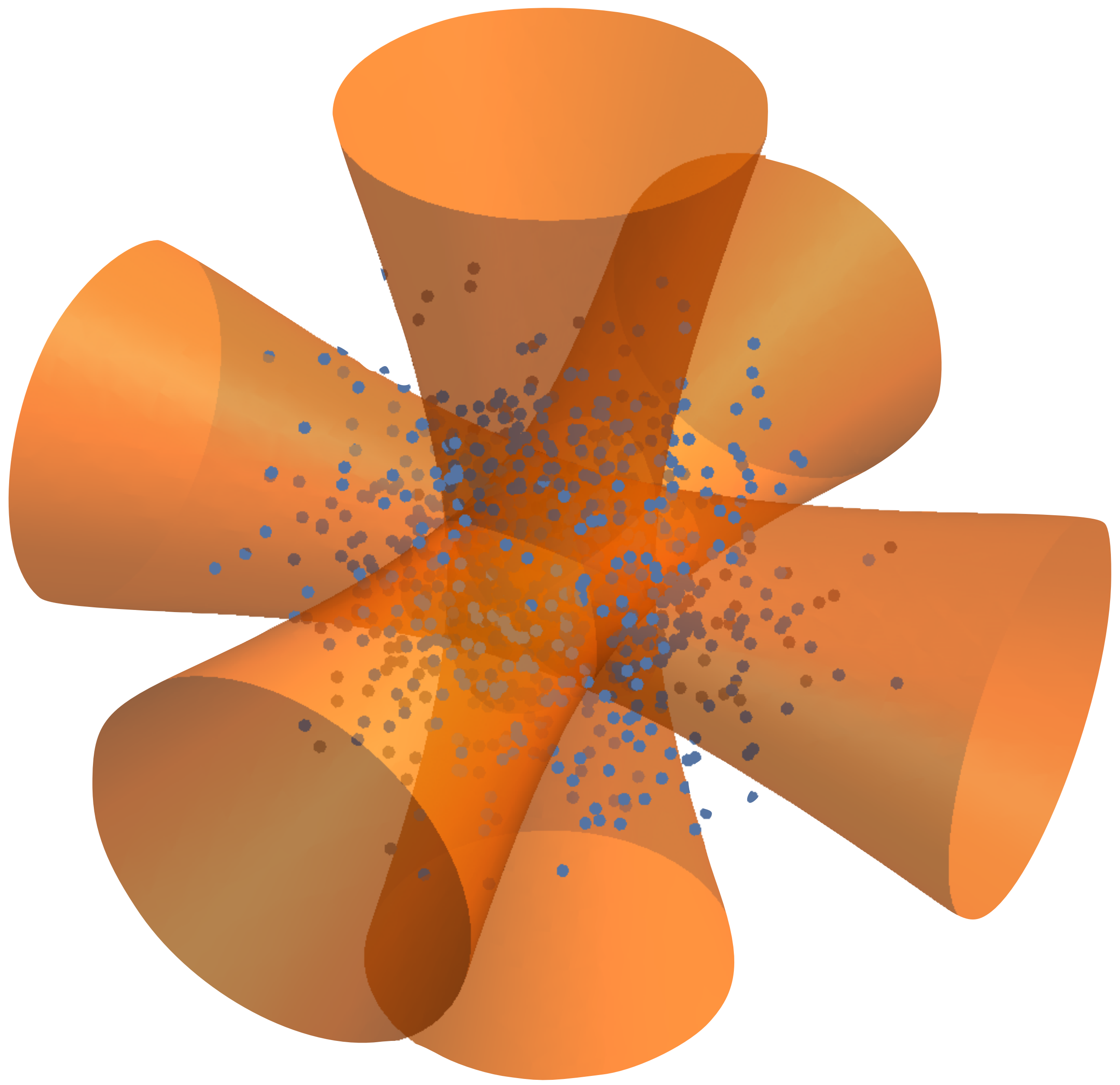

Light scattering

Single two-level atom in **free space**

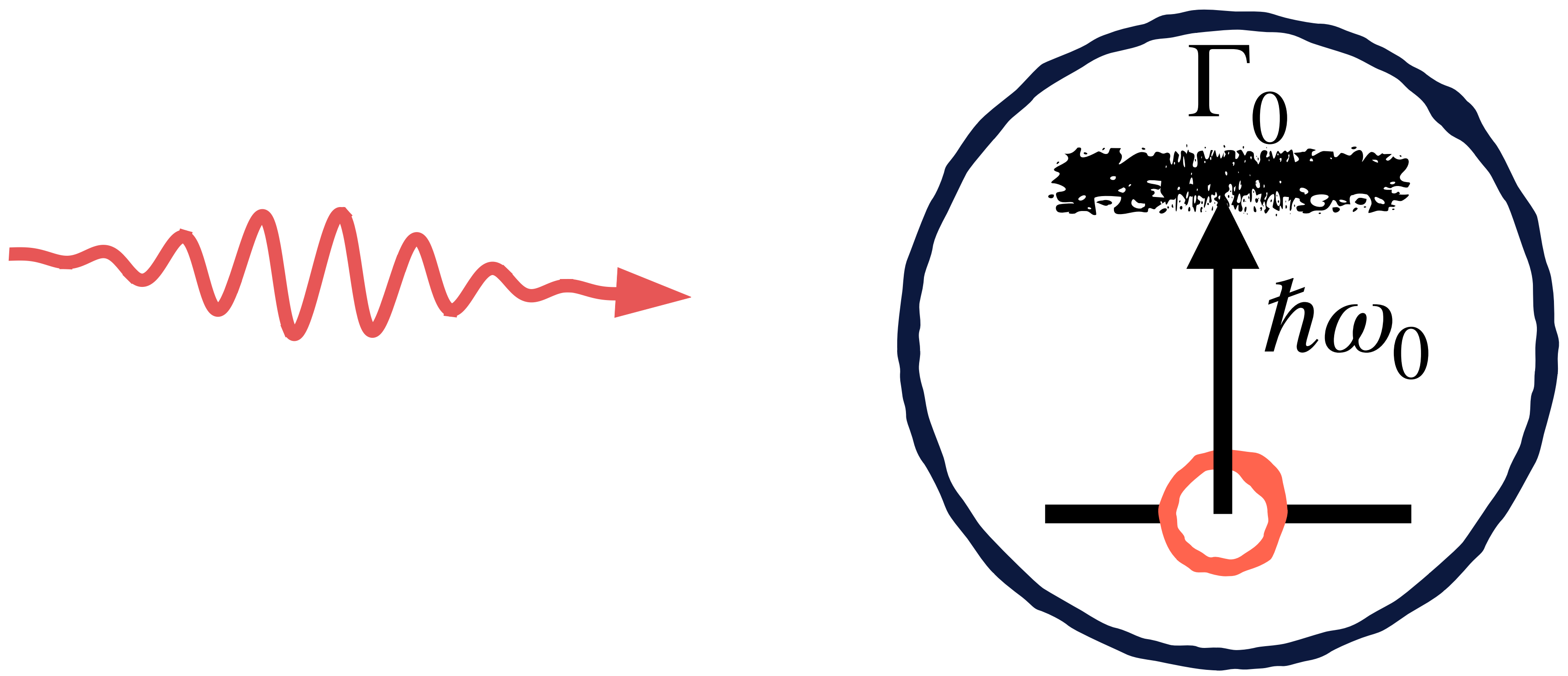

Scattered power vs detuning

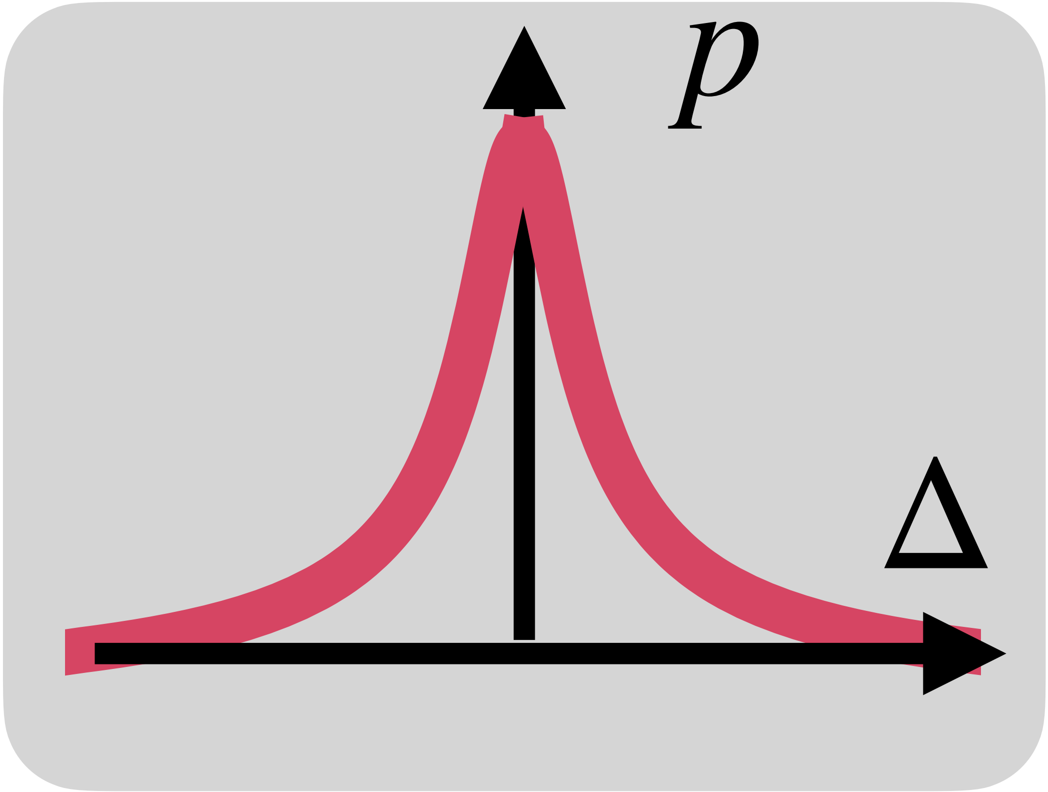

$$p(\Delta) \propto \frac{\Gamma}{2}\frac{s}{1+s+(2\Delta/\Gamma_0)^2}$$

Scattered power vs time

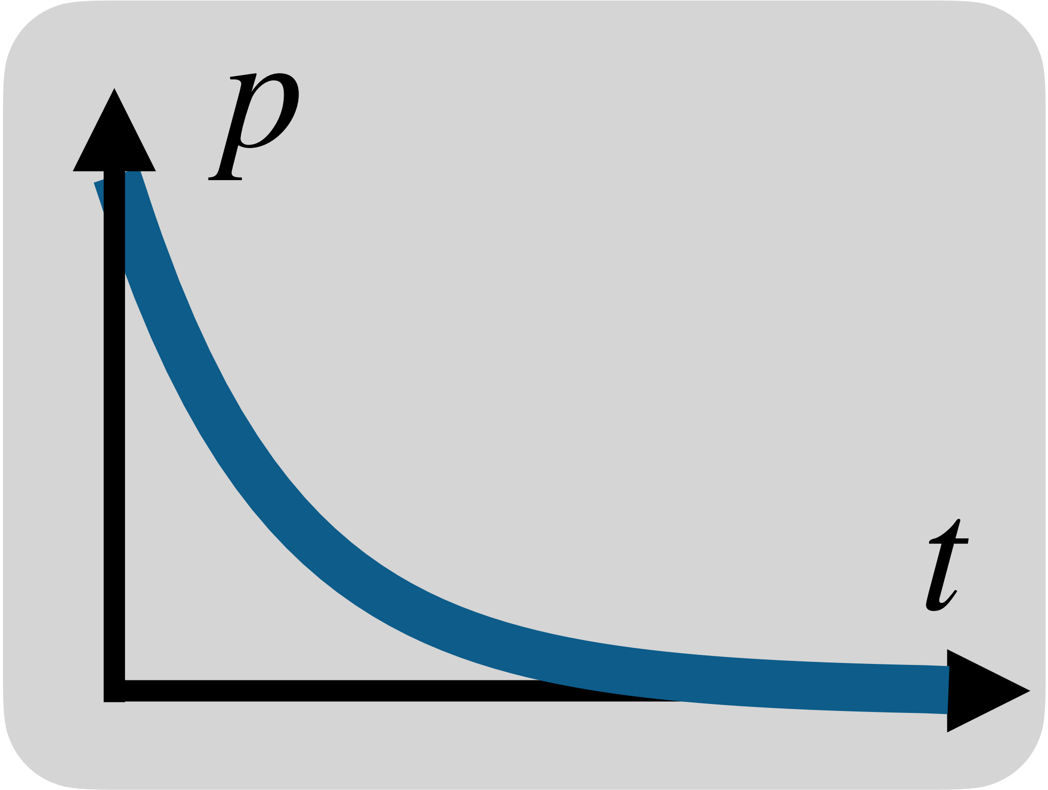

$$p(t) \propto e^{-\Gamma_0 t}$$

Collective light scattering

Single atom in **free space**

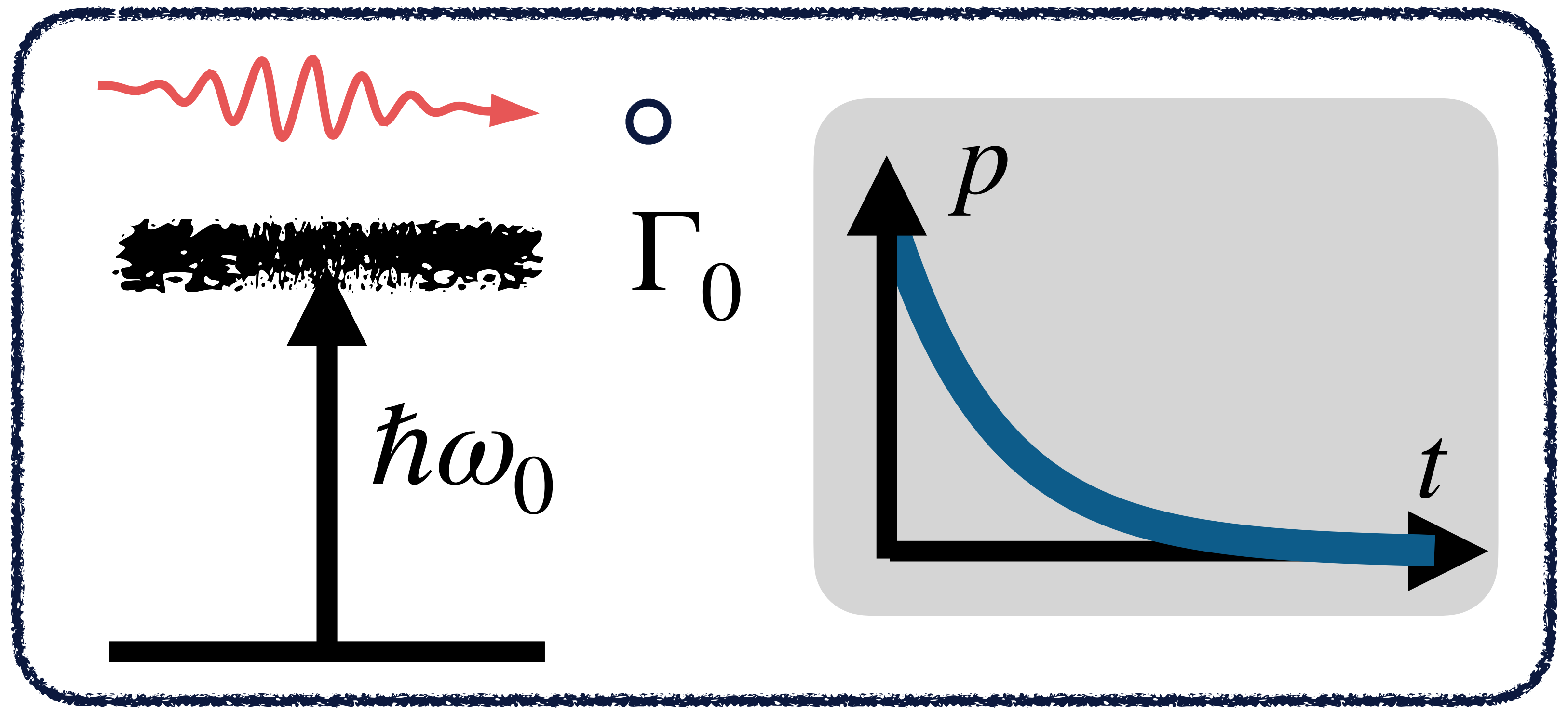

N-atom collective response

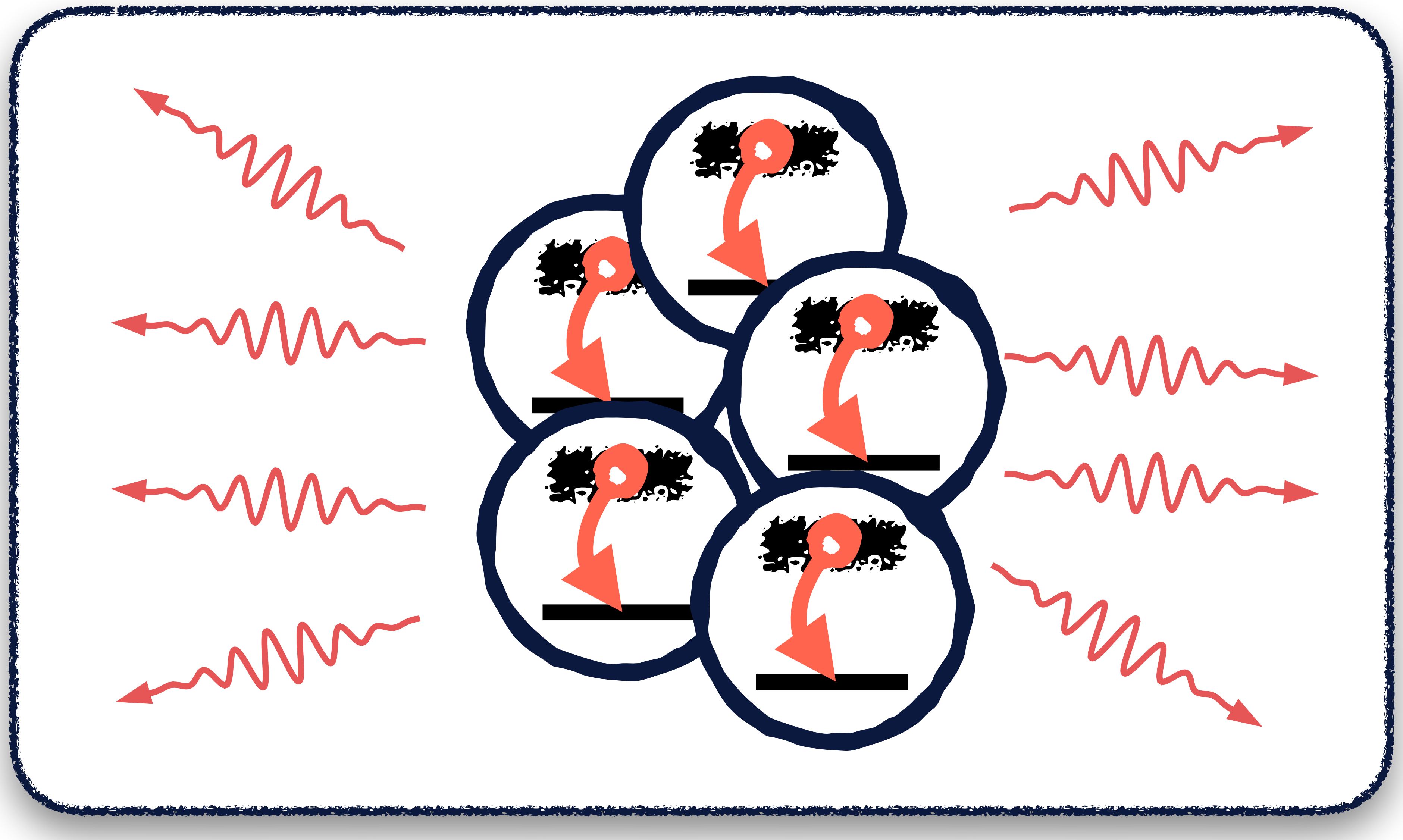

Outline

Lecture 1: Quantum optics of single atoms

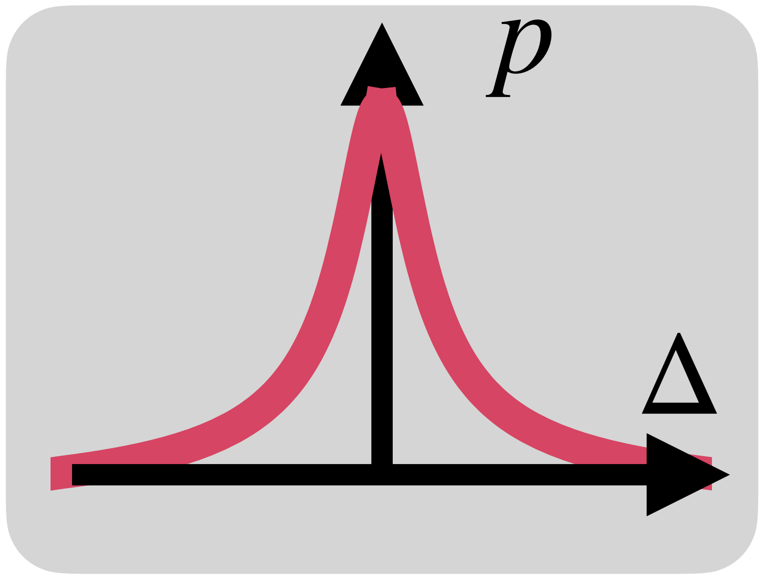

Lecture 2: Collective light scattering by *N* atoms

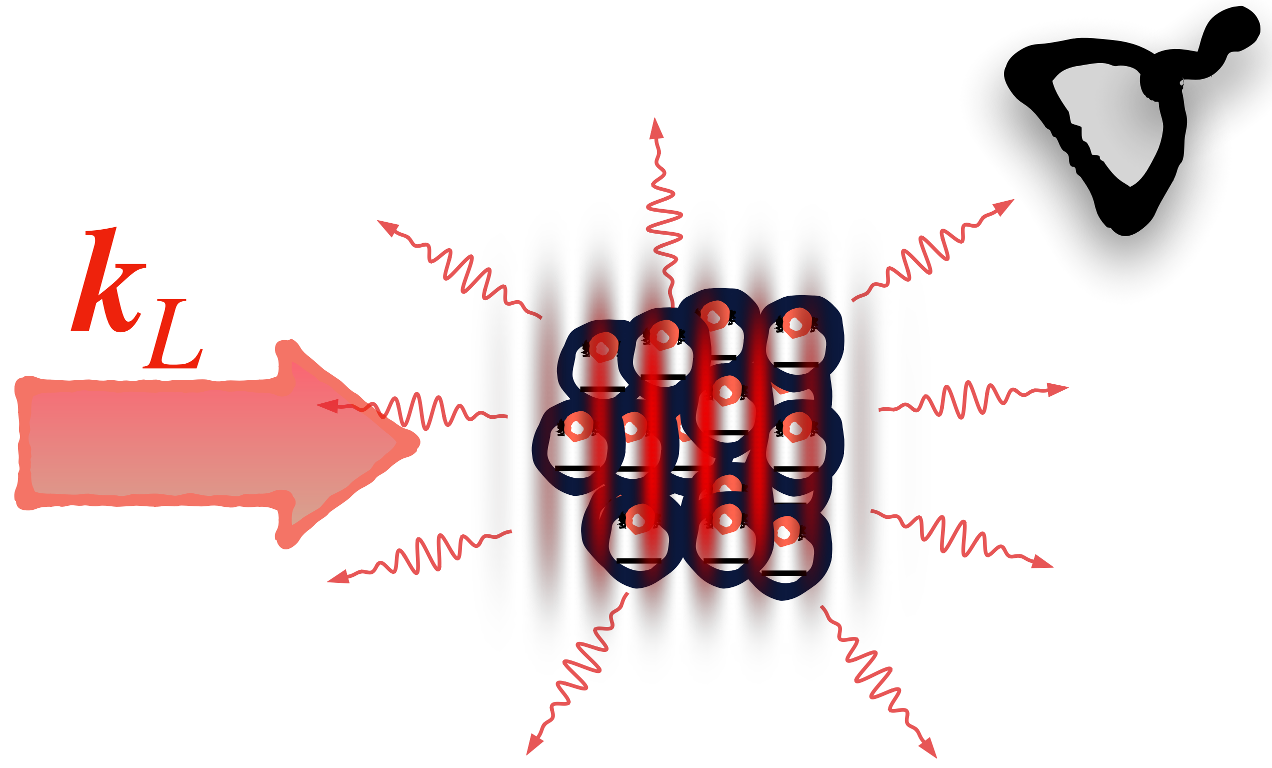

Lecture 3: Many-body quantum optics

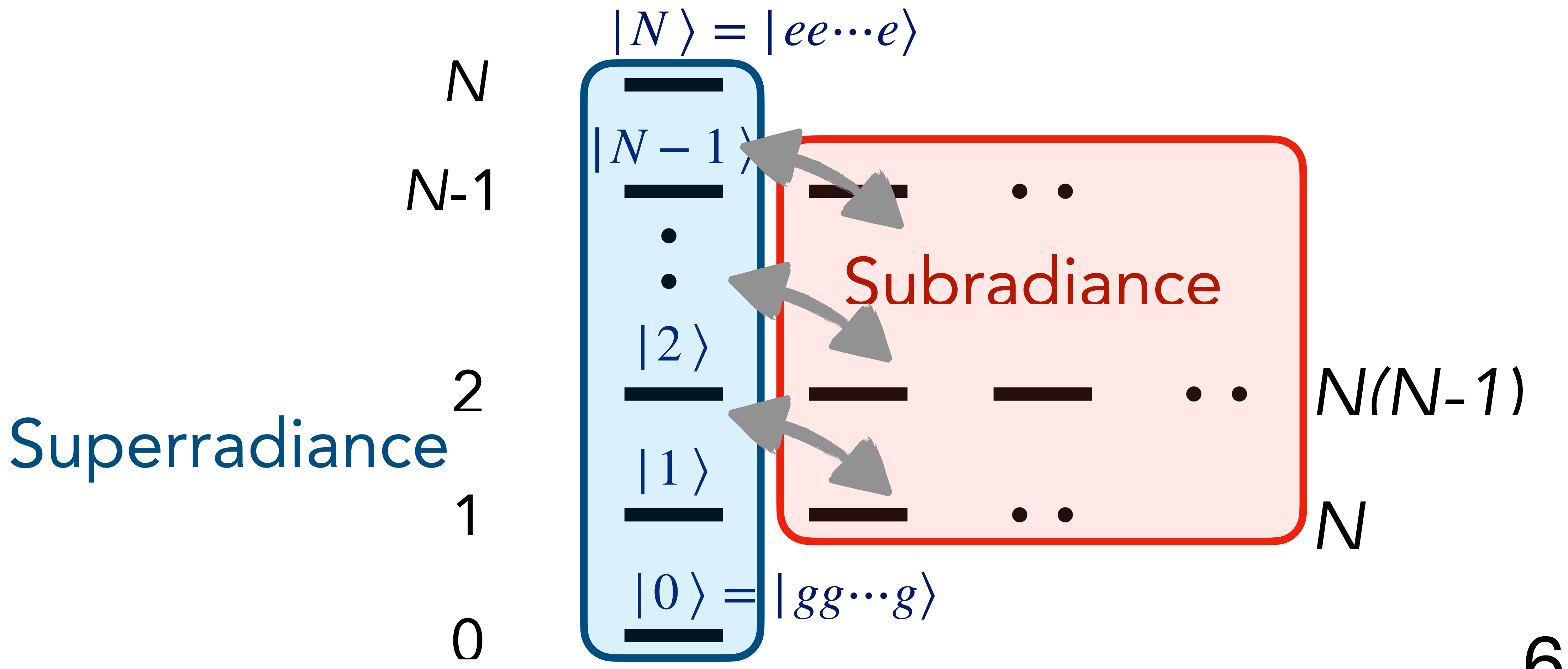

The atomic dipole

Classical dipole

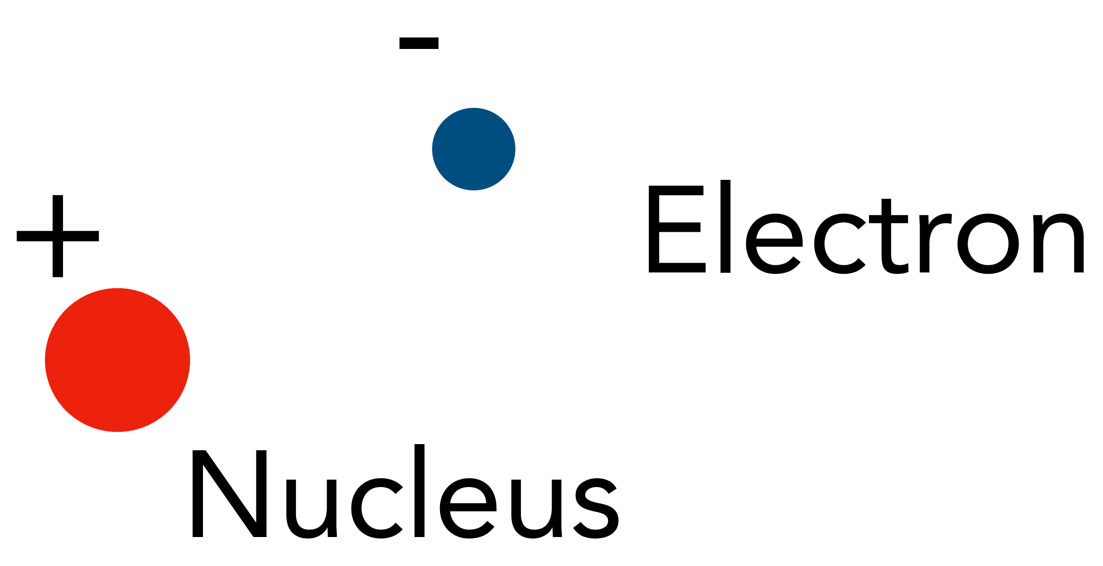

Quantized electronic motion

$$\hat{\boldsymbol{d}} = q\hat{\boldsymbol{r}} \qquad \hat{\boldsymbol{D}} = \sum_i q\hat{\boldsymbol{r}}_i$$

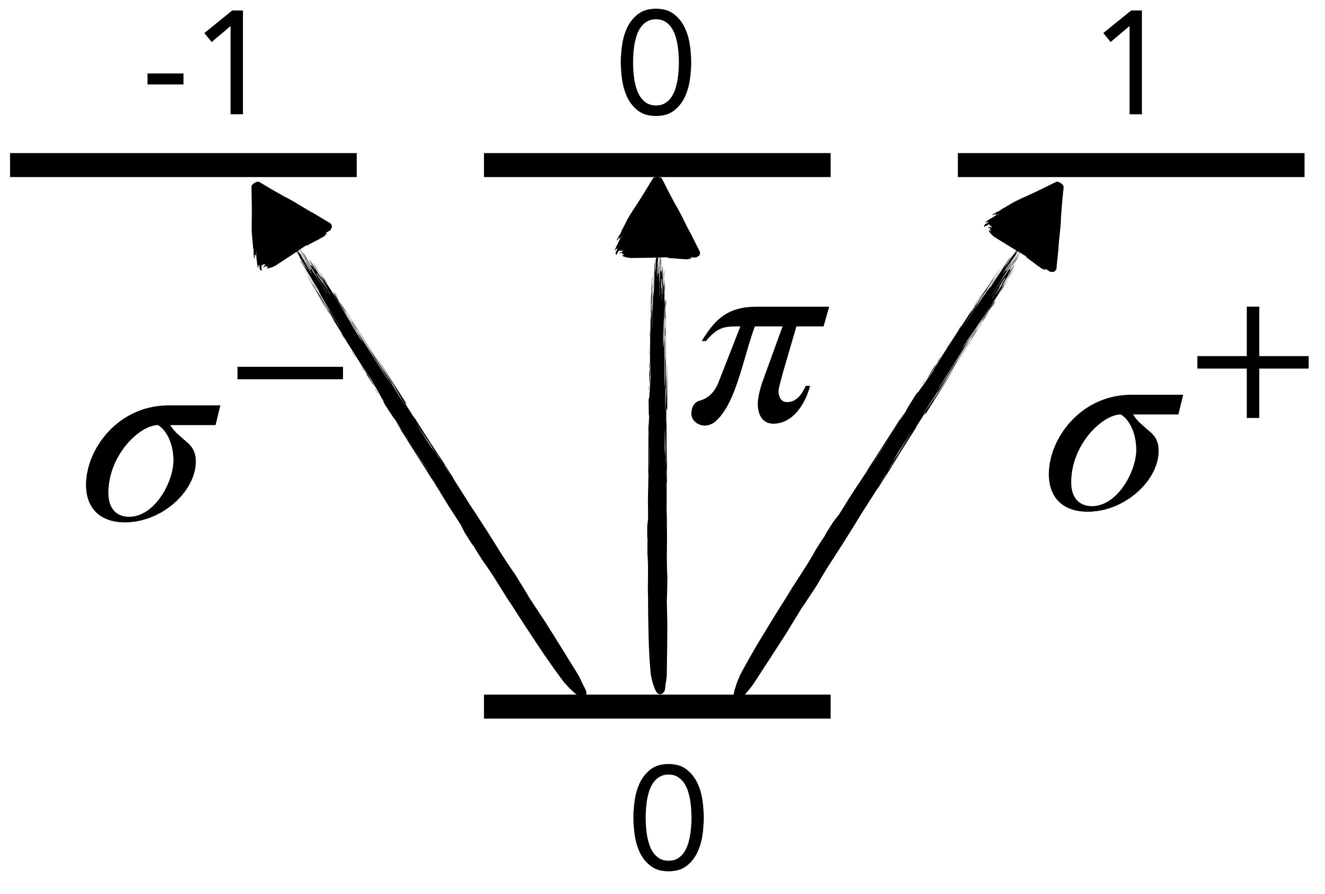

$$|n', l', m_l'\rangle$$

$$|n, l, m_l\rangle$$

Dipole elements: $\langle n', l', m_l' | \hat{\boldsymbol{D}} | n, l, m_l \rangle$

Spontaneous emission

Fermi's golden rule $\Gamma = \dfrac{2\pi}{\hbar} |\langle g, 1_k | \hat{\boldsymbol{D}} \cdot \hat{\boldsymbol{E}} | e, 0 \rangle|^2 \rho(\hbar\omega_0)$

$$\Gamma = \frac{\omega_0^3}{3\pi\hbar\varepsilon_0 c^3} |d_{eg}|^2 \qquad |d_{eg}|^2 = |\langle e | \hat{\boldsymbol{D}} | g \rangle|^2$$

Atoms and field are entangled: $|\psi\rangle = \alpha |e, 0\rangle + \sum_k \beta_k |g, 1_k\rangle$

$\rho_{at} = \alpha^2 |e\rangle\langle e| + \beta^2 |g\rangle\langle g|$ ➡ $\langle \hat{\boldsymbol{D}} \rangle = 0$ during spontaneous emission

Description of the atomic systems tracing out the field: Master equation

Optical Bloch equations

Master equation $\dot{\rho} = \frac{1}{i\hbar}\left[H, \rho\right] + L(\rho)$

$$\dot{\rho}_{ee} = -\frac{i\Omega}{2}(\rho_{eg} - \rho_{ge}) - \Gamma\rho_{ee}$$

$$\dot{\rho}_{eg} = -\frac{i\Omega}{2}(\rho_{ee} - \rho_{gg}) - \frac{\Gamma}{2}\rho_{eg} + i\Delta\,\rho_{eg}$$

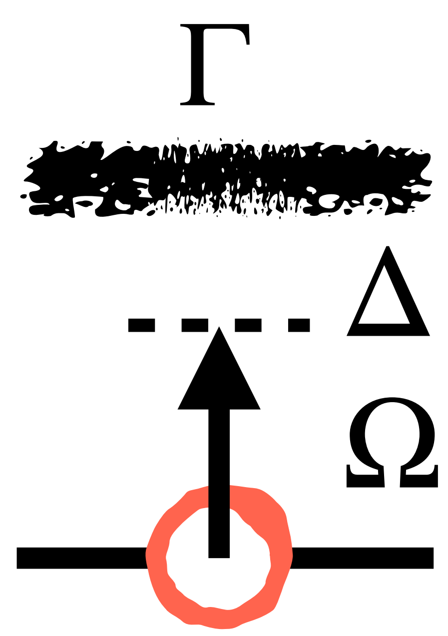

Rabi oscillations

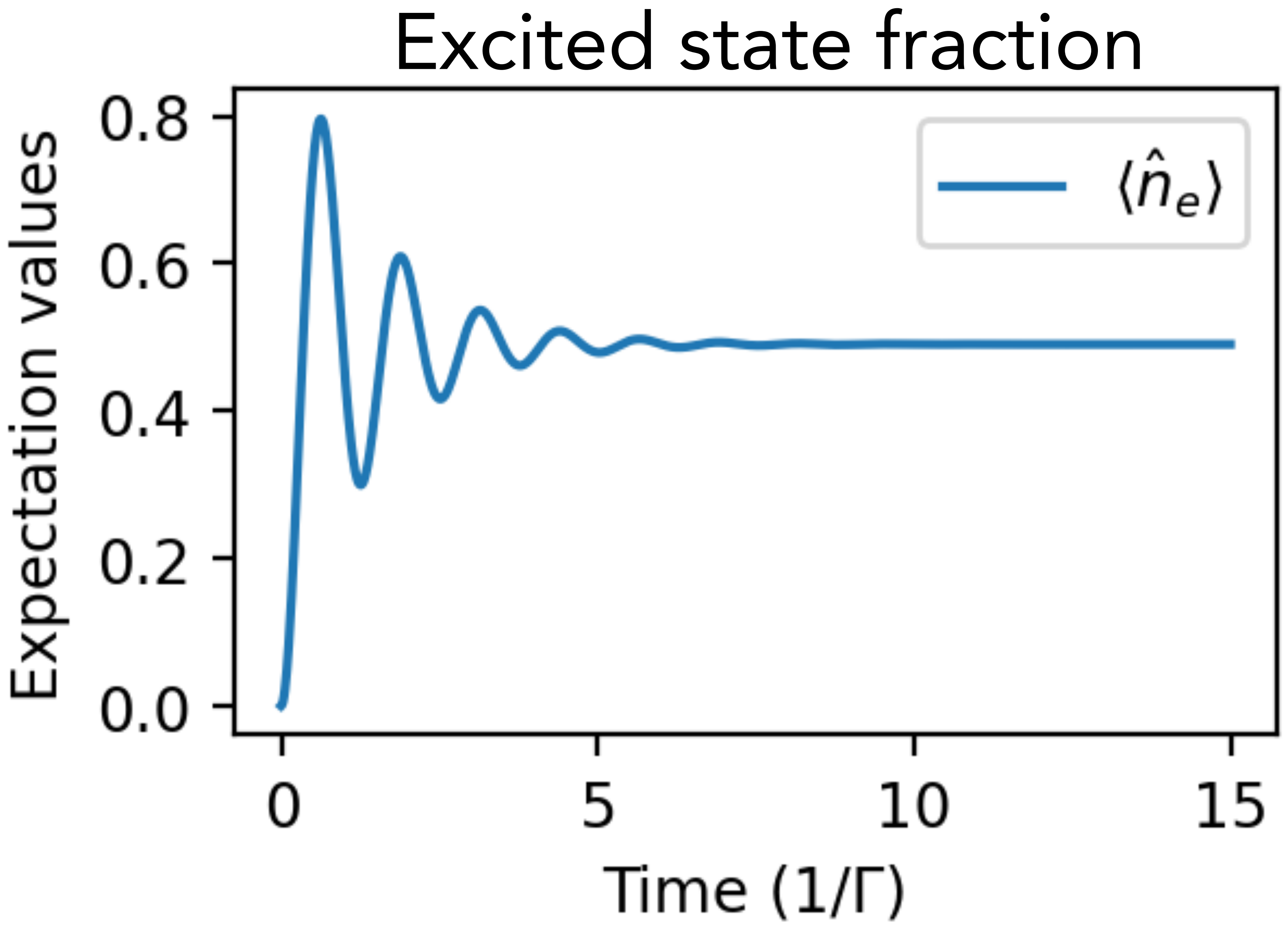

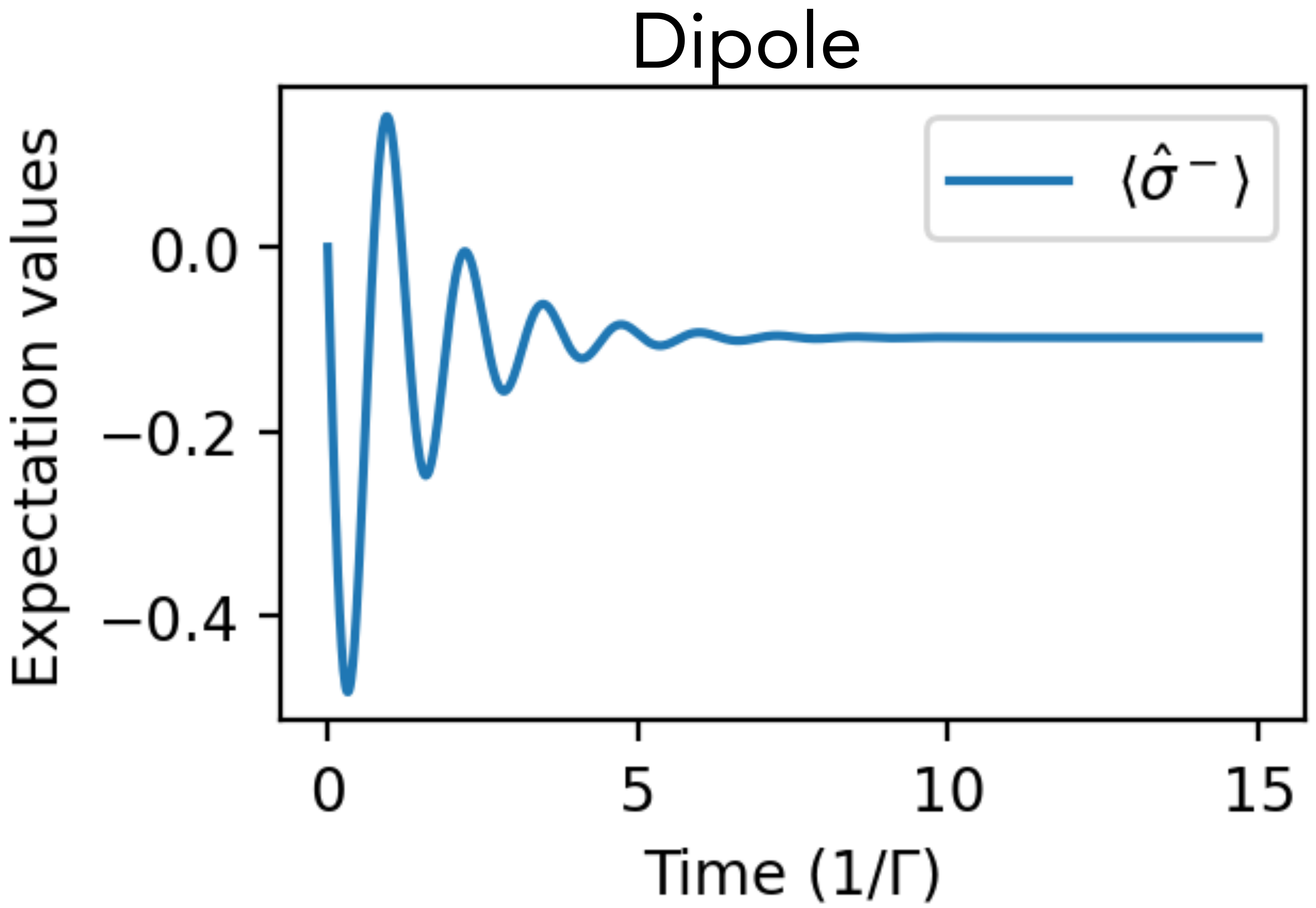

Optical Bloch equations

Steady-state solutions: $$\rho_{ee} = \frac{1}{2}\frac{2\Omega^2/\Gamma^2}{1 + 2\Omega^2/\Gamma^2 + 4\Delta^2/\Gamma^2}$$

$$s = I/I_{\text{sat}} = \frac{2\Omega^2}{\Gamma^2}$$

$$\rho_{eg} = i\frac{\Omega}{2}\frac{\Gamma/2 + i\Delta}{\Gamma^2/4 + \Omega^2/2 + \Delta^2}$$

$$I_{\text{sat}} = \frac{2\pi^2\hbar\Gamma c}{3\lambda^3}$$

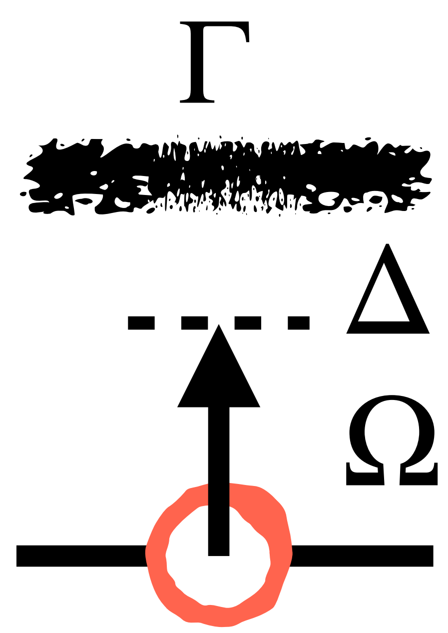

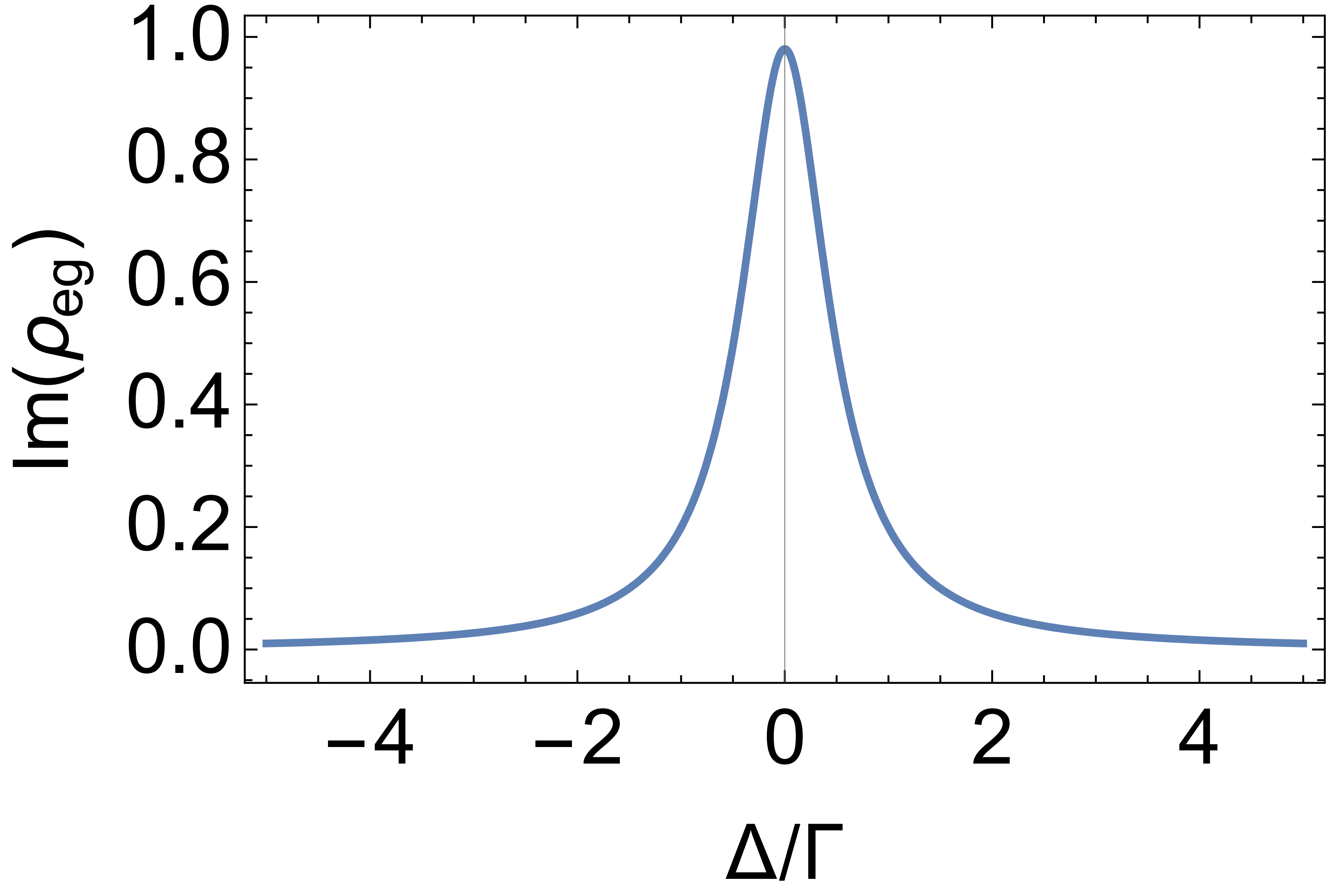

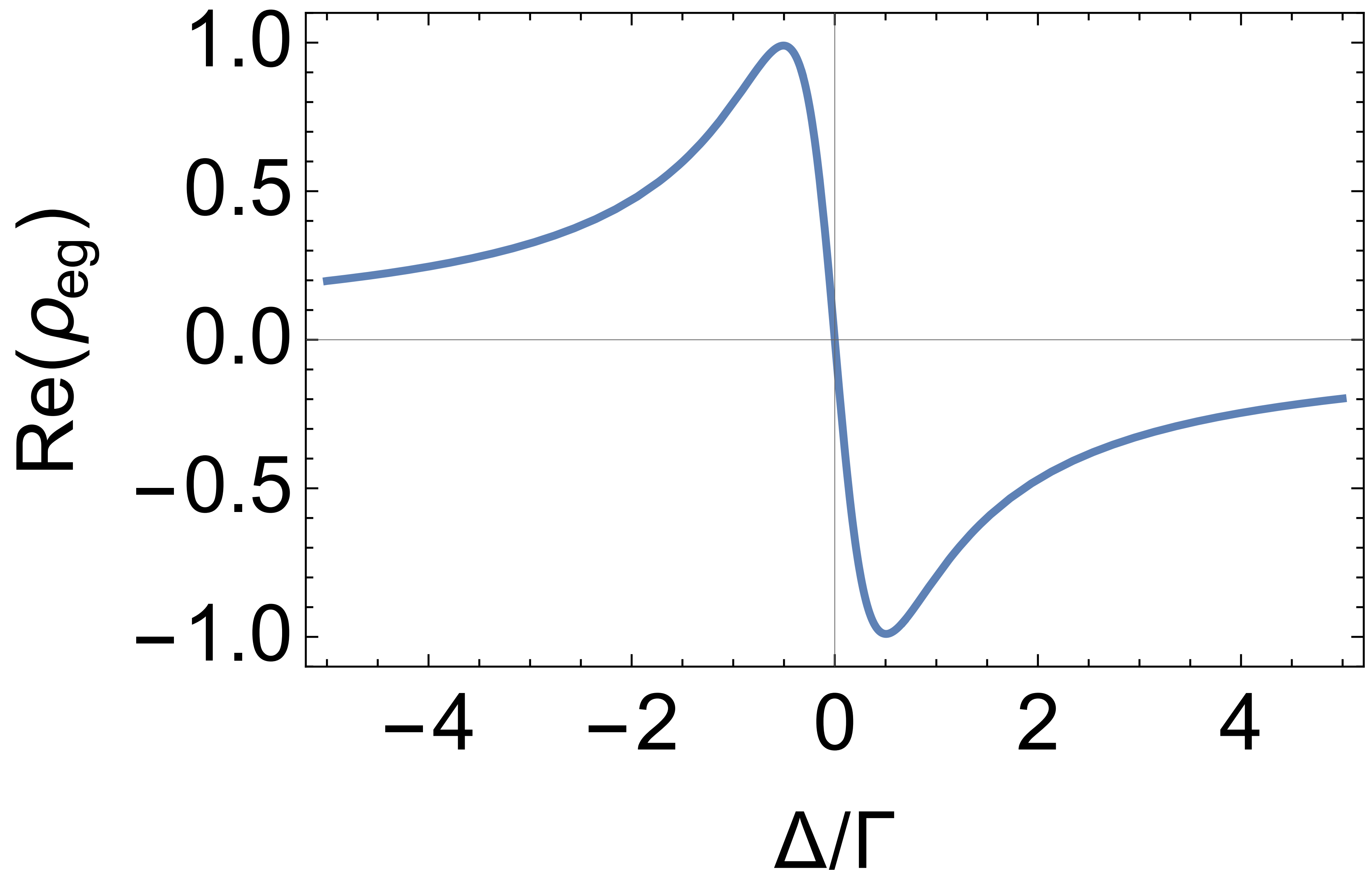

Dipole radiation

Classical dipole field

$$E_z = \frac{\langle d \rangle k^3}{4\pi\varepsilon_0} e^{ikr} [\frac{\sin^2\theta}{kr} + (3\cos^2\theta - 1)(\frac{1}{(kr)^3} - i\frac{1}{(kr)^2})]$$

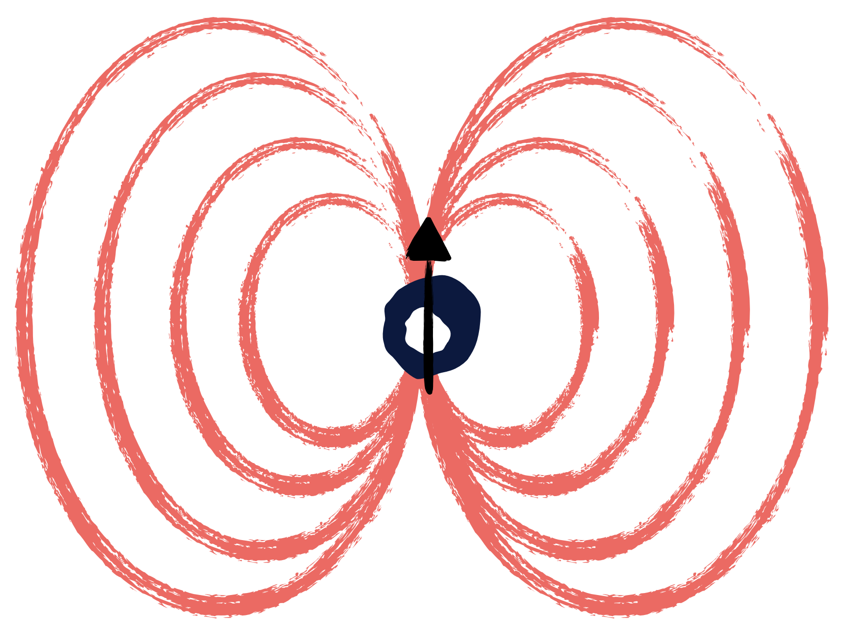

Weak driving: classical dipole

$$\langle d \rangle = d_{eg}\rho_{eg} = \frac{6\pi\varepsilon_0}{k^3} iE_0$$

Dipole radiation

Classical dipole field

$$E_z = \frac{\langle d \rangle k^3}{4\pi\varepsilon_0} e^{ikr} \left[\frac{\sin^2\theta}{kr} + (3\cos^2\theta - 1)\left(\frac{1}{(kr)^3} - i\frac{1}{(kr)^2}\right)\right]$$

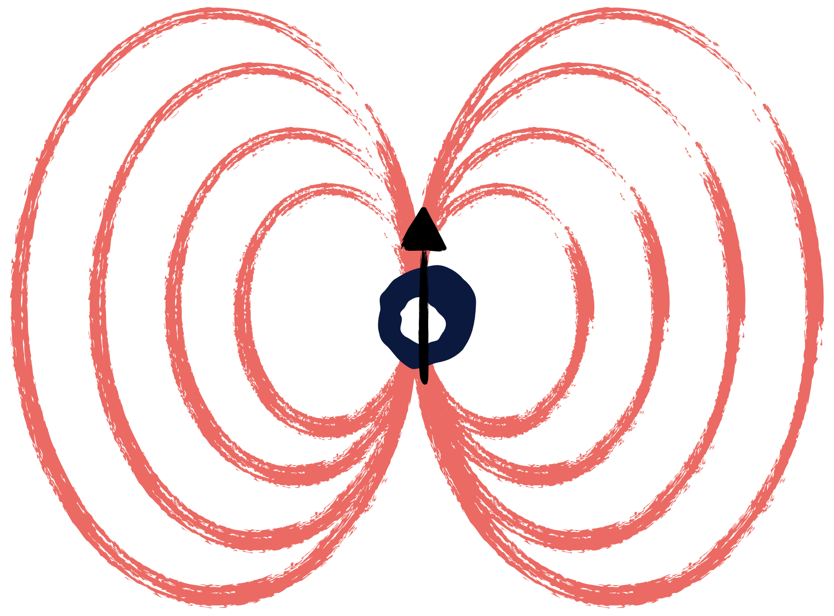

Weak driving: classical dipole

$$\langle d \rangle = d_{eg}\rho_{eg} = \frac{6\pi\varepsilon_0}{k^3} iE_0$$

Two-level atom

$$\hat{E}^+(\boldsymbol{r}) = \frac{k^3}{\varepsilon_0} G(\boldsymbol{r} - \boldsymbol{r}_{at})\hat{\sigma}^-$$

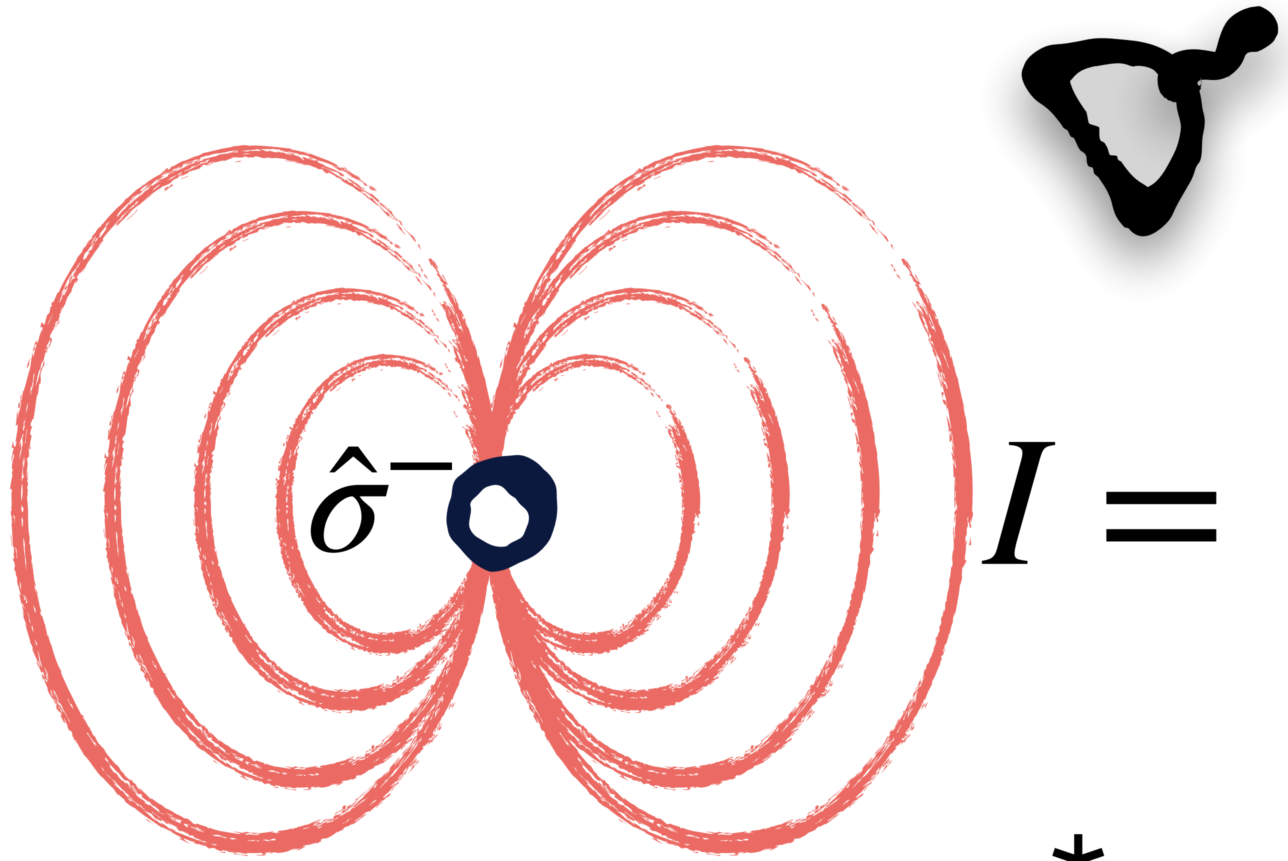

$\hat{E}^+(\boldsymbol{r})$

$$I = \langle \hat{E}^-(\boldsymbol{r})\hat{E}^+(\boldsymbol{r}) \rangle$$

*see many-atom case

Single atom absorption

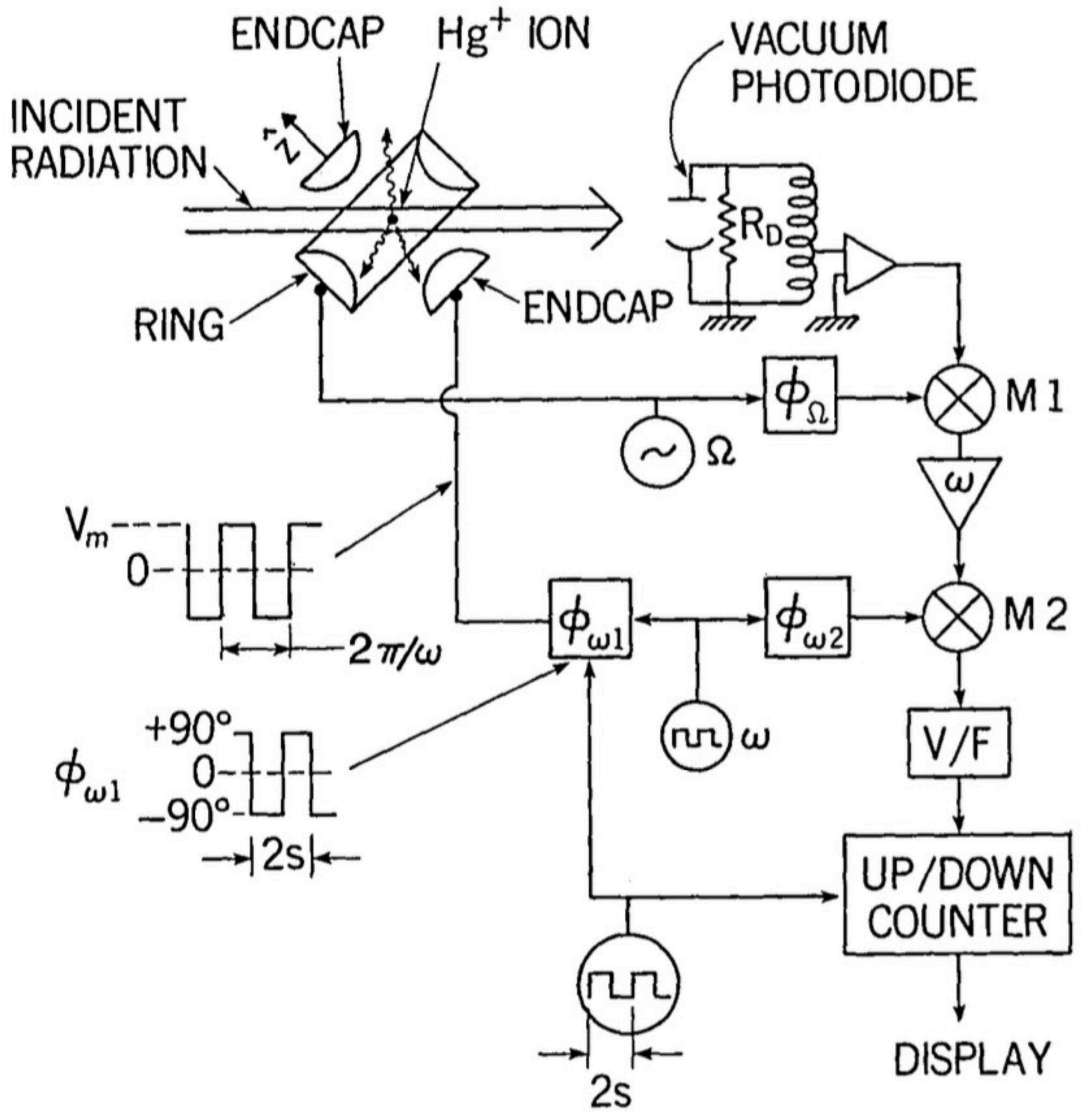

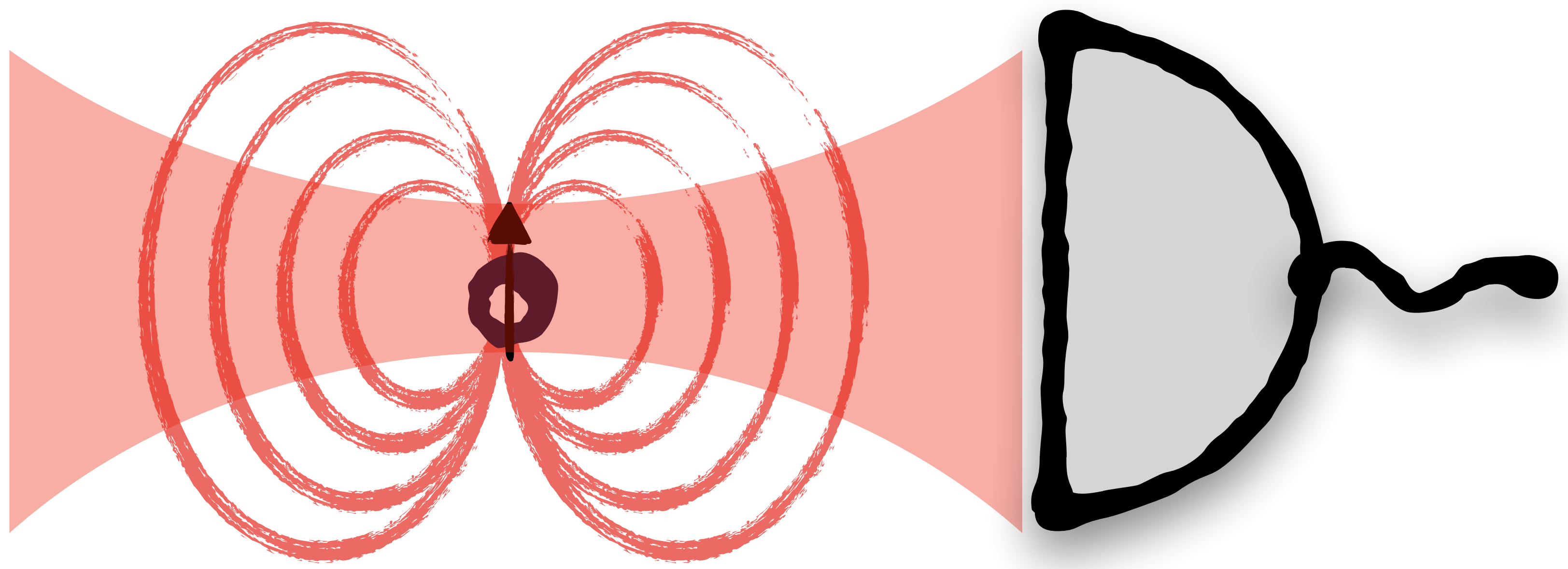

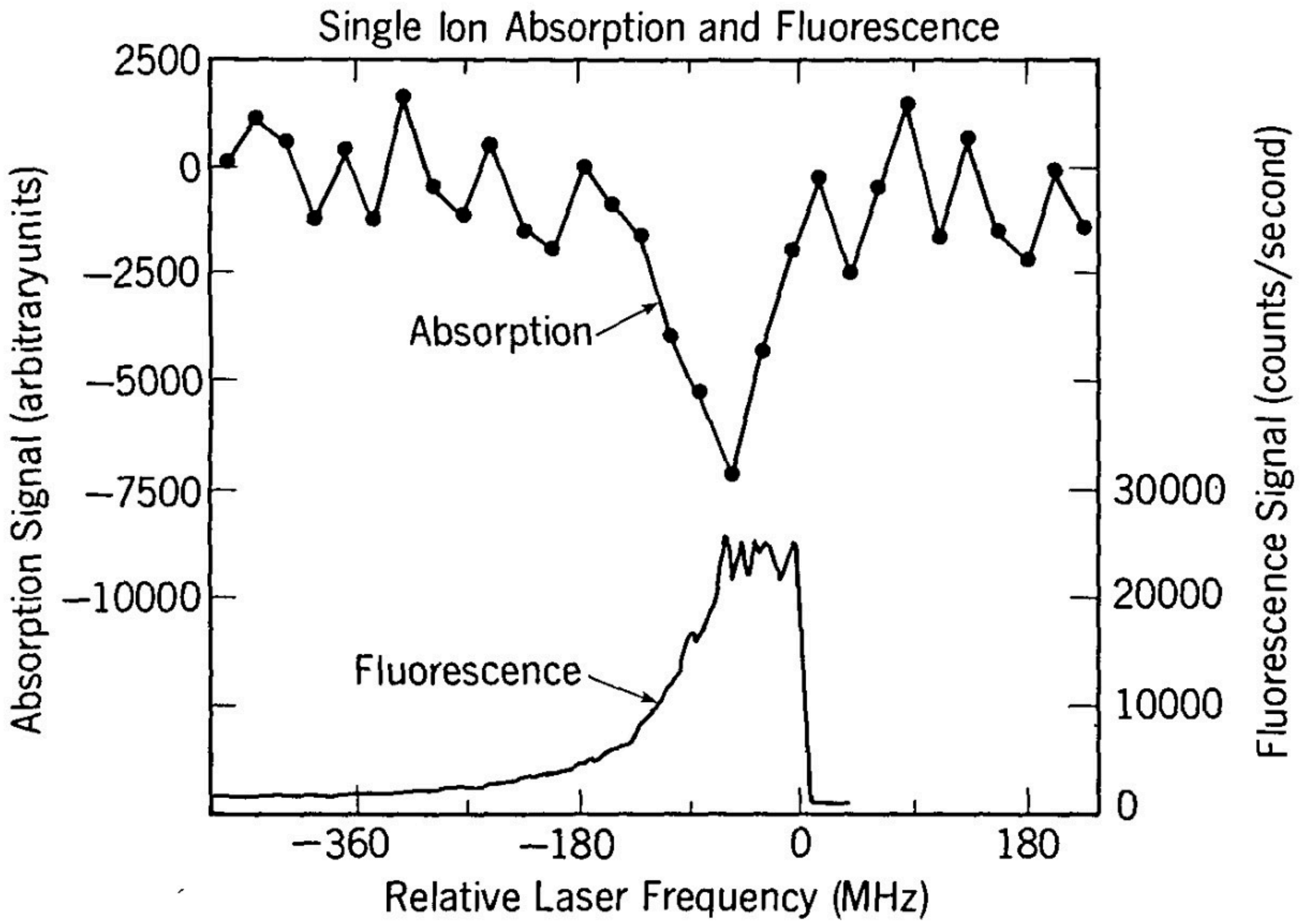

Fig. 2. Absorption signal observed as the 194-nm source is tuned through ν_0. Lower trace shows the simultaneously observed fluorescence scattering; the flat-topped appearance of this curve is due to the frequency modulation of the ion resonance. Integration times per point are 50 and 10 sec in the upper and lower traces, respectively.

Wineland, Itano, & Bergquist, *Opt Lett* **12**, 389 (1987).

Single atom absorption

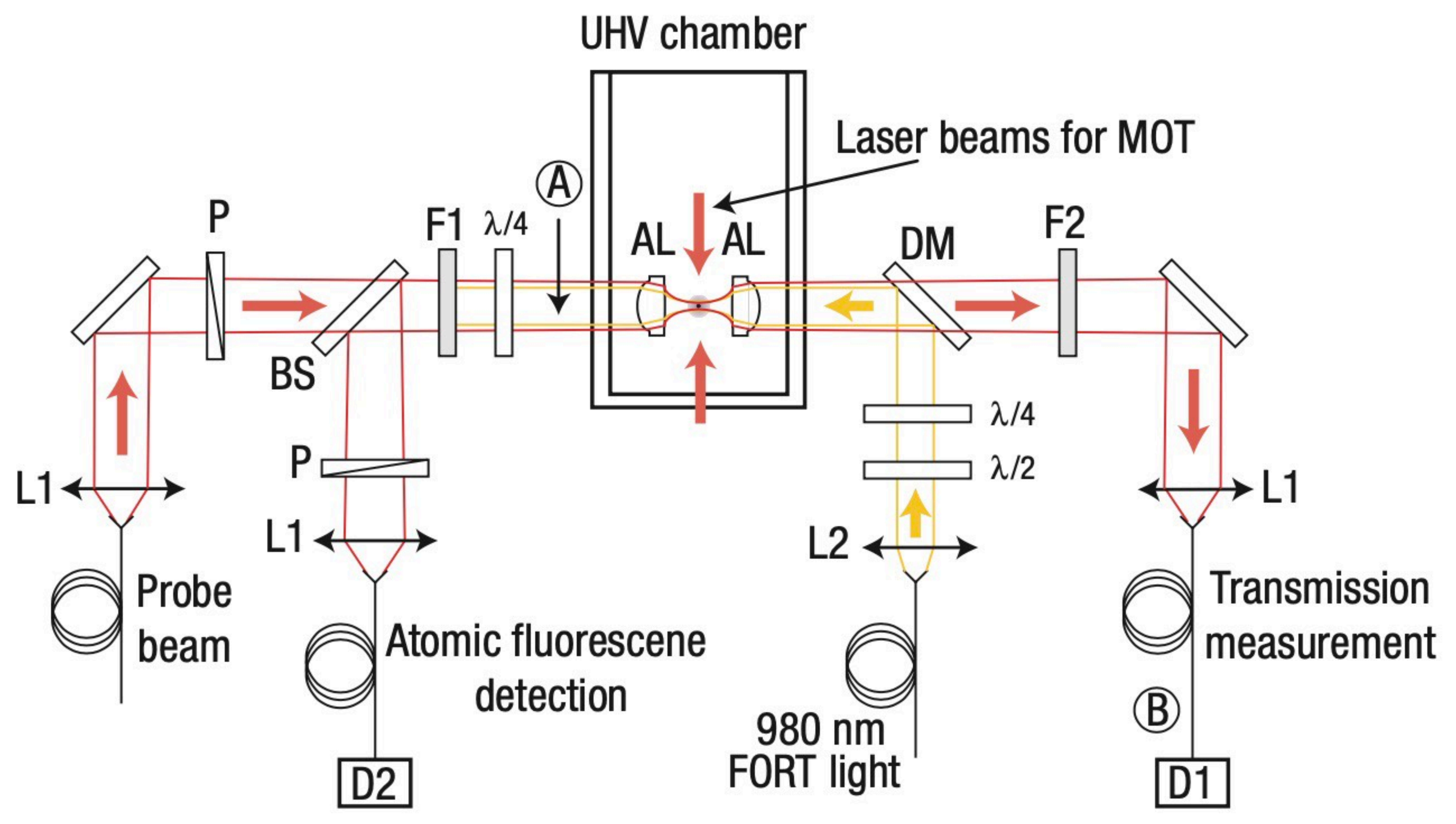

Figure 1 Experimental set-up for measuring the extinction of a light beam by a single atom. AL: aspheric lens ($f = 4.5$ mm, full NA $= 0.55$), P: polarizer, DM: dichroic mirror, BS: beam splitter with 99% reflectivity, $\lambda/4$, $\lambda/2$: quarter- and half-wave plates, F1: filters for blocking the 980 nm FORT light, F2: interference filter centred at 780 nm, D1 and D2: Si avalanche photodiodes, UHV: ultrahigh vacuum. Four more laser beams forming the MOT lie in an orthogonal plane and are not shown explicitly.

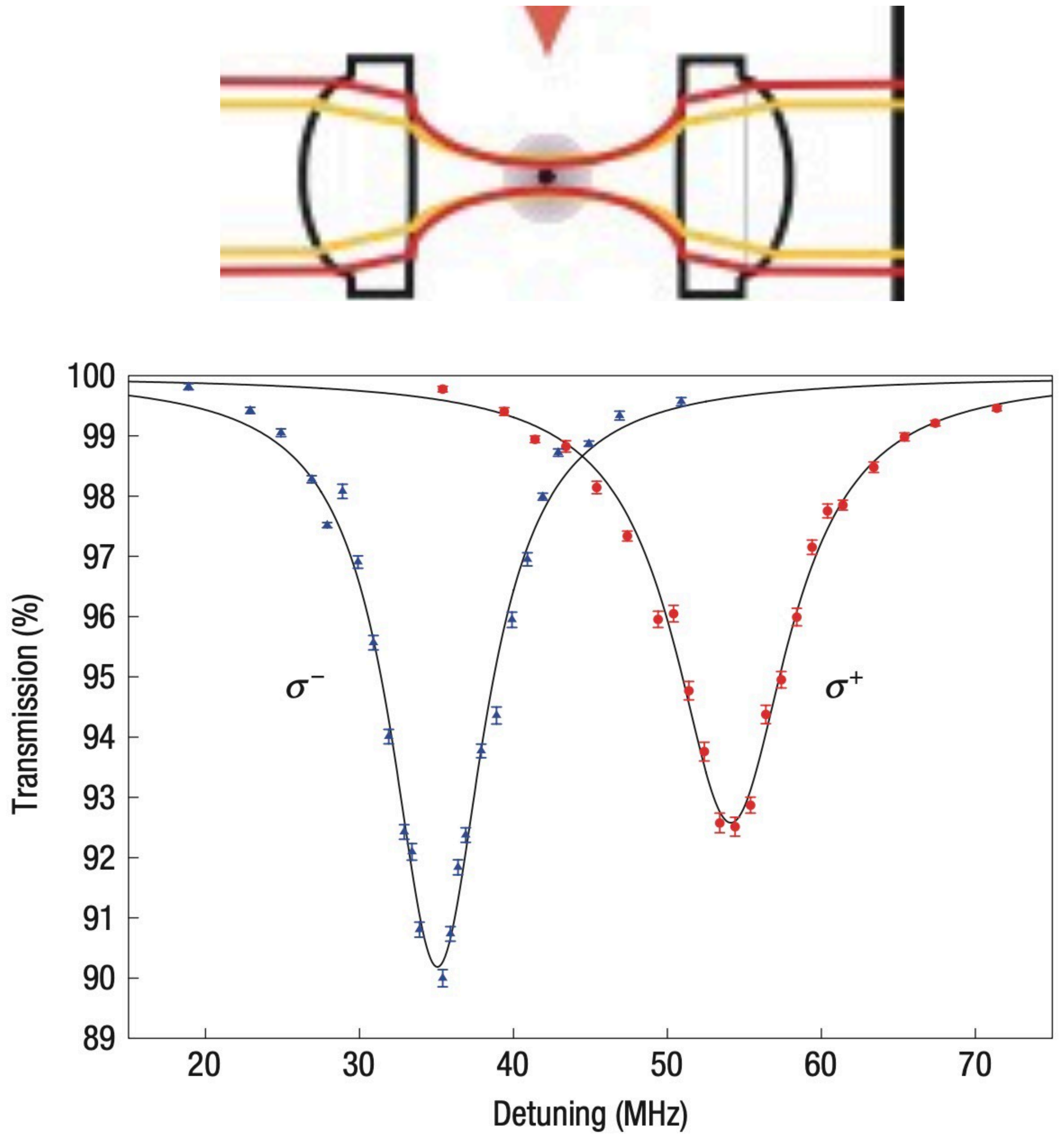

Figure 4 Transmission of the probe beam versus detuning from the natural resonant frequency of the $|g\rangle$ to $|e\rangle$ transition. The absolute photon scattering rate is kept at $\approx$2,500 s^{-1} for every point by adjusting the probe intensity according to the measured extinction. The solid lines are Lorentzian fits. Error bars indicate $\pm$1 standard deviations obtained from propagated Poissonian counting statistics (see the Methods section).

Tey *et al.*, *Nat Phys* **4**, 924–927 (2008).

Resonance fluorescence

First order coherence $$g^{(1)}(\tau) = \lim_{t\to\infty} \langle E^-(t)E^+(t+\tau)\rangle$$

Interference between the field at t and $t+\tau$

Resonance spectrum $$S(\omega) = \int_0^\infty g^{(1)} e^{-i\omega\tau} d\tau$$

Resonance fluorescence

First order coherence $$g^{(1)}(\tau) = \lim_{t \to \infty} \langle E^{-}(t) E^{+}(t+\tau) \rangle$$

Interference between the field at t and $t+\tau$

Resonance spectrum $$S(\omega) = \int_0^\infty g^{(1)} e^{-i\omega\tau} d\tau$$

Weak drive

$\Omega < \Gamma$

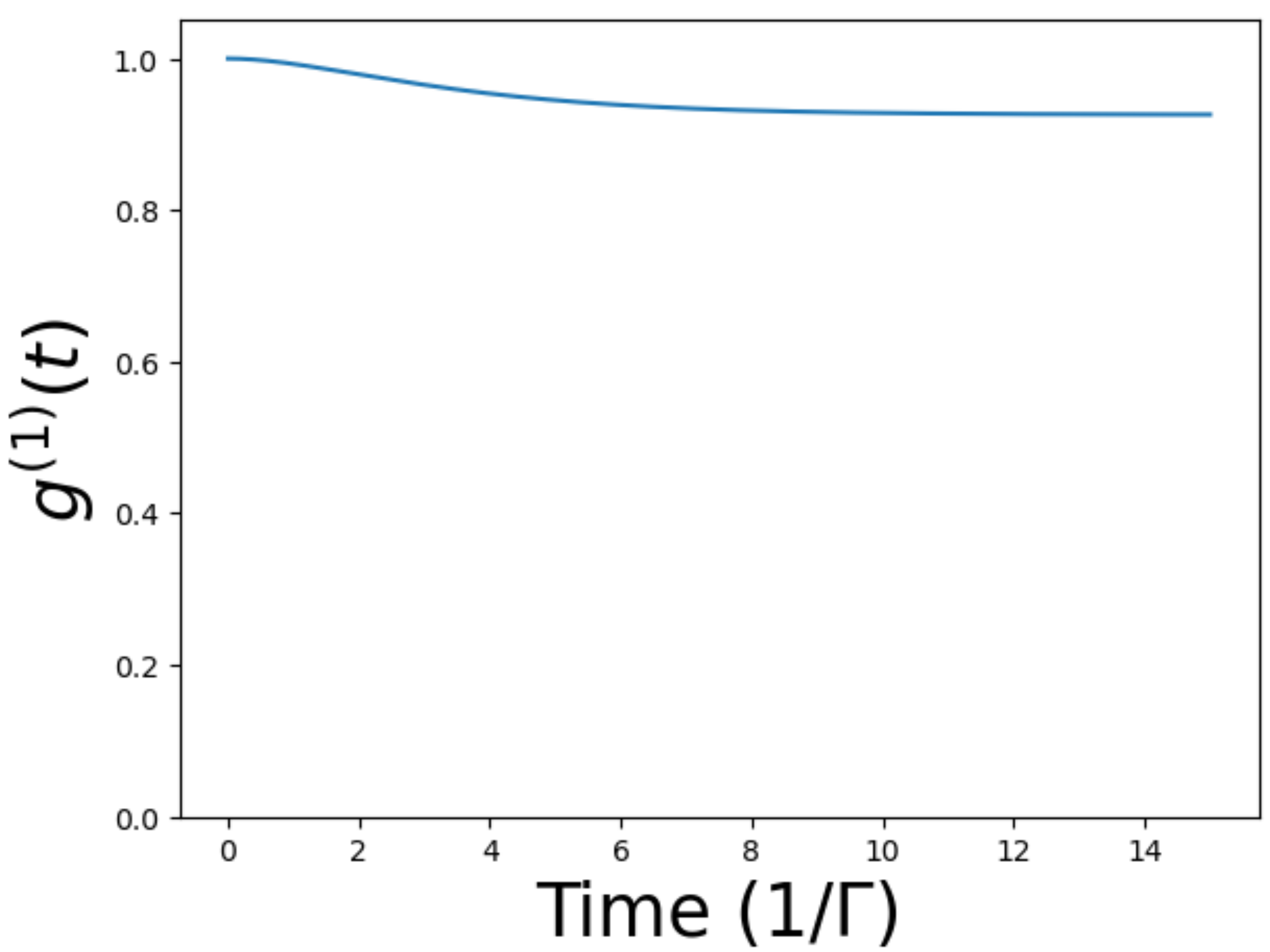

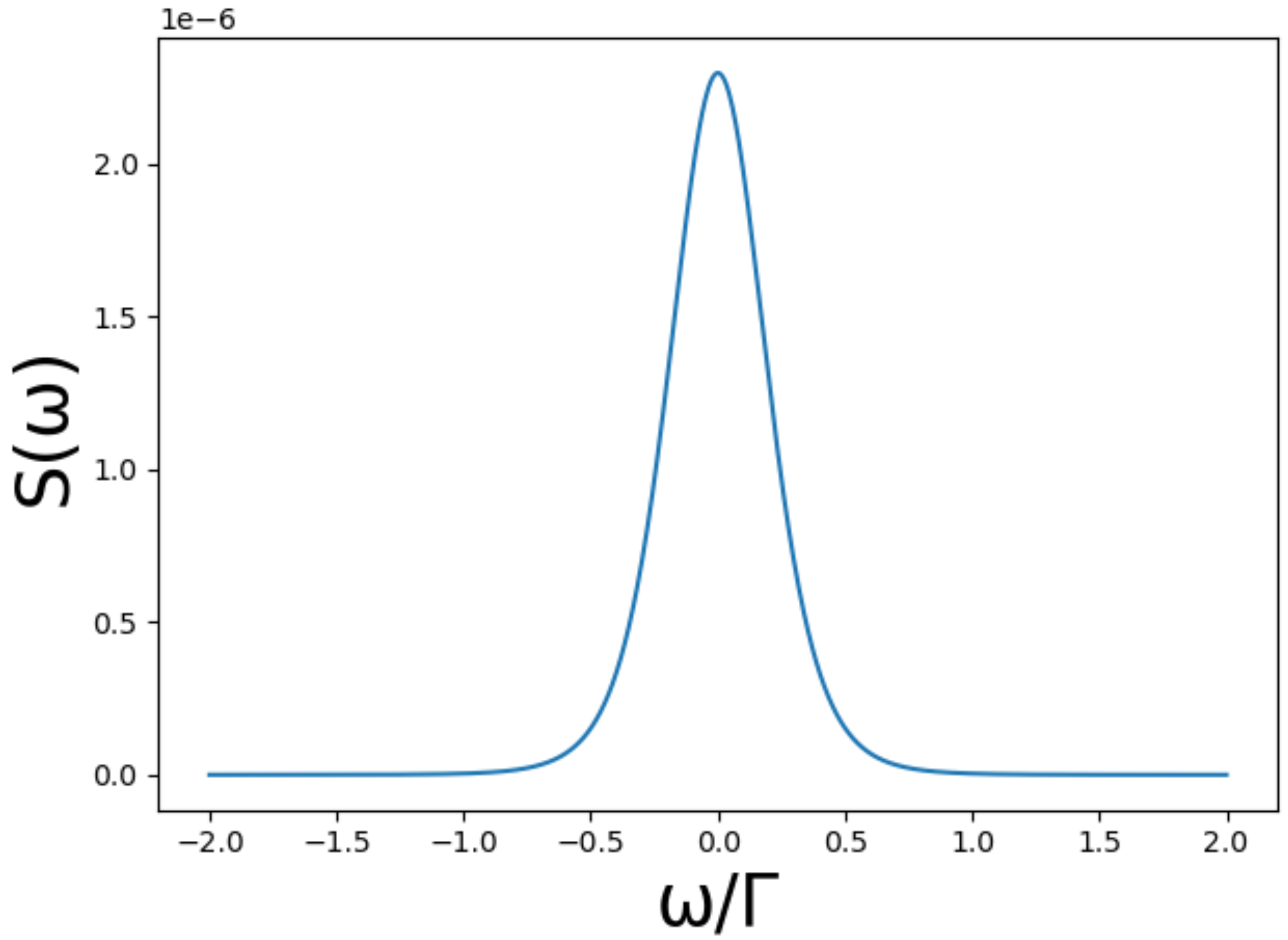

Resonance fluorescence

First order coherence $$g^{(1)}(\tau) = \lim_{t\to\infty} \langle E^{-}(t)E^{+}(t+\tau)\rangle$$

Interference between the field at t and $t+\tau$

Resonance spectrum $$S(\omega) = \int_0^\infty g^{(1)} e^{-i\omega\tau} d\tau$$

Strong drive

$\Omega \gg \Gamma$

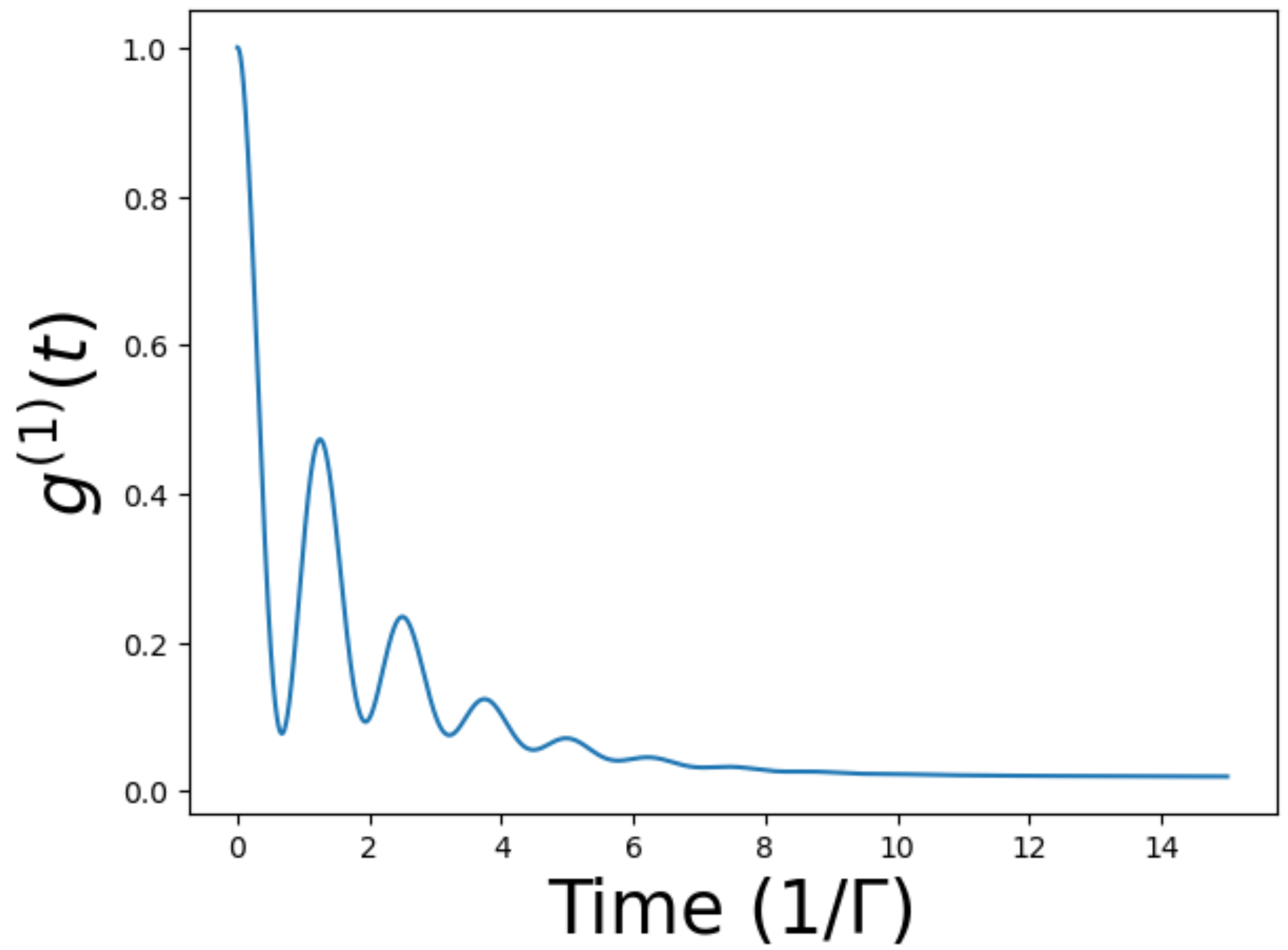

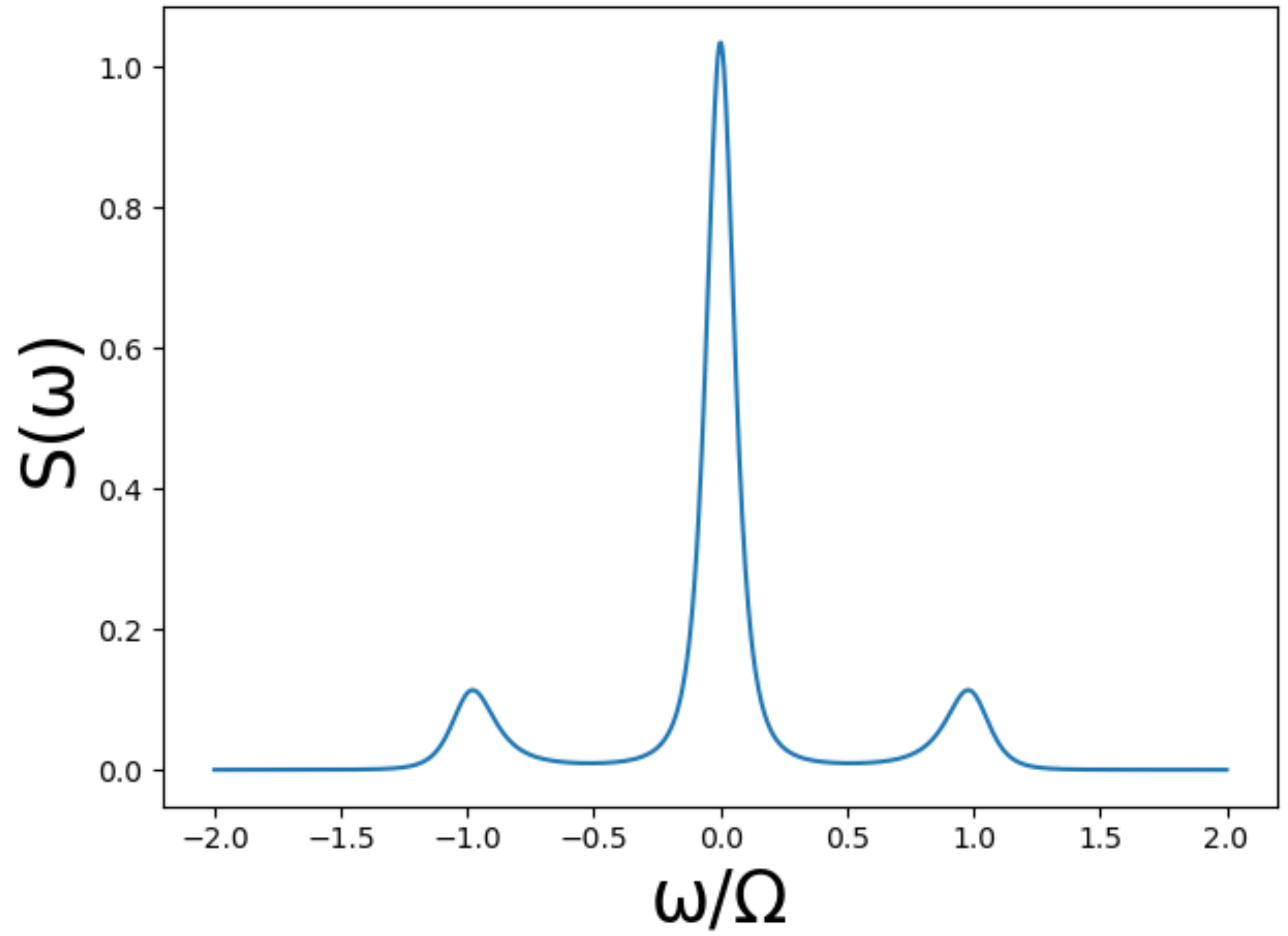

Resonance Fluorescence

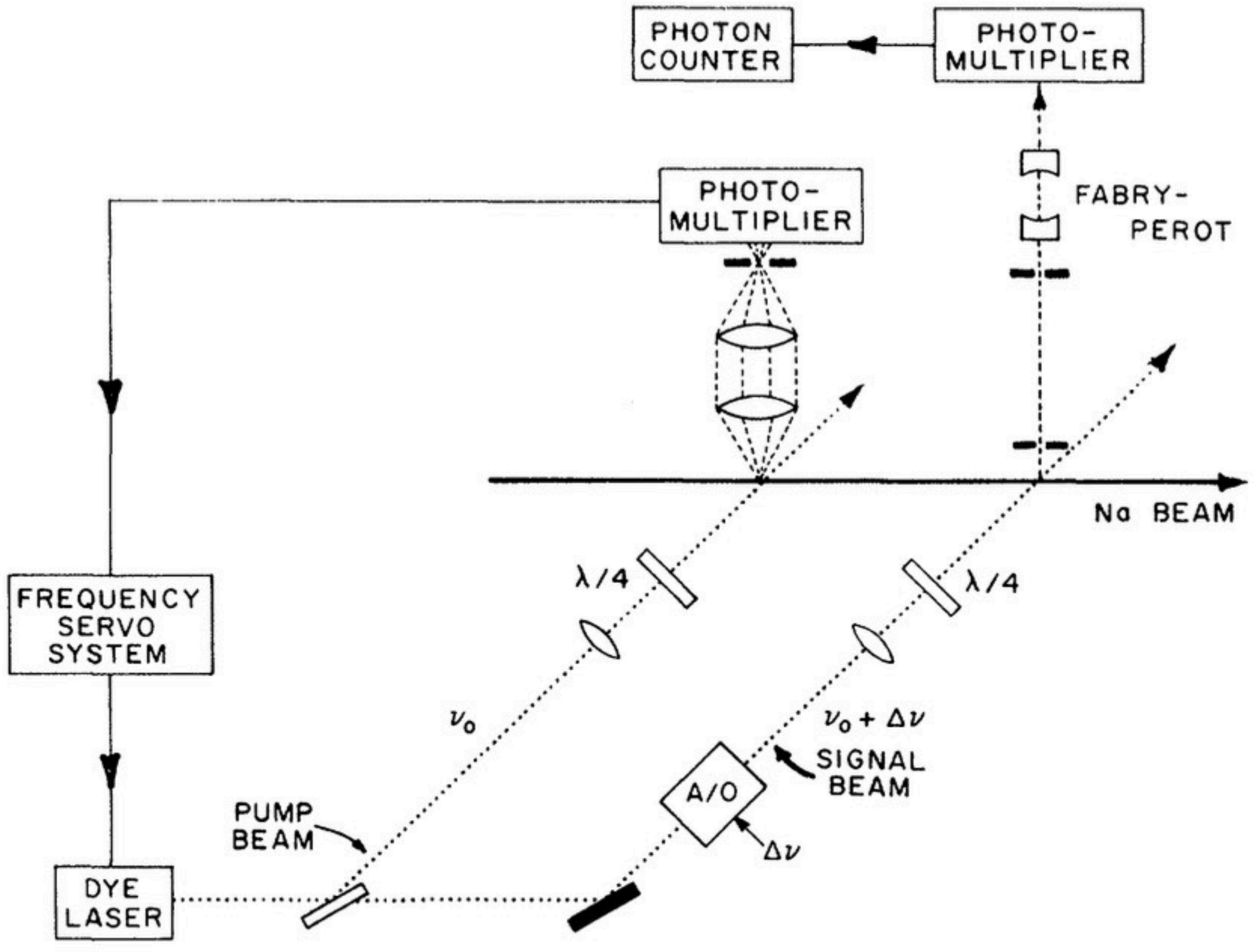

FIG. 4. Experimental setup used to measure the spectrum of resonance fluorescence. The A/O shifter is removed to obtain on-resonance data.

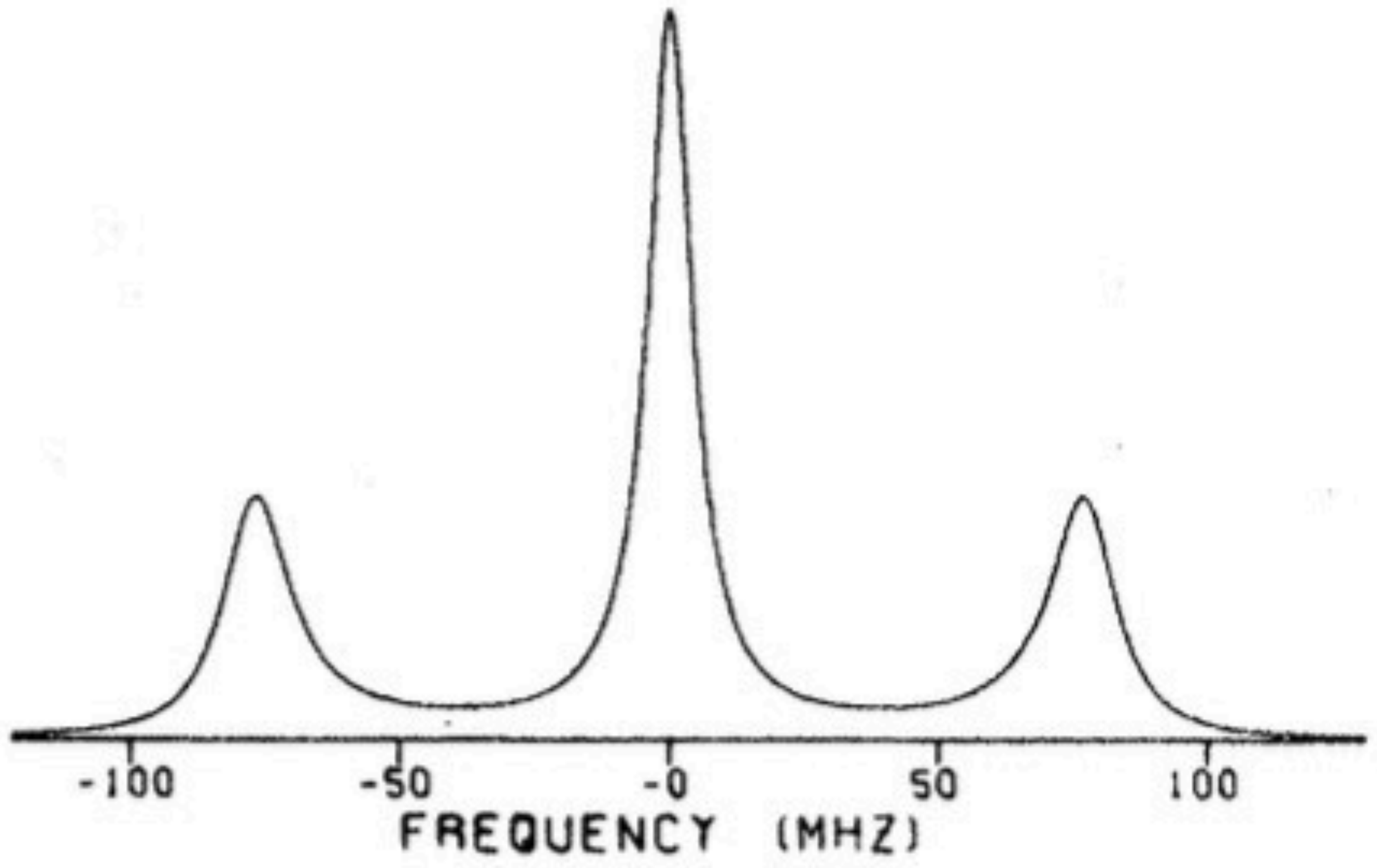

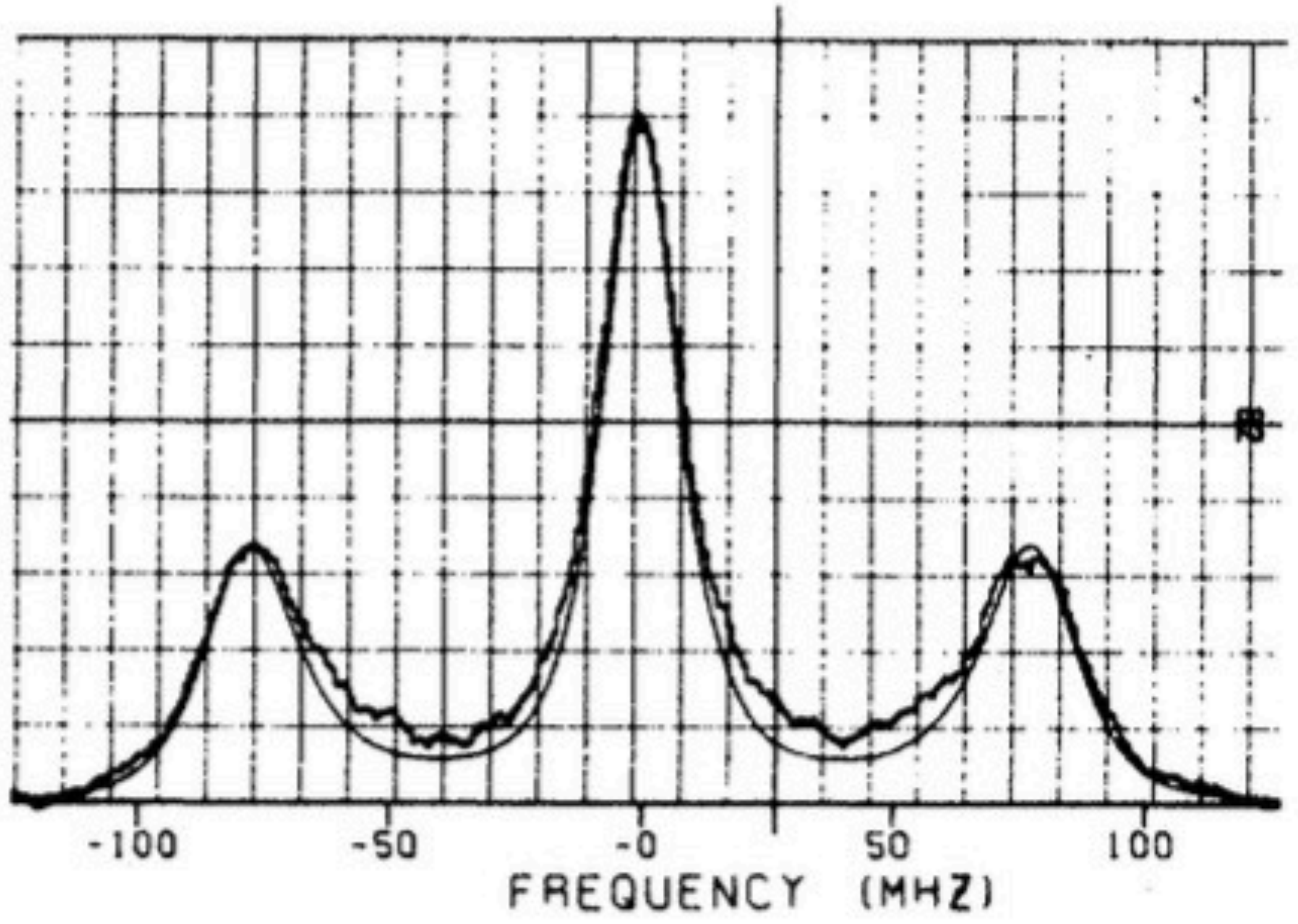

Grove, Wu & Ezekiel. *Phys. Rev. A* **15**, 227(1977).

Resonance Fluorescence

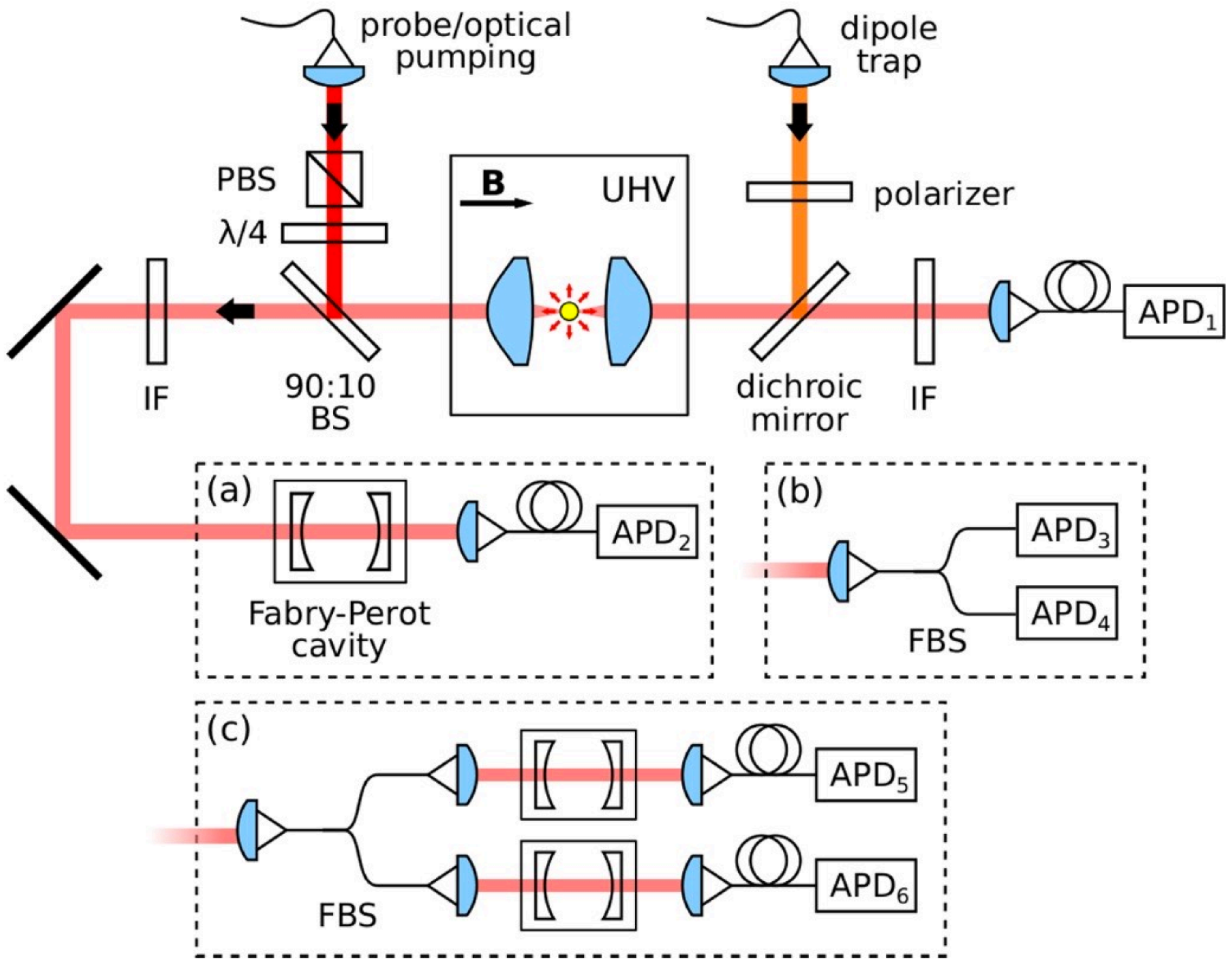

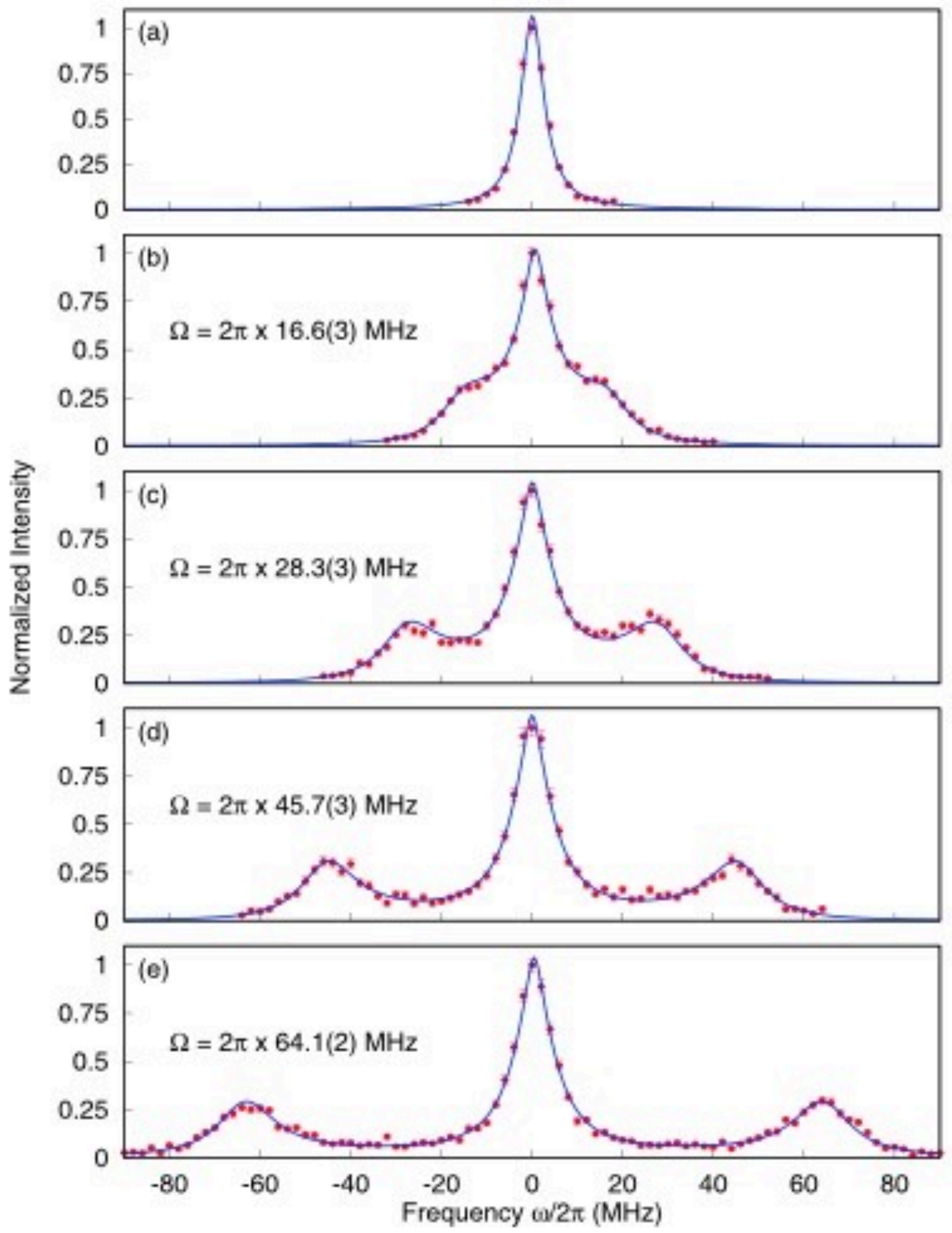

FIG. 4. Normalized resonance atomic emission spectra at different excitation intensities recorded by scanning the Fabry-Perot cavity with the setup in Fig. 2(a). For (b)–(e), the solid line is a fit to Eq. (1) convoluted with the cavity transfer function and the effect of laser reflection. The Rabi frequency Ω extracted from the fit is labeled in (b)–(e).

Ng, Chow & Kurtsiefer, *Phys. Rev. A* **106**, 063719 (2022).

Original expt: Aspect, Roger, Reynaud, Dalibard & Cohen-Tannoudji, *Phys Rev Lett* **45**, 617 (1980).

Resonance Fluorescence

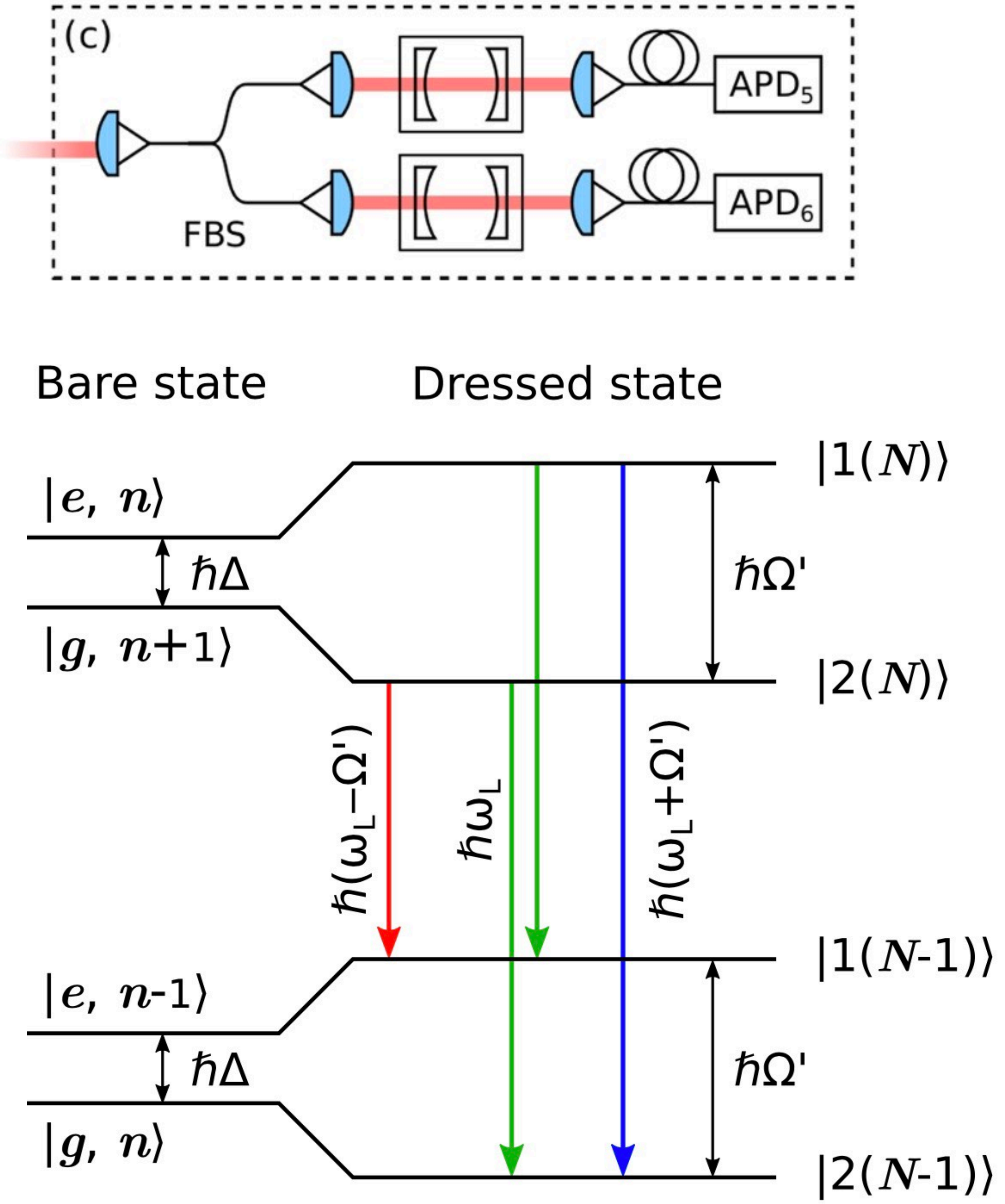

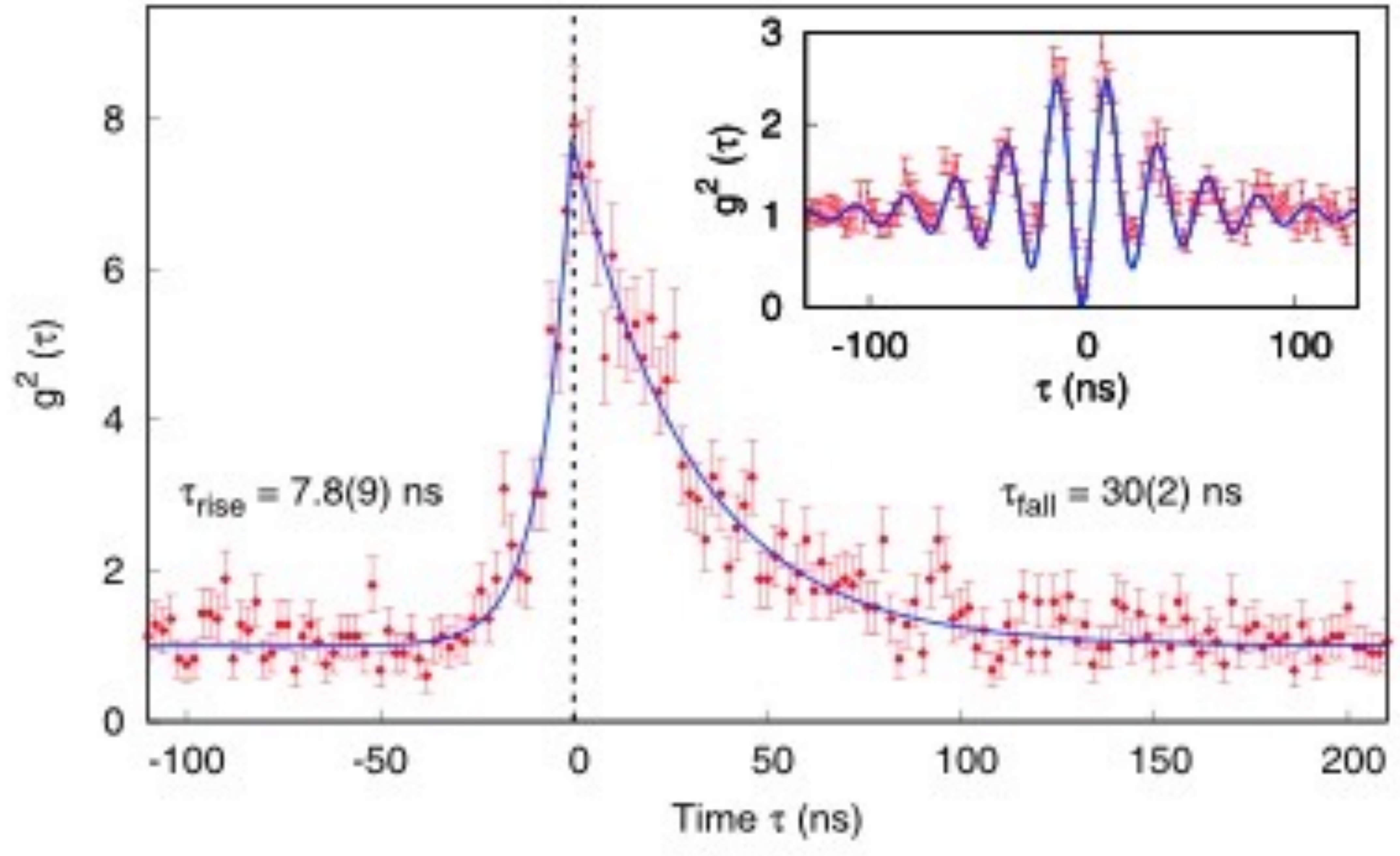

FIG. 6. Normalized cross-correlation between photons from two opposite Mollow sidebands as a function of delay τ between detection of a photon from the higher-energy sideband after detection of a photon from lower-energy sideband. Inset: Normalized intensity autocorrelation of the unfiltered off-resonance atomic fluorescence to extract Ω'.

Ng, Chow & Kurtsiefer, *Phys. Rev. A* **106**, 063719 (2022).

Original expt: Aspect, Roger, Reynaud, Dalibard & Cohen-Tannoudji, *Phys Rev Lett* **45**, 617 (1980).

$g^{(2)}(0)$ with large optical depth

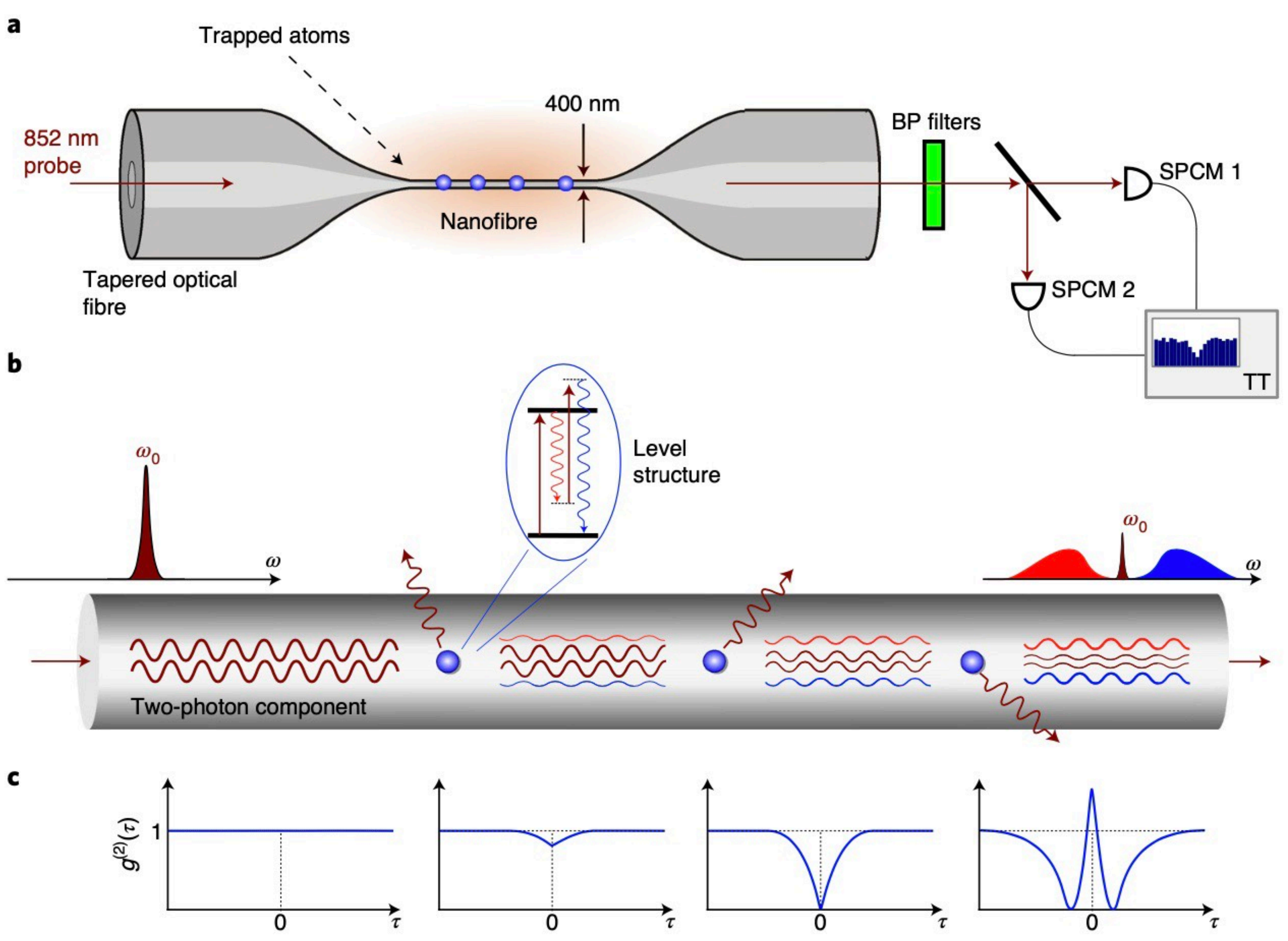

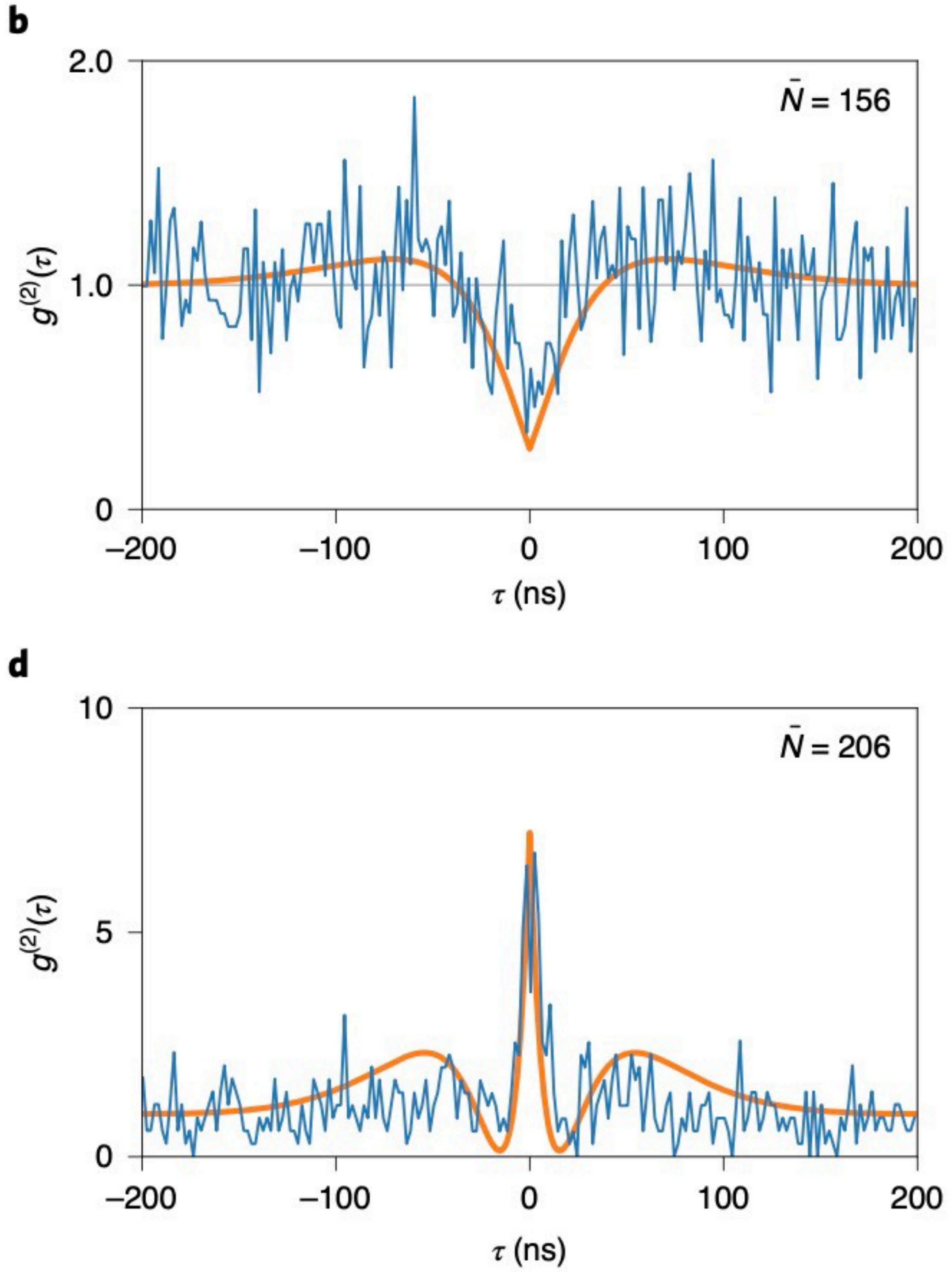

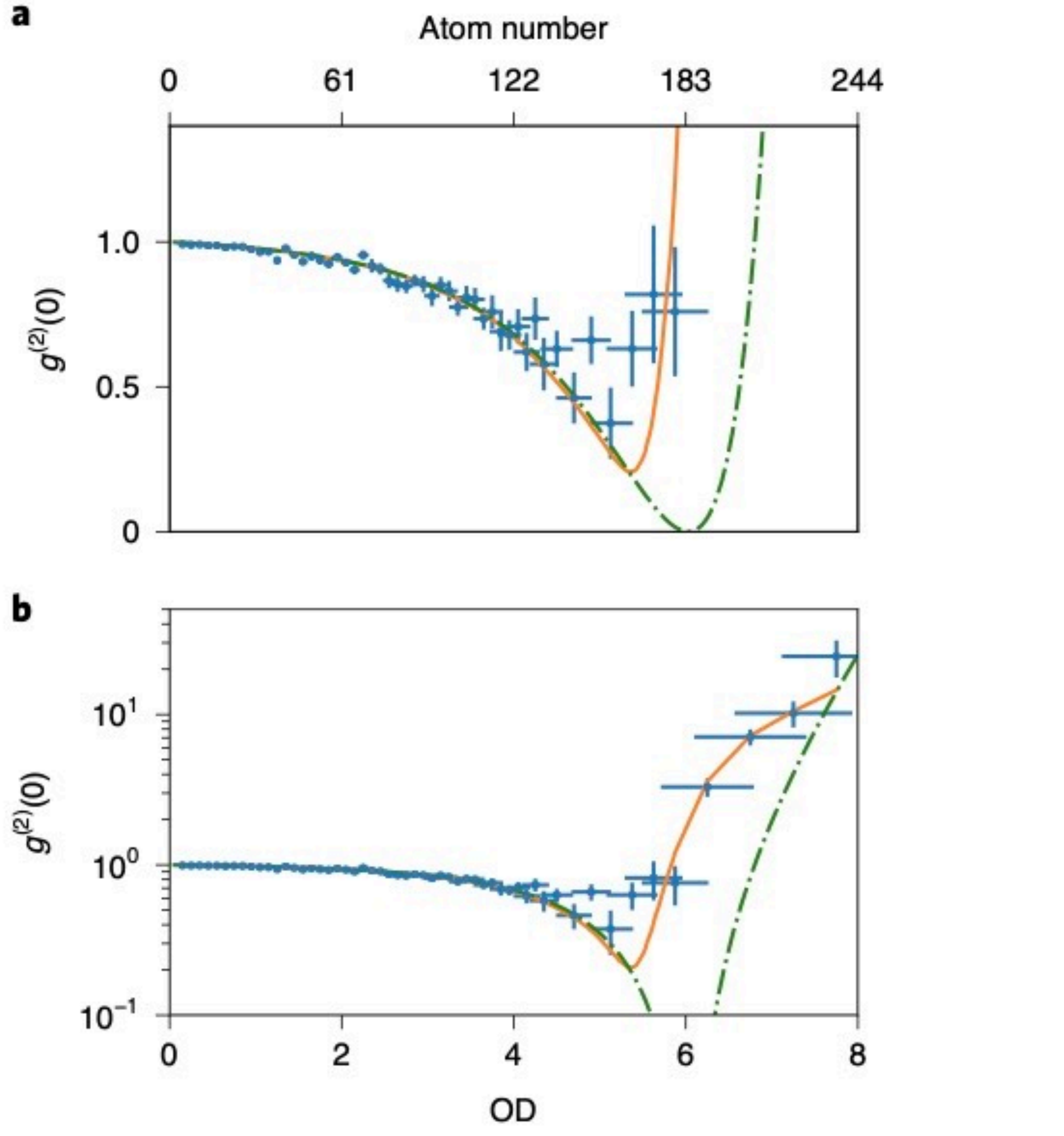

Fig. 3 | Correlations at zero time delay versus the number of trapped atoms. a,**b**, The zero time delay-value, $g^{(2)}(0)$ of the measured second-order correlation functions (blue data points) plotted on a linear (**a**) or logarithmic (**b**) scale versus the OD of the atomic ensemble (bottom *x* axes) or average number of trapped atoms (top *x* axes). The values of $g^{(2)}(0)$ stem from maximum-likelihood fits to the individual correlation functions. The vertical and horizontal error bars indicate the 1σ error in $g^{(2)}(0)$ and the atom number, respectively (see Methods). The solid orange line is the theory prediction taking into account the experimental uncertainty in OD using the coupling strength β as the only fit parameter (see Methods). For comparison, the dashed green curve shows the theory prediction without uncertainty in OD for the same value of β.

Optical depth is narrow in frequency: does not absorb the sidebands

Prasad *et al.*. *Nat. Photonics* **14**, 719 (2020).

Outline

Lecture 1: Quantum optics of single atoms

Lecture 2: Collective light scattering by *N* atoms

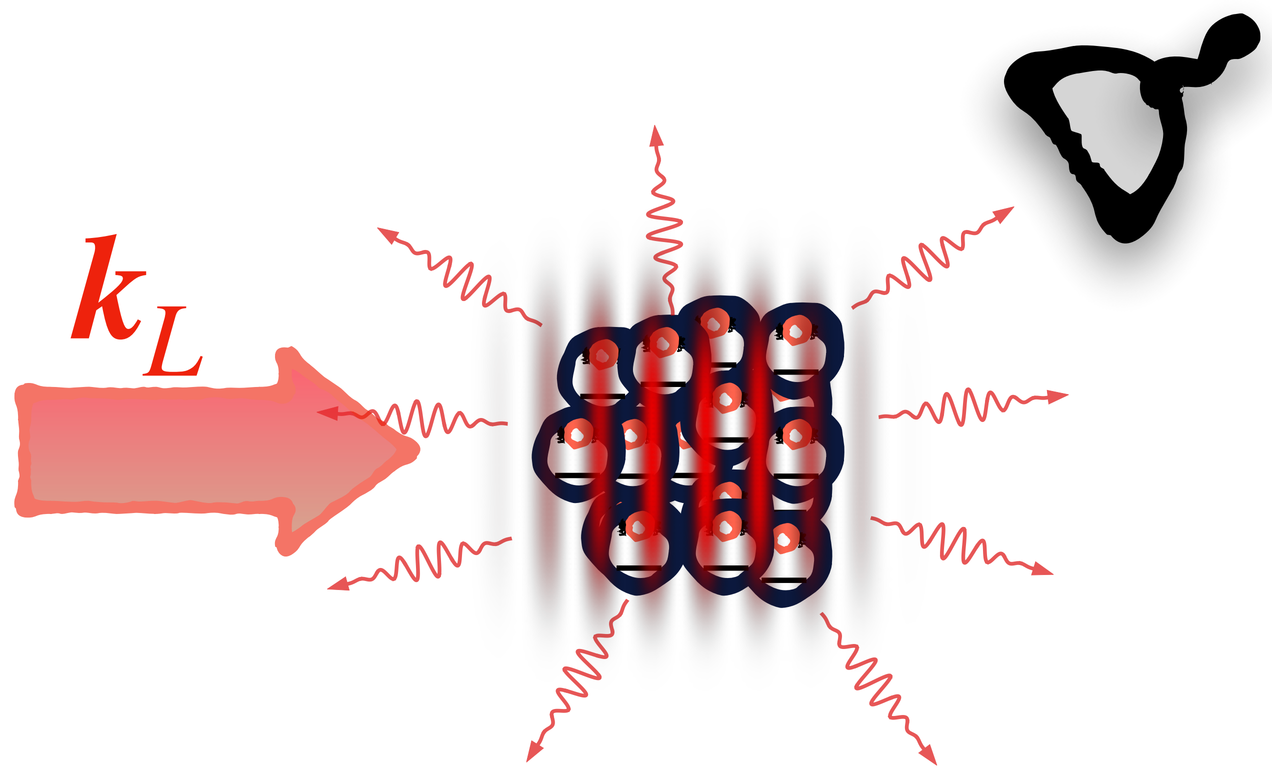

Lecture 3: Many-body quantum optics

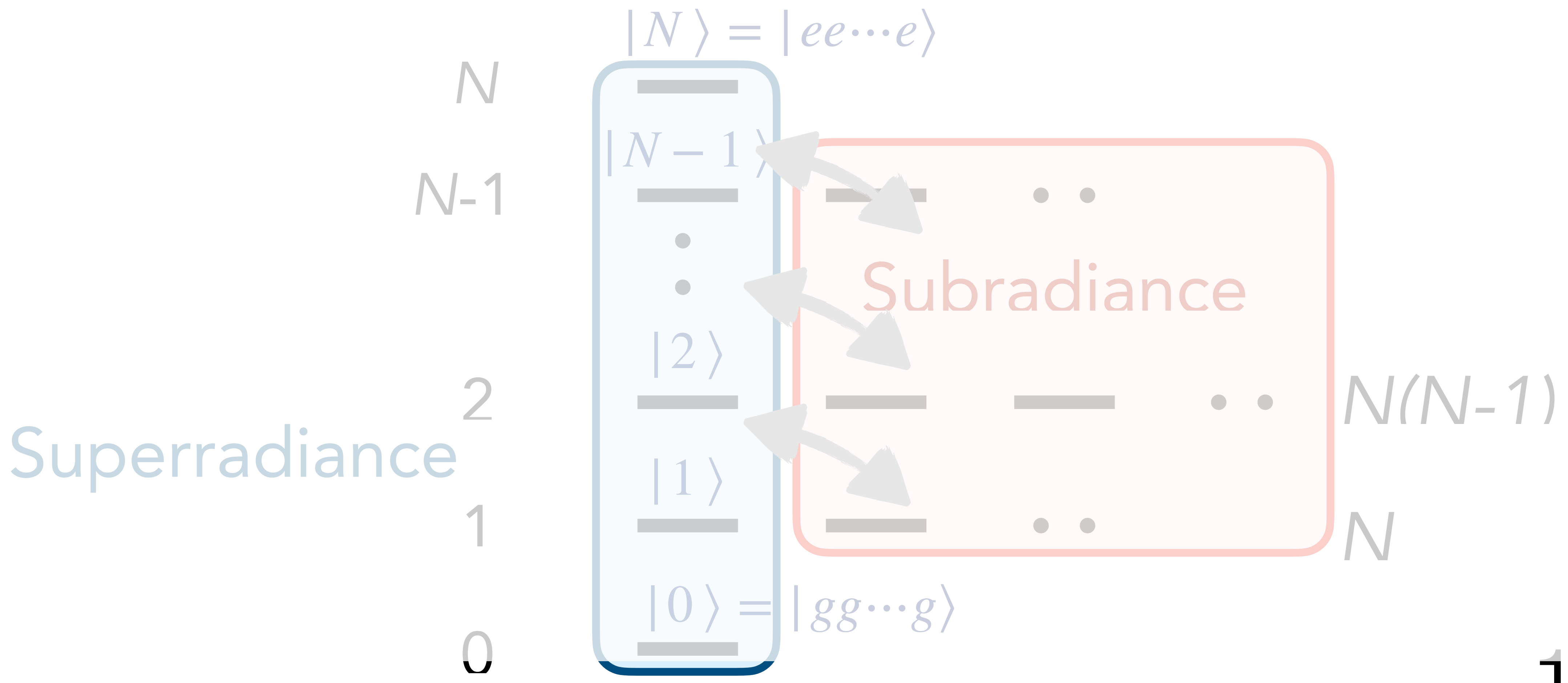

Collective light scattering

Single atom in **free space**

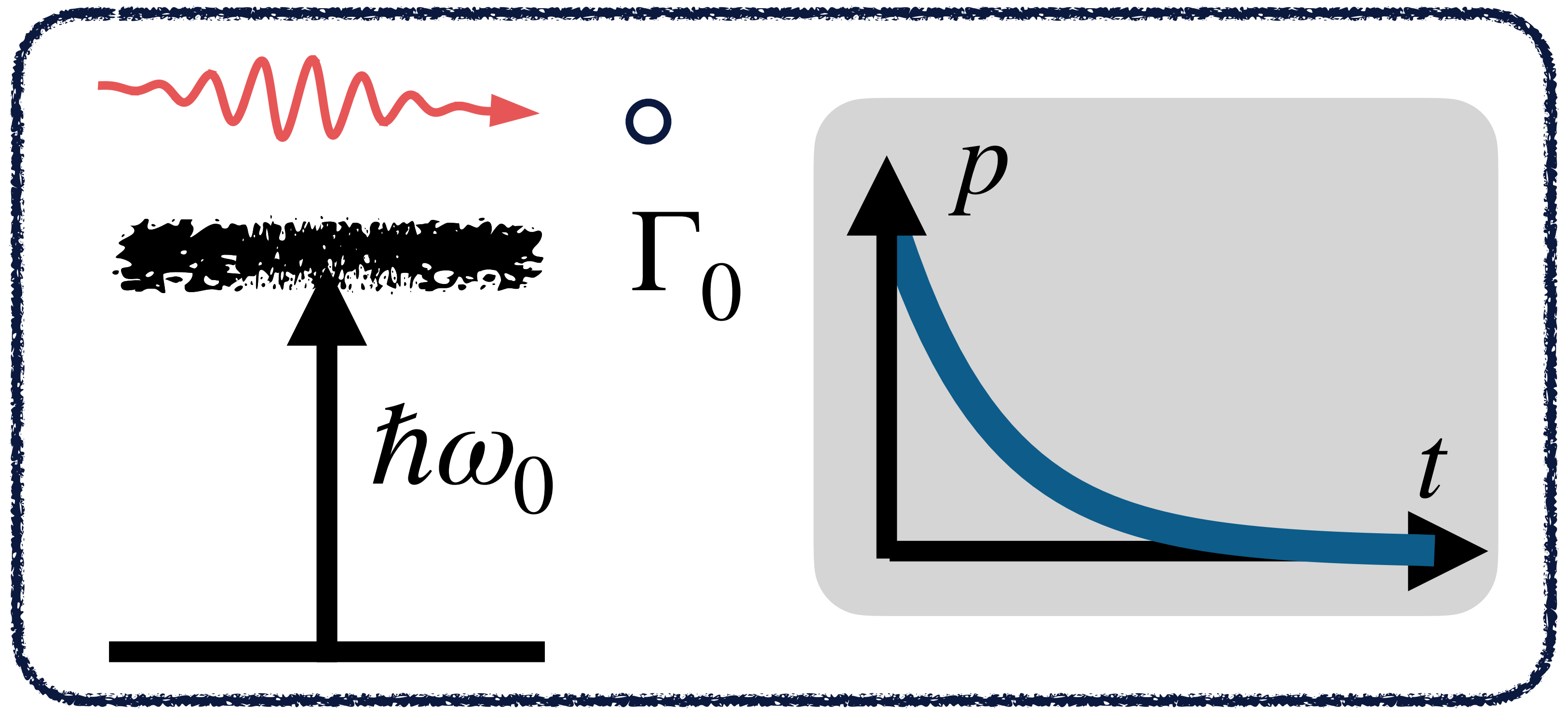

N-atom spontaneous emission

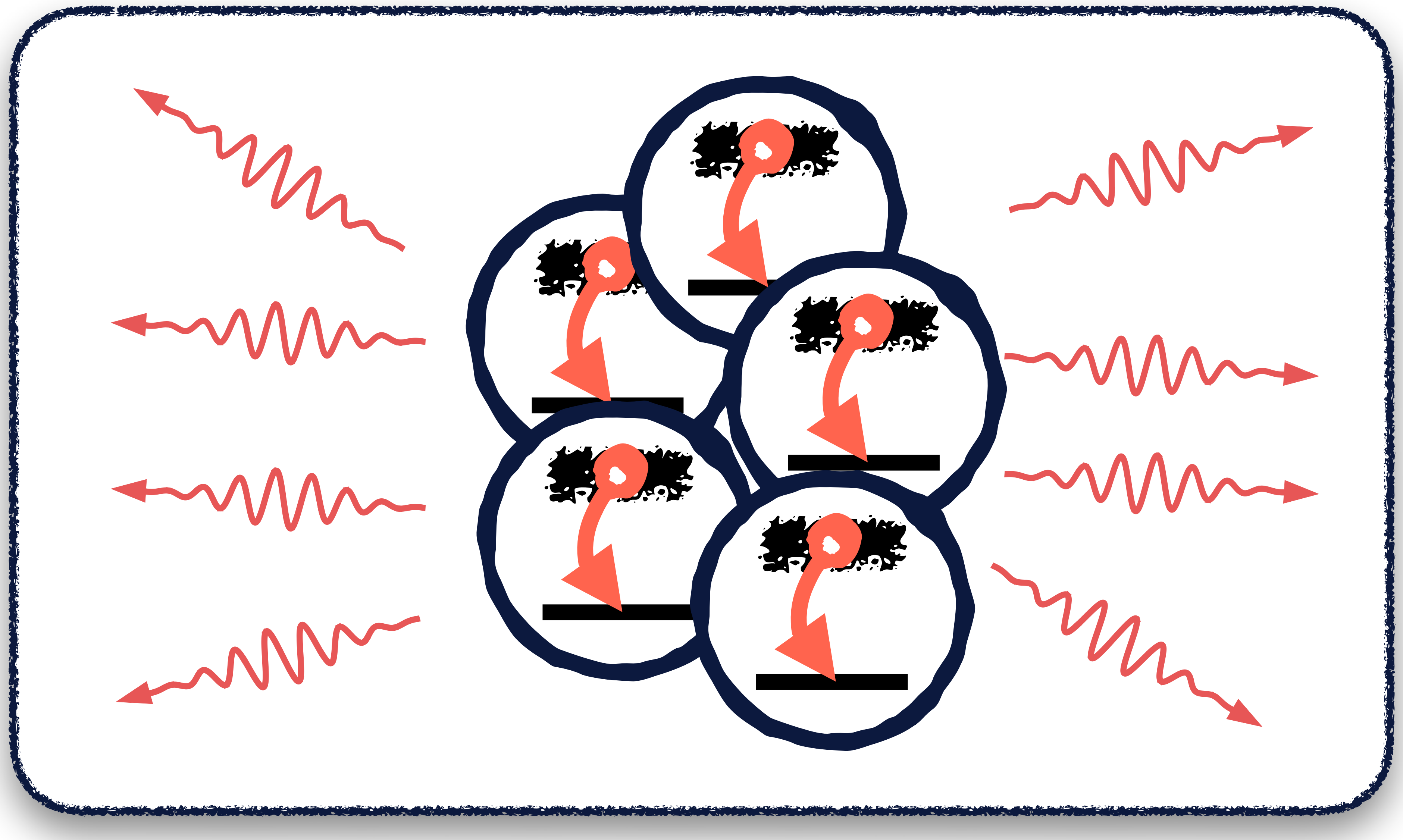

Resonant dipole dipole interaction

Two dipoles interact with light: resonant dipole-dipole interaction

$$E_z^1 = \frac{d_1 k^3}{4\pi\varepsilon_0} e^{ikr} \left[\frac{\sin^2\theta}{kr} + (3\cos^2\theta - 1)\left(\frac{1}{(kr)^3} - i\frac{1}{(kr)^2}\right)\right]$$

$-\boldsymbol{d}_2^* \cdot \boldsymbol{E}_1$

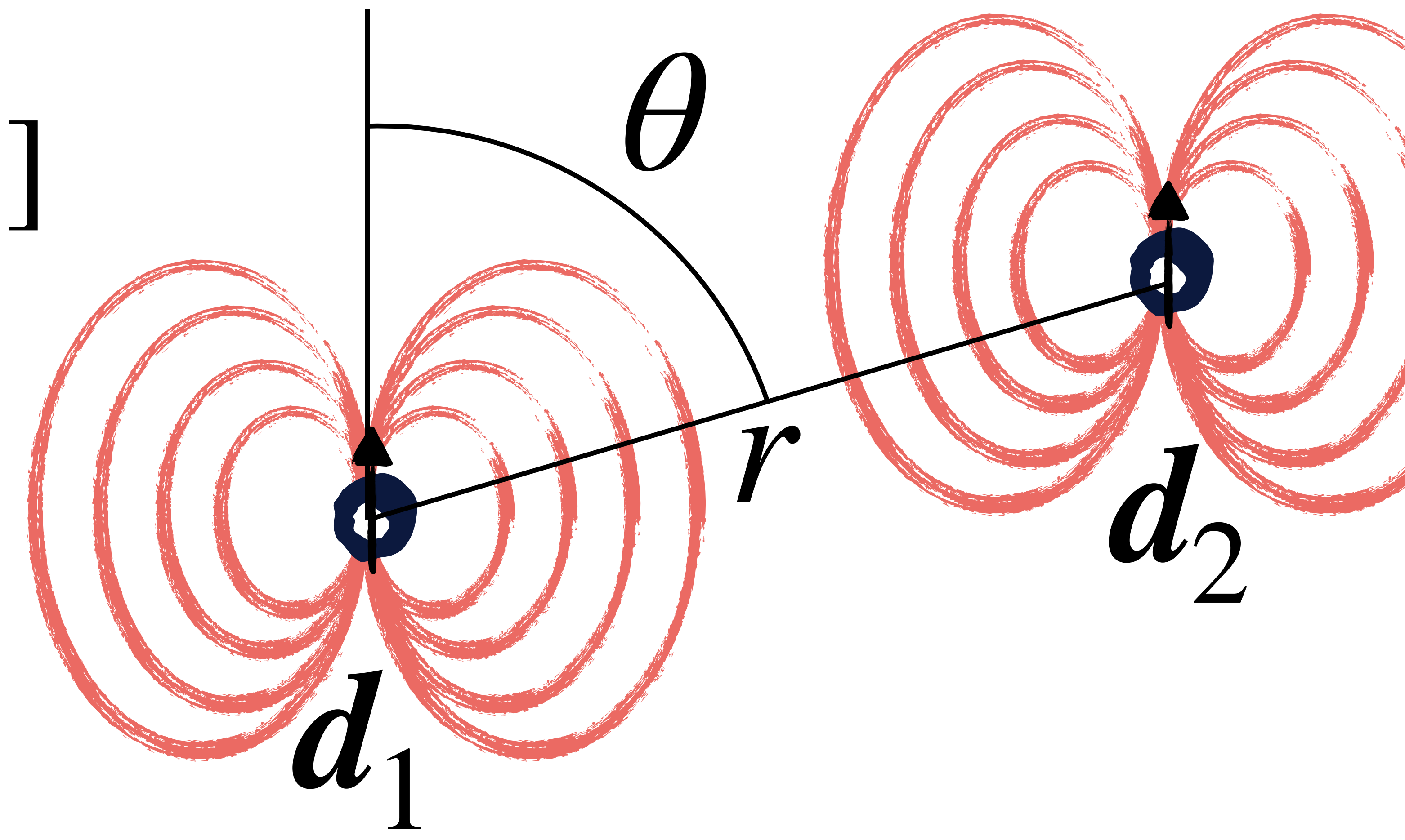

Resonant dipole dipole interaction

Two dipoles interact with light: resonant dipole-dipole interaction

$$-\boldsymbol{d}_2^* \cdot \boldsymbol{E}_1$$

$$V_{\mathrm{dd}}(r,\theta) = -\frac{3\hbar\Gamma}{4} e^{ikr}\left[\frac{\sin^2\theta}{kr} + (3\cos^2\theta - 1)\left(\frac{1}{(kr)^3} - i\frac{1}{(kr)^2}\right)\right]$$

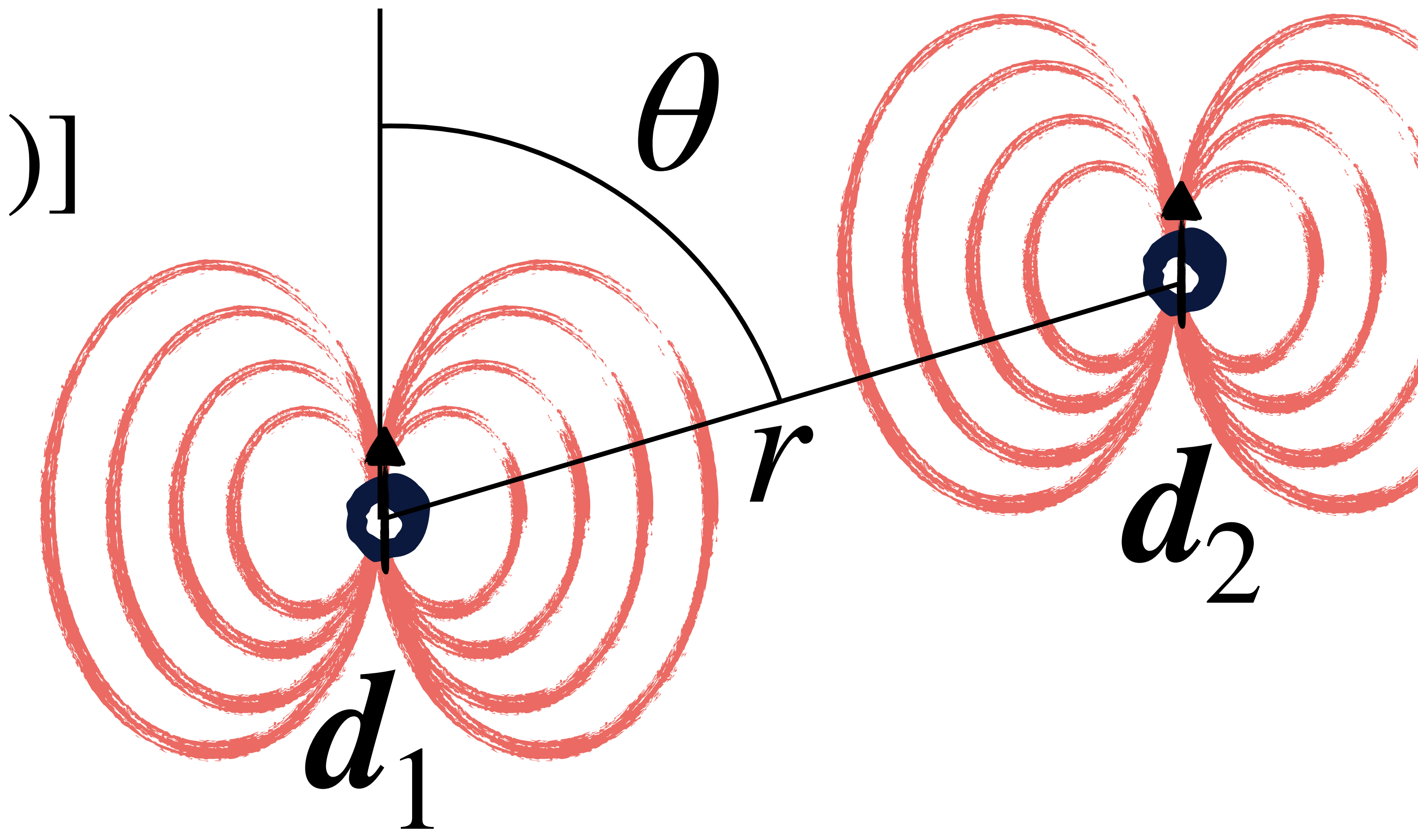

Resonant dipole dipole interaction

Two dipoles interact with light: resonant dipole-dipole interaction

$$V_{\mathrm{dd}}(r,\theta) = -\frac{3\hbar\Gamma}{4}e^{ikr}[\frac{\sin^2\theta}{kr} + (3\cos^2\theta - 1)(\frac{1}{(kr)^3} - i\frac{1}{(kr)^2})]$$

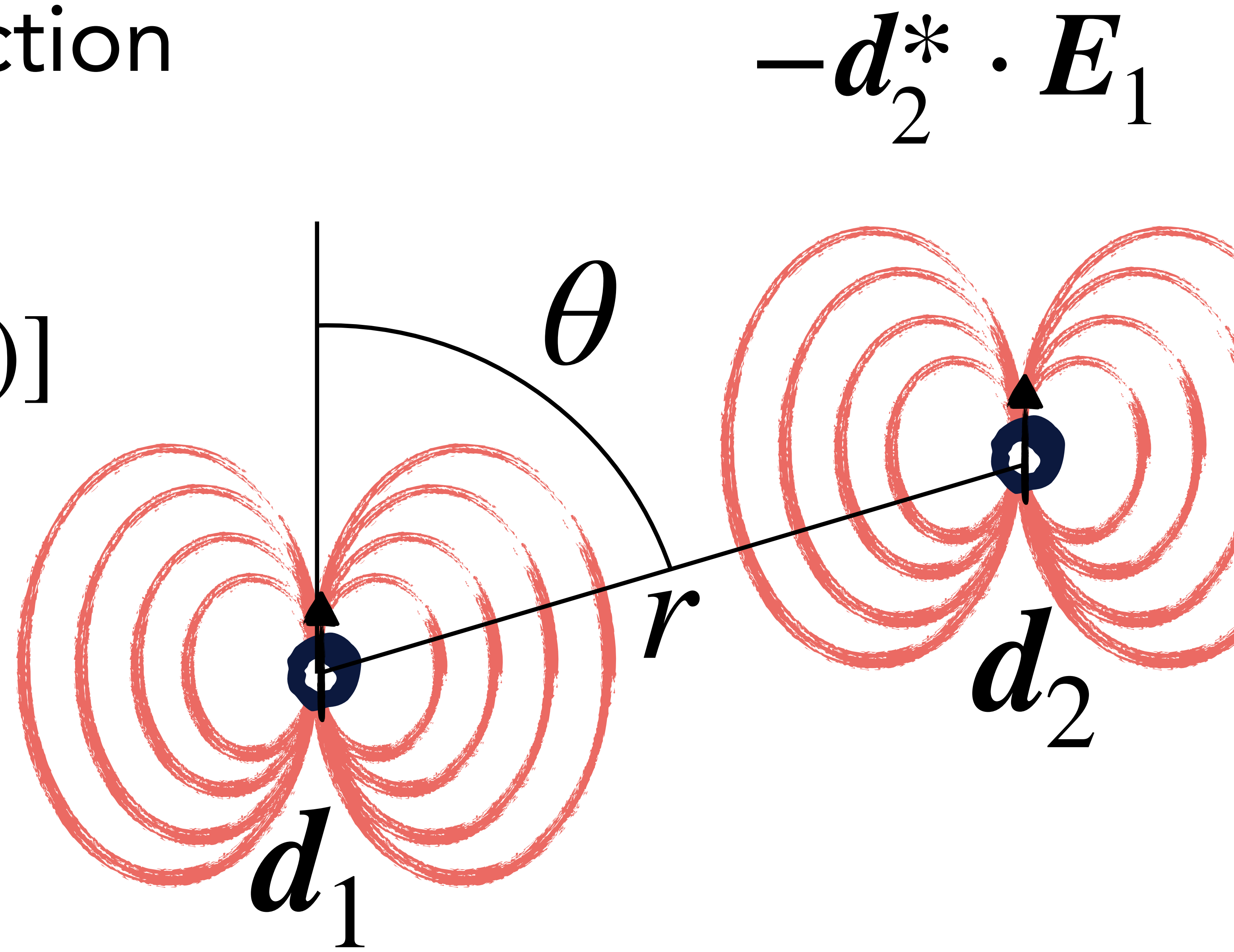

Coupled equations

$$\dot{d}_n = (i\Delta - \frac{\Gamma}{2})d_n - i\frac{\Omega}{2} + i\sum_{m\neq n} d_m^* V_{\mathrm{dd}}(\boldsymbol{r}_m - \boldsymbol{r}_n)$$

Two modes

$$\omega_\pm = \Delta \pm \mathrm{Re}[V_{\mathrm{dd}}]$$

$$\Gamma_{12} = \Gamma \pm 2\,\mathrm{Im}[V_{\mathrm{dd}}]$$

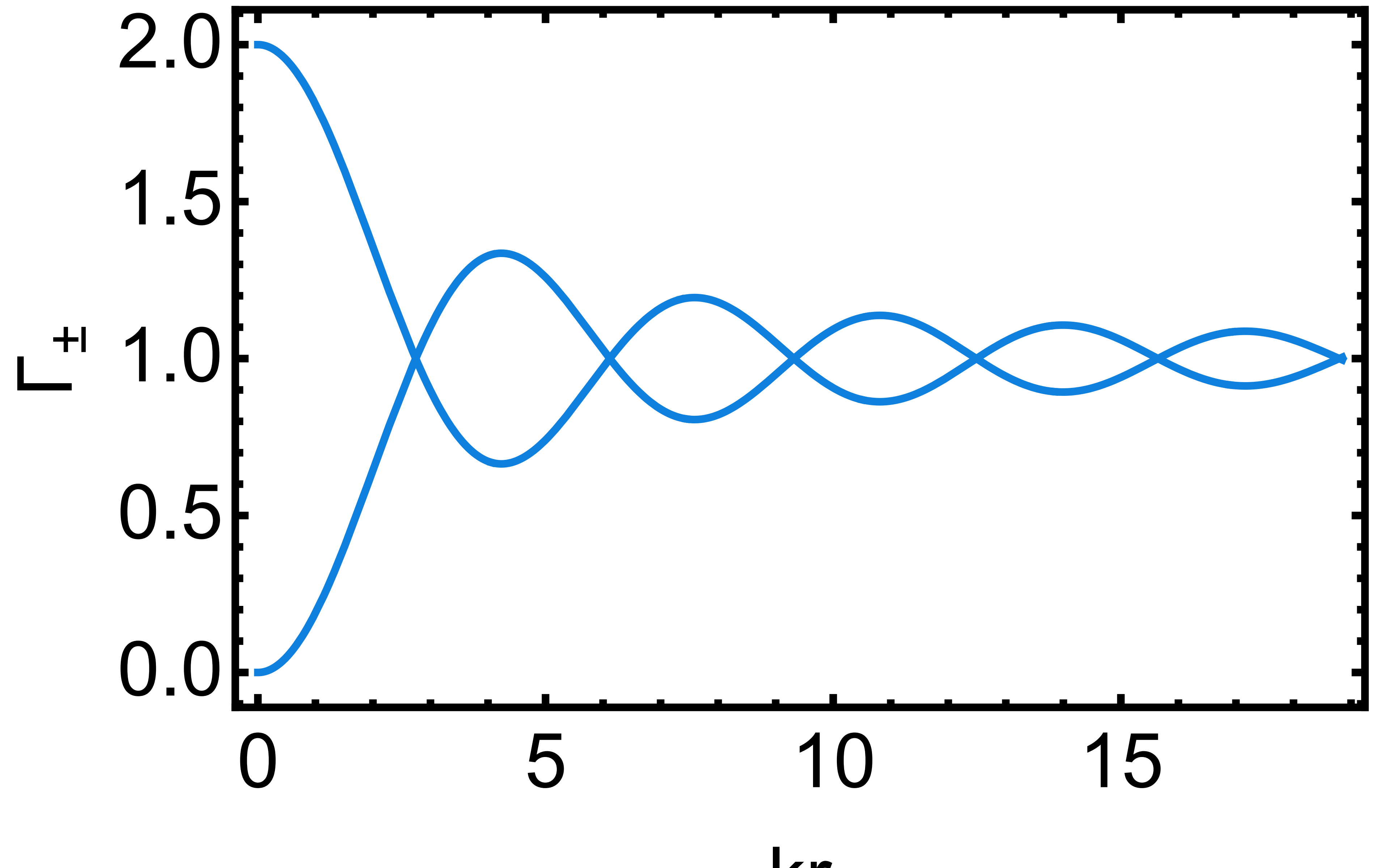

Resonant dipole dipole interaction

$\Gamma_{12} = \Gamma \pm 2\,\mathrm{Im}[V_{\mathrm{dd}}]$

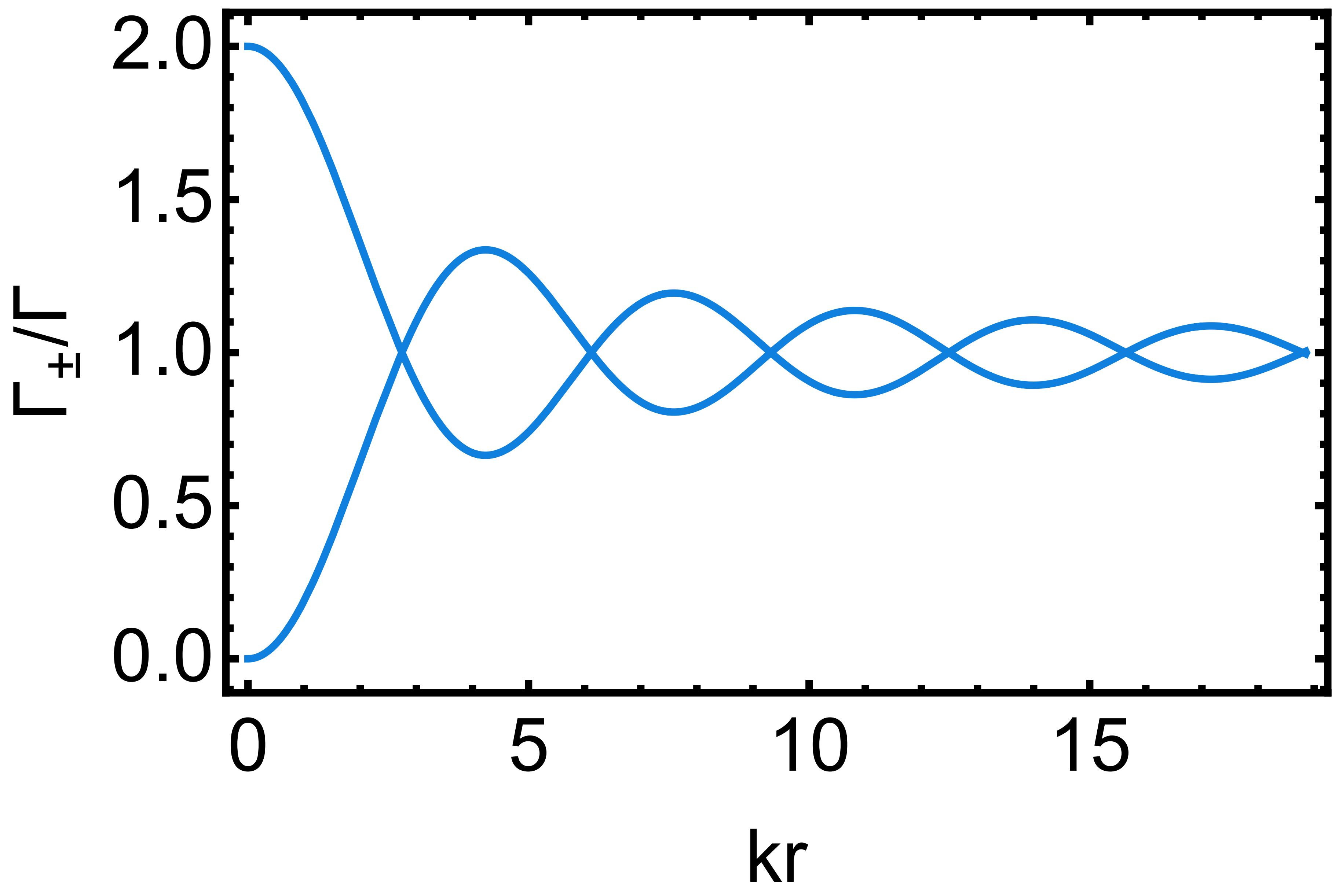

$\omega_{\pm} = \Delta \pm \mathrm{Re}[V_{\mathrm{dd}}]$

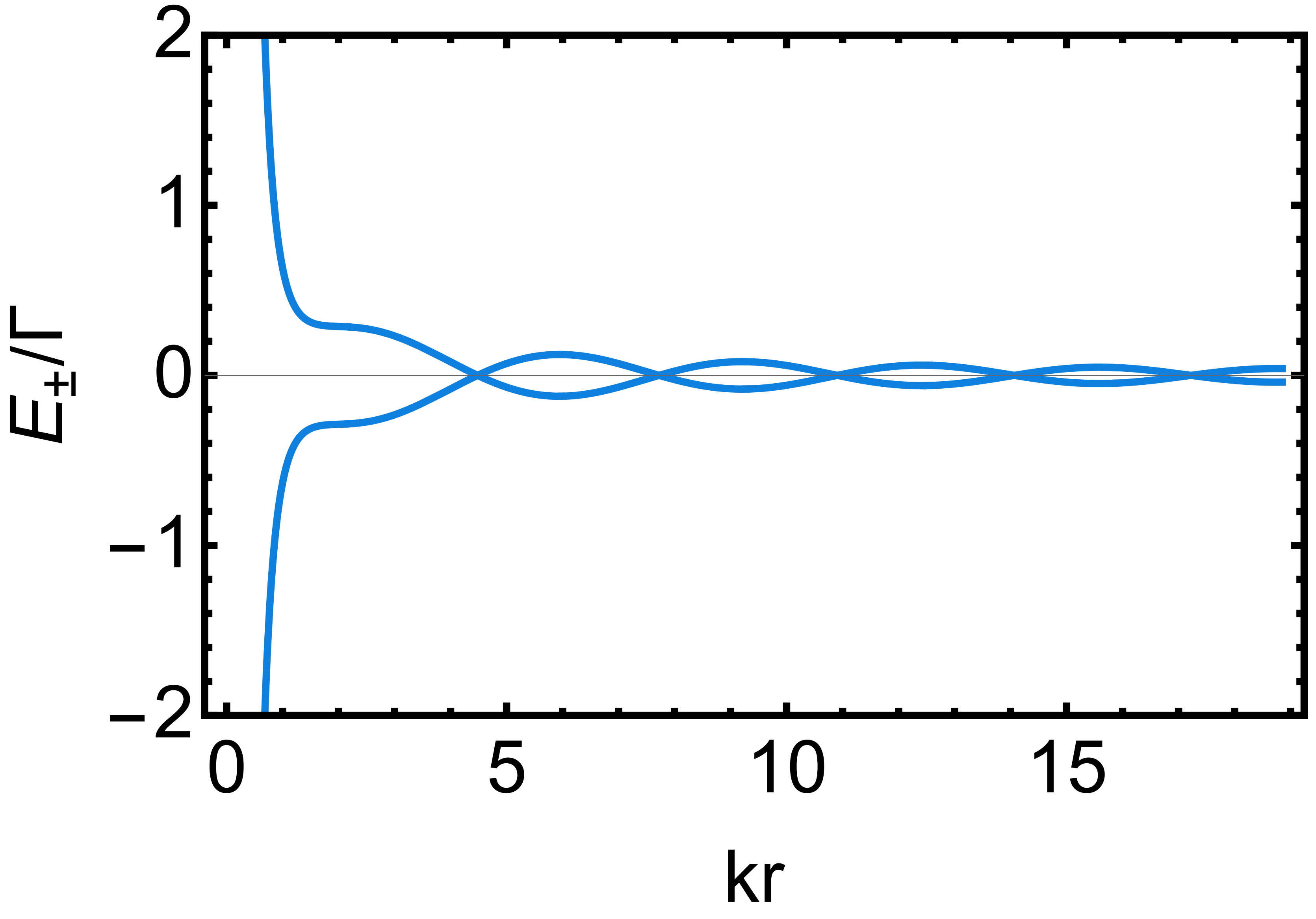

In-phase mode: constructive interference

Out-of-phase mode: destructive interference

Divergence of shift with $1/(kr)^3$

Classical case: $-\boldsymbol{d}_2^* \cdot \boldsymbol{E}_1 \sim -\boldsymbol{d}_2^* \cdot \boldsymbol{d}_1$

Quantum case: $\hat{d} = d_{\mathrm{eg}}\hat{\sigma}^-$ Flip-flop interaction $V_{\mathrm{dd}}\,\hat{\sigma}_2^+\sigma_1^-$

2 atoms and 1 cavity mode

Cavity atom coupling = g $$\hat{H} = \sum_i g(\hat{a}\,\hat{\sigma}_i^+ + \hat{a}^\dagger\,\hat{\sigma}_i^-) + \Delta \sum_i |e_i\rangle\langle e_i|$$

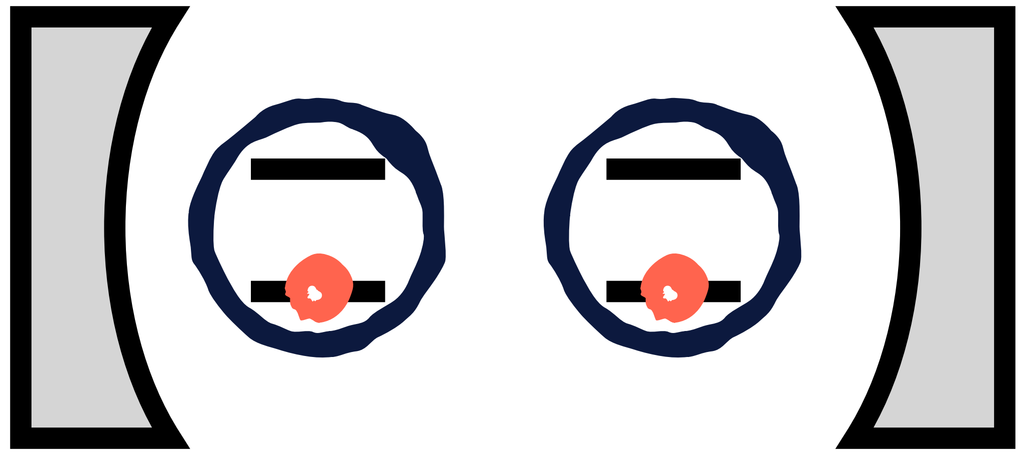

Far-detuned cavity $\Delta > g$ ($\Delta \ll \omega_0$)

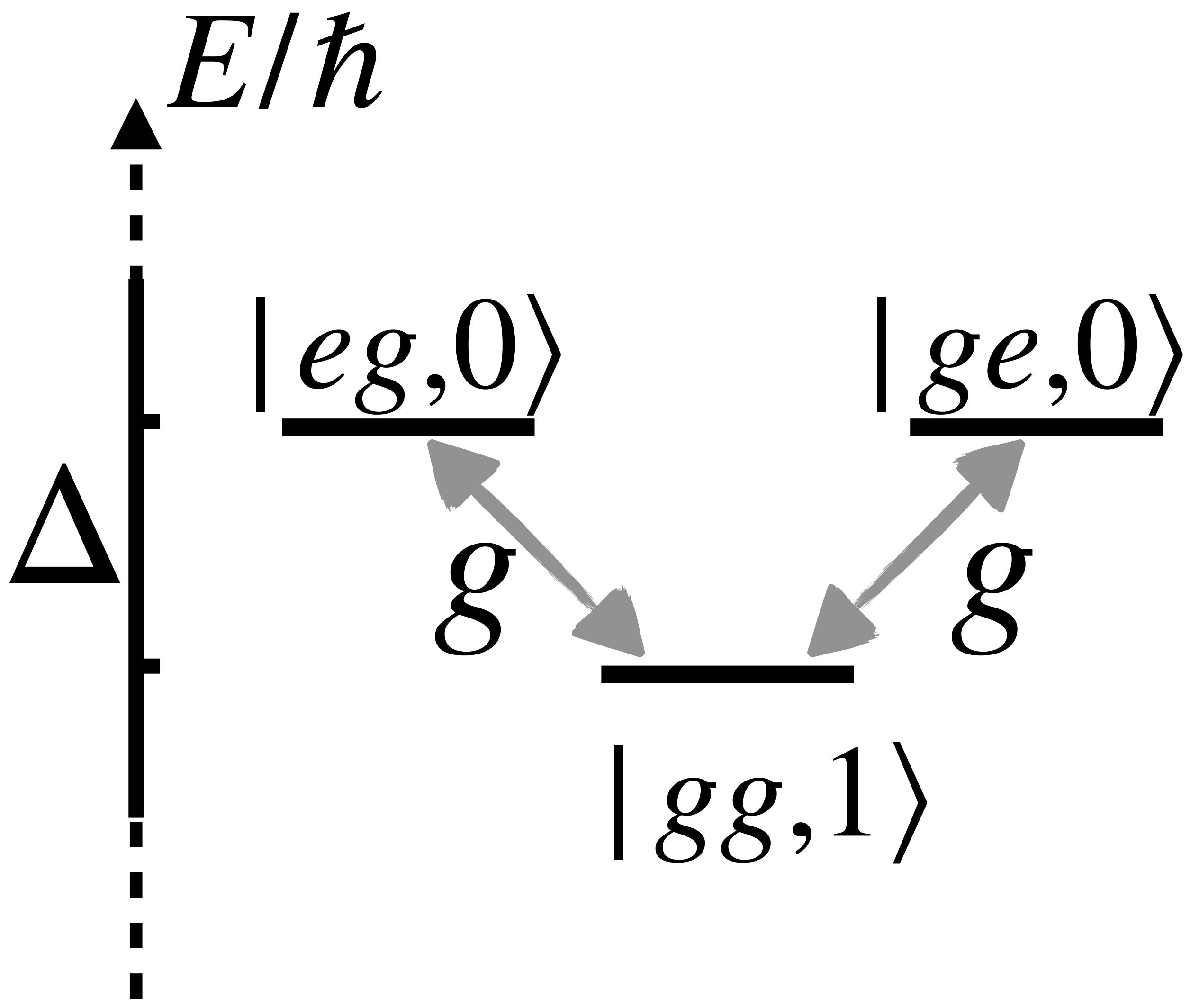

Adiabatic elimination of $|gg,1\rangle$

Flip-flop interaction : $$V_{dd} = -\frac{g^2}{\Delta}(|eg\rangle\langle ge| + (|ge\rangle\langle eg|)$$

2 atoms and 1 cavity mode

Flip-flop interaction : $$V_{dd} = -\frac{g^2}{\Delta}(|eg\rangle\langle ge| + (|ge\rangle\langle eg|)$$

Superconducting qubits and microwave cavity

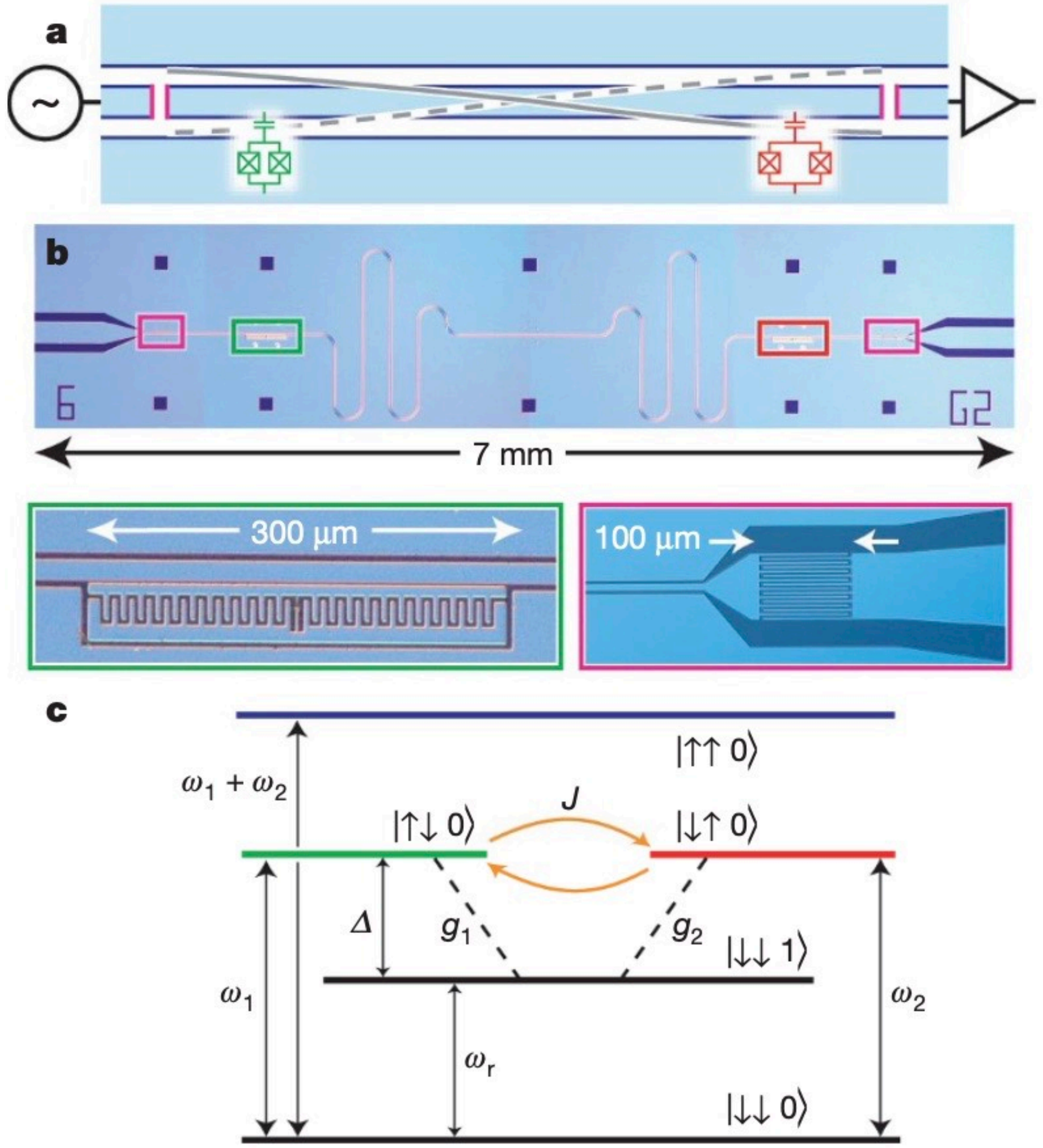

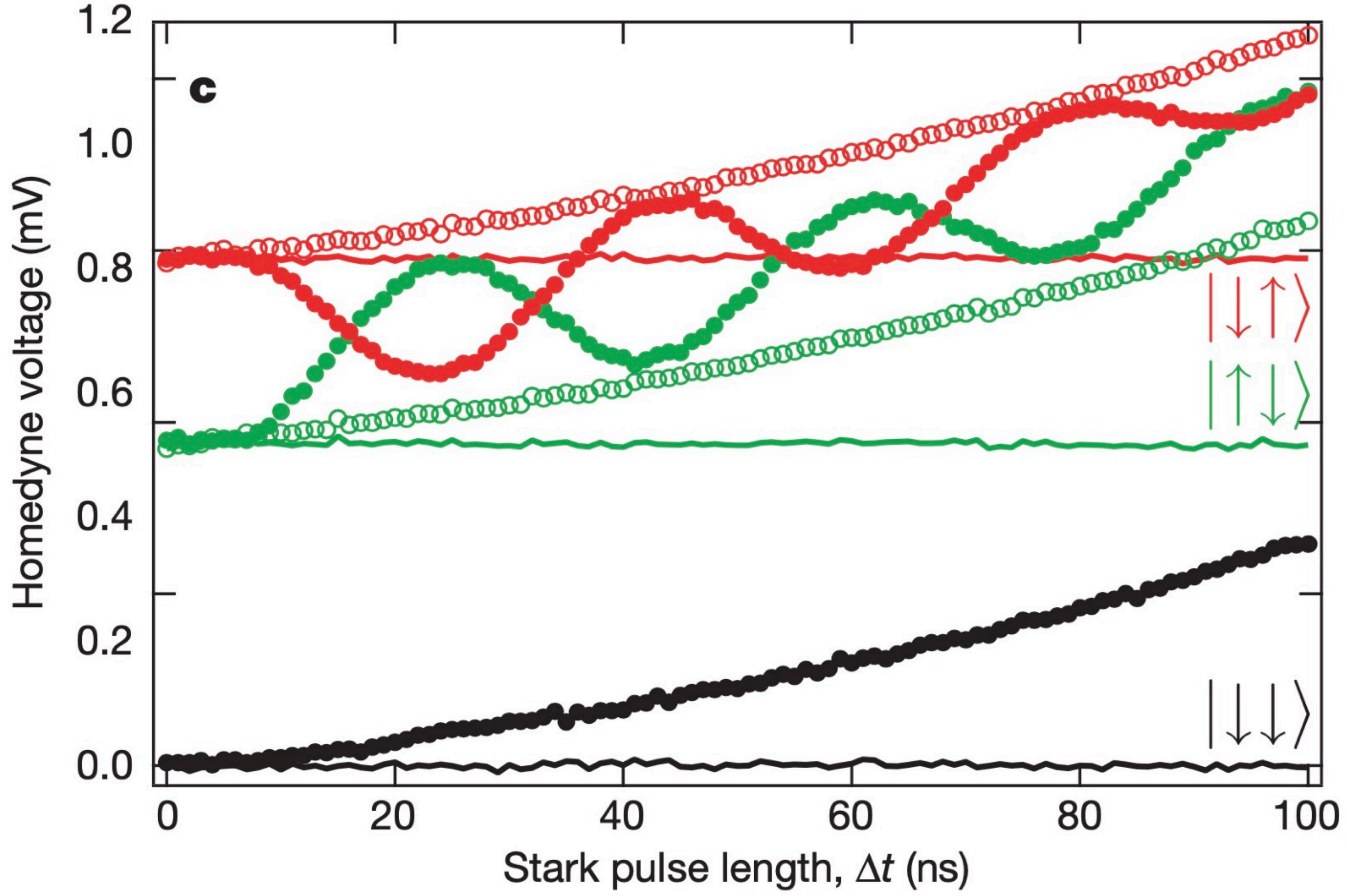

Majer *et al.*. *Nature* **449**, 443 (2007).

Original expt. with Rydberg atoms: Hagley *et al. Phys. Rev. Lett.* **79**, 1 (1997)

2-atom spontaneous emission

Collective decay

$$I(\boldsymbol{R}) = \langle \hat{E}^{-}(\boldsymbol{R}) \hat{E}^{+}(\boldsymbol{R}) \rangle$$

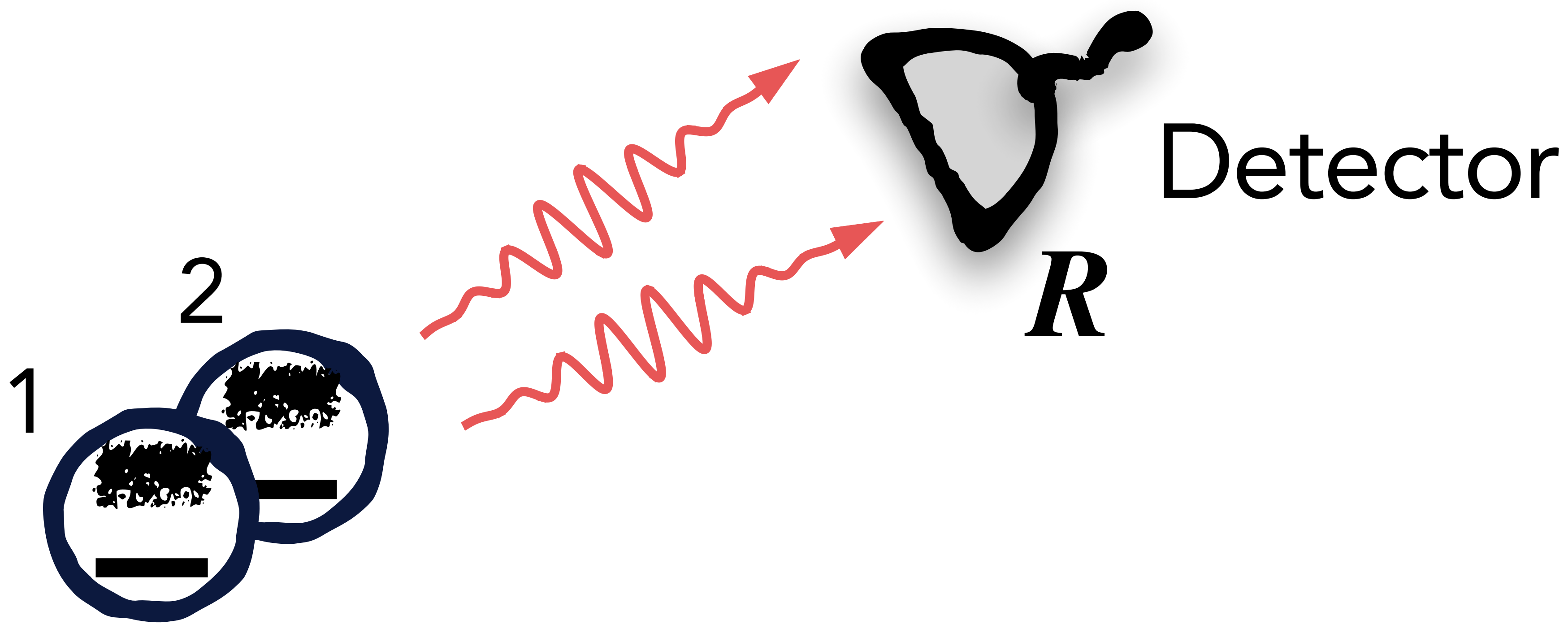

2-atom spontaneous emission

Collective decay

$$I(\boldsymbol{R}) = \langle \hat{E}^{-}(\boldsymbol{R})\hat{E}^{+}(\boldsymbol{R})\rangle$$

$$\hat{E}^{+}(\boldsymbol{R}) \propto \sum_{n} G(\boldsymbol{R}-\boldsymbol{r}_n,\omega_0)\hat{\sigma}_n^{-}$$

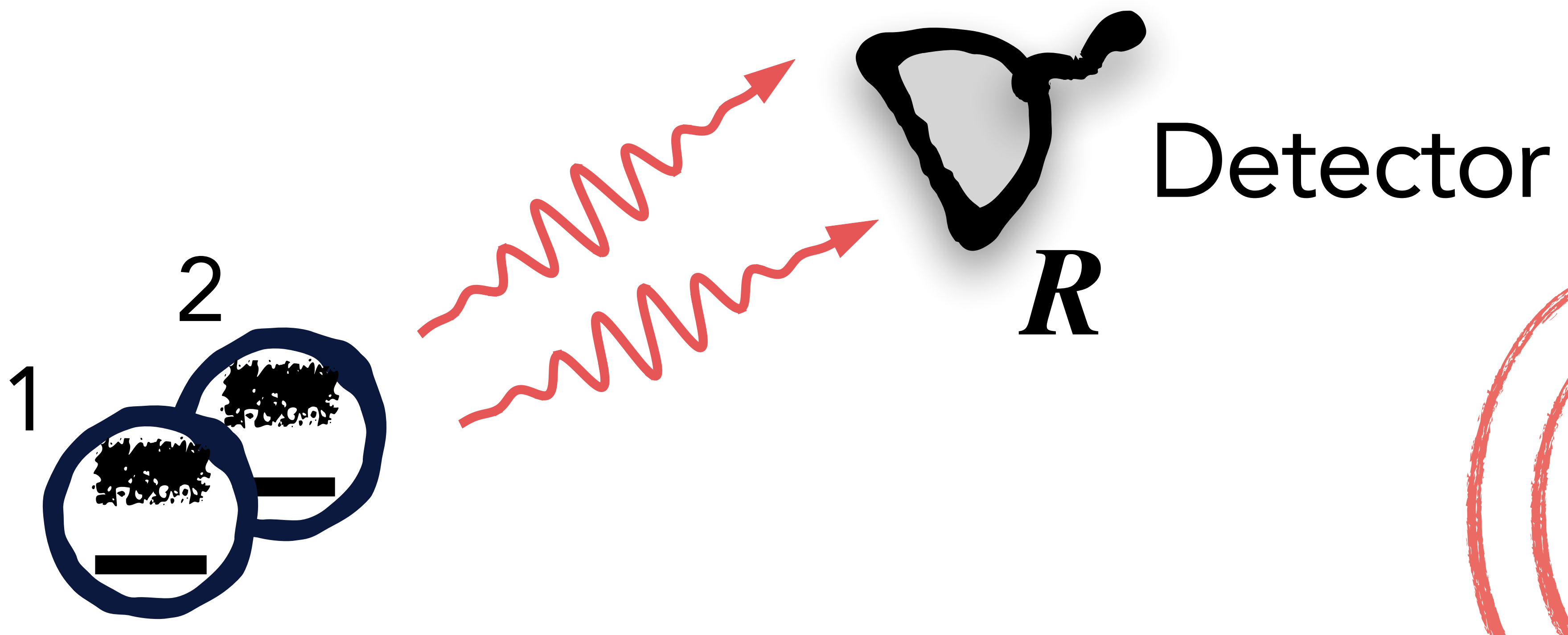

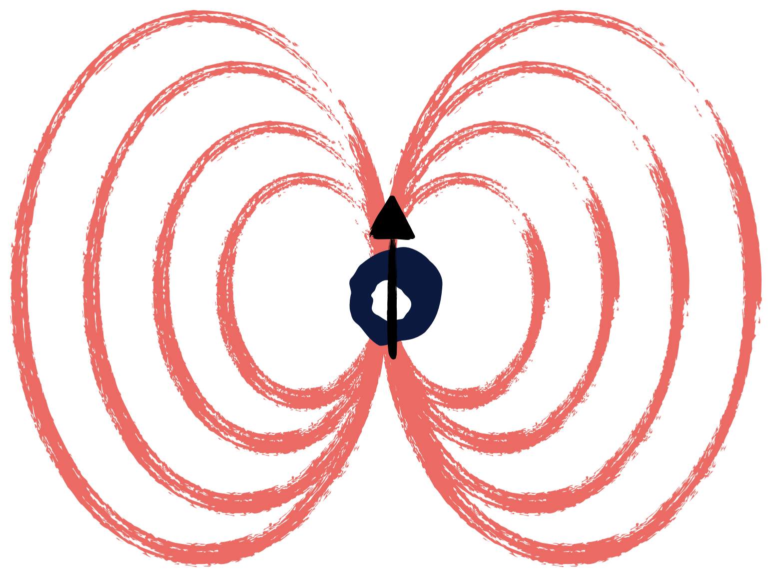

$$G(\boldsymbol{x},\omega_0) \sim \frac{e^{ik_0 x}}{4\pi\, k_0 x} \qquad \hat{\sigma}_n^{-} = |\, g_n \rangle\langle\, e_n \,|$$

Far field Green's function

2-atom spontaneous emission

Collective decay

$$I(\boldsymbol{R}) = \langle \hat{E}^-(\boldsymbol{R})\hat{E}^+(\boldsymbol{R})\rangle$$

$$\hat{E}^+(\boldsymbol{R}) \propto \sum_n G(\boldsymbol{R} - \boldsymbol{r}_n, \omega_0)\hat{\sigma}_n^-$$

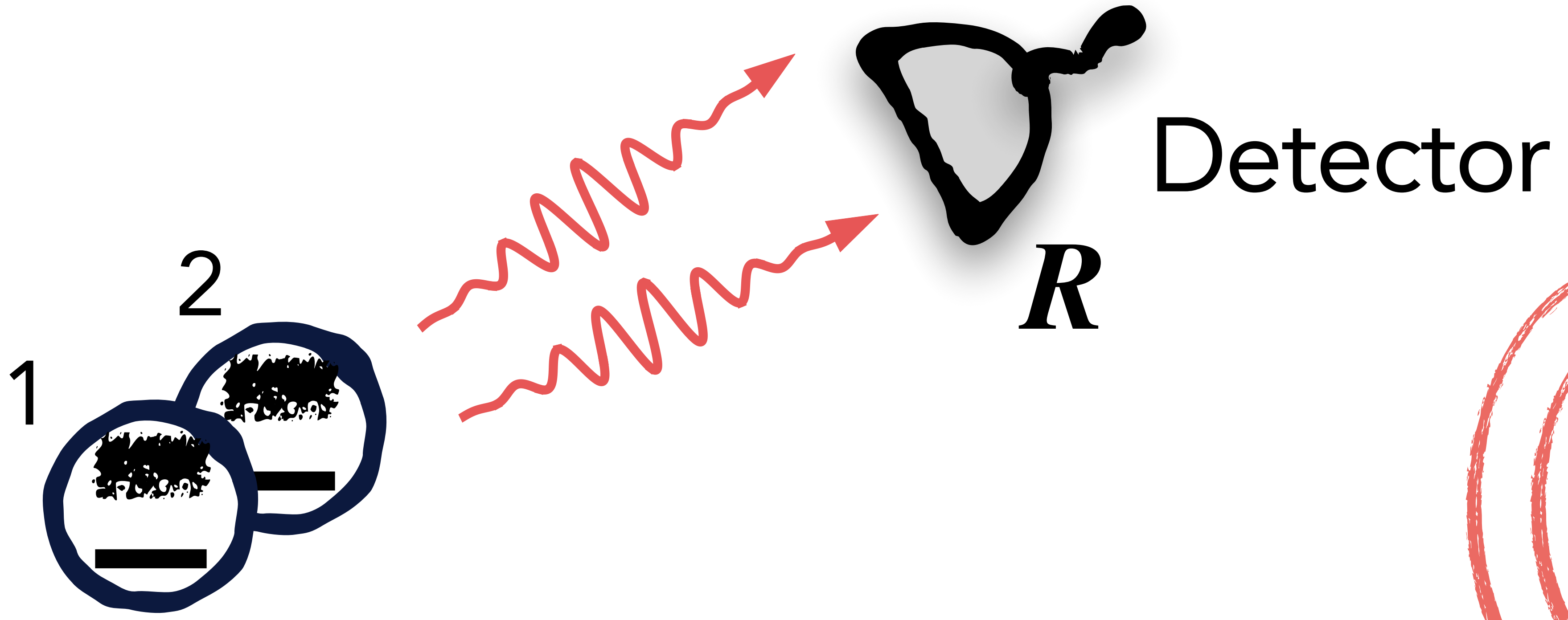

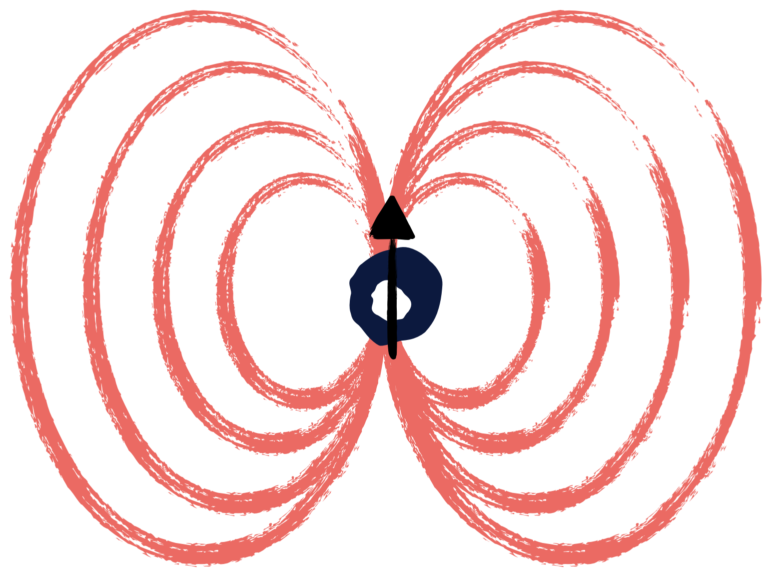

$$G(\boldsymbol{x}, \omega_0) \sim \frac{e^{ik_0 x}}{4\pi\, k_0 x}$$

$$\hat{\sigma}_n^- = |\, g_n \rangle\langle\, e_n |$$

Far field Green's function

Far field intensity in direction $\boldsymbol{k} = k_0\hat{k}$

$$I(\boldsymbol{k}) = I_1(\boldsymbol{k})\left[\langle \hat{e}_1\rangle + \langle \hat{e}_2\rangle + e^{i\boldsymbol{k}\cdot(\boldsymbol{r}_2-\boldsymbol{r}_1)}\langle \hat{\sigma}_2^+\hat{\sigma}_1^-\rangle + \mathrm{cc}\right]$$

2-atom spontaneous emission

$$I(\boldsymbol{k}) = I_1(\boldsymbol{k})\left[\langle \hat{e}_1 \rangle + \langle \hat{e}_2 \rangle + e^{i\boldsymbol{k}\cdot(\boldsymbol{r}_2 - \boldsymbol{r}_1)} \langle \hat{\sigma}_2^+ \hat{\sigma}_1^- \rangle + \mathrm{cc}\right]$$

2-atom spontaneous emission

$$I(\boldsymbol{k}) = I_1(\boldsymbol{k})\left[\langle \hat{e}_1 \rangle + \langle \hat{e}_2 \rangle + e^{i\boldsymbol{k}\cdot(\boldsymbol{r}_2-\boldsymbol{r}_1)}\langle \hat{\sigma}_2^+ \hat{\sigma}_1^- \rangle + \mathrm{cc}\right]$$

2 excitations: $|ee\rangle$ $\quad I(\boldsymbol{k}) = 2I_1(\boldsymbol{k})$

$$\Gamma_{ee} = 2\,\Gamma_0$$

2-atom spontaneous emission

$$I(\boldsymbol{k}) = I_1(\boldsymbol{k})\left[\langle \hat{e}_1 \rangle + \langle \hat{e}_2 \rangle + e^{i\boldsymbol{k}\cdot(\boldsymbol{r}_2-\boldsymbol{r}_1)}\langle \hat{\sigma}_2^+ \hat{\sigma}_1^- \rangle + \mathrm{cc}\right]$$

2 excitations: $|ee\rangle$ $\quad I(\boldsymbol{k}) = 2I_1(\boldsymbol{k})$

$$\Gamma_{ee} = 2\,\Gamma_0$$

1 excitation: $|\pm\rangle = (|eg\rangle \pm |ge\rangle)/\sqrt{2})$ $\quad \langle \pm | \hat{\sigma}_2^+ \hat{\sigma}_1^- | \pm \rangle = \pm \dfrac{1}{2}$

$$I_\pm(\boldsymbol{k}) = I_1(\boldsymbol{k})\left[1 \pm \cos(\boldsymbol{k}\cdot(\boldsymbol{r}_2 - \boldsymbol{r}_1))\right]$$

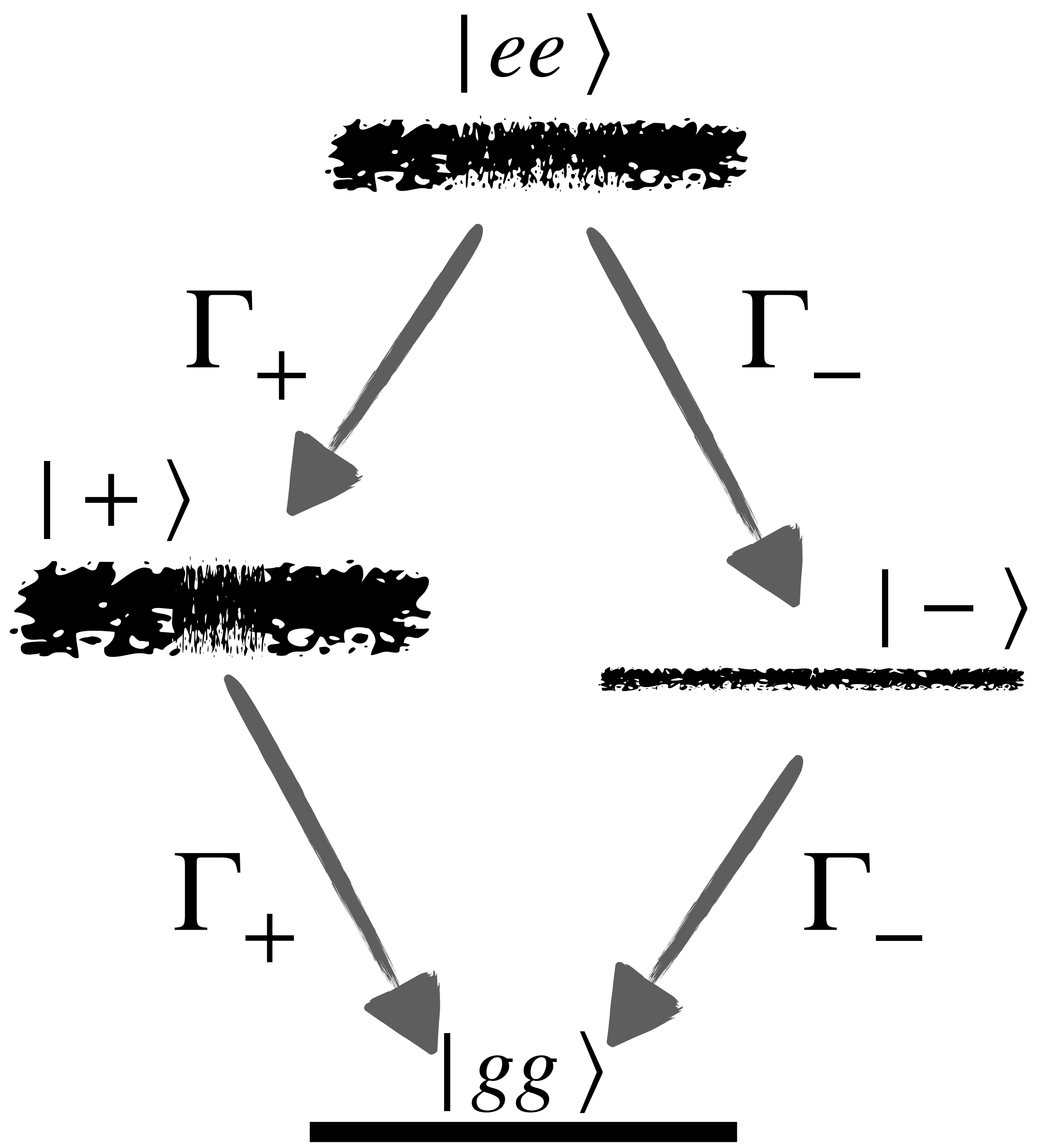

Integrate: $\quad \Gamma_\pm = \Gamma_0(1 + 2\mathrm{Im}V_{dd}(\boldsymbol{r}))$

Faraway atoms $\quad \Gamma_\pm \sim \Gamma_0(1 \pm \dfrac{3}{2}\sin(k_0 r)/k_0 r)$

2-atom spontaneous emission

$$\Gamma_{\pm} \sim \Gamma_0 \left(1 \pm \frac{3}{2} \frac{\sin(k_0 r)}{k_0 r}\right)$$

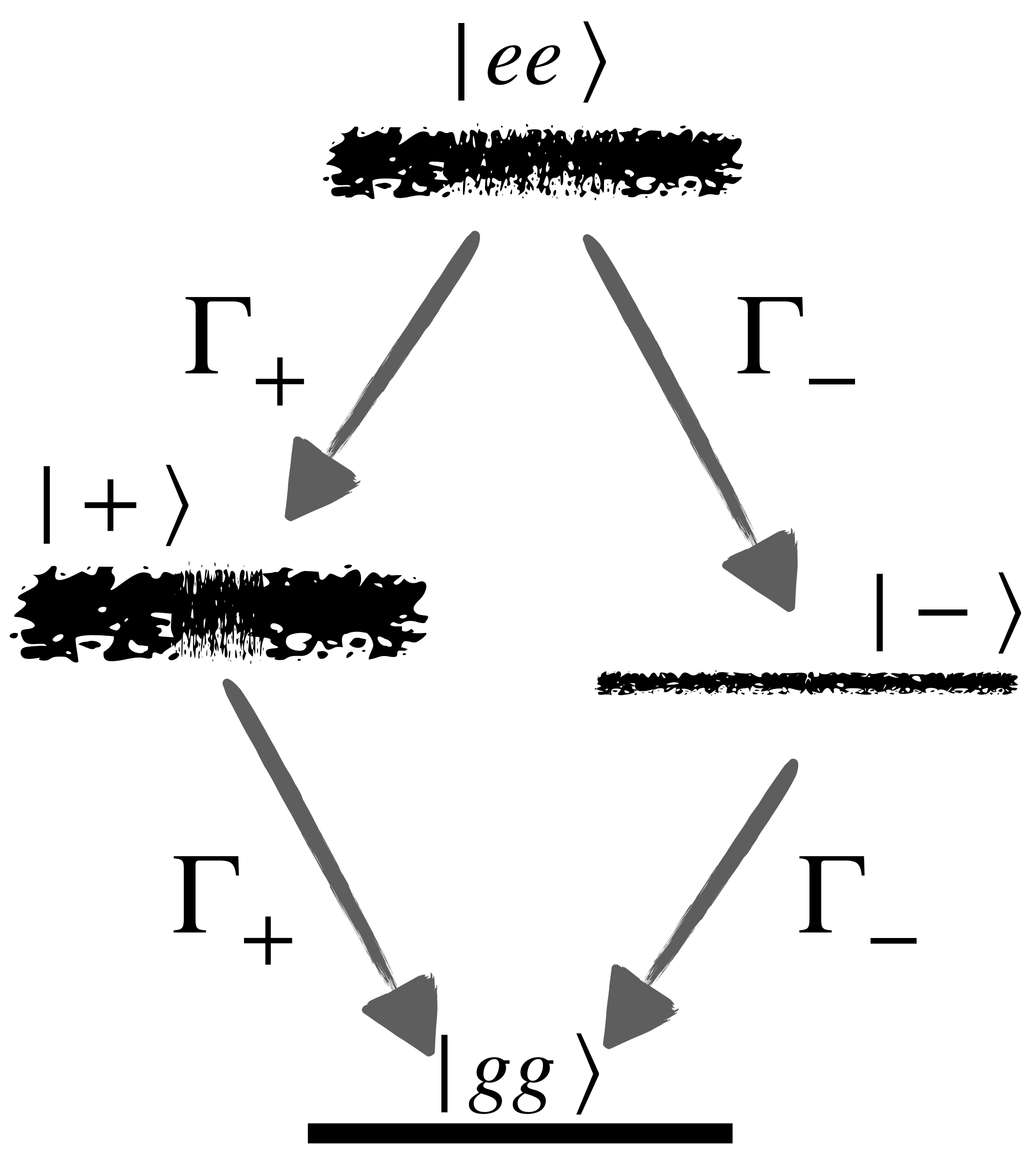

2-atom spontaneous emission

2 ions at variable distance

DeVoe & Brewer *Phys Rev Lett* **76**, 2049 (1996).

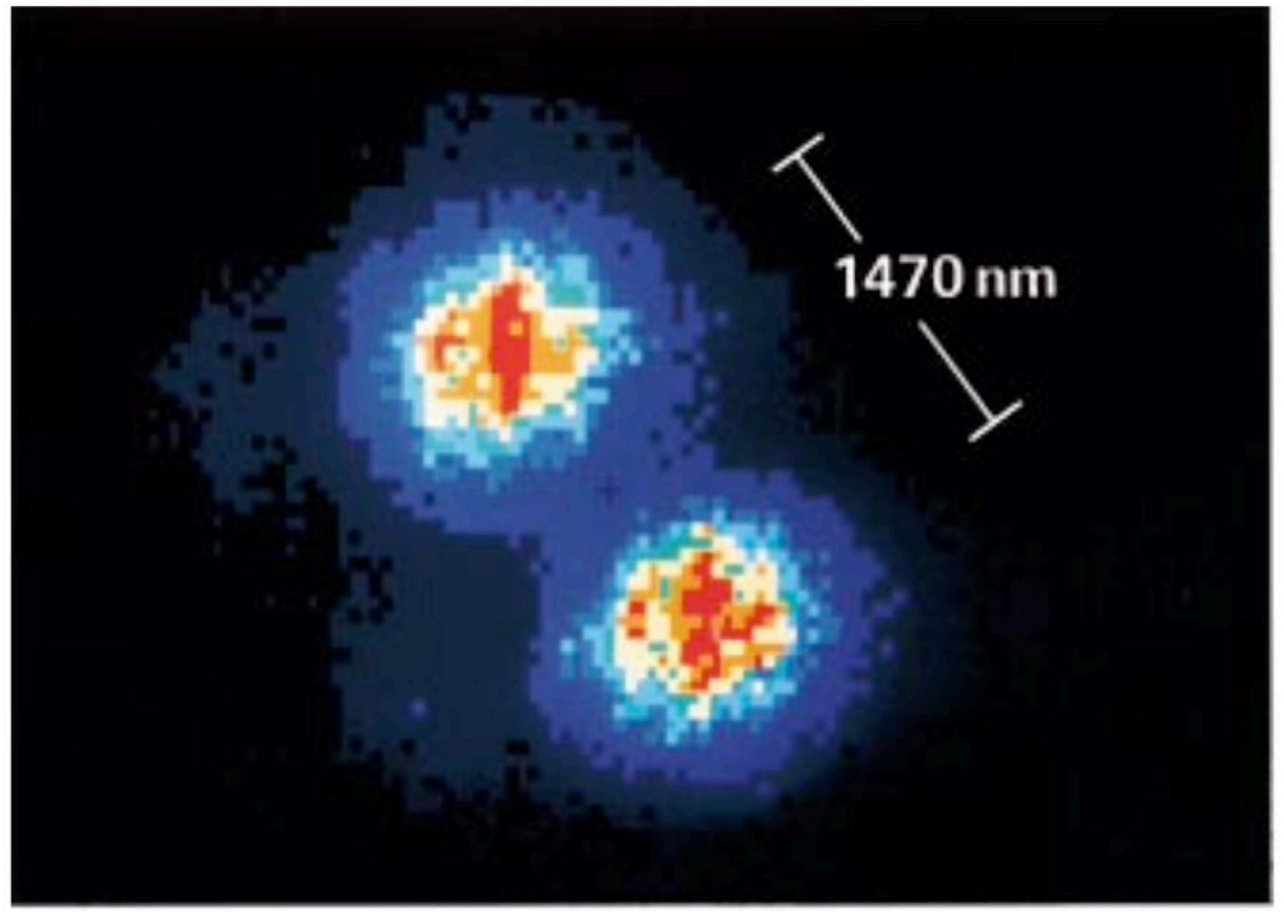

FIG. 4. (color) Diffraction-limited image of a two-ion crystal with $R = 1470$ nm. This determines the orientation of the interatomic vector $\vec{R}$ enabling a no-free-parameter fit.

$$\Gamma_{\pm} \sim \Gamma_0 \left(1 \pm \frac{3}{2}\frac{\sin(k_0 r)}{k_0 r}\right)$$

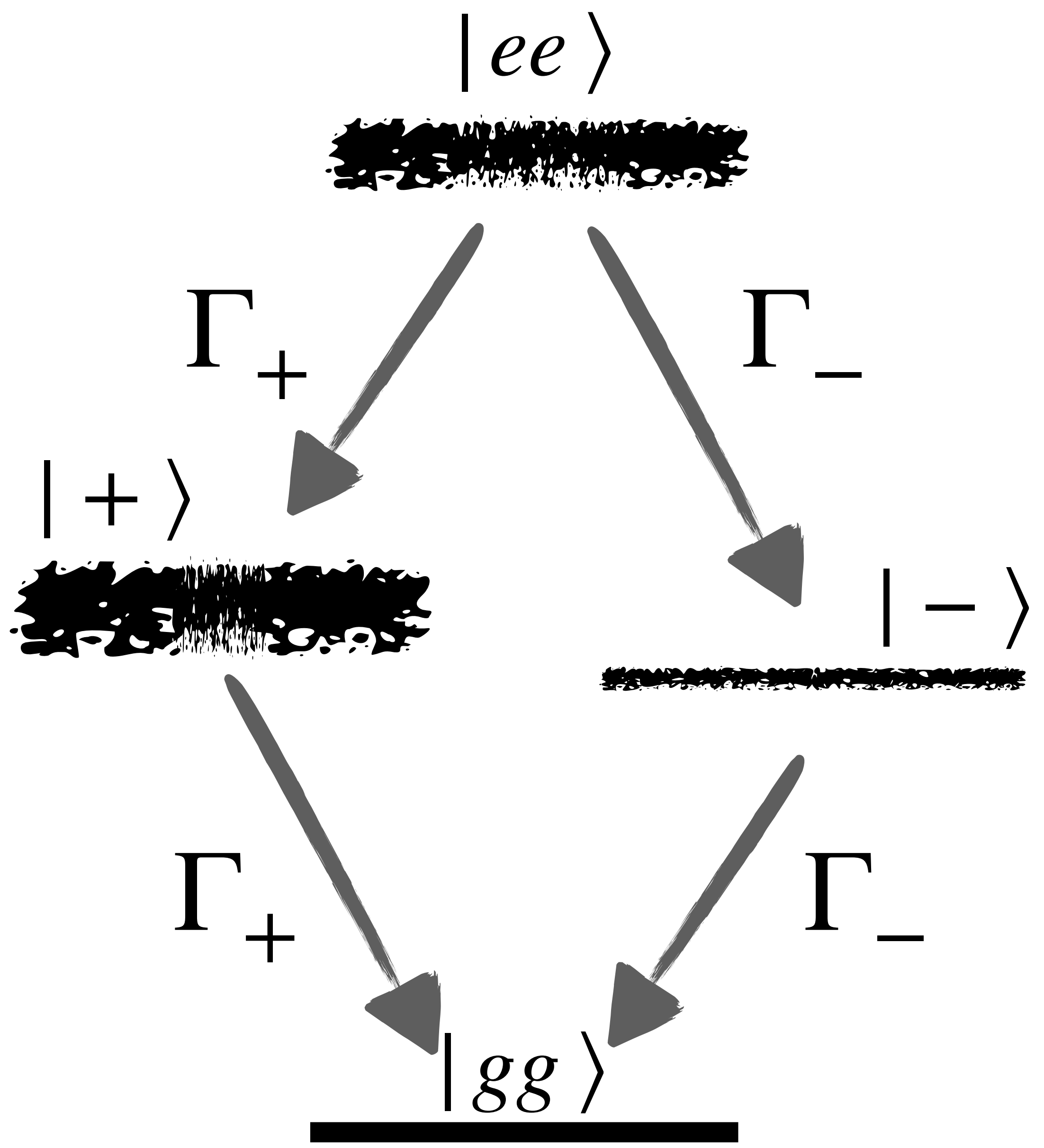

2-atom spontaneous emission

2 ions at variable distance

DeVoe & Brewer *Phys Rev Lett* **76**, 2049 (1996).

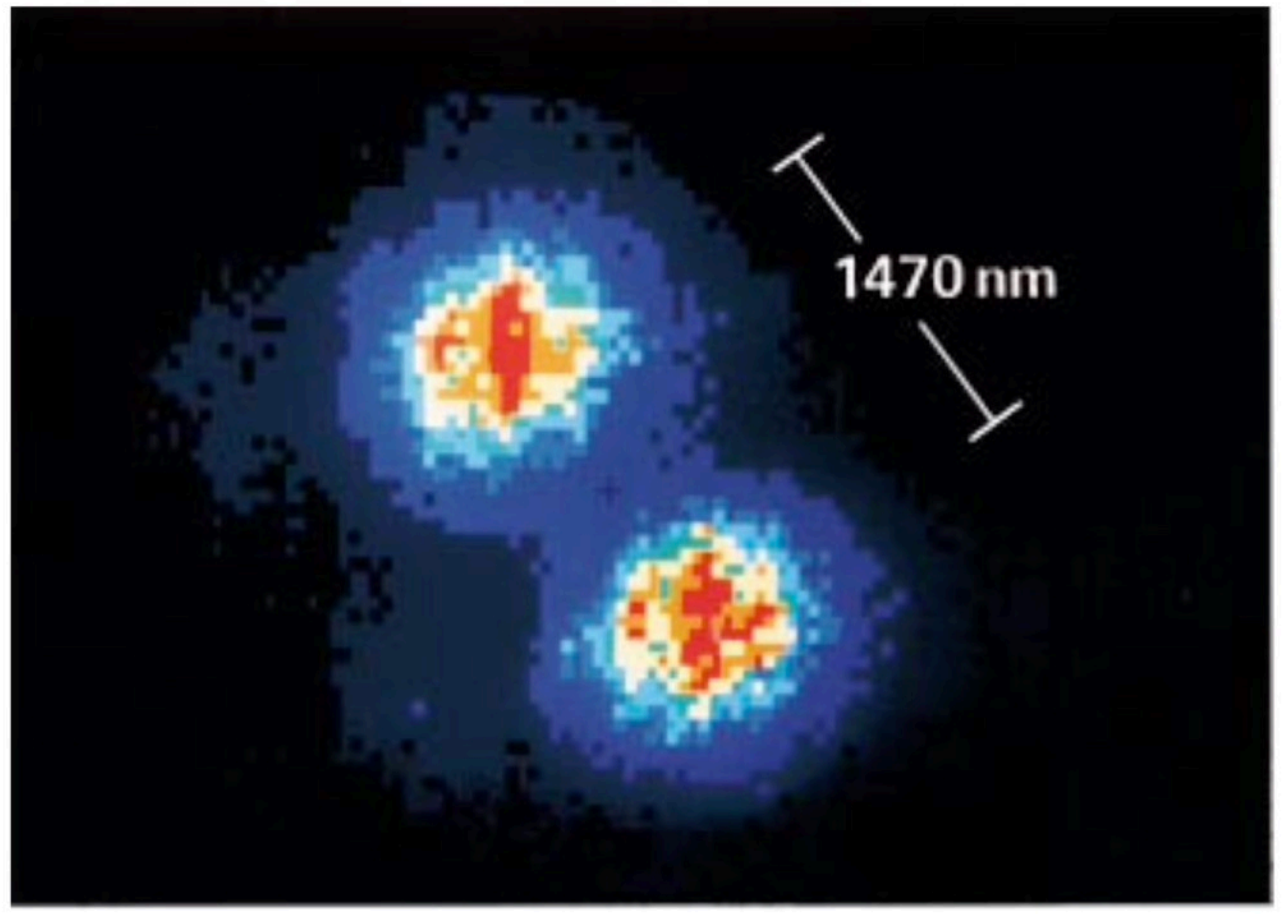

FIG. 4. (color) Diffraction-limited image of a two-ion crystal with $R = 1470$ nm. This determines the orientation of the interatomic vector $\vec{R}$ enabling a no-free-parameter fit.

$$\Gamma_{\pm} \sim \Gamma_0 \left(1 \pm \frac{3}{2} \frac{\sin(k_0 r)}{k_0 r}\right)$$

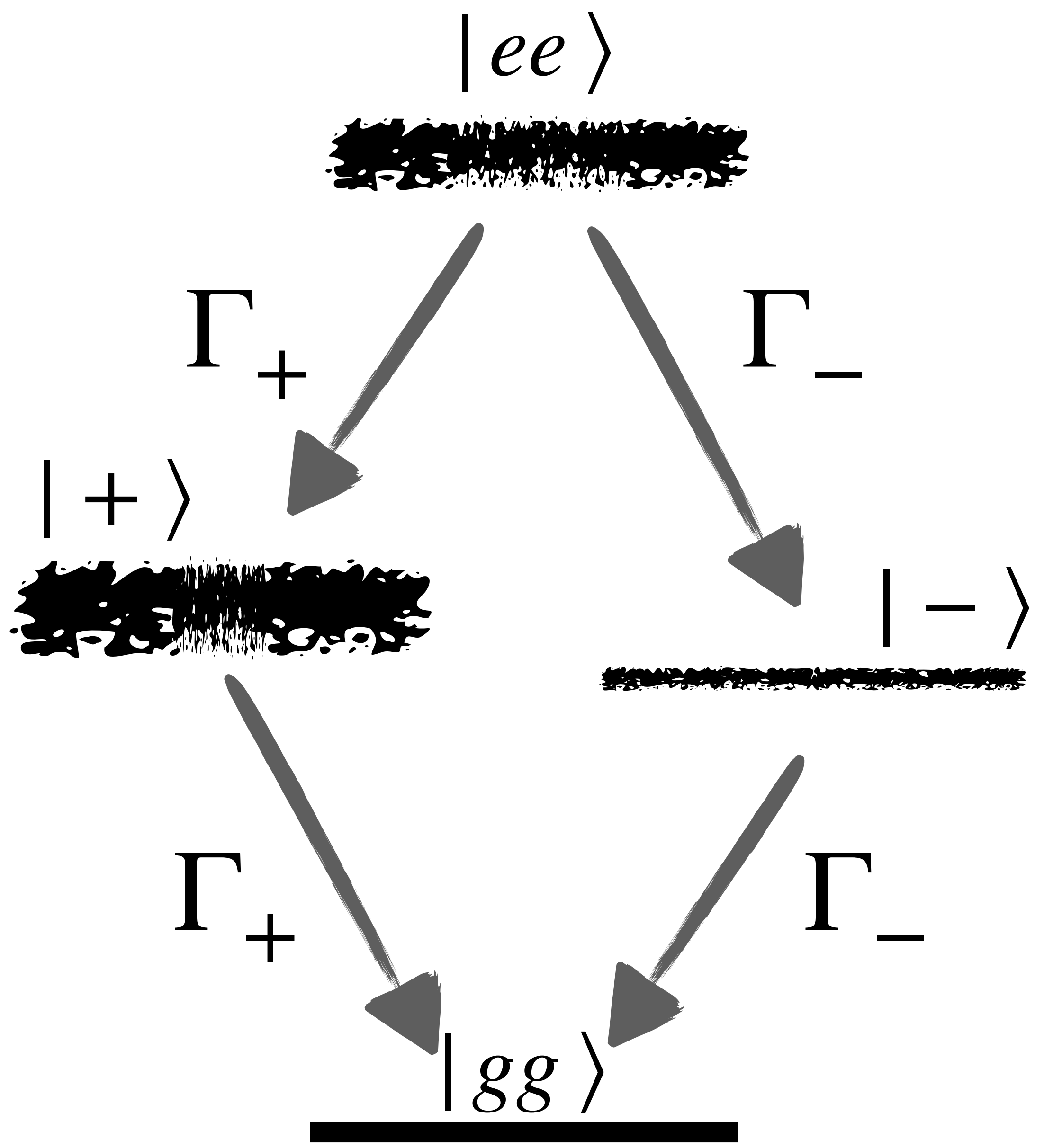

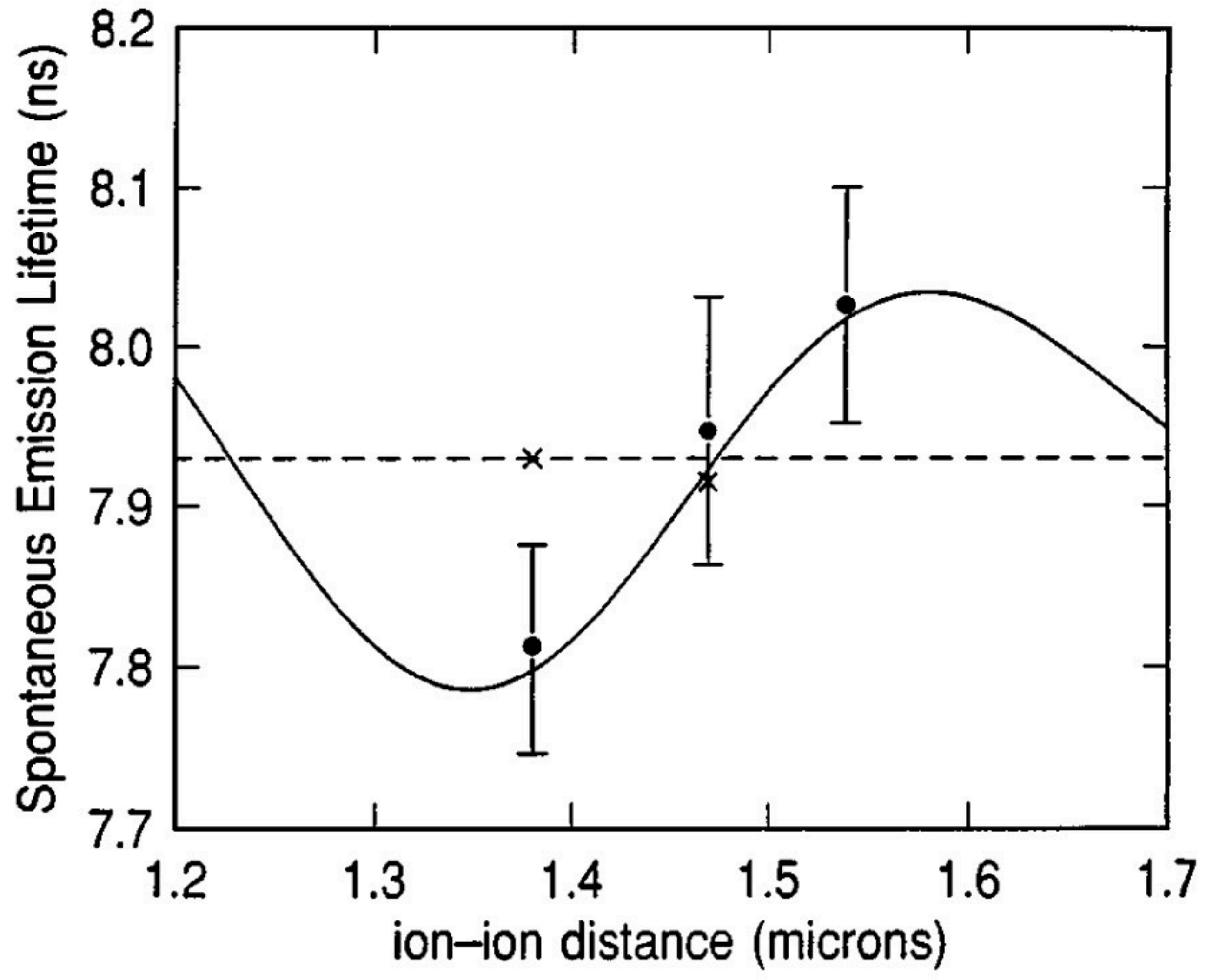

FIG. 6. Comparison of theory to experimental points at 1380, 1470, and 1540 nm (see text). The ion-ion distance is independently known by measuring the secular oscillation frequency of one ion. The lifetime is calibrated by comparison to 7.930 ± 0.03 ns measured for a single ion in the same apparatus. Note the polarization sensitivity (crosses, with error bars omitted for clarity).

Master equation

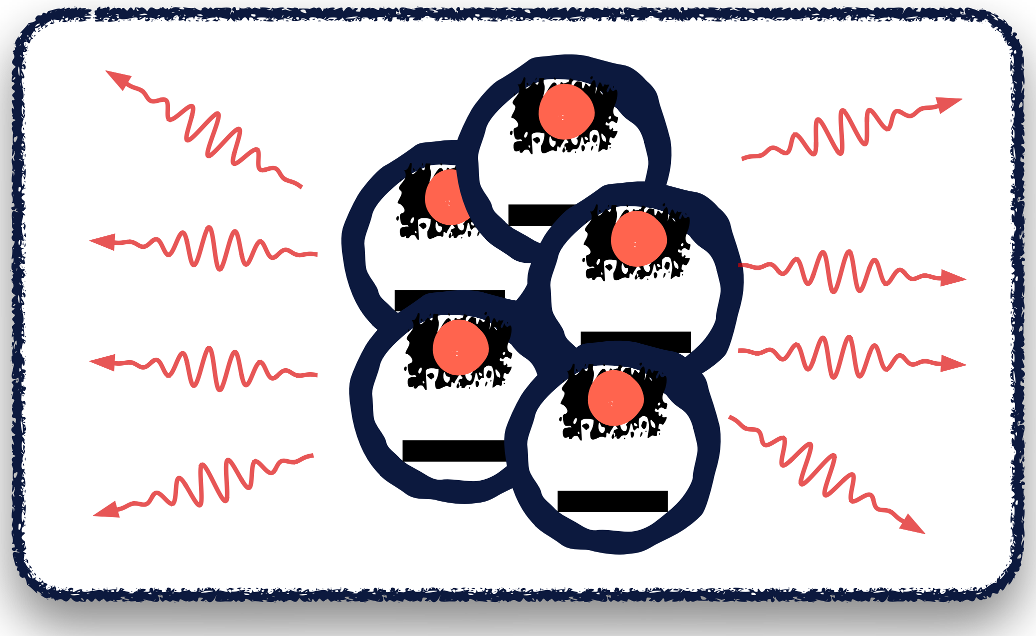

$$\dot{\rho} = -\frac{i}{\hbar}\left[H, \rho\right] + L(\rho)$$

$$H = H_0 + \sum_{nm} V_{nm} \hat{\sigma}_n^+ \hat{\sigma}_m^-$$

$$V_{nm} = \mathrm{Re}[V_{\mathrm{dd}}(\boldsymbol{r}_{nm})]$$

$$L(\rho) = \frac{1}{2}\sum_{nm} \Gamma_{nm}(2\hat{\sigma}_m^- \rho \hat{\sigma}_n^+ - \rho \hat{\sigma}_n^+ \hat{\sigma}_m^- - \hat{\sigma}_n^+ \hat{\sigma}_m^- \rho)$$

$$\Gamma_{nm} = 2\,\mathrm{Im}[V_{\mathrm{dd}}(\boldsymbol{r}_{nm})]$$

Equation valid under the Born-Markov approximation

Ignore correlations between field and atoms (free space)

Ignore propagation time $L/c \ll 1/\Gamma$ typical evolution time

Emission from N weakly excited atoms

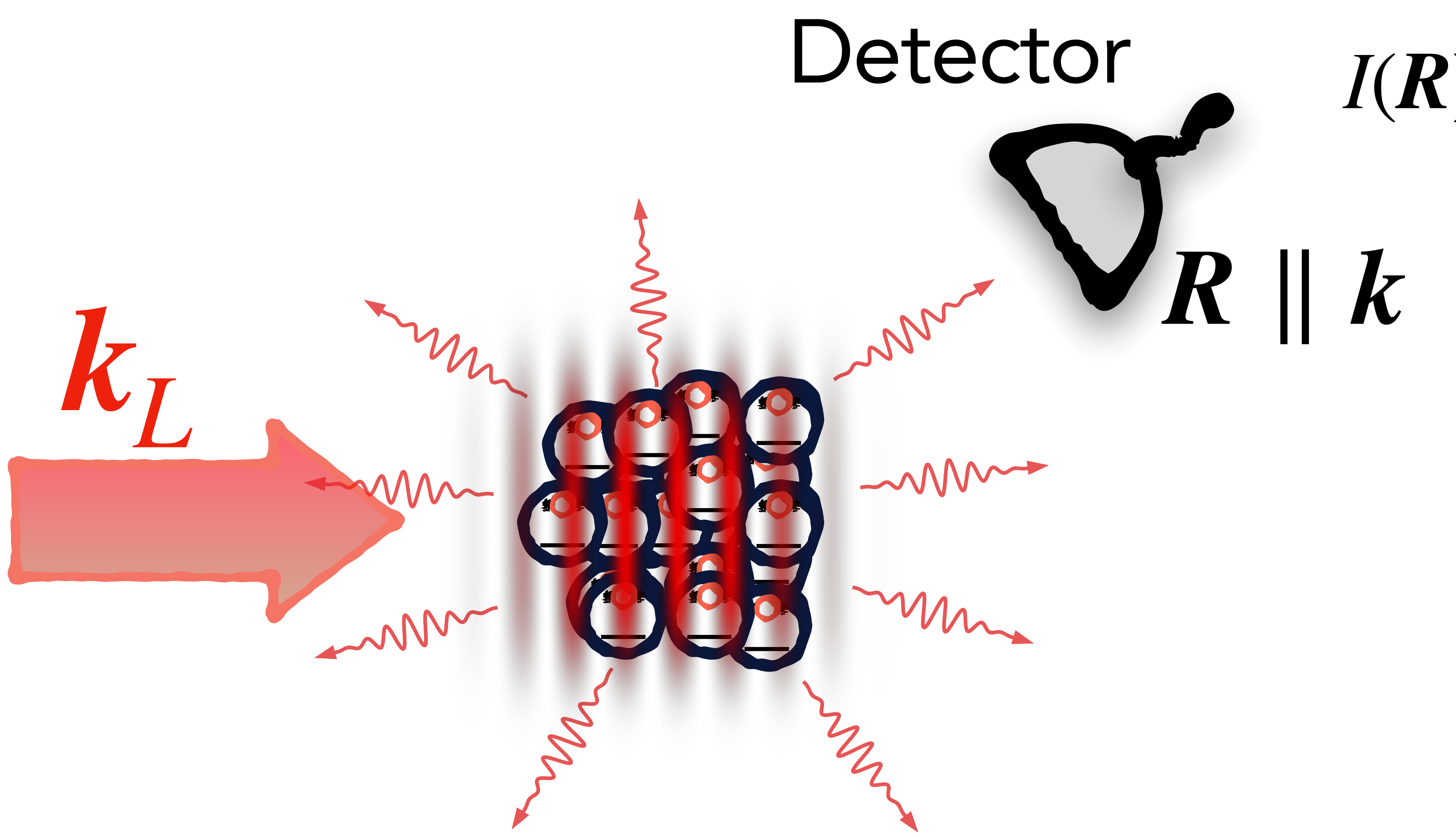

$$I(\boldsymbol{R}) = \langle \hat{E}^{-}(\boldsymbol{R})\hat{E}^{+}(\boldsymbol{R})\rangle \qquad \hat{E}^{+}(\boldsymbol{R}) \propto \sum_{n=1}^{N} G(\boldsymbol{R} - \boldsymbol{r}_n, \omega_0)\hat{\sigma}_n^{-}$$

$$I_N(\boldsymbol{k}) = I_1(\boldsymbol{k}) \sum_{n} \left[\langle \hat{e}_n \rangle + \sum_{m \neq n} e^{i\boldsymbol{k}\cdot(\boldsymbol{r}_m - \boldsymbol{r}_n)} \langle \hat{\sigma}_m^{+} \hat{\sigma}_n^{-} \rangle \right]$$

Emission from N weakly excited atoms

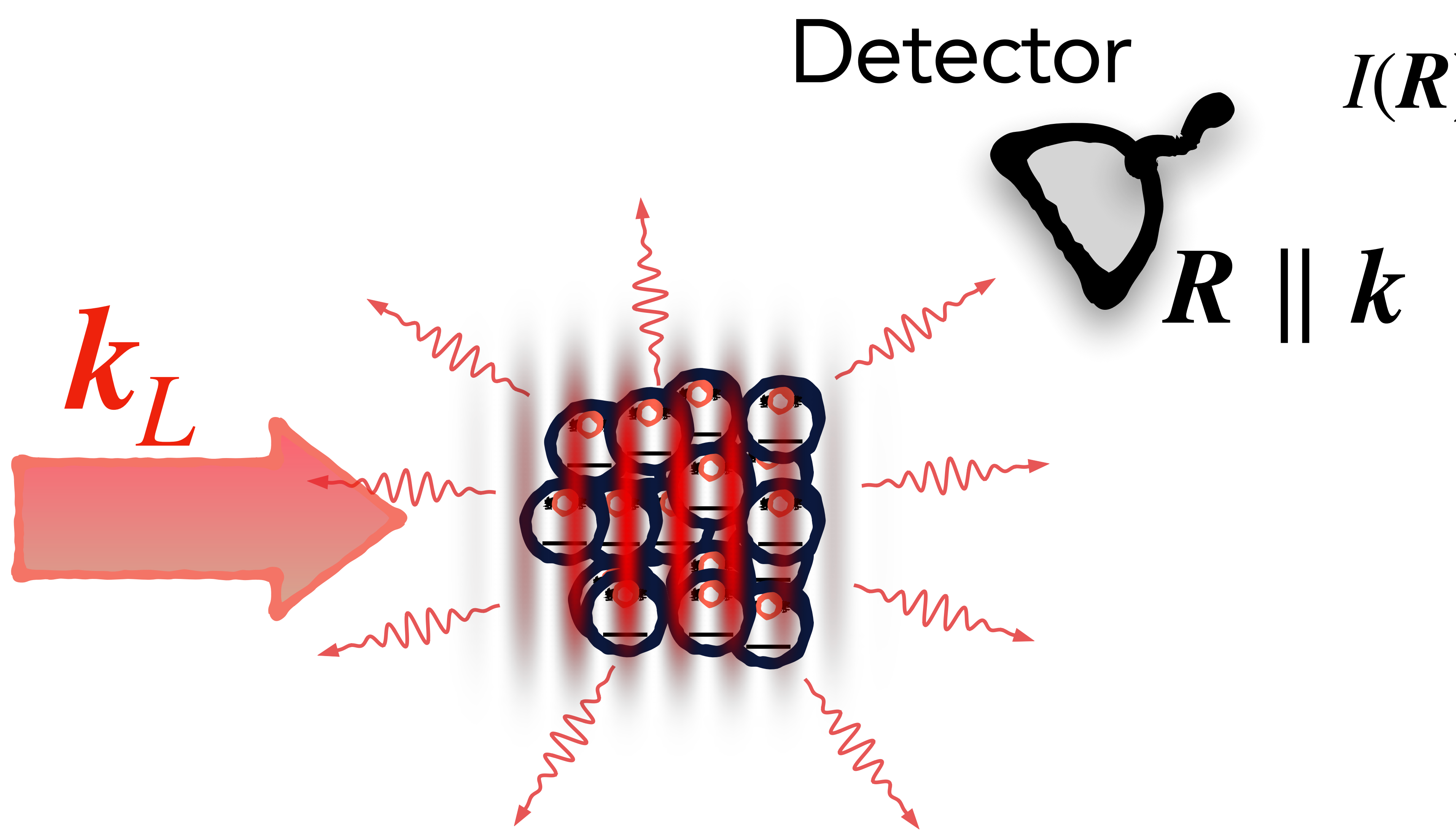

$$I(\boldsymbol{R}) = \langle \hat{E}^{-}(\boldsymbol{R})\hat{E}^{+}(\boldsymbol{R})\rangle \qquad \hat{E}^{+}(\boldsymbol{R}) \propto \sum_{n=1}^{N} G(\boldsymbol{R}-\boldsymbol{r}_n, \omega_0)\hat{\sigma}_n^{-}$$

$$I_N(\boldsymbol{k}) = I_1(\boldsymbol{k}) \sum_n \left[\langle \hat{e}_n \rangle + \sum_{m \neq n} e^{i\boldsymbol{k}\cdot(\boldsymbol{r}_m - \boldsymbol{r}_n)} \langle \hat{\sigma}_m^{+} \hat{\sigma}_n^{-} \rangle \right]$$

Laser propagating along $\boldsymbol{k}_L$ excites each atom to: $\quad |\psi_n\rangle \propto (|g_n\rangle + \varepsilon\, e^{i\boldsymbol{k}_L\cdot\boldsymbol{r}_n}|e_n\rangle) \quad |\psi\rangle = \Pi_{\otimes n}|\psi_n\rangle$

Emission from N weakly excited atoms

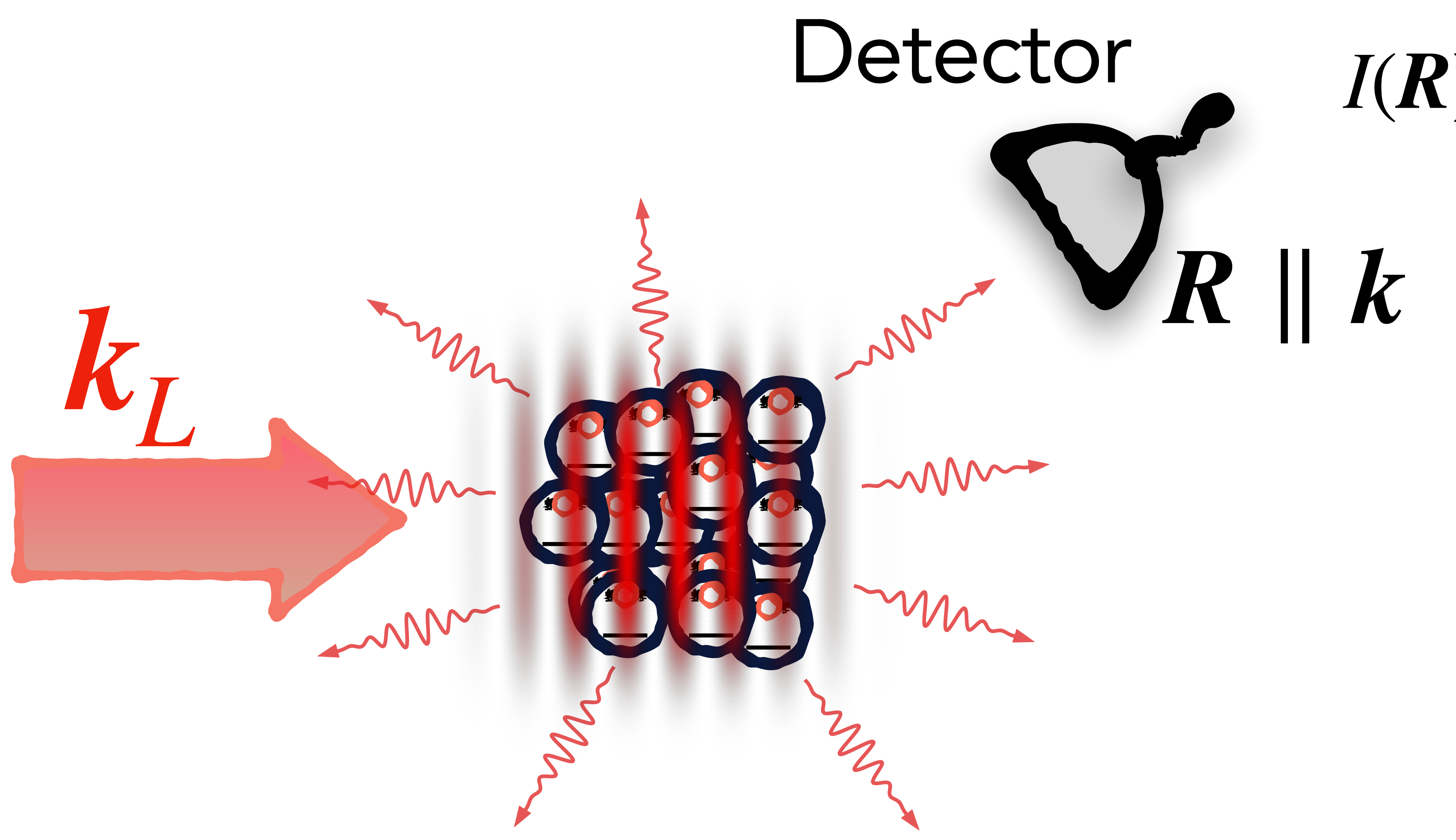

$$I(\boldsymbol{R}) = \langle \hat{E}^{-}(\boldsymbol{R}) \hat{E}^{+}(\boldsymbol{R}) \rangle \qquad \hat{E}^{+}(\boldsymbol{R}) \propto \sum_{n=1}^{N} G(\boldsymbol{R} - \boldsymbol{r}_n, \omega_0) \hat{\sigma}_n^{-}$$

$$I_N(\boldsymbol{k}) = I_1(\boldsymbol{k}) \sum_n \left[\langle \hat{e}_n \rangle + \sum_{m \neq n} e^{i\boldsymbol{k}\cdot(\boldsymbol{r}_m - \boldsymbol{r}_n)} \langle \hat{\sigma}_m^{+} \hat{\sigma}_n^{-} \rangle \right]$$

Laser propagating along $\boldsymbol{k}_L$ excites each atom to: $\quad |\psi_n\rangle \propto (|g_n\rangle + \varepsilon\, e^{i\boldsymbol{k}_L\cdot\boldsymbol{r}_n} |e_n\rangle) \quad |\psi\rangle = \Pi_{\otimes n} |\psi_n\rangle$

Weak excitation ($\varepsilon \ll 1$) $\quad \langle \hat{e}_n \rangle = \varepsilon^2 \quad \langle \hat{\sigma}_m^{+} \hat{\sigma}_n^{-} \rangle = \varepsilon^2 e^{i\boldsymbol{k}_L\cdot(\boldsymbol{r}_n - \boldsymbol{r}_m)}$

$$I_N(\boldsymbol{k}) = \varepsilon^2 I_1(\boldsymbol{k}) \left[N + \sum_{m \neq n} e^{i(\boldsymbol{k} - \boldsymbol{k}_L)\cdot(\boldsymbol{r}_m - \boldsymbol{r}_n)} \right]$$

Emission from N weakly excited atoms

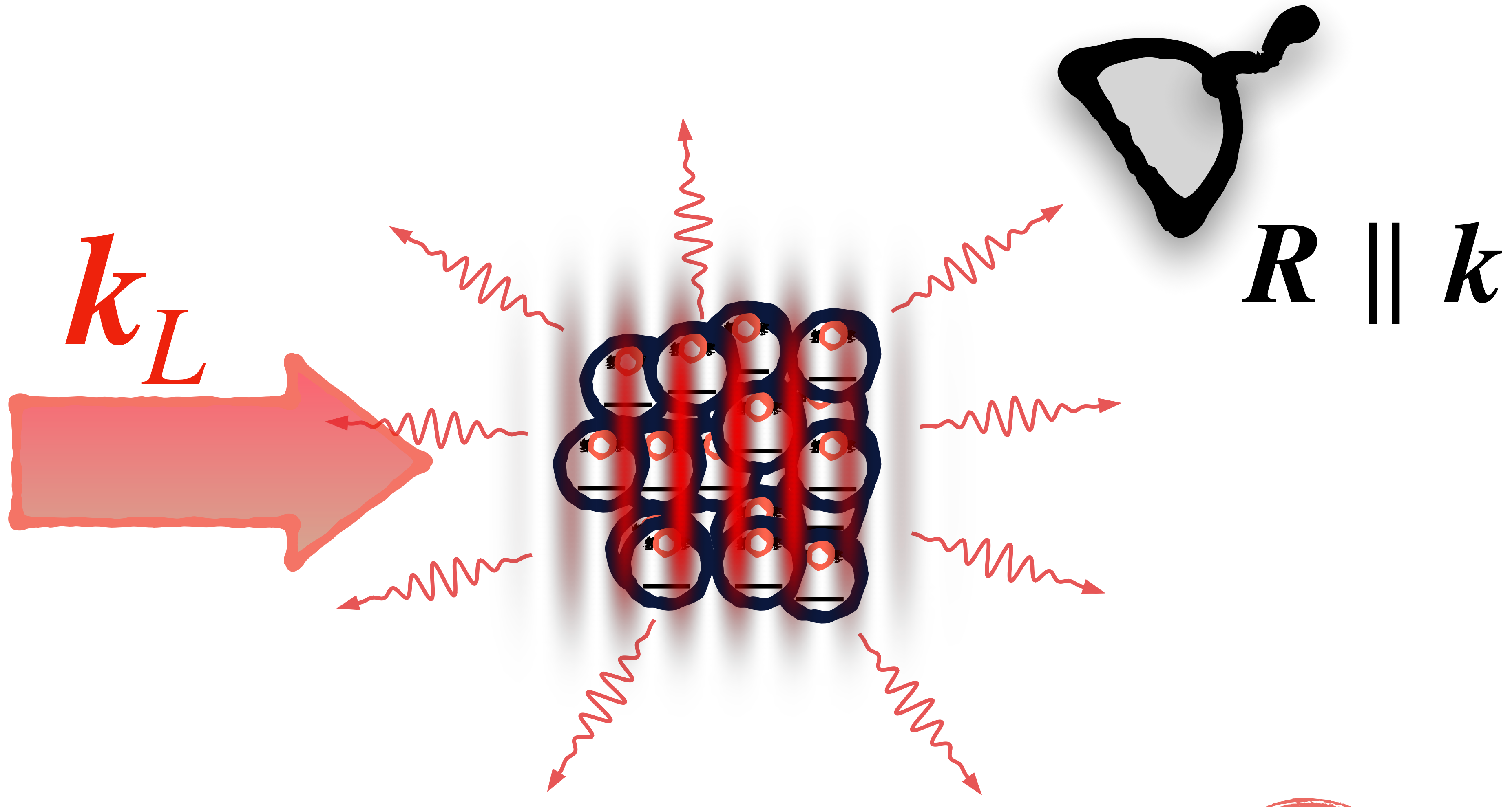

$$I_N(\boldsymbol{k}) \propto \frac{I_1(\boldsymbol{k})}{N}\left[N + \sum_{m\neq n} e^{i\,(\boldsymbol{k}-\boldsymbol{k}_L)\cdot(\boldsymbol{r}_m-\boldsymbol{r}_n)}\right]$$

$$I_N(\boldsymbol{k}) \propto N I_1(\boldsymbol{k}) + N^2 I_1(\boldsymbol{k}) \left|\frac{1}{N}\sum_{m\neq n} e^{i\,(\boldsymbol{k}-\boldsymbol{k}_L)\cdot\boldsymbol{r}_m}\right|^2$$

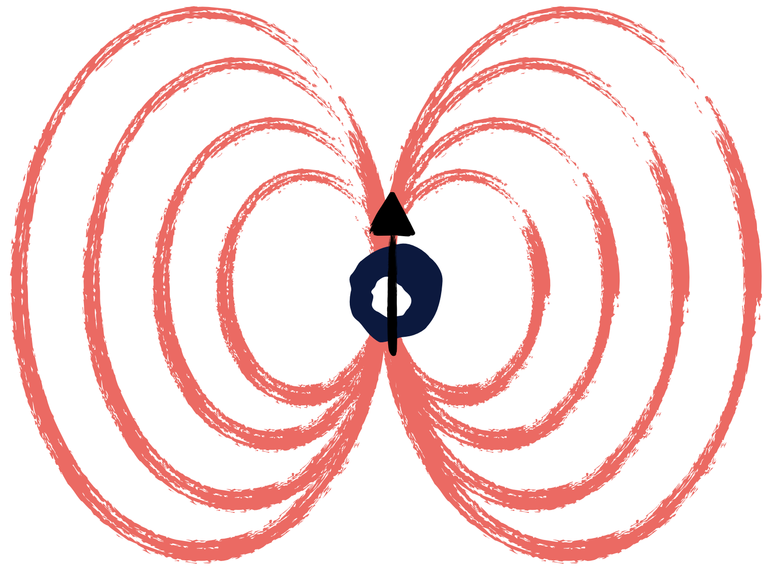

$\sin^2\theta$

$$= I_{\mathrm{incoh}}(\boldsymbol{k}) + I_{\mathrm{coop}}(\boldsymbol{k})$$

$$= S(\boldsymbol{k} - \boldsymbol{k}_L)$$

Structure factor

Emission from N weakly excited atoms

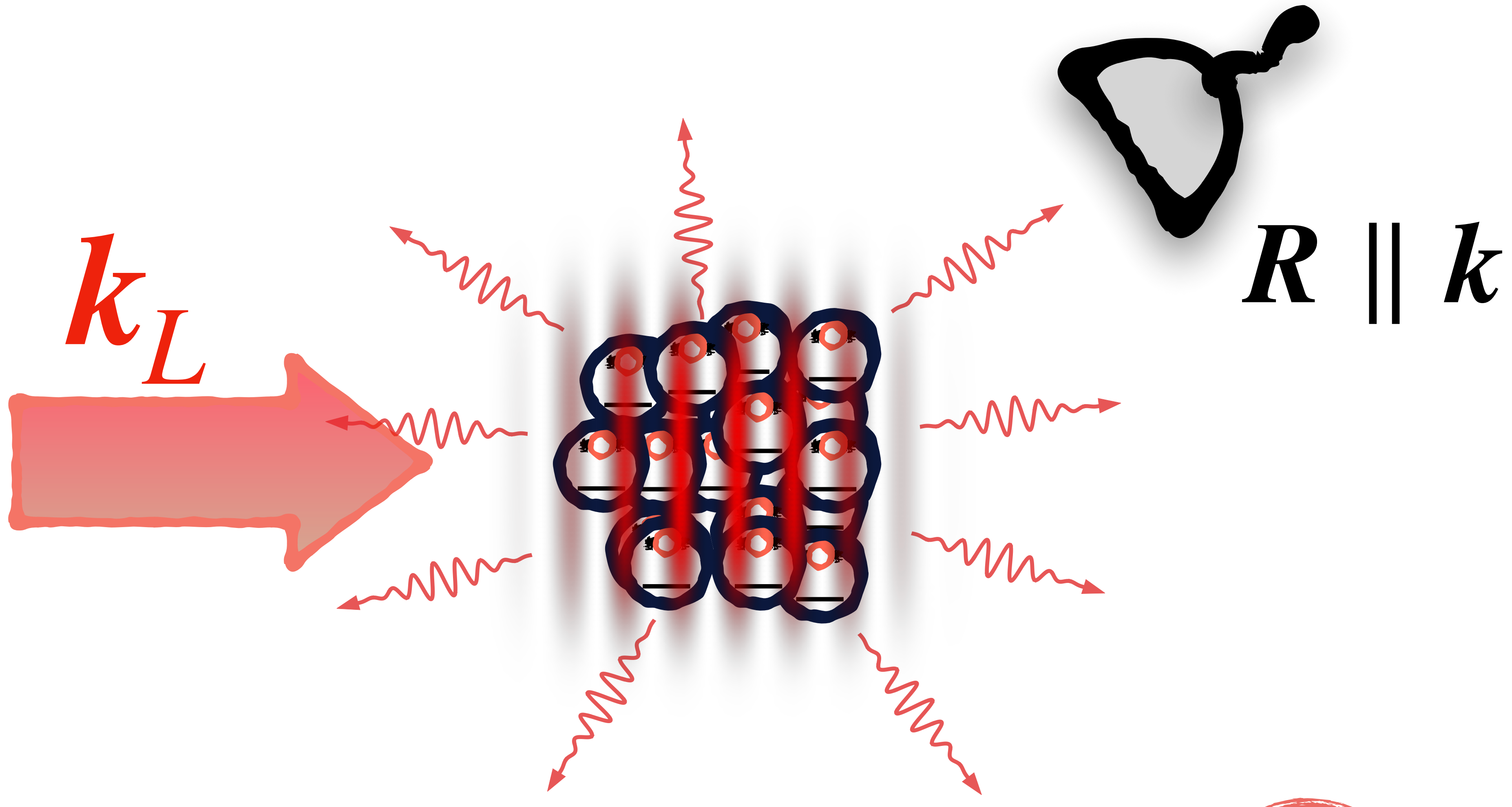

$$I_N(\boldsymbol{k}) \propto \frac{I_1(\boldsymbol{k})}{N}\left[N + \sum_{m \neq n} e^{i(\boldsymbol{k}-\boldsymbol{k}_L)\cdot(\boldsymbol{r}_m - \boldsymbol{r}_n)}\right]$$

$$I_N(\boldsymbol{k}) \propto N I_1(\boldsymbol{k}) + N^2 I_1(\boldsymbol{k}) \left| \frac{1}{N} \sum_{m \neq n} e^{i(\boldsymbol{k}-\boldsymbol{k}_L)\cdot \boldsymbol{r}_m} \right|^2$$

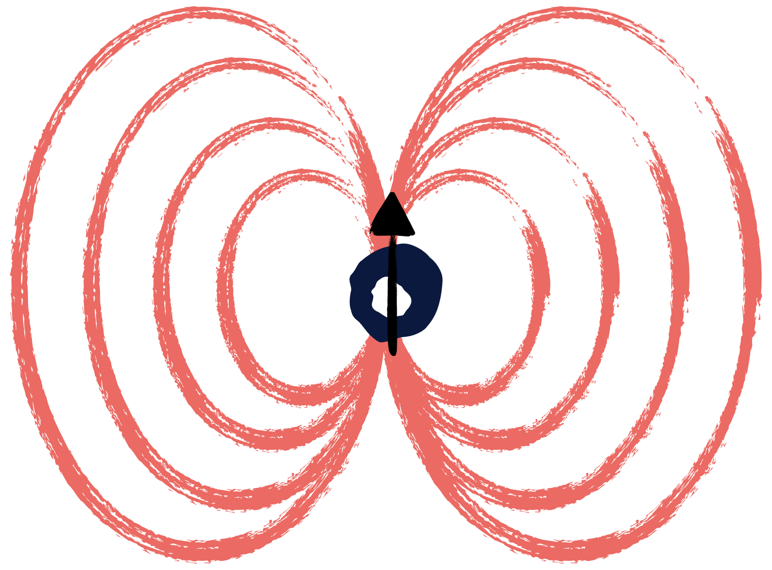

$\sin^2\theta$

$$= I_{\mathrm{incoh}}(\boldsymbol{k}) + I_{\mathrm{coop}}(\boldsymbol{k})$$

$$= S(\boldsymbol{k} - \boldsymbol{k}_L)$$

Structure factor

Defines the **cooperativity** μ

$$\mu = \frac{P_{\mathrm{coop}}}{P_{\mathrm{incoh}}}$$

$$\mu = \frac{\int d\Omega\, I_1(\boldsymbol{k})\, |S(\boldsymbol{k} - \boldsymbol{k}_L)|^2}{\int d\Omega\, I_1(\boldsymbol{k})}$$

Emission from N weakly excited atoms

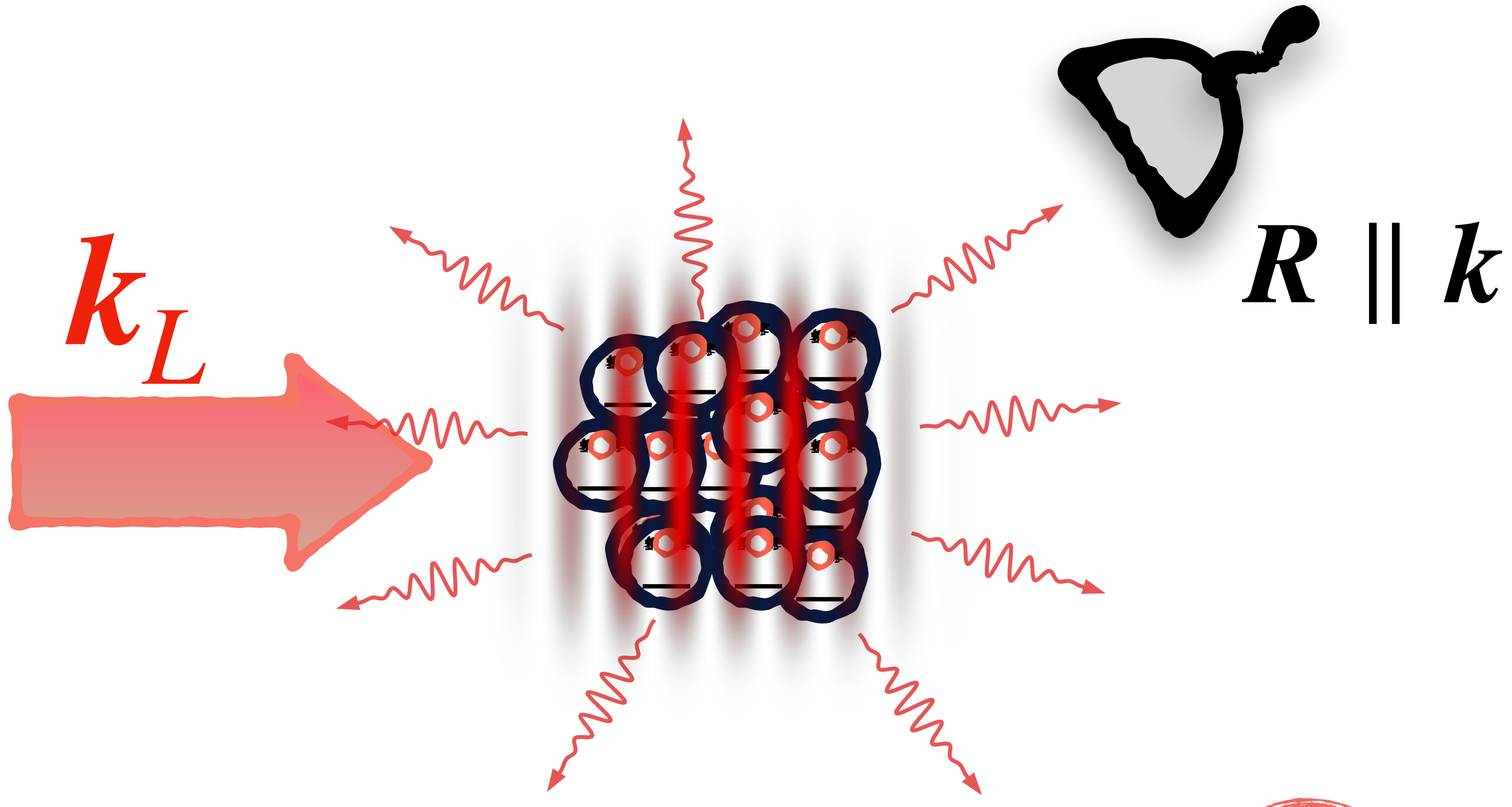

$$I_N(\boldsymbol{k}) \propto \frac{I_1(\boldsymbol{k})}{N}\left[N + \sum_{m\neq n} e^{i\,(\boldsymbol{k}-\boldsymbol{k}_L)\cdot(\boldsymbol{r}_m-\boldsymbol{r}_n)}\right]$$

$$I_N(\boldsymbol{k}) \propto N I_1(\boldsymbol{k}) + N^2 I_1(\boldsymbol{k})\left|\frac{1}{N}\sum_{m\neq n} e^{i\,(\boldsymbol{k}-\boldsymbol{k}_L)\cdot\boldsymbol{r}_m}\right|^2$$

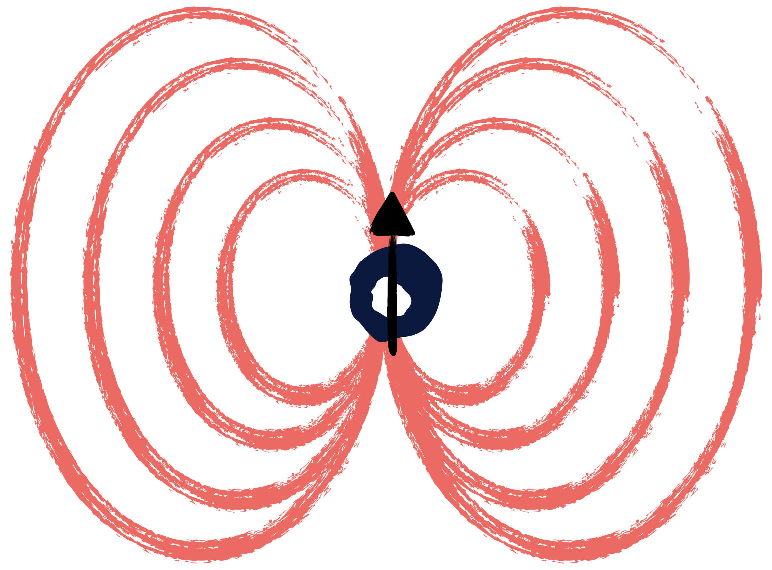

$\sin^2\theta$

$$= I_{\text{incoh}}(\boldsymbol{k}) + I_{\text{coop}}(\boldsymbol{k})$$

$$= S(\boldsymbol{k}-\boldsymbol{k}_L)$$

Structure factor

Defines the **cooperativity** μ

$$\mu = \frac{P_{\text{coop}}}{P_{\text{incoh}}} \qquad \mu = \frac{\int d\Omega\, I_1(\boldsymbol{k})\,|\,S(\boldsymbol{k}-\boldsymbol{k}_L)\,|^2}{\int d\Omega\, I_1(\boldsymbol{k})}$$

Collective initial scattering rate

$$\Gamma_N = \Gamma_0(1+\mu N)$$

Cooperativity

$$I(\boldsymbol{k}) = I_{\text{incoh}}(\boldsymbol{k}) + I_{\text{coop}}(\boldsymbol{k})$$

$$\mu = \frac{P_{\text{coop}}}{N P_1} \sim \frac{\Delta\Omega}{4\pi}$$

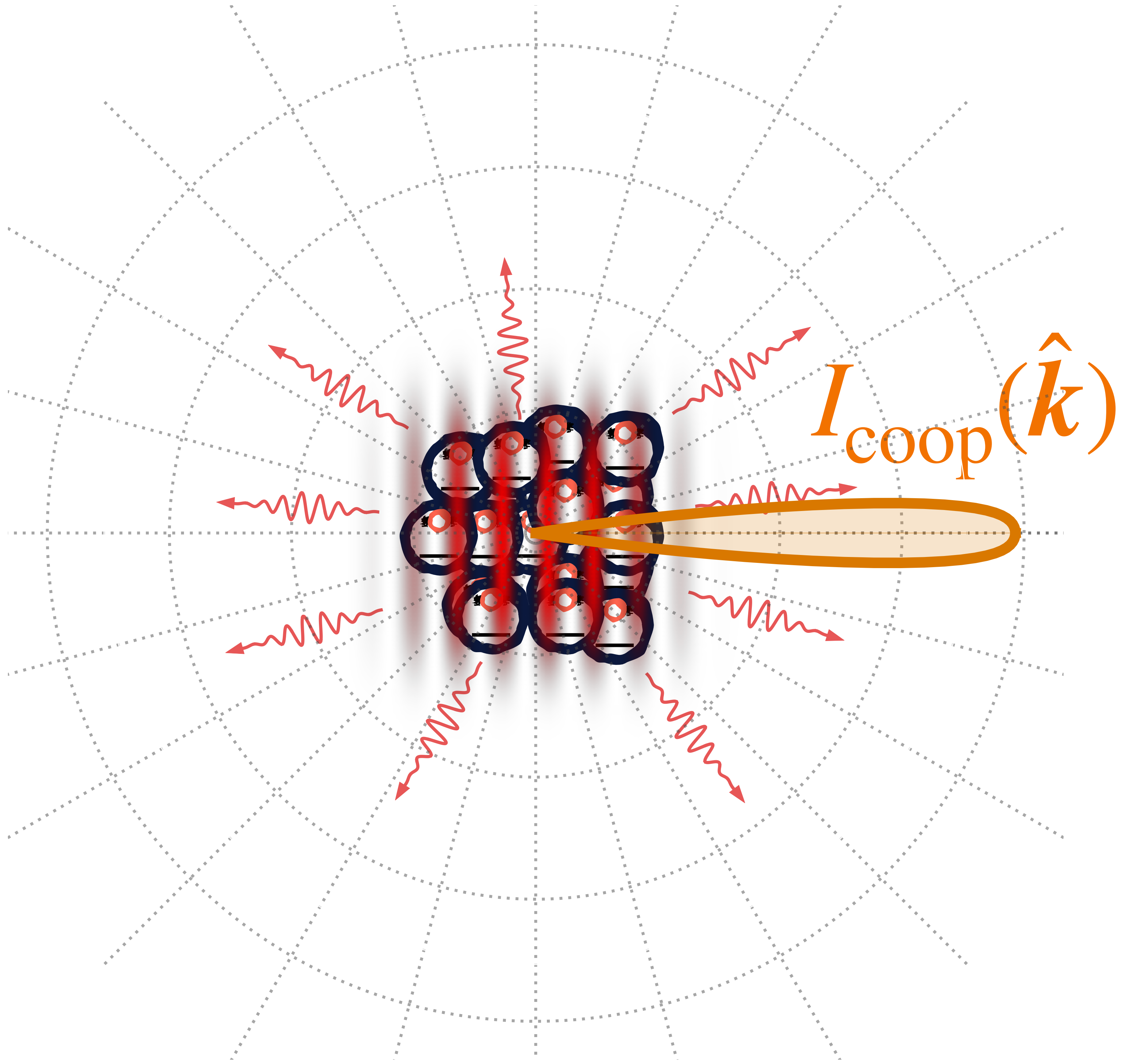

Cooperative scattering in solid angle $\Delta\Omega$

Gross & Haroche, *Physics Reports* **93**, 301 (1982).

Allen & Eberly, *Optical resonance and two-level atoms*, Courier Corp. (1987)

“Classical” superradiance

Cooperativity
$$\mu = \frac{N^2 \int d\Omega\, I_1(\boldsymbol{k})\,|\,S(\boldsymbol{k}-\boldsymbol{k}_L)\,|^2}{N \int d\Omega\, I_1(\boldsymbol{k})}$$

Smal subwavelength clouds

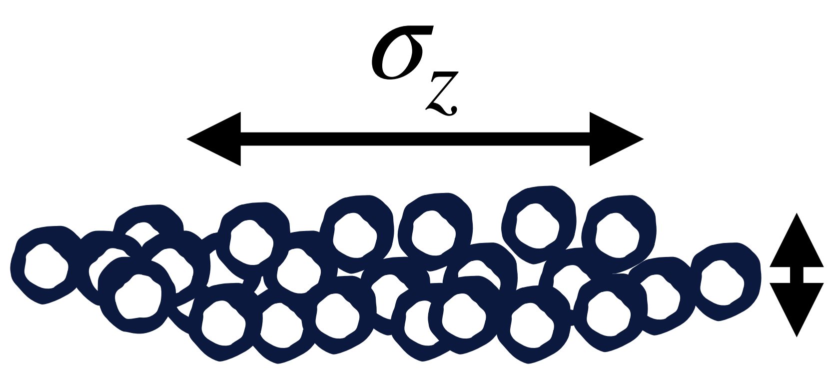

$\sigma_r < \lambda$
$$\mu \sim \frac{\Delta\Omega}{4\pi} \sim \frac{\lambda}{2\pi\sigma_z}$$

Couples to one diffraction mode set by cloud dimensions

Couping set by the optical depth in the direction of excitation

"Classical" superradiance

Cooperativity
$$\mu = \frac{N^2 \int d\Omega\, I_1(\boldsymbol{k})\, |\, S(\boldsymbol{k} - \boldsymbol{k}_L)\, |^2}{N \int d\Omega\, I_1(\boldsymbol{k})}$$

σ_z

Smal subwavelength clouds 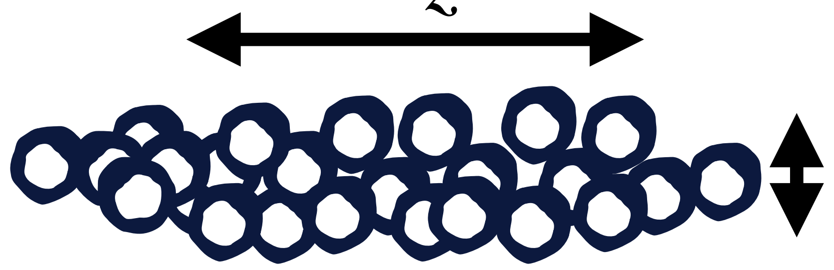 $\sigma_r < \lambda$ $\quad \mu \sim \dfrac{\Delta\Omega}{4\pi} \sim \dfrac{\lambda}{2\pi\sigma_z}$

Couples to one diffraction mode set by cloud dimensions

Cloud $\sigma \gg \lambda_0$ 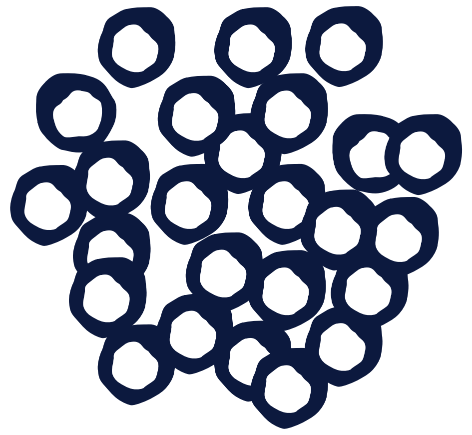 $\quad \mu N = \mathrm{OD} = \dfrac{3\,N}{k_0^2\,\sigma^2}$ optical depth

Couping set by the optical depth in the direction of excitation

Analogies

	Clouds	Clouds in cavity	WQED
	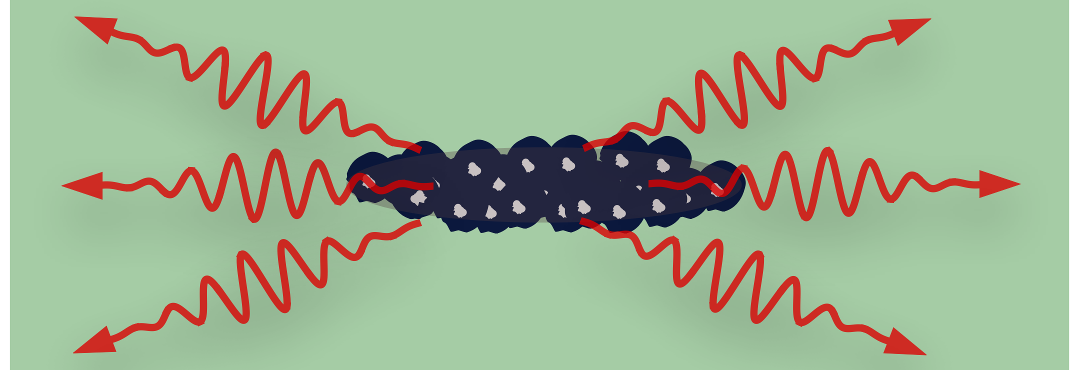	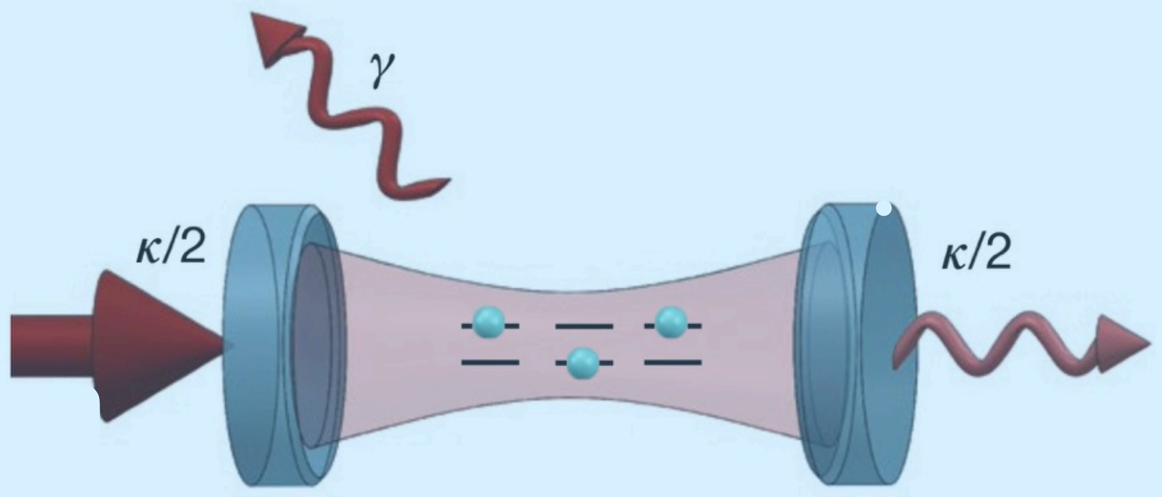 from: *Nature* **580**, 602 (2020)	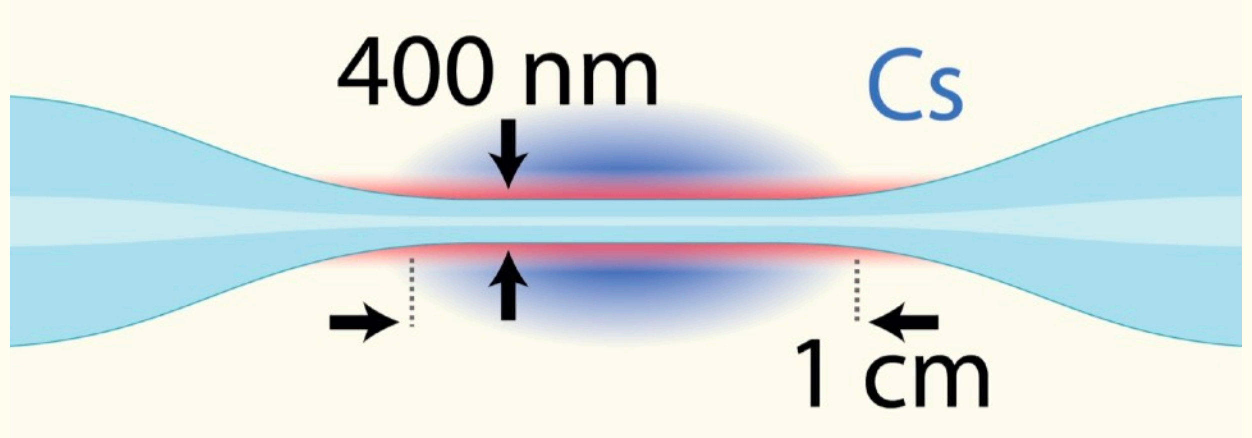 from arXiv: 2211.08940 (2022)
Collective mode	Diffraction pattern	Cavity mode	Waveguide mode
N-atom cooperativity	μN	$N\,4g^2/\kappa\gamma$	$N\beta = N\,\Gamma_{1D}/\Gamma'$

Classical (“single-photon”) superradiance

Mark Havey, ODU

Roof. *et al.*, *Phys Rev Lett* **117**, 073003 (2016).
Araújo *et al.*, *Phys Rev Lett* **117**, 073002 (2016).

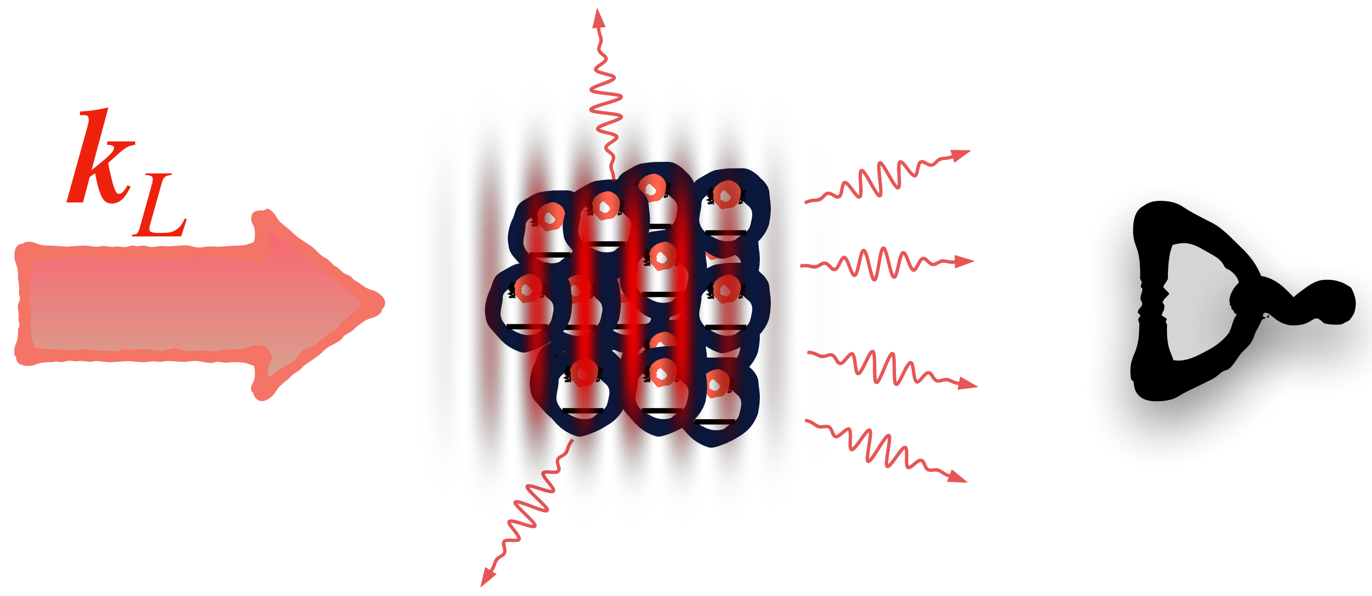

On-axis detector

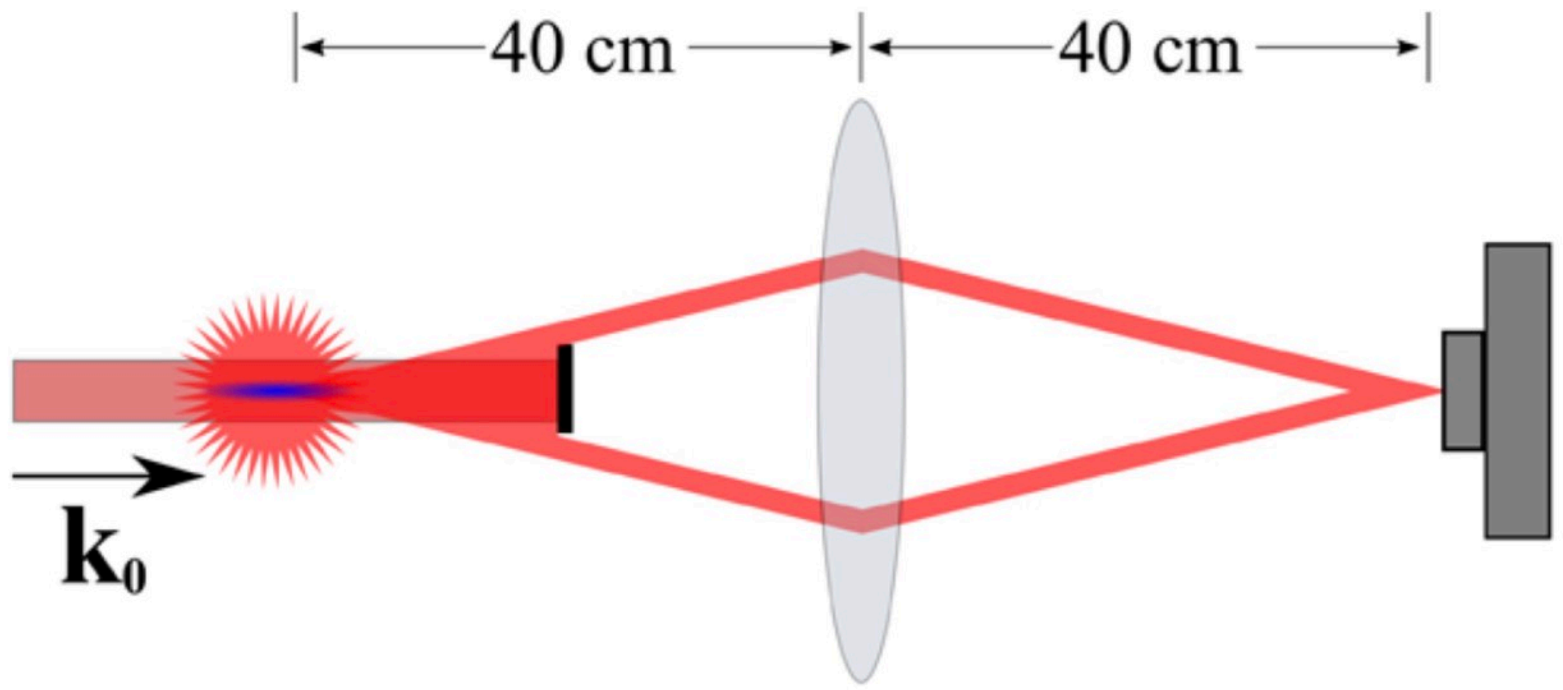

Classical ("single-photon") superradiance

Mark Havey, ODU

Roof. *et al.*, *Phys Rev Lett* **117**, 073003 (2016).
Araújo *et al.*, *Phys Rev Lett* **117**, 073002 (2016).

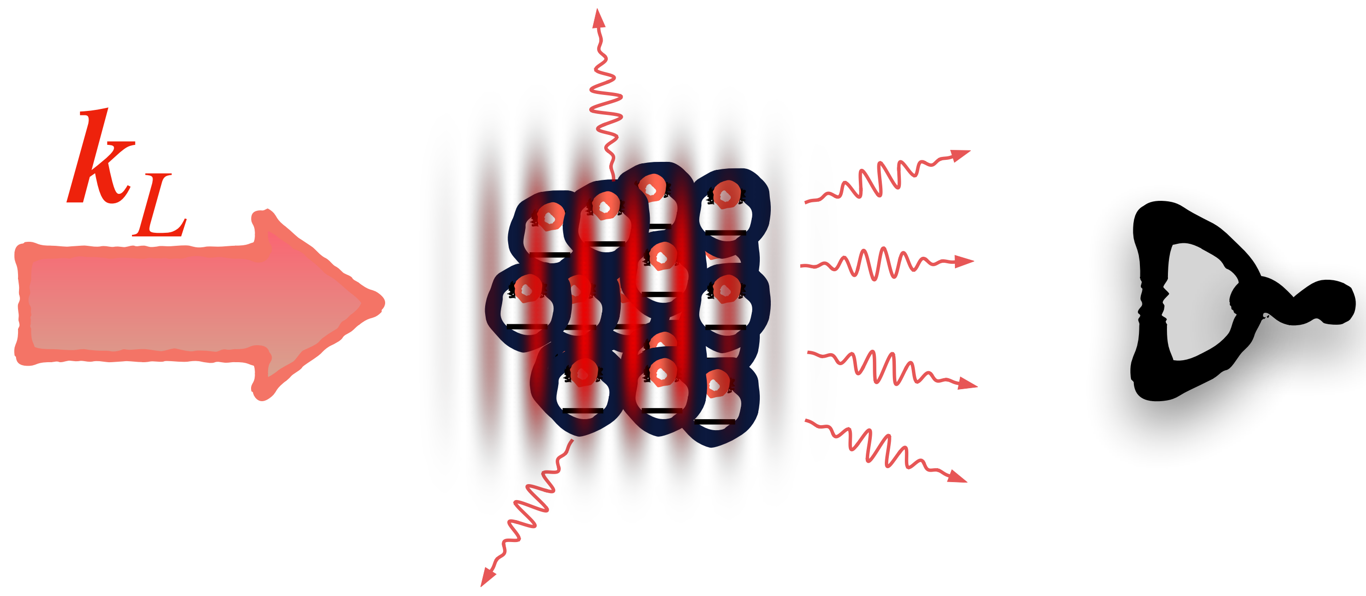

On-axis detector

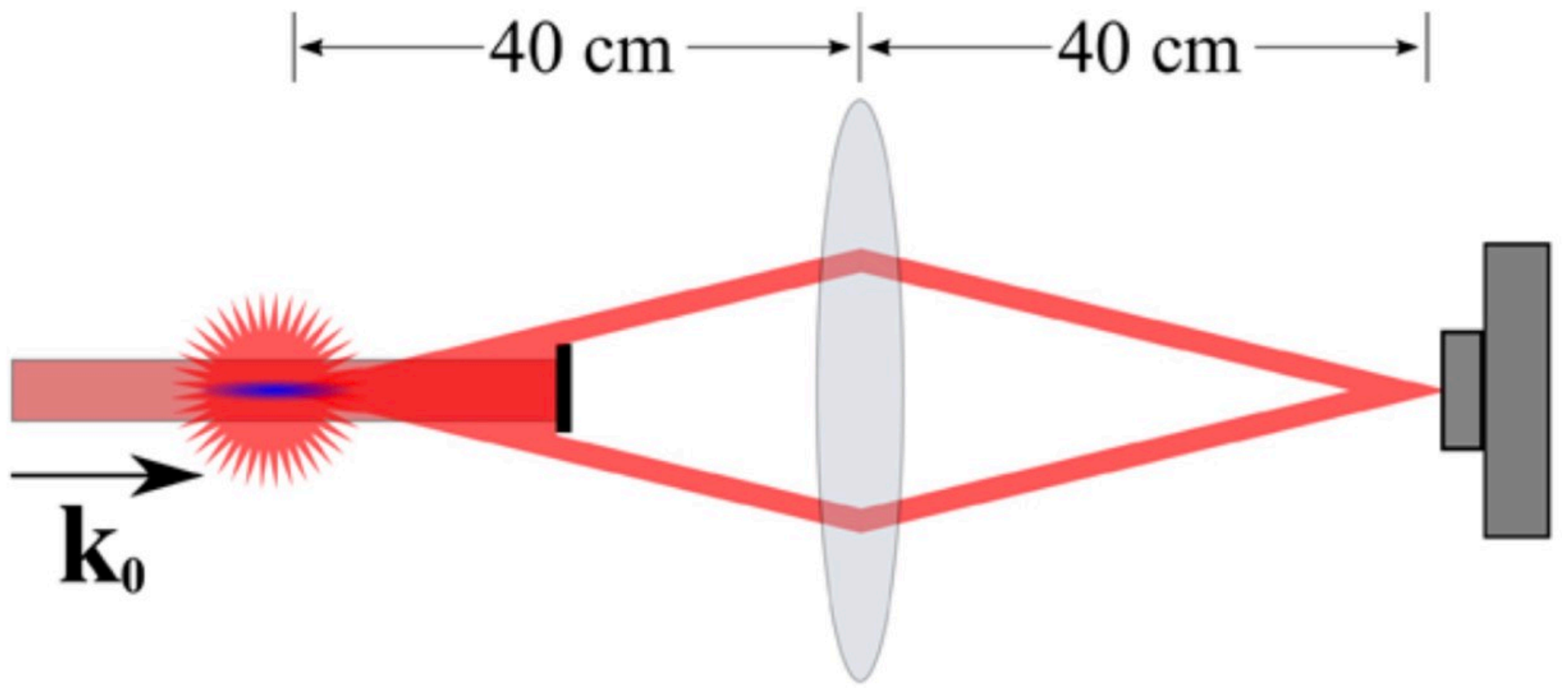

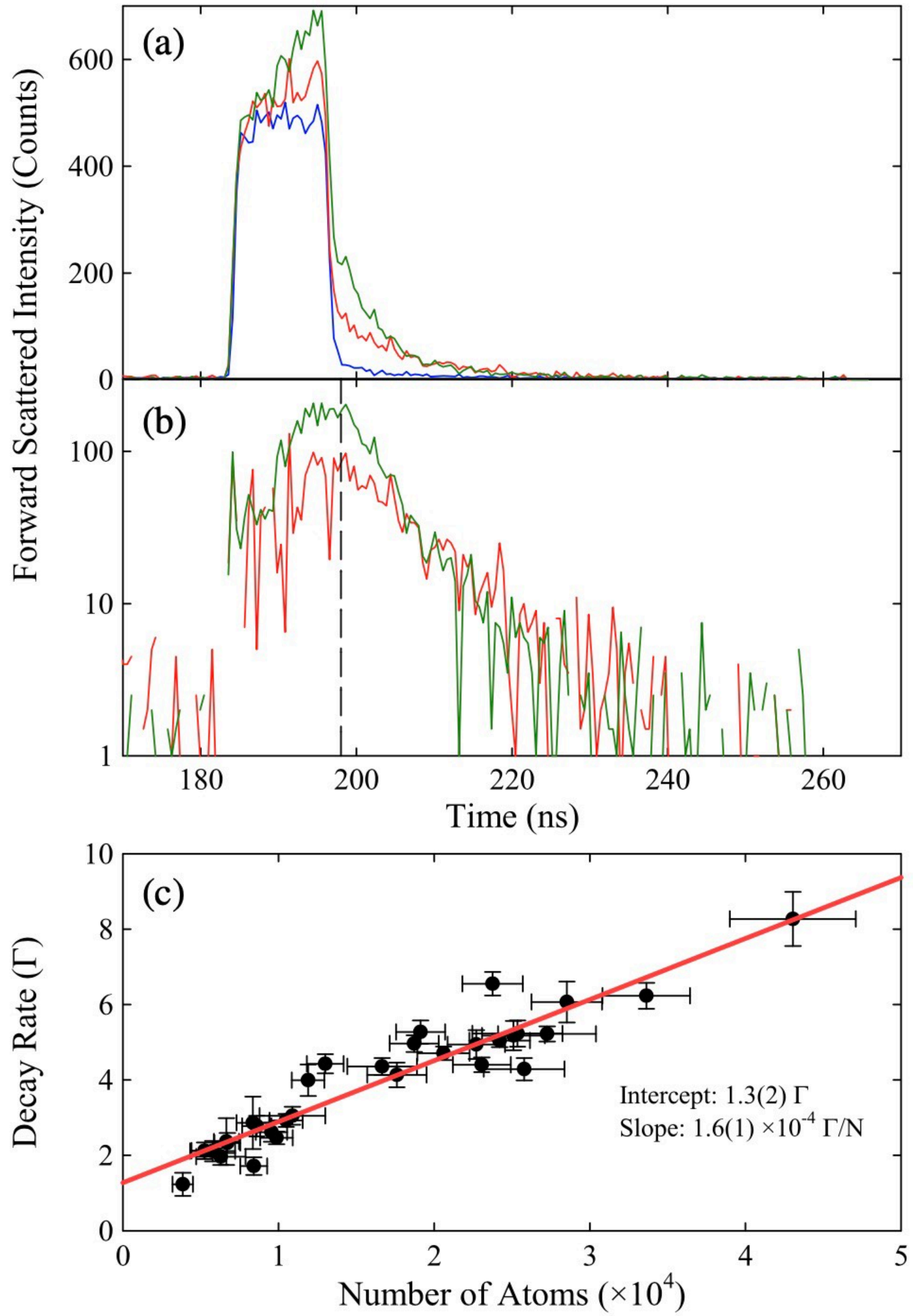

Quantum memory efficiency

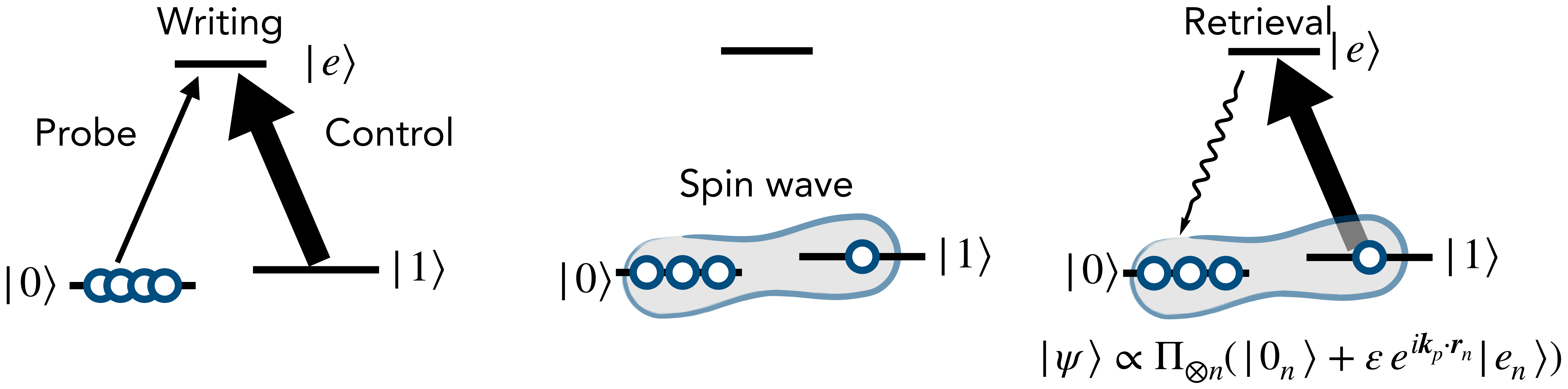

Total emission $\Gamma_0(1+\mathrm{OD})$ $\quad \mu N = \mathrm{OD}$

Cooperative emission $\Gamma_0\mathrm{OD}$

Efficiency of retrieval: $\eta = \dfrac{\mathrm{OD}}{1+\mathrm{OD}}$

Quantum memory efficiency

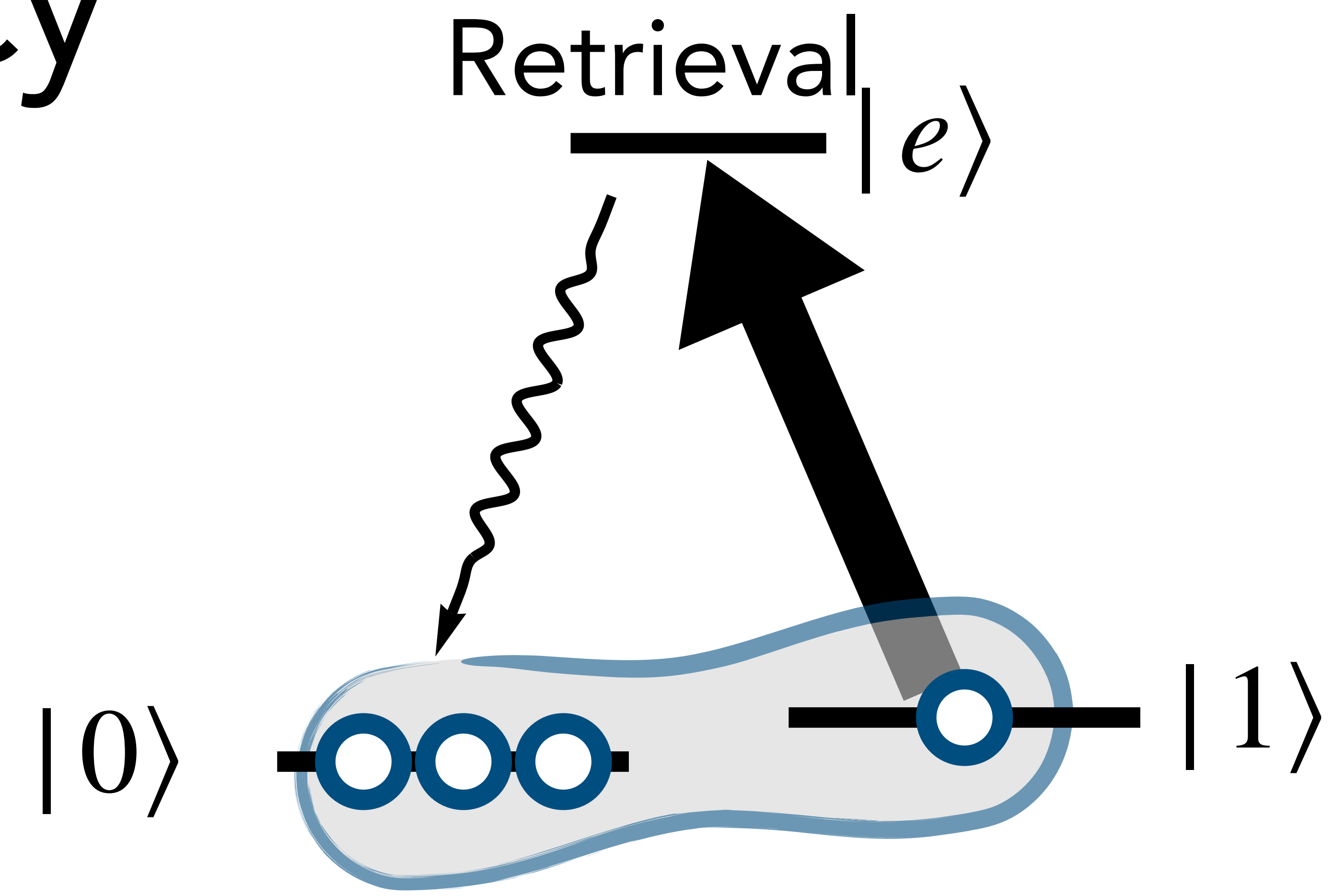

$$|\psi\rangle \propto \Pi_{\otimes n}(|0_n\rangle + \varepsilon\, e^{i\boldsymbol{k}_p\cdot\boldsymbol{r}_n}|e_n\rangle)$$

Efficiency of retrieval: $$\eta = \frac{\mathrm{OD}}{1+\mathrm{OD}}$$

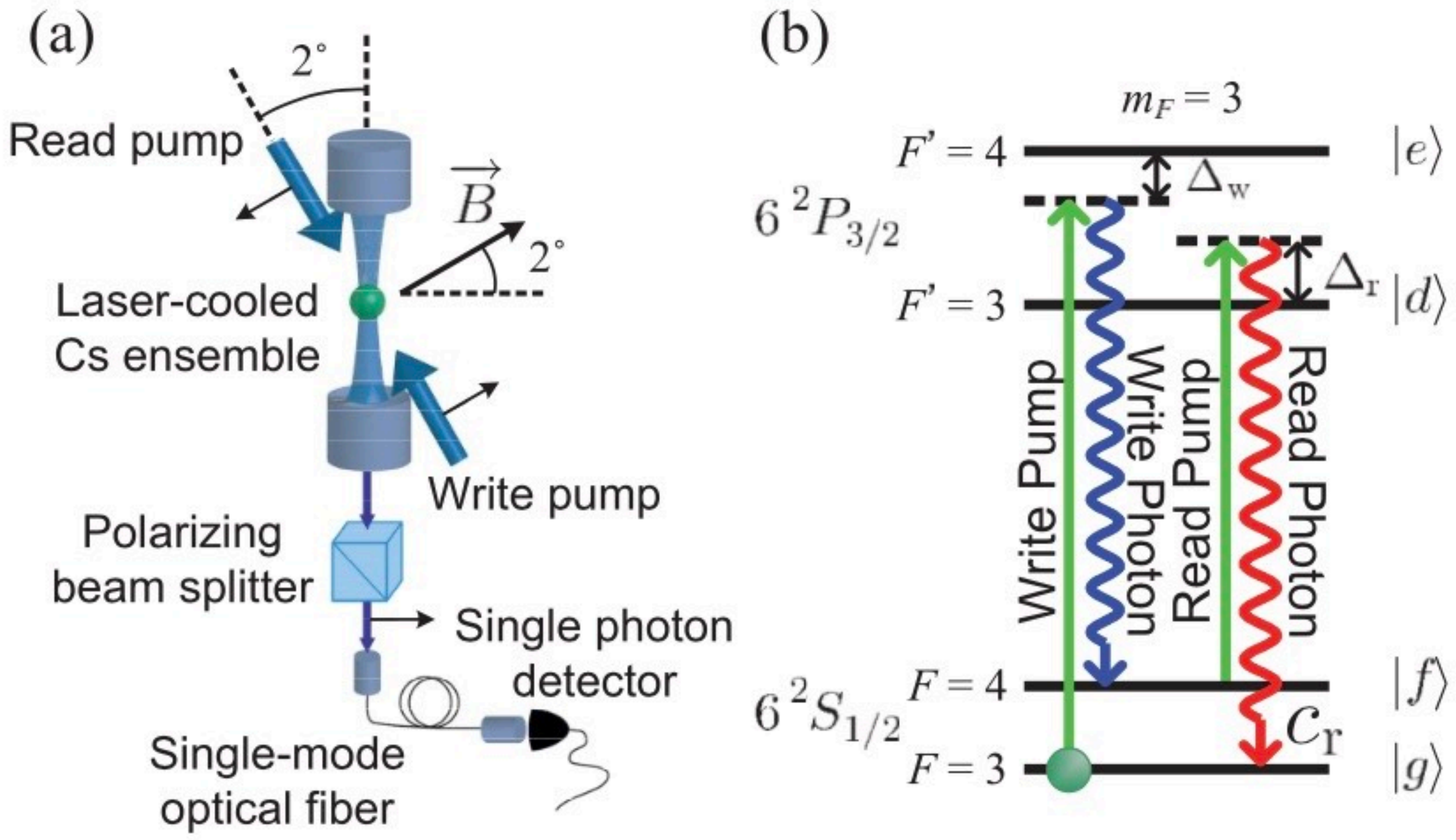

FIG. 1 (color online). (a) Setup for the conditional generation of single photons using a sample of laser-cooled Cs atoms inside an optical resonator. (b) Level scheme for the system with hyperfine and magnetic sublevels $|F, m_F\rangle$. The atomic sample is initially prepared in $|g\rangle$ by optical pumping.

Simon *et al.*, *Phys. Rev. Lett.* **98**, 183601 (2007).

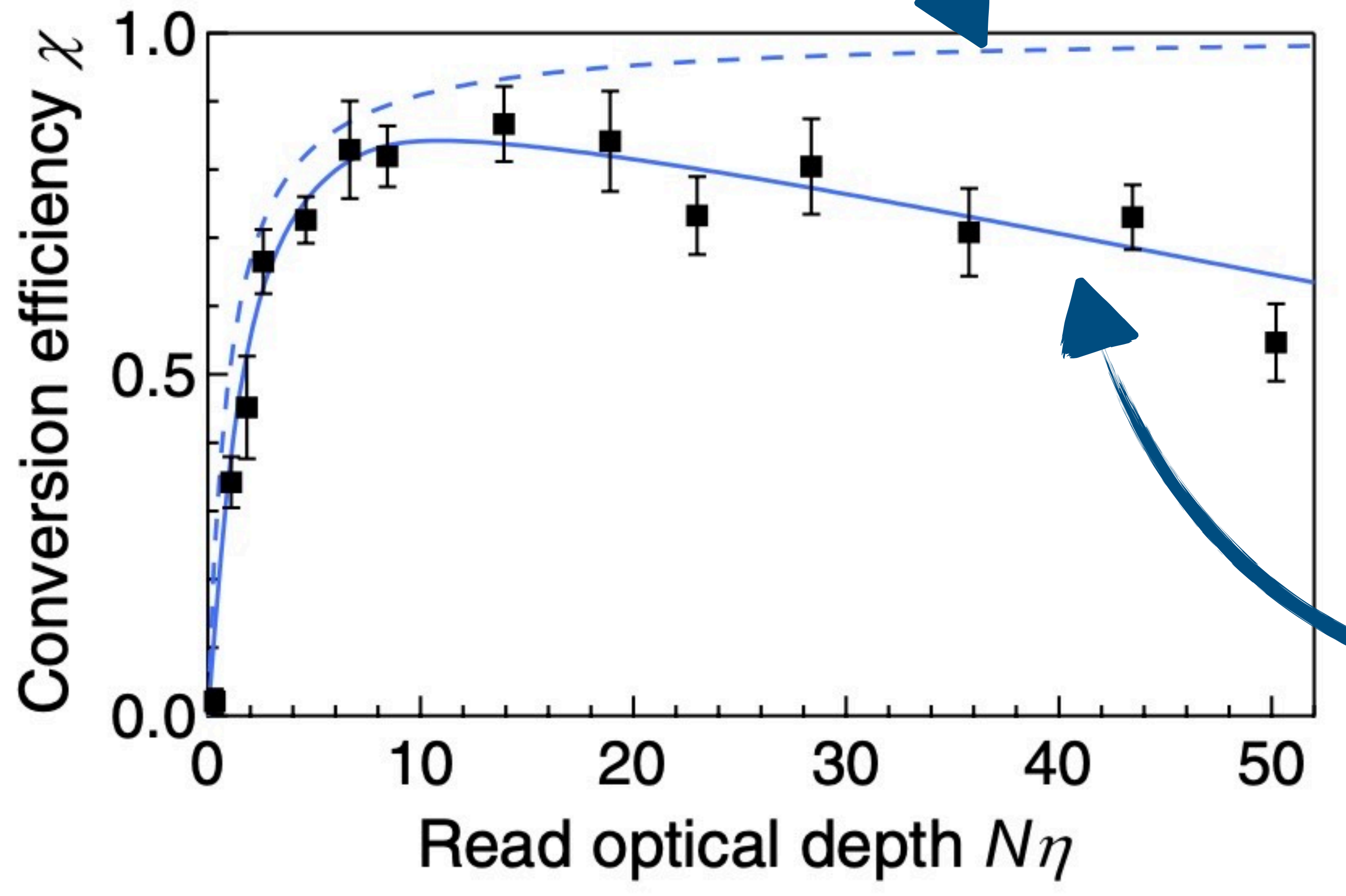

FIG. 3 (color online). Magnon-photon conversion efficiency χ versus read optical depth $N\eta$ at a write-read delay of 120 ns. The optical depth is extracted from the write scattering rate and known intensities and detunings. The dashed line shows the predicted conversion χ_0 for a three-level system; the solid line is the prediction from a model including dephasing from additional excited states.

Additional dephasings

Atom arrays

Equivalent with Bragg: diffraction orders

At subwavelength spacing: can switch all orders off

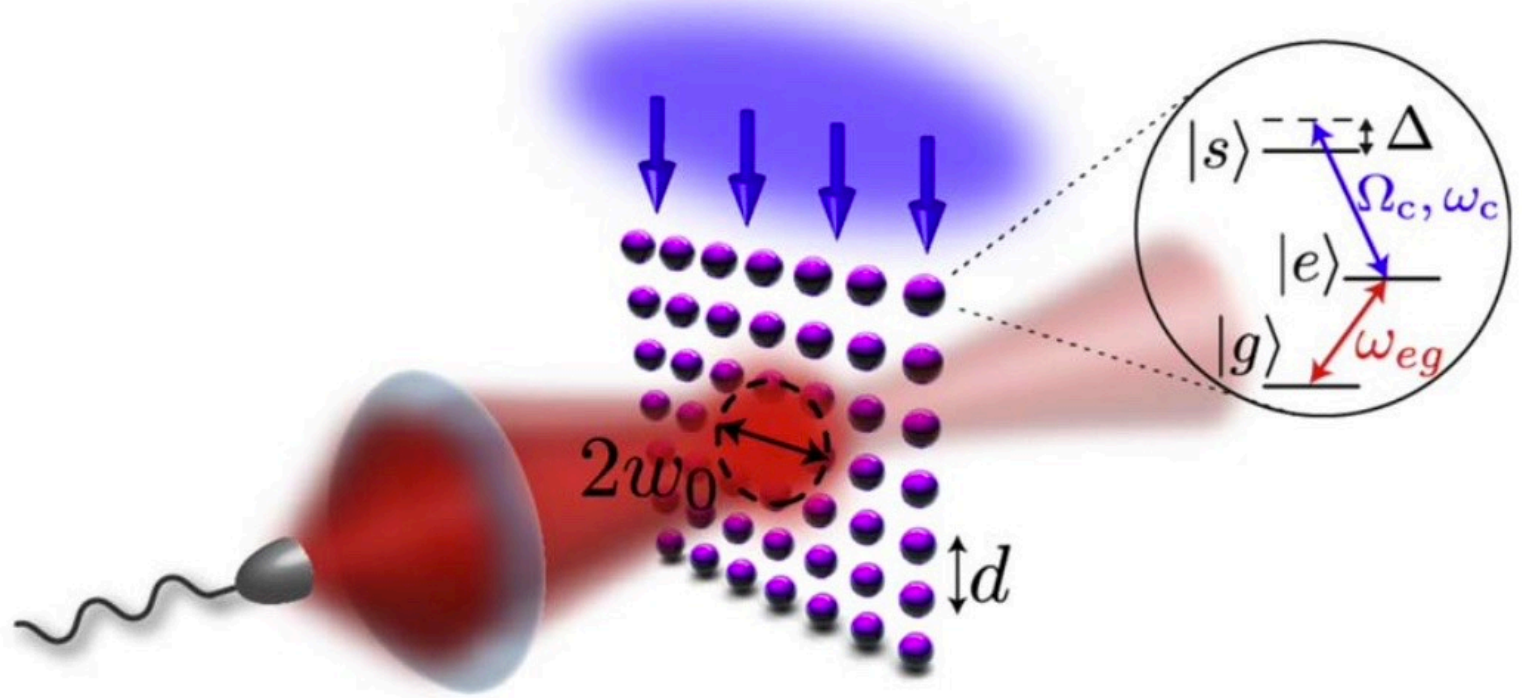

Figure 1. Schematic of a quantum memory using a two-dimensional atomic array. An excitation initially stored in the $|s\rangle$-manifold is retrieved as a photon by turning on the classical control field Ω_c (blue arrows), which then creates a Raman scattered photon from the $|g\rangle - |e\rangle$ transition. The photon is detected in some given mode, illustrated here as a Gaussian beam.

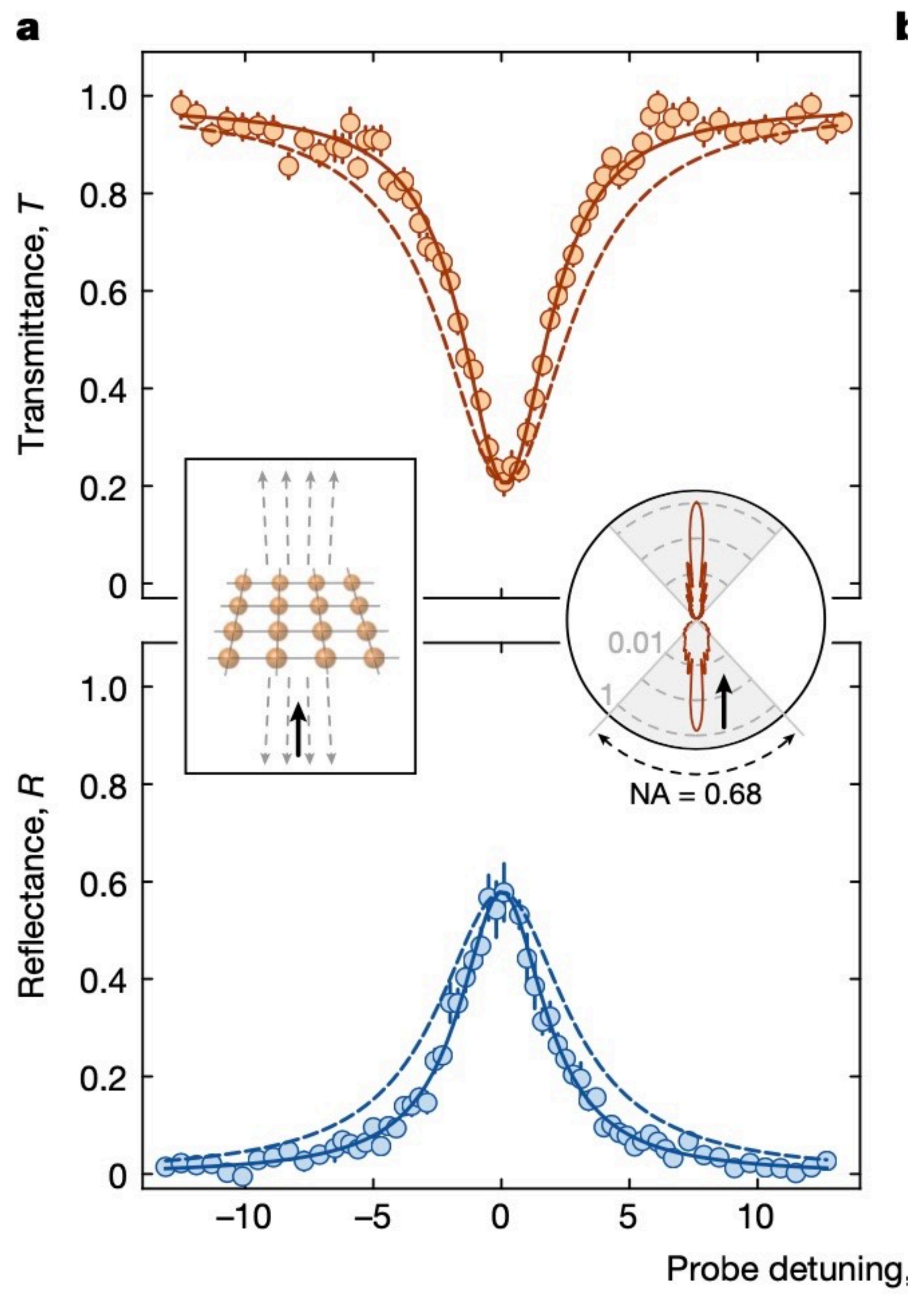

Manzoni *et al. New J Phys* **20**, 083048 (2018).

Rui *et al. Nature* **583**, 369 (2020).

Outline

Lecture 1: Quantum optics of single atoms

Lecture 2: Collective light scattering by N atoms

Lecture 3: Many-body quantum optics

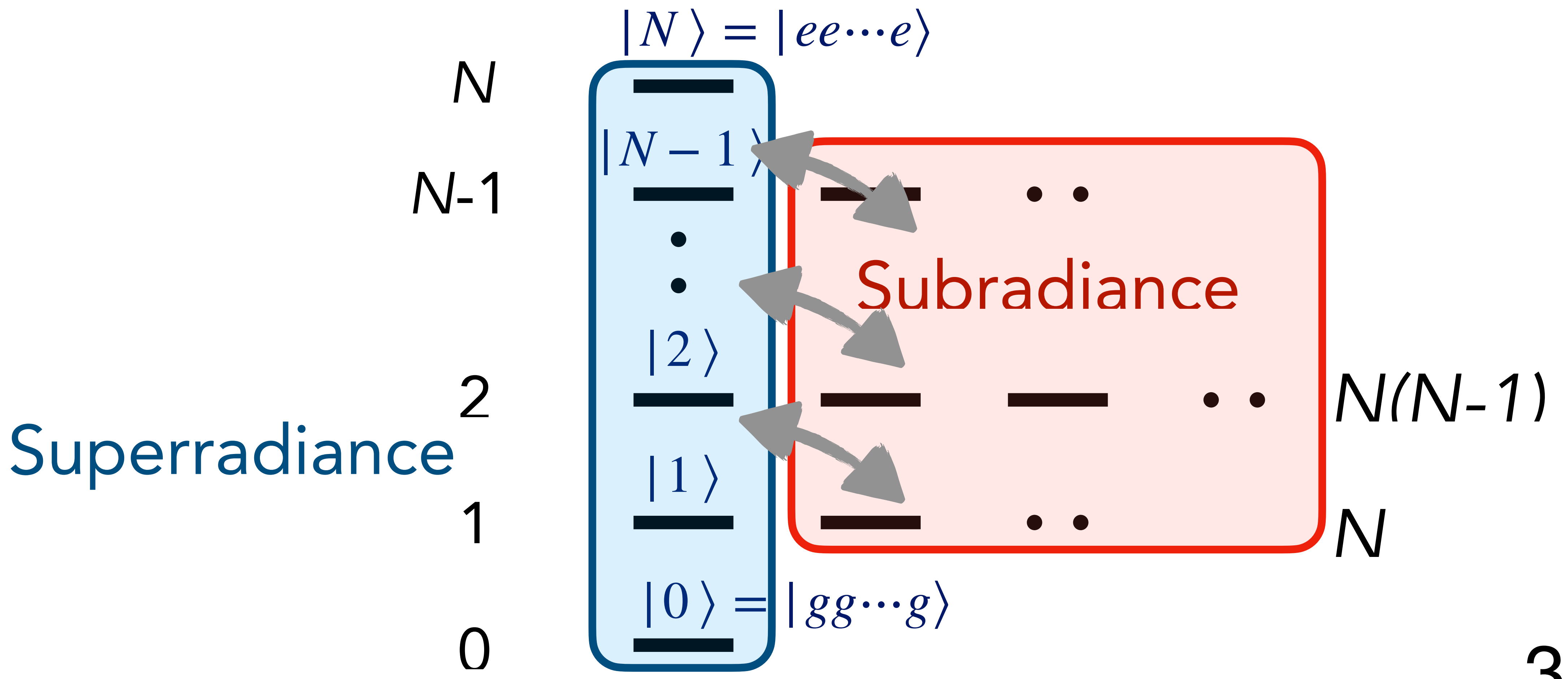

Master equation

$$\dot{\rho} = -\frac{i}{\hbar}\left[H, \rho\right] + L(\rho)$$

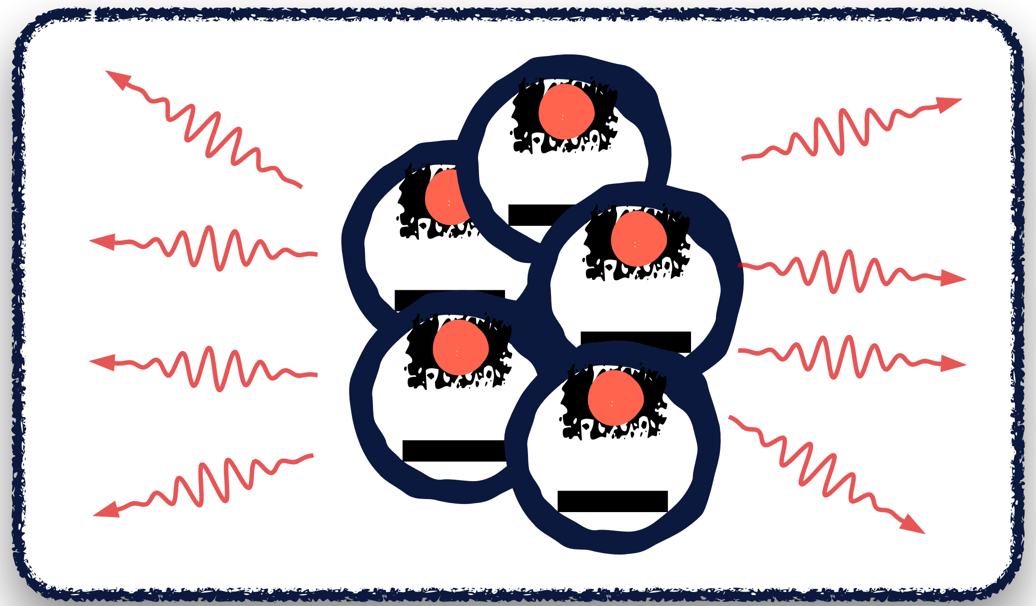

$$H = H_0 + \sum_{nm} V_{nm}\hat{\sigma}_n^+\hat{\sigma}_m^-$$

$$V_{nm} = \mathrm{Re}[V_{\mathrm{dd}}(\boldsymbol{r}_{nm})]$$

$$L(\rho) = \frac{1}{2}\sum_{nm}\Gamma_{nm}(2\hat{\sigma}_m^-\rho\hat{\sigma}_n^+ - \rho\hat{\sigma}_n^+\hat{\sigma}_m^- - \hat{\sigma}_n^+\hat{\sigma}_m^-\rho)$$

$$\Gamma_{nm} = 2\,\mathrm{Im}[V_{\mathrm{dd}}(\boldsymbol{r}_{nm})]$$

Equation valid under the Born-Markov approximation

Ignore correlations between field and atoms (free space)

Ignore propagation time $L/c \ll 1/\Gamma$ typical evolution time

Dicke superradiance

R. H. Dicke, *Phys. Rev.* **93**, 99 (1954).

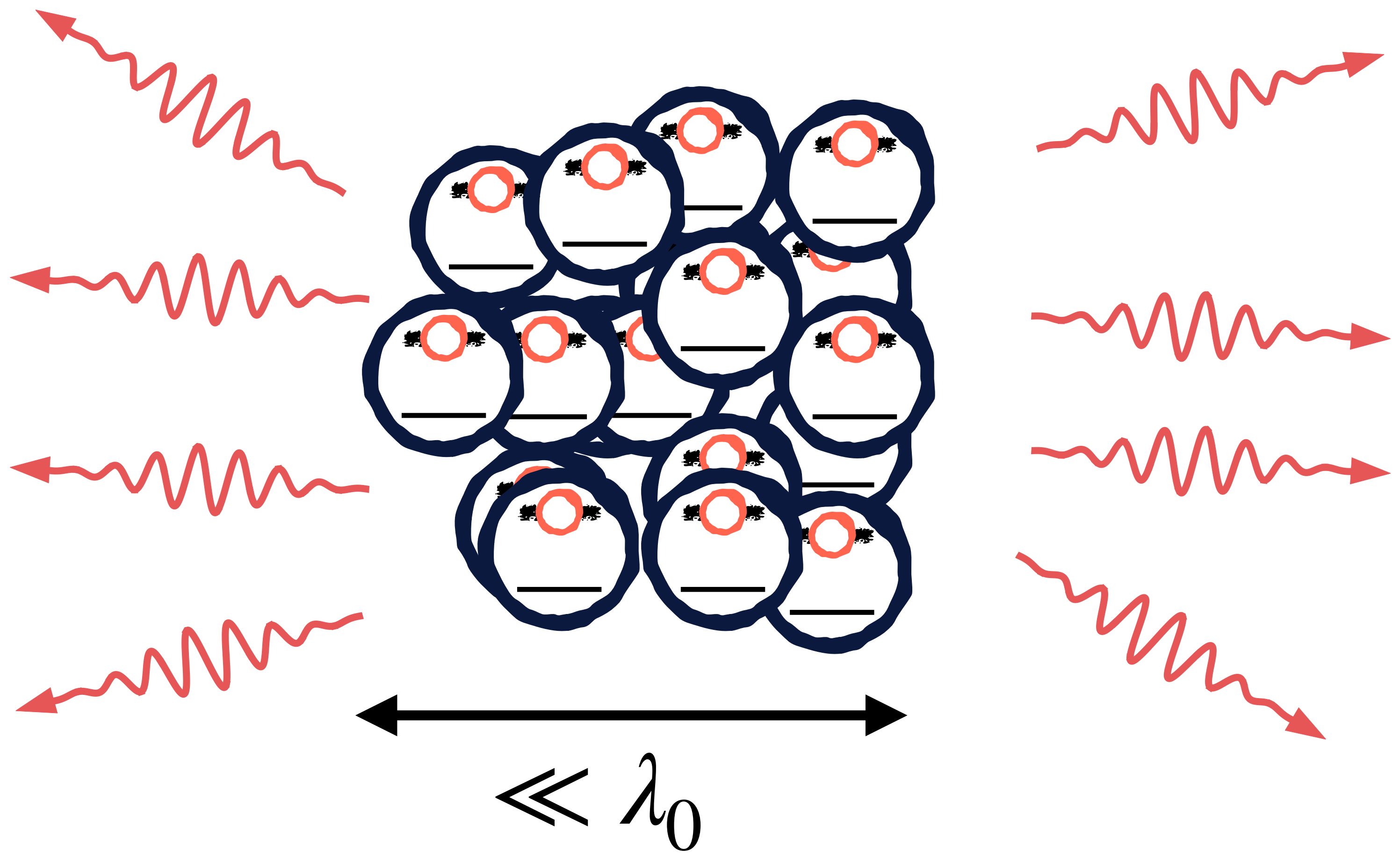

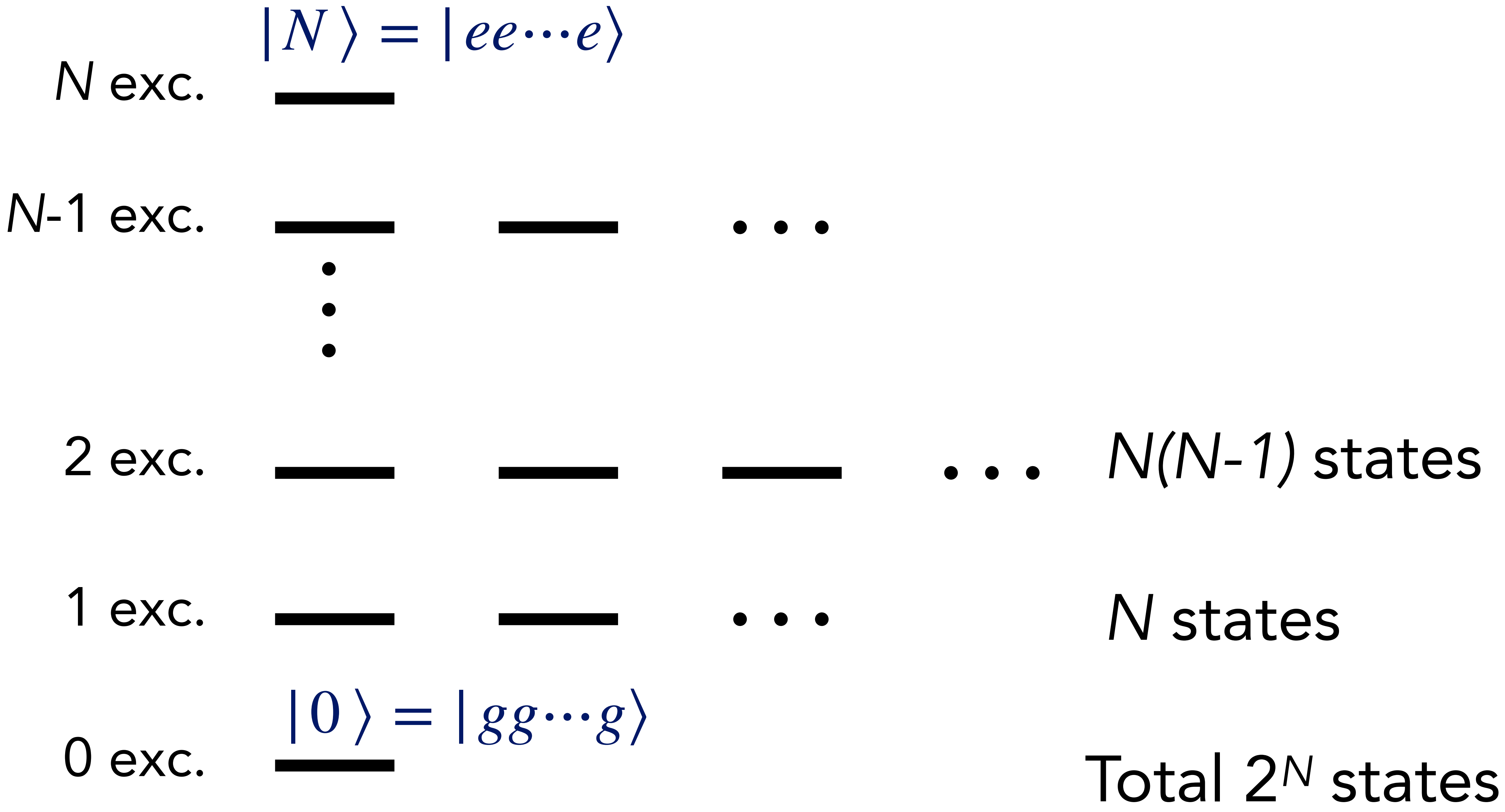

Dicke superradiance

R. H. Dicke, *Phys. Rev.* **93**, 99 (1954).

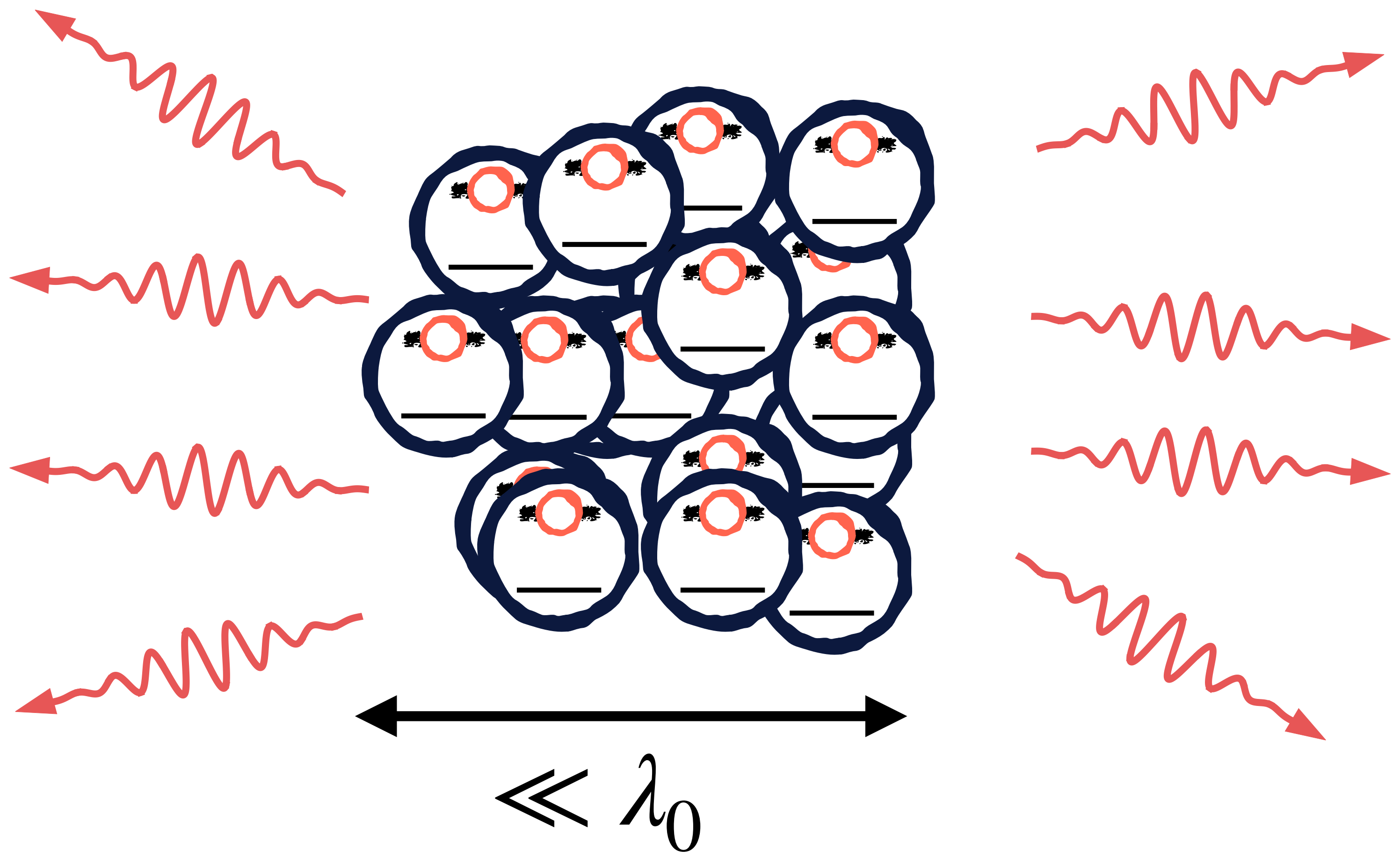

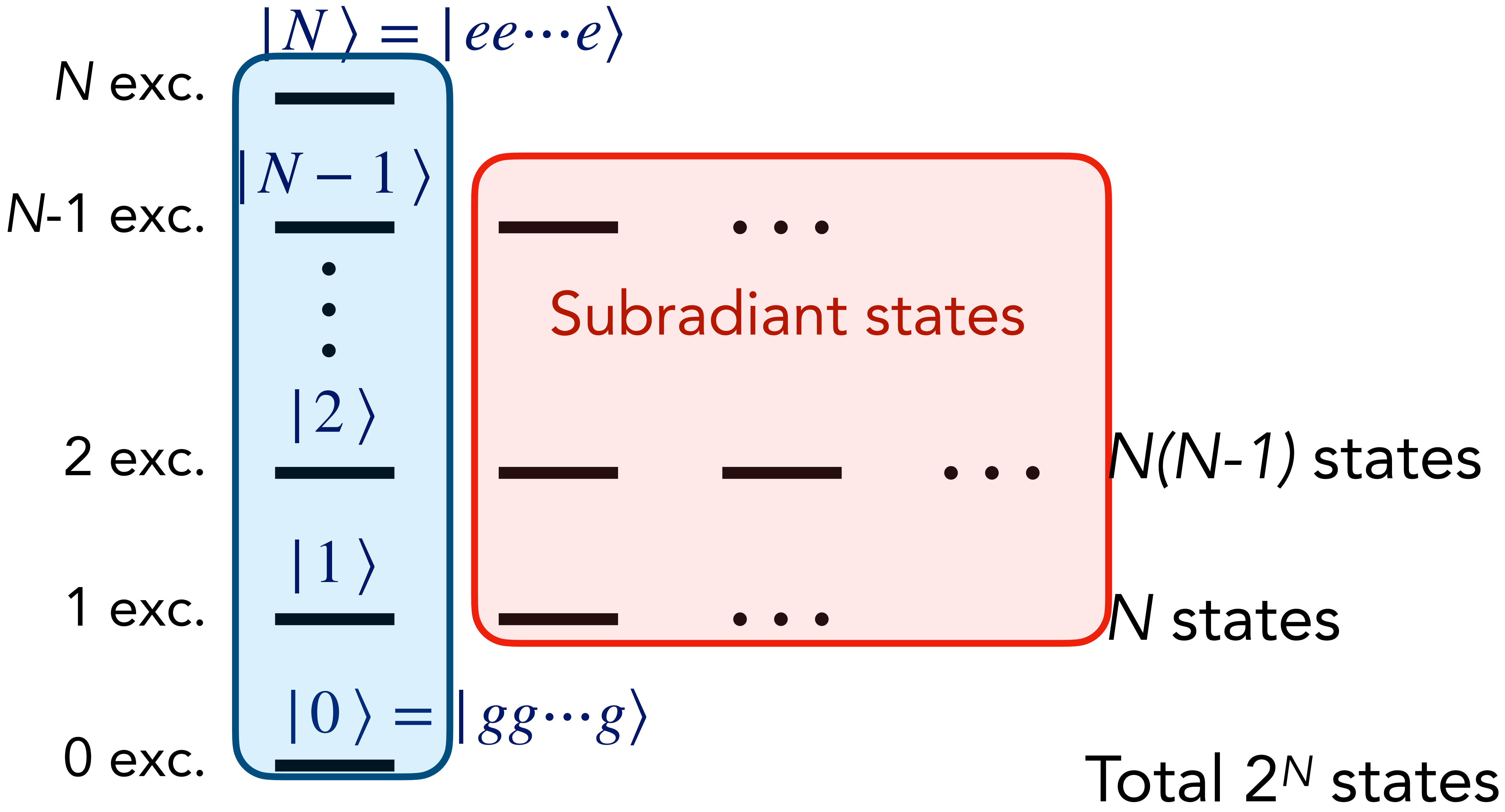

Dicke superradiance

R. H. Dicke, *Phys. Rev.* **93**, 99 (1954).

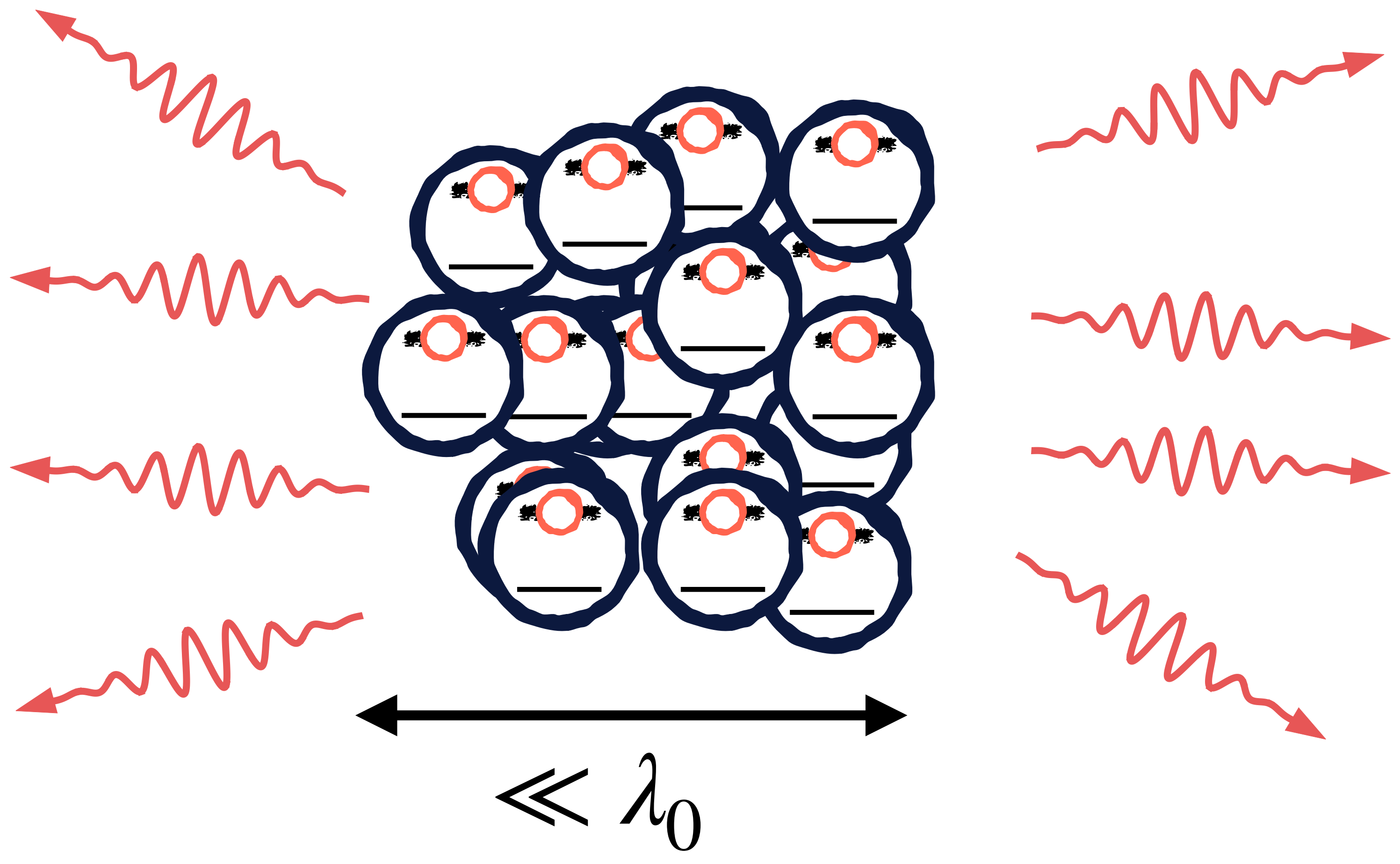

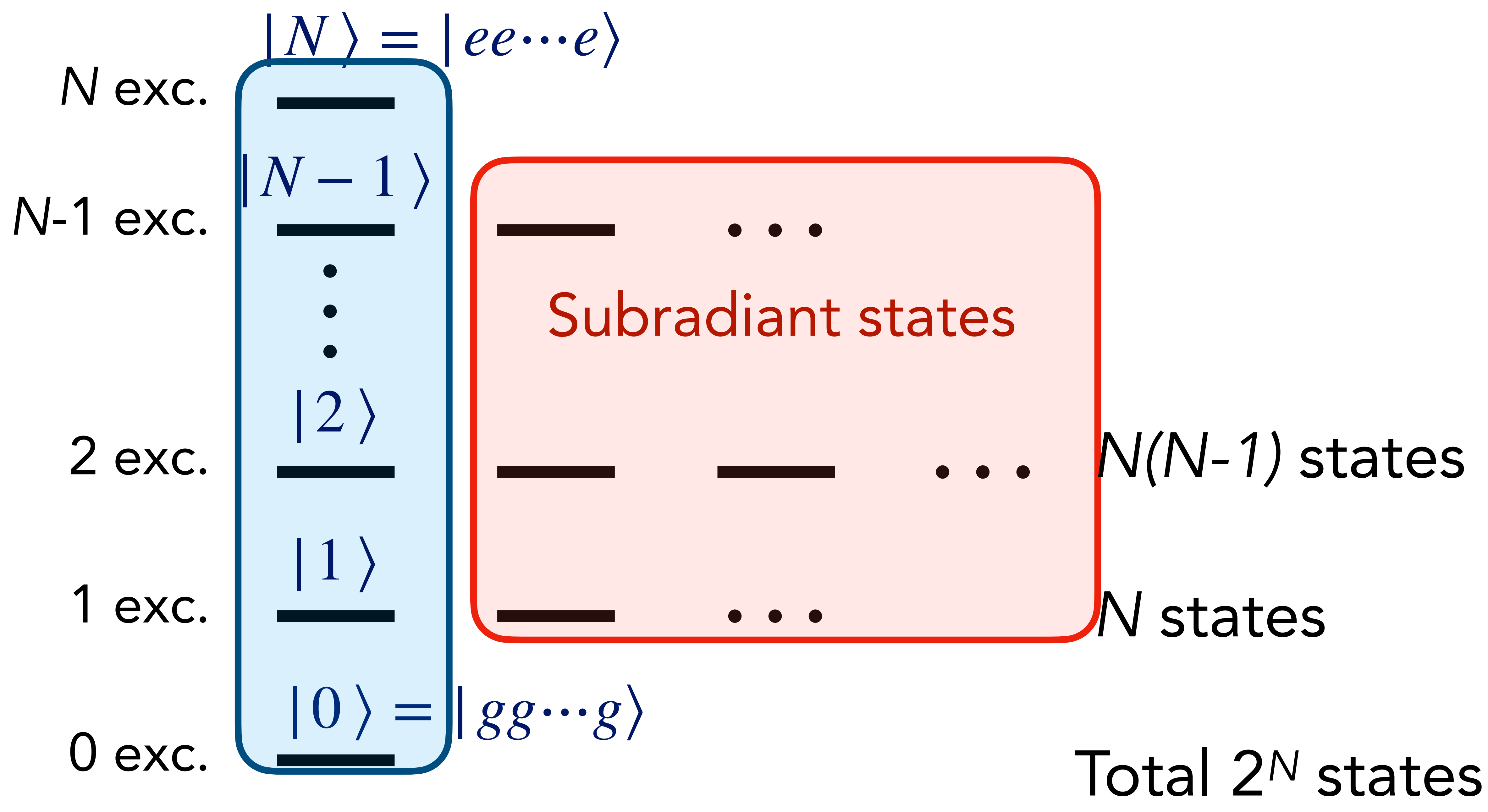

Dicke states $\quad |n\rangle \propto (\hat{S}^+)^n |0\rangle \quad |n\rangle = |J, m\rangle \quad J = \dfrac{N}{2},\ m = n - J \quad \hat{S}^+ = \sum_{i=1}^{N} \hat{S}_i^+$

$$H = \frac{\Omega}{2}\left(\hat{S}^- + \hat{S}^+\right) \qquad L(\rho) = \frac{\Gamma}{2}\left(2\hat{S}^-\rho\hat{S}^+ - \hat{S}^+\hat{S}^-\rho - \rho\hat{S}^+\hat{S}^-\right)$$

Dicke superradiance

R. H. Dicke, *Phys. Rev.* **93**, 99 (1954).

$$I(\boldsymbol{R}) = \langle \hat{E}^{-}(\boldsymbol{R})\hat{E}^{+}(\boldsymbol{R})\rangle$$

$$\hat{E}^{+}(\boldsymbol{R}) \propto \sum_{n=1}^{N} G(\boldsymbol{R} \cancel{- \boldsymbol{r}_n}, \omega_0)\hat{\sigma}_n^{-}$$

$$I = I_1\langle \hat{S}^{+}\hat{S}^{-}\rangle \qquad \Gamma_N = \Gamma_0\langle \hat{S}^{+}\hat{S}^{-}\rangle$$

$$\langle n-1\,|\,\hat{S}^{-}\,|\,n\rangle = \sqrt{n(-n+N+1)}$$

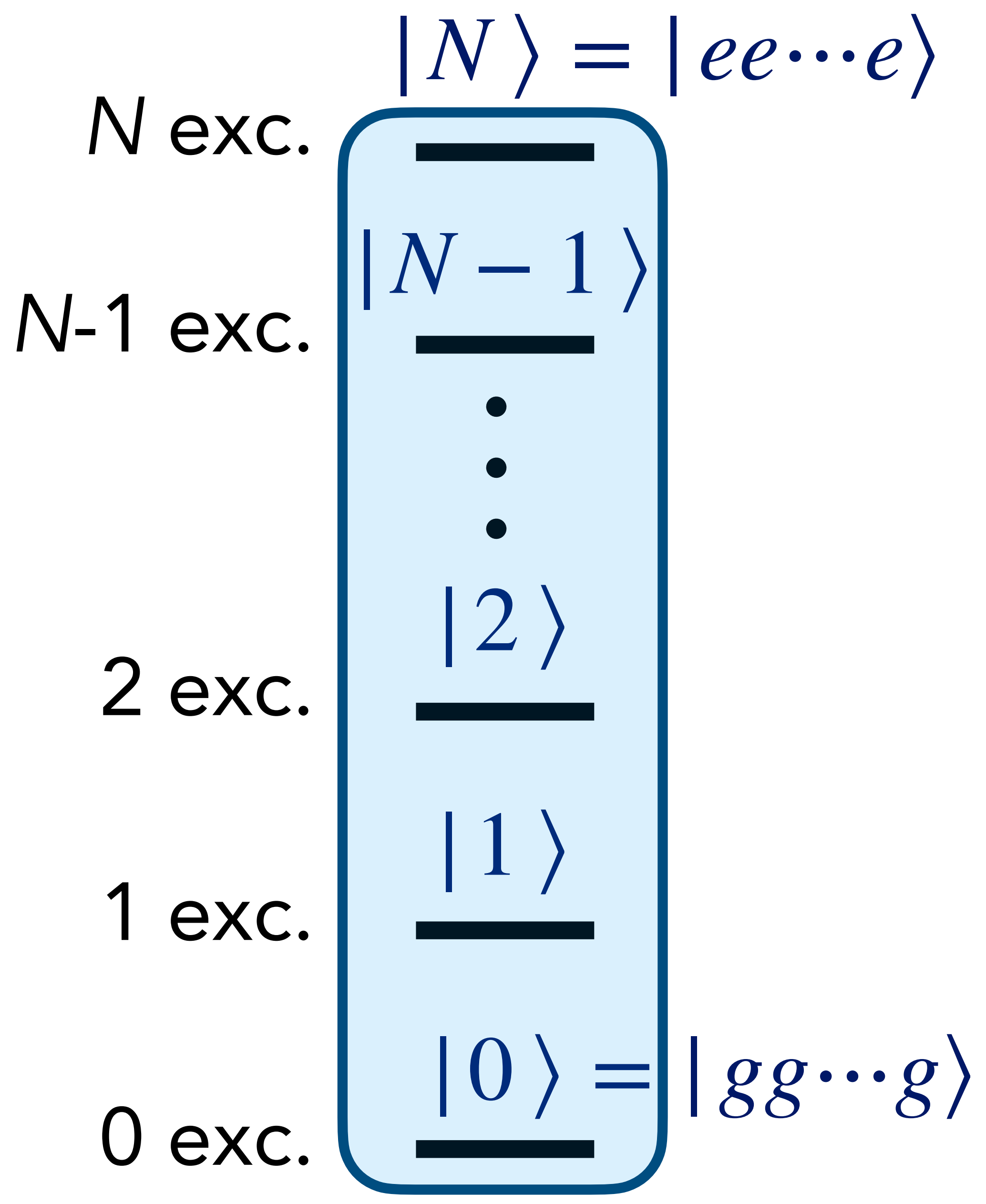

Dicke superradiance

R. H. Dicke, *Phys. Rev.* **93**, 99 (1954).

$$I(\boldsymbol{R}) = \langle \hat{E}^{-}(\boldsymbol{R})\hat{E}^{+}(\boldsymbol{R})\rangle$$

$$\hat{E}^{+}(\boldsymbol{R}) \propto \sum_{n=1}^{N} G(\boldsymbol{R} \cancel{- \boldsymbol{r}_n}, \omega_0)\hat{\sigma}_n^{-}$$

$$I = I_1\langle \hat{S}^{+}\hat{S}^{-}\rangle \qquad \Gamma_N = \Gamma_0\langle \hat{S}^{+}\hat{S}^{-}\rangle$$

$$\langle n-1 \,|\, \hat{S}^{-} \,|\, n\rangle = \sqrt{n(-n+N+1)}$$

$$\Gamma_N = \Gamma_0\, n(N-n+1)$$ in state $|\, n\,\rangle$

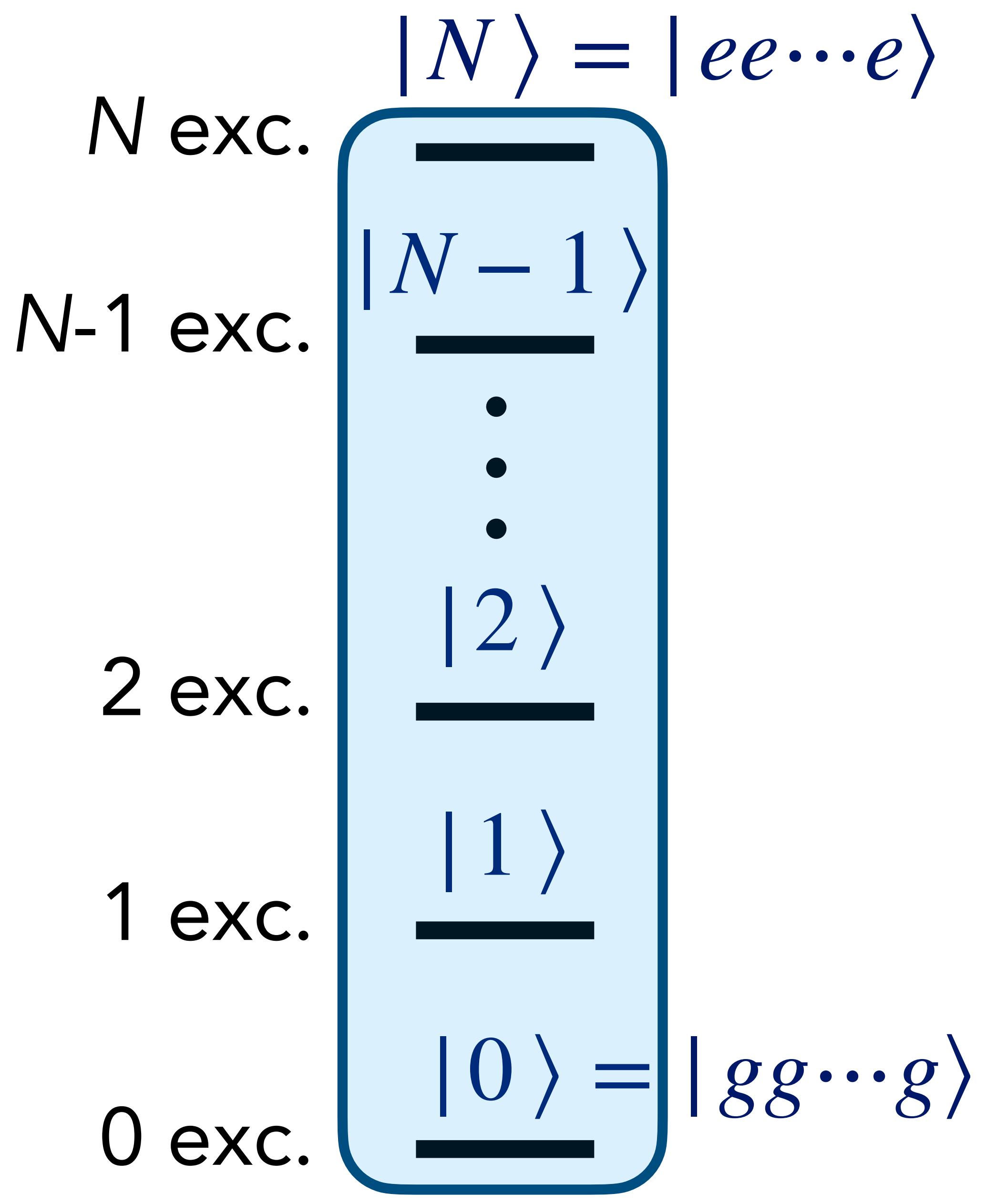

Reaches maximum for $|\, n\,\rangle = |\, N/2\,\rangle$, with $\Gamma_N \simeq N^2\Gamma_0/4$

Dicke superradiance

$\Gamma_N = \Gamma_0 \, n(N - n + 1)$ in state $|\, n \,\rangle$

Starting from fully excited state: pulse of light

Peak power $\propto N^2$

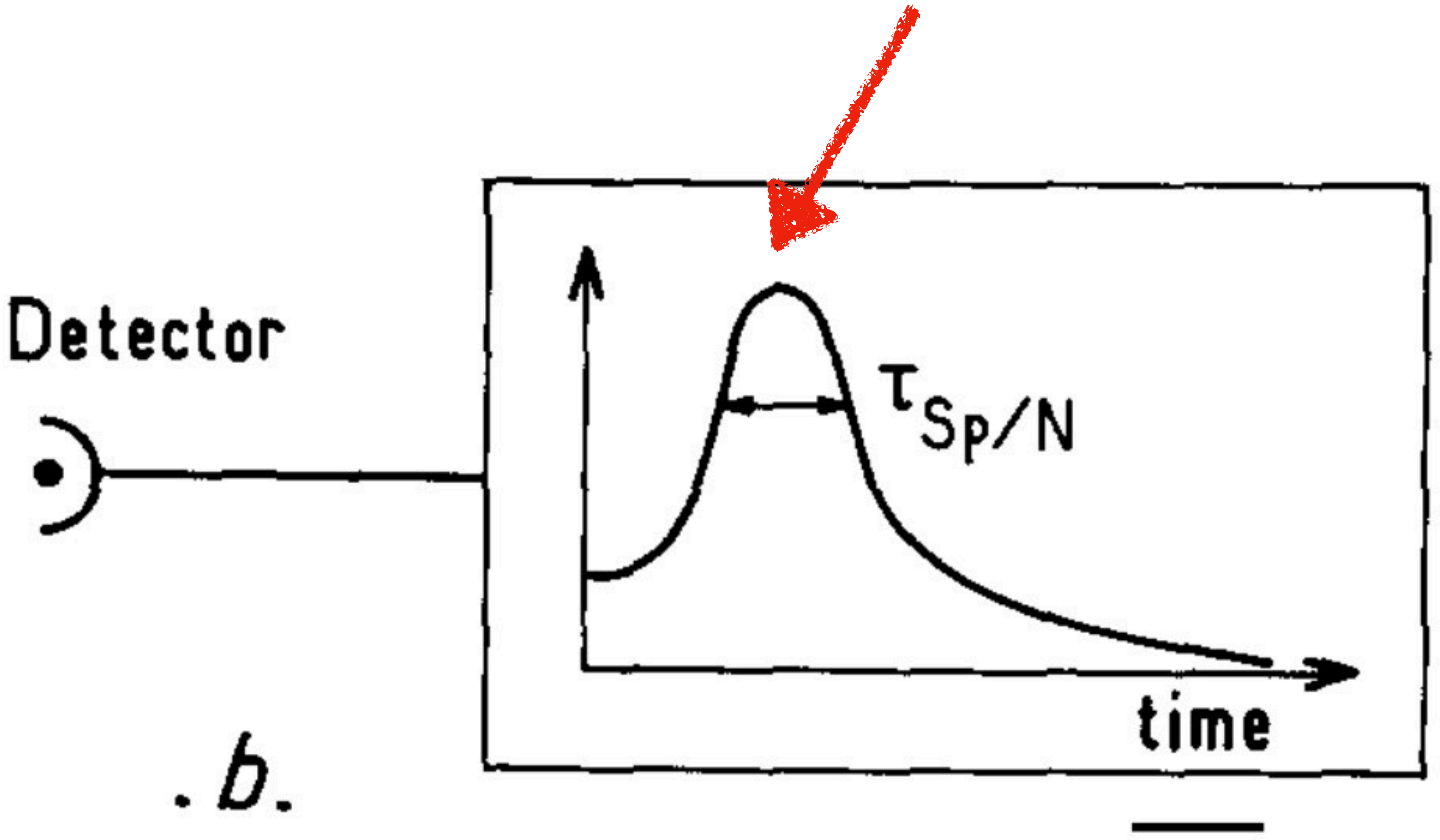

Gross & Haroche, *Physics Reports* **93**, 301 (1982).

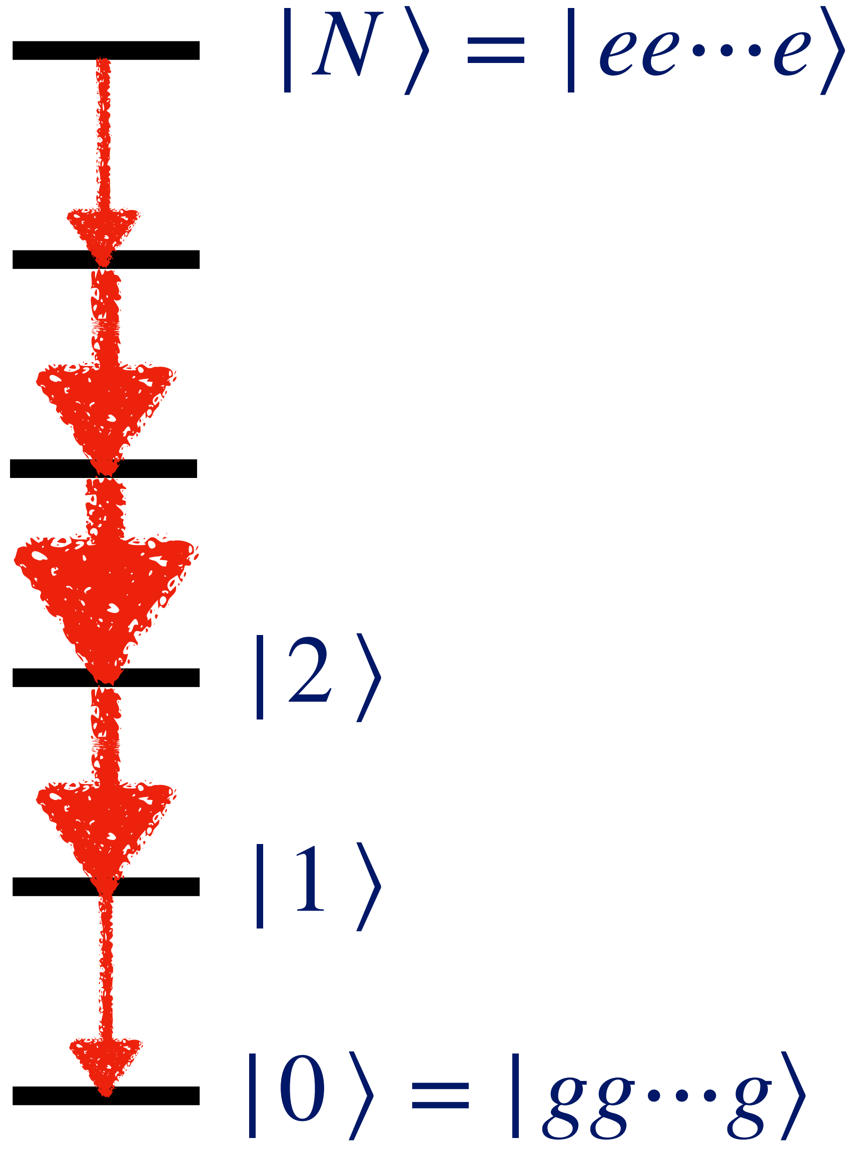

$\langle \hat{\sigma}_i^+ \hat{\sigma}_j^- \rangle = 0$

$\langle \hat{\sigma}_i^+ \hat{\sigma}_j^- \rangle \simeq \dfrac{1}{4}$

$\langle \hat{\sigma}_i^+ \hat{\sigma}_j^- \rangle = 0$

Superradiance induces correlations during decay

Despite $\langle \hat{\sigma}_i^- \rangle = \langle \hat{S}^- \rangle / N = 0$ at all times

Dicke superradiance

Extended clouds (size $\gg \lambda_0$): dynamics governed by effective atom number

$$\mu = \frac{P_{\mathrm{coop}}}{N P_1}$$

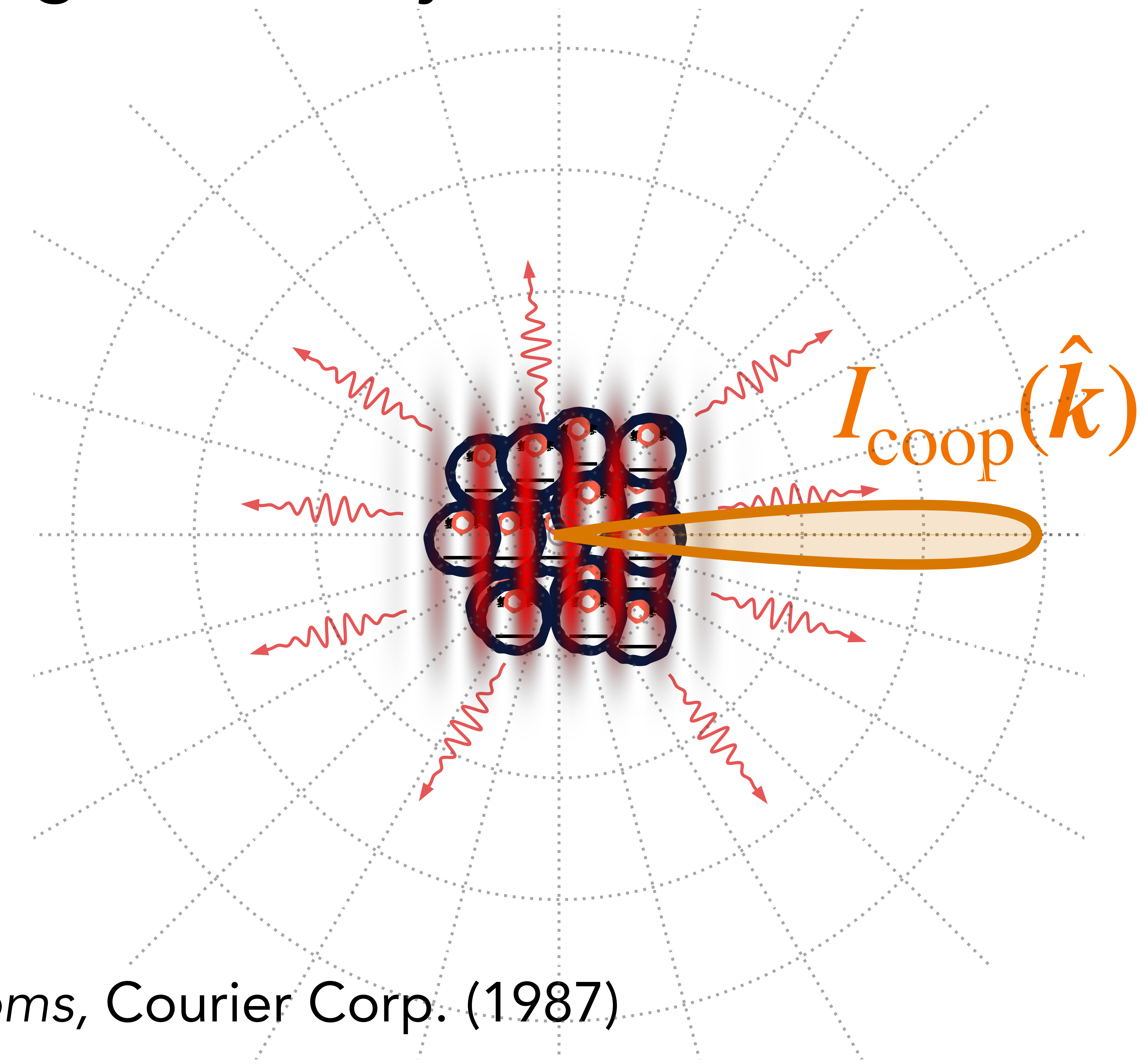

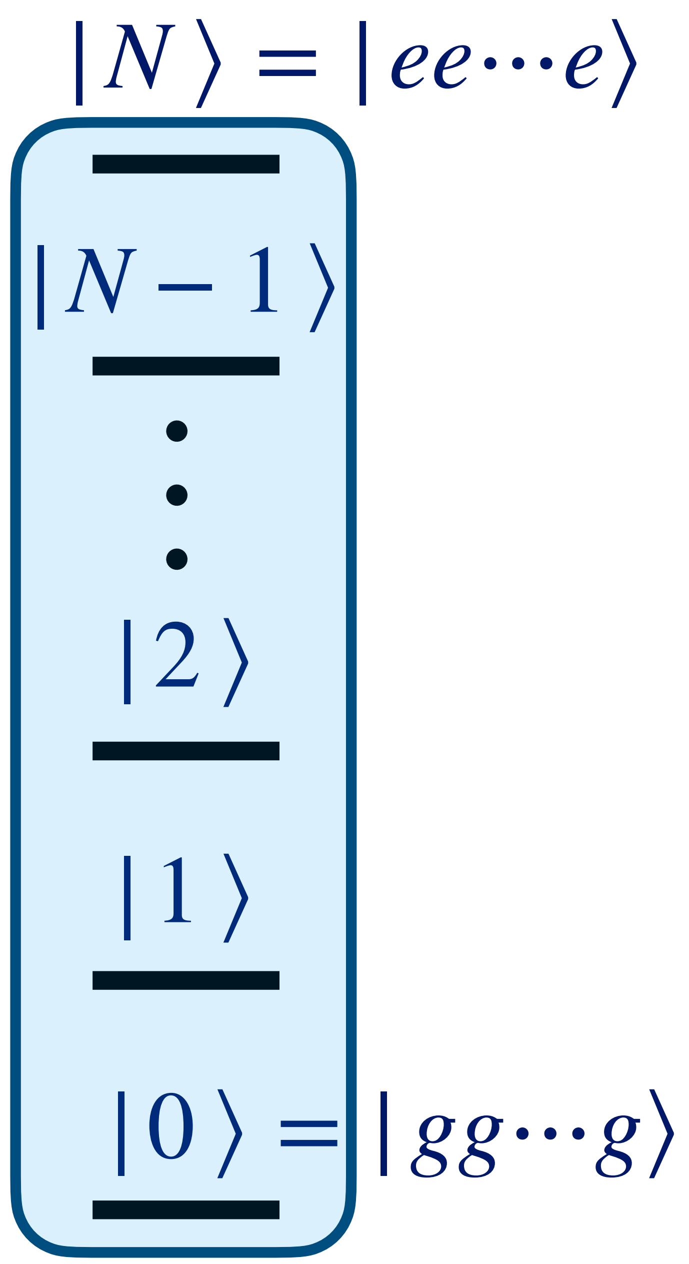

Dicke case: $\mu = 1$

General case: $N \to \tilde{N} = \mu N$

Gross & Haroche, *Physics Reports* **93**, 301 (1982).

Allen & Eberly, *Optical resonance and two-level atoms*, Courier Corp. (1987)

Dicke superradiance

Extended clouds (size $\gg \lambda_0$): dynamics governed by effective atom number

$$\mu = \frac{P_{\mathrm{coop}}}{N P_1}$$

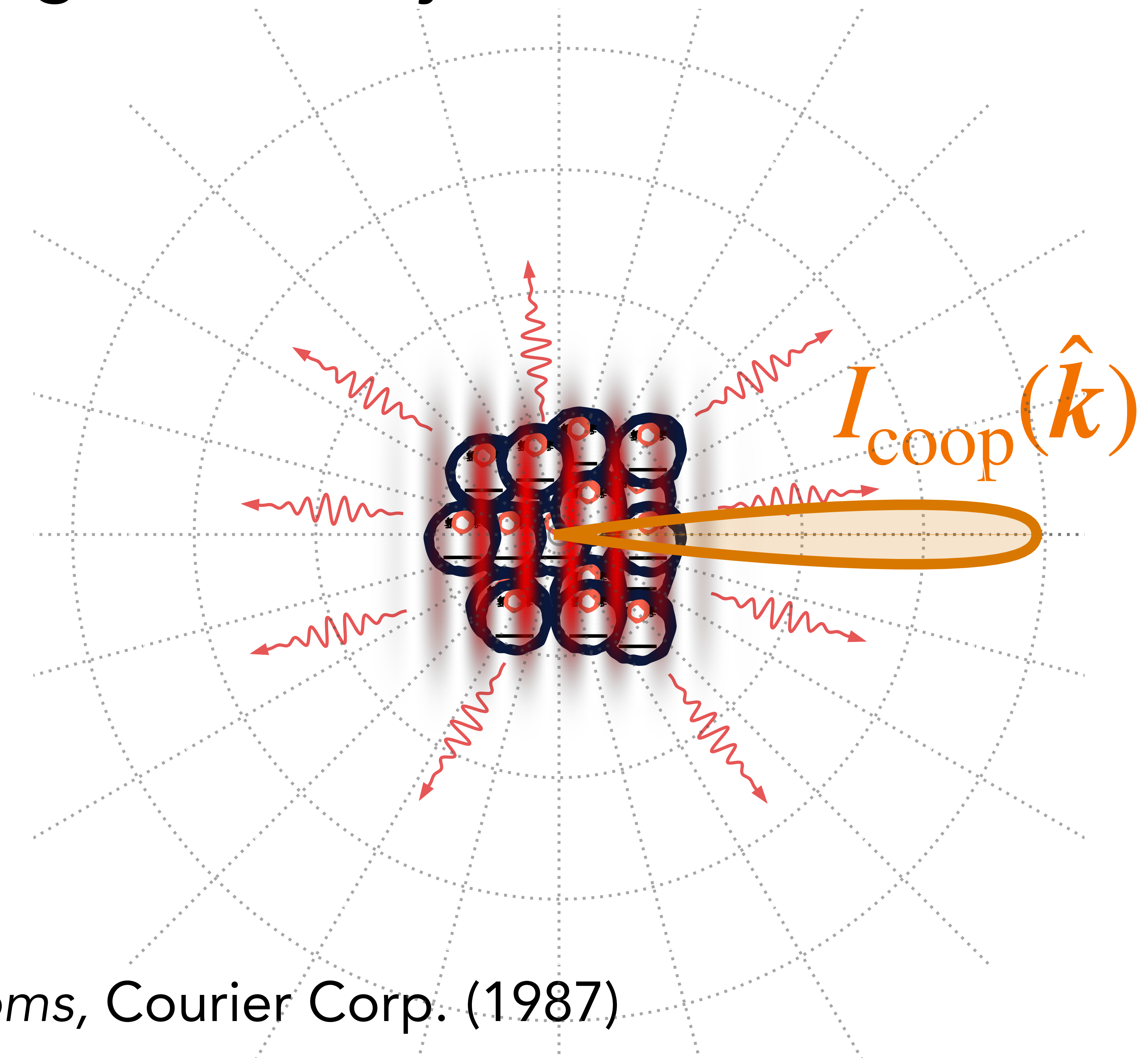

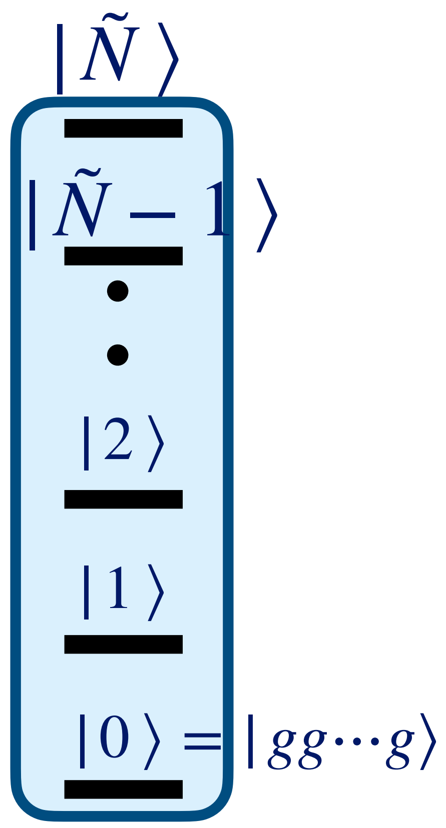

Dicke case: $\mu = 1$

General case: $N \to \tilde{N} = \mu N$

Gross & Haroche, *Physics Reports* **93**, 301 (1982).

Allen & Eberly, *Optical resonance and two-level atoms*, Courier Corp. (1987)

Dicke superradiance, first observations

Skribanowitz *et al.*, *Phys Rev Lett* **30**, 309–312 (1973).

Gross *et al.*, *Phys Rev Lett* **36**, 1035–1038 (1976).

Multilevel molecules of atoms, pumped via auxiliary transition

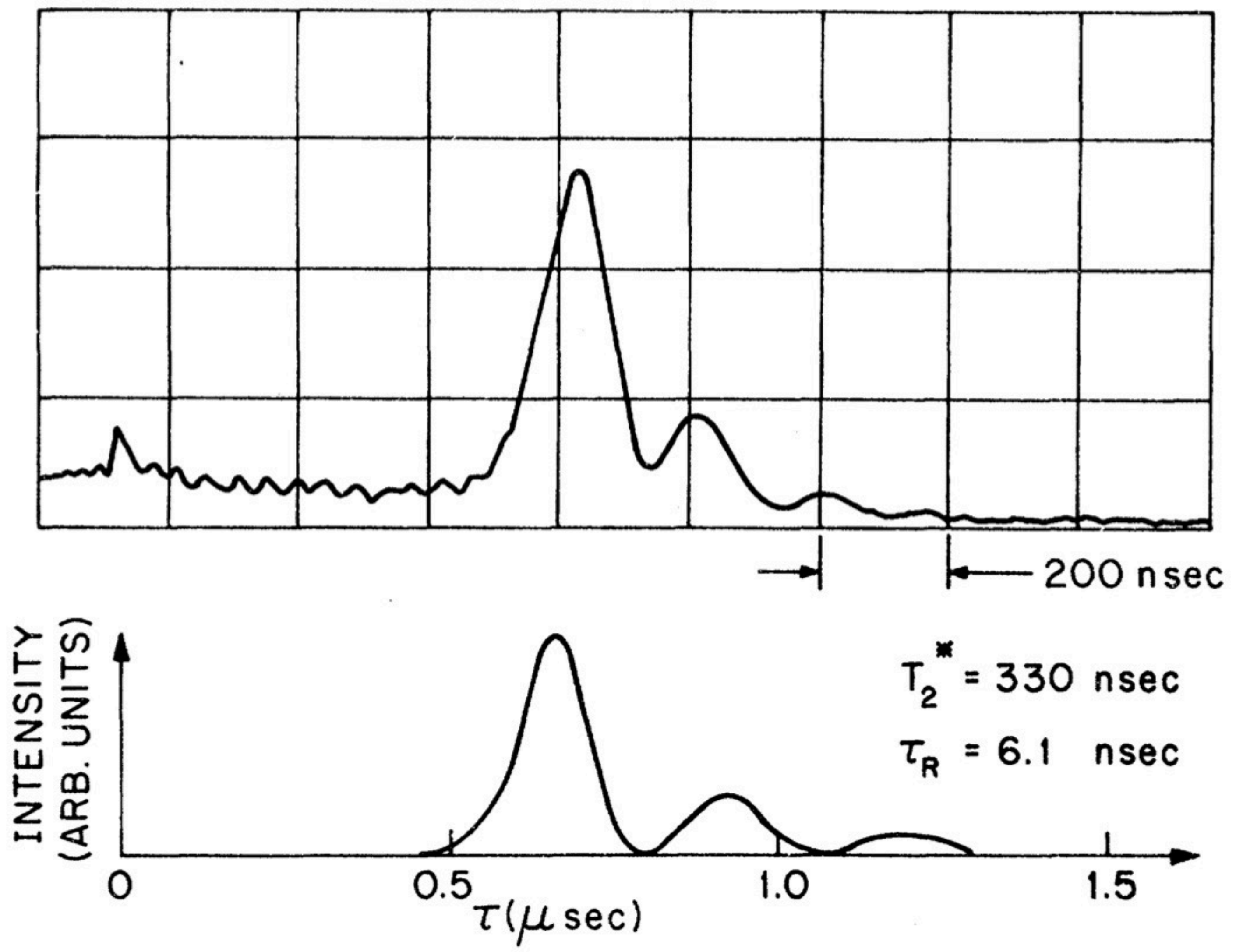

FIG. 1. Oscilloscope trace of superradiant pulse at 84 μm ($J=3\to 2$), pumped by the $R_1(2)$ laser line, and theoretical fit. The parameters are $I=1$ kW/cm^2, $p=1.3$ mTorr, and $kl=2.5$ for $l=100$ cm. The small peak on the scope trace at $\tau=0$ is the 3-μm pump pulse, highly attenuated.

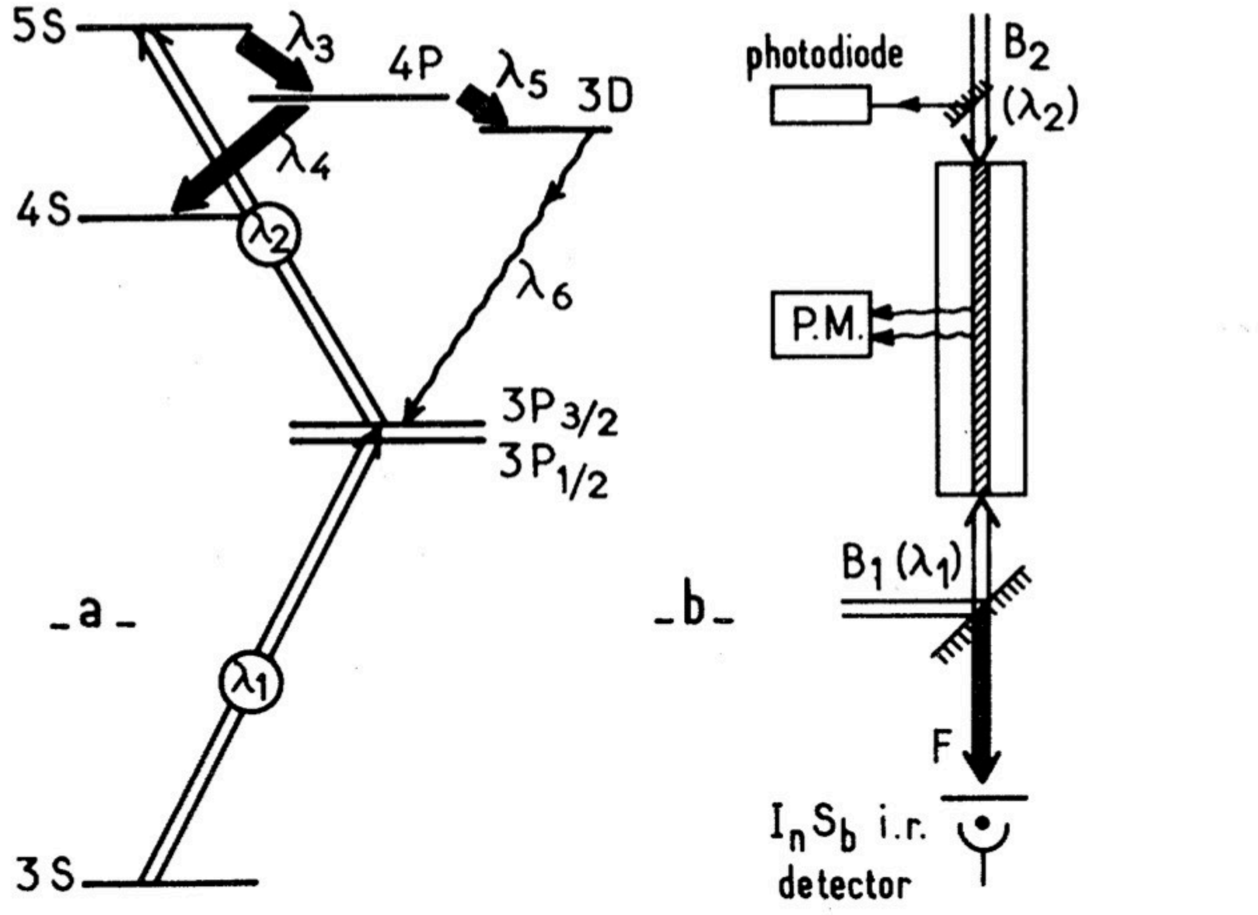

FIG. 1. (a) Diagram of Na energy levels relevant for superradiance experiment. Double-line arrows, pumping transition at $\lambda_1=0.5890$ and $\lambda_2=0.6160$ μm; solid-line arrows, superradiant transitions $\lambda_3=3.41$, $\lambda_4=2.21$, and $\lambda_5=9.10$ μm; wavy line, transition at $\lambda_6=0.8191$ μm detected off-axis by the photomultiplier. (b) Sketch of experimental setup showing collinear pumping beams B_1 and B_2, on-axis InSb detector, and off-axis photomultiplier.

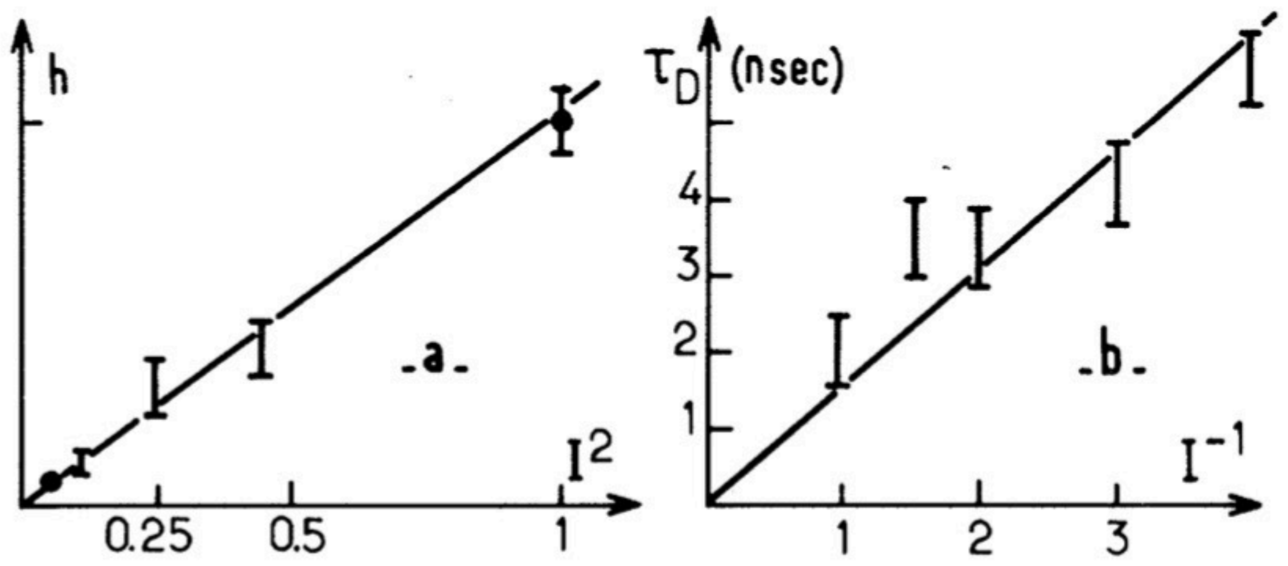

FIG. 3. (a) Height h of 3.41-μm pulse versus I^2, square of B_2 pumping beam intensity. (b) Delay of 3.41-μm pulse versus I^{-1} (I in arbitrary units).

Dicke superradiance, recent experiments

Modern tools: dense clouds of 2-level atoms, resonantly driven

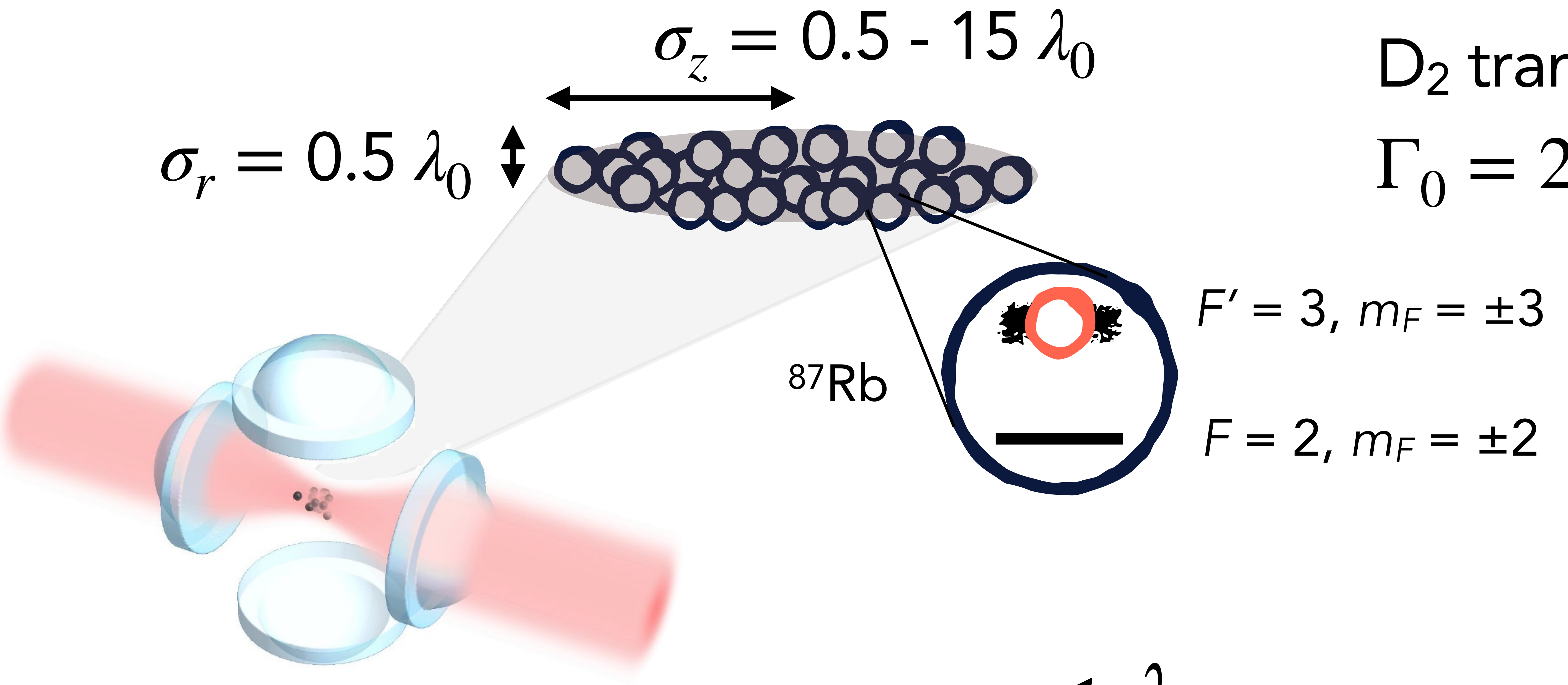

D_2 transition, $\lambda_0 = 780$ nm,
$\Gamma_0 = 2\pi \times 6$ MHz, $\tau_0 \simeq 25$ ns

$$\sigma_r < \lambda_0 \rightarrow \mu \sim \frac{1}{k_0 \sigma_z}$$

Dense clouds of 2-level atoms

Observations

Single photon detection (NA=0.45)

Along two directions

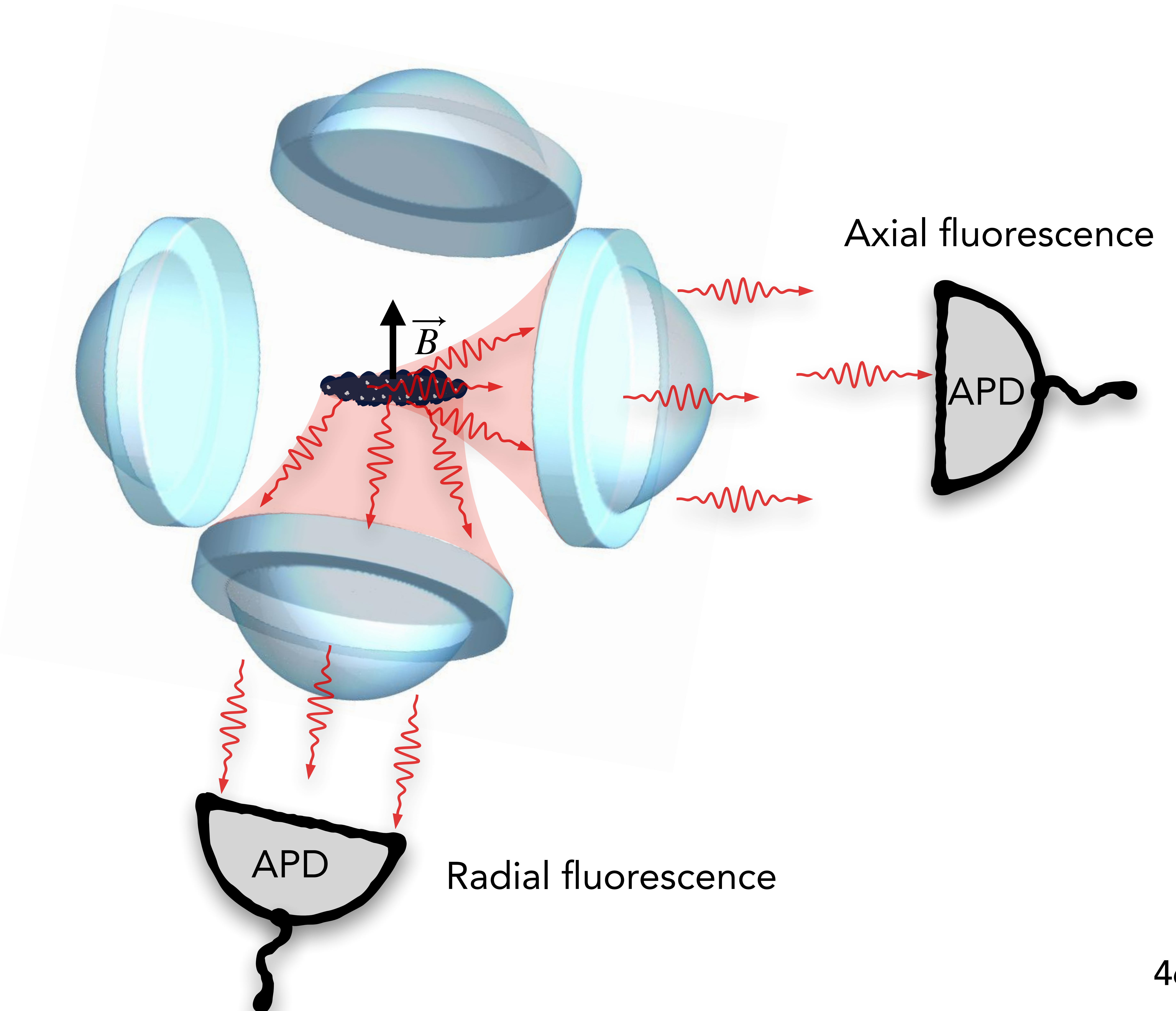

Rabi oscillations

Low atom number

Record axial fluorescence

Very good fit with optical Bloch equations

Independent atoms

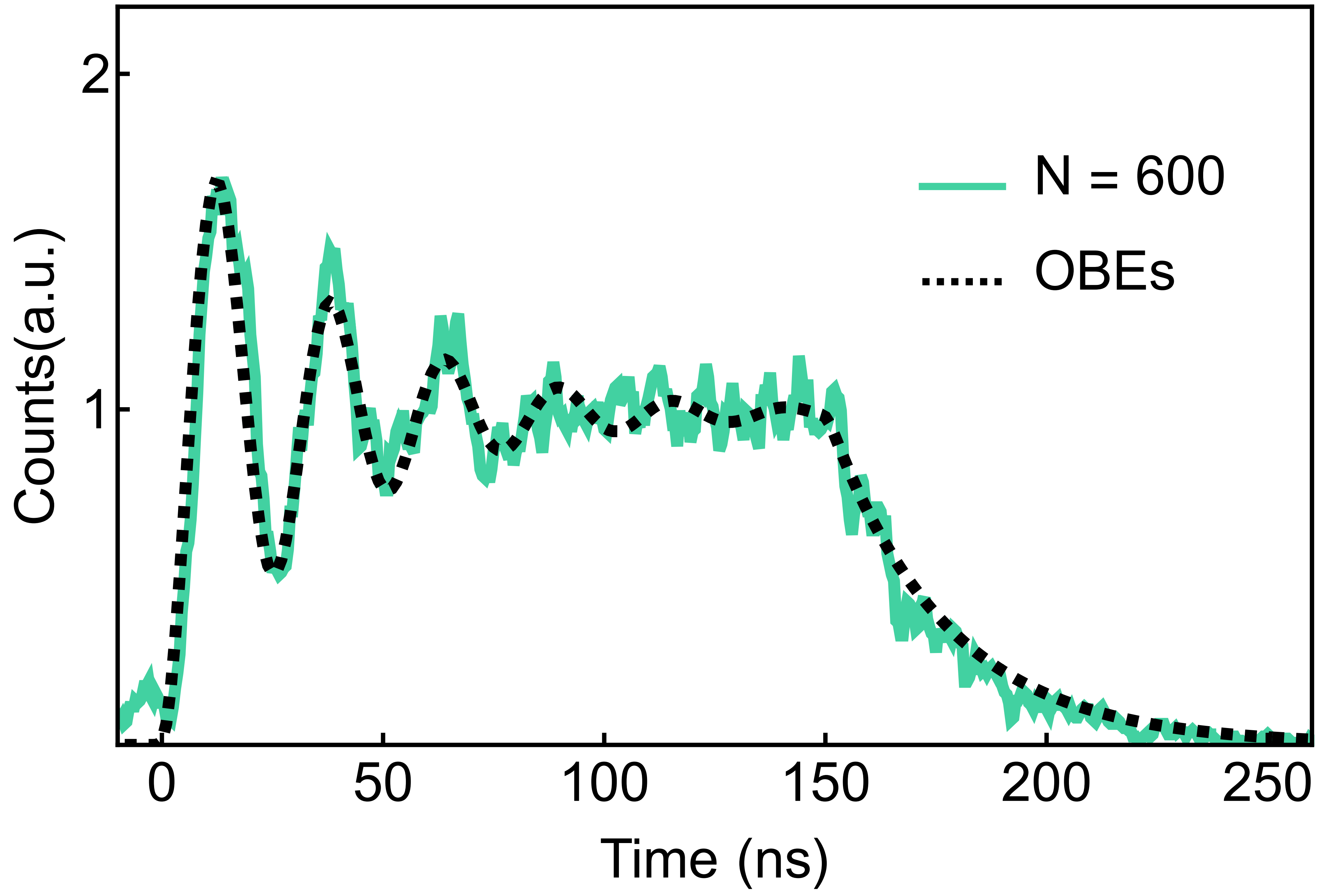

Rabi oscillations

Low atom number

π - time, 85 % in $|e\rangle$

Record axial fluorescence

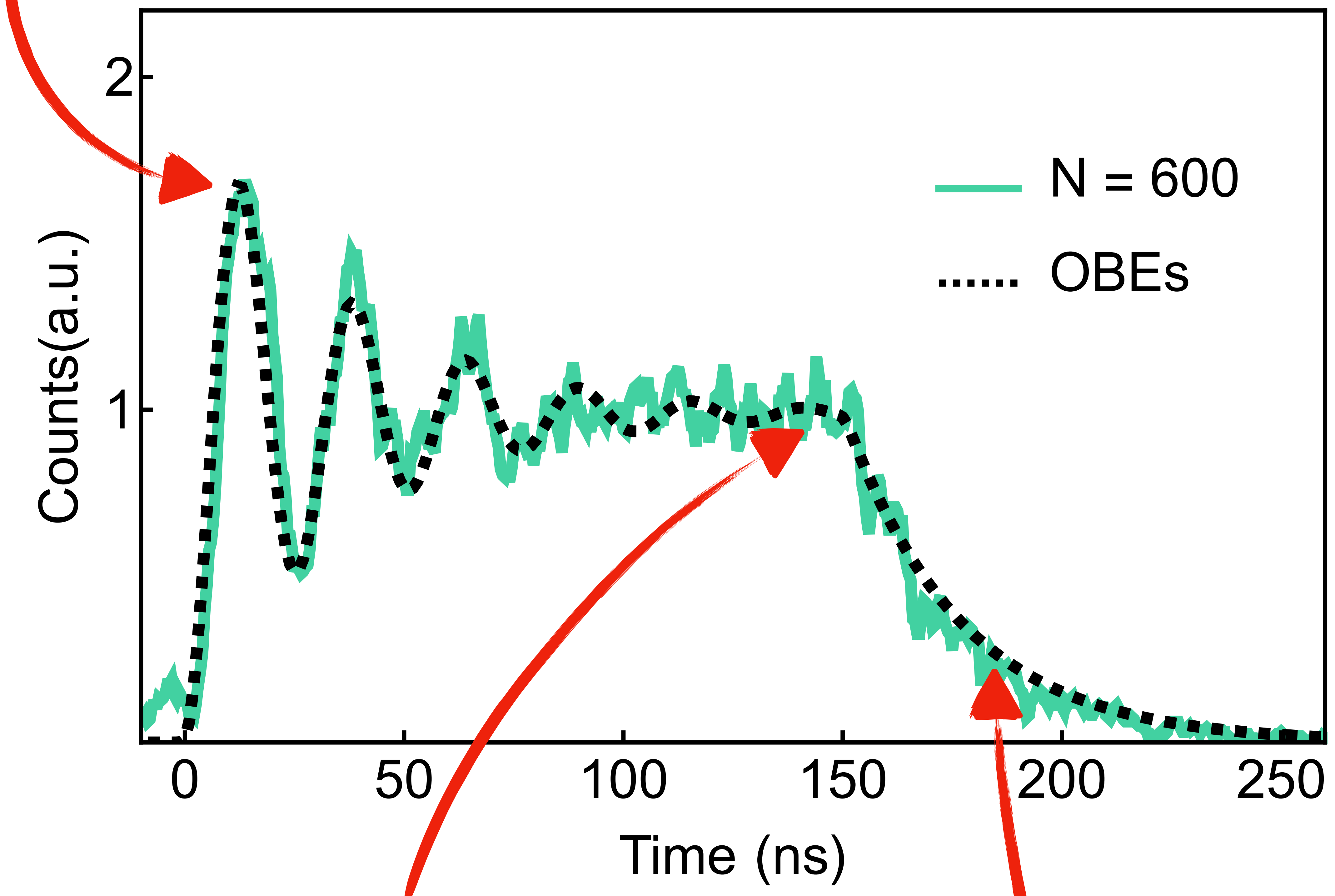

Very good fit with optical Bloch equations

Independent atoms

$$\rho = \left(\frac{|e\rangle\langle e| + |g\rangle\langle g|}{2} \right)^{\otimes N}$$

Decay $\propto e^{-\Gamma_0 t}$

Dicke superradiance

π - pulse (12 ns, s = 85)

Increasing atom number

Axial fluorescence

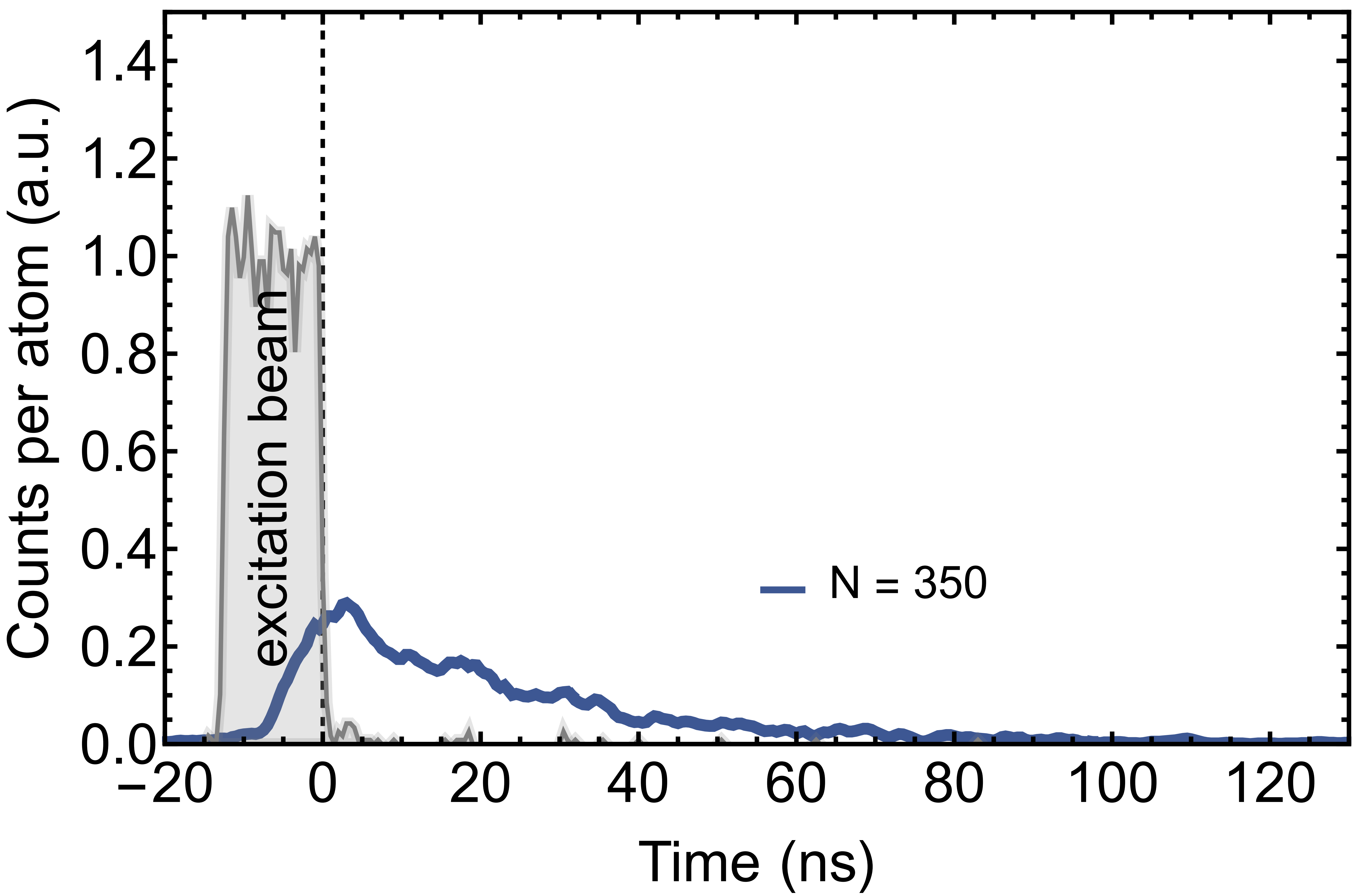

G. Ferioli et al., Phys. Rev. Lett. 127, 243602 (2021)

Dicke superradiance

π - pulse (12 ns, s = 85)

Increasing atom number

Axial fluorescence

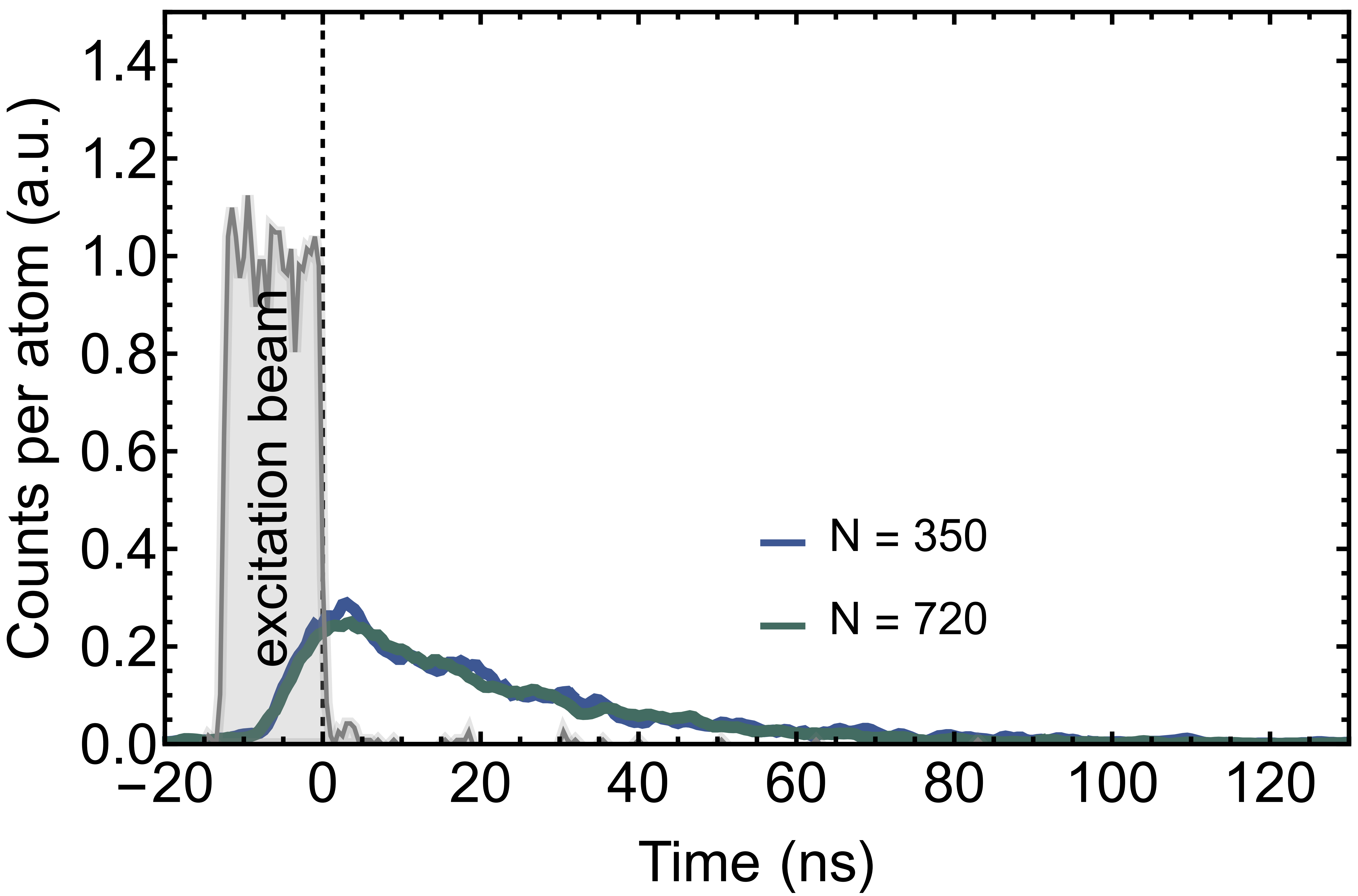

G. Ferioli et al., Phys. Rev. Lett. 127, 243602 (2021)

Dicke superradiance

Superradiant flash

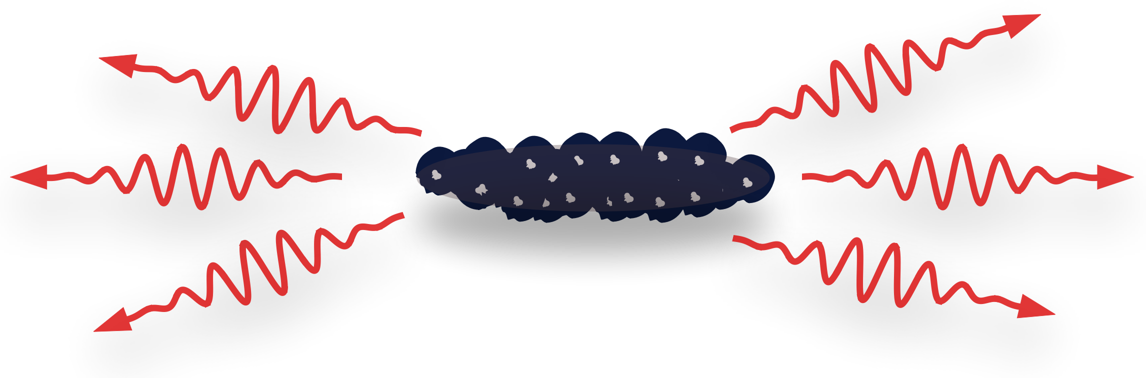

π - pulse (12 ns, s = 85)

Increasing atom number

Axial fluorescence

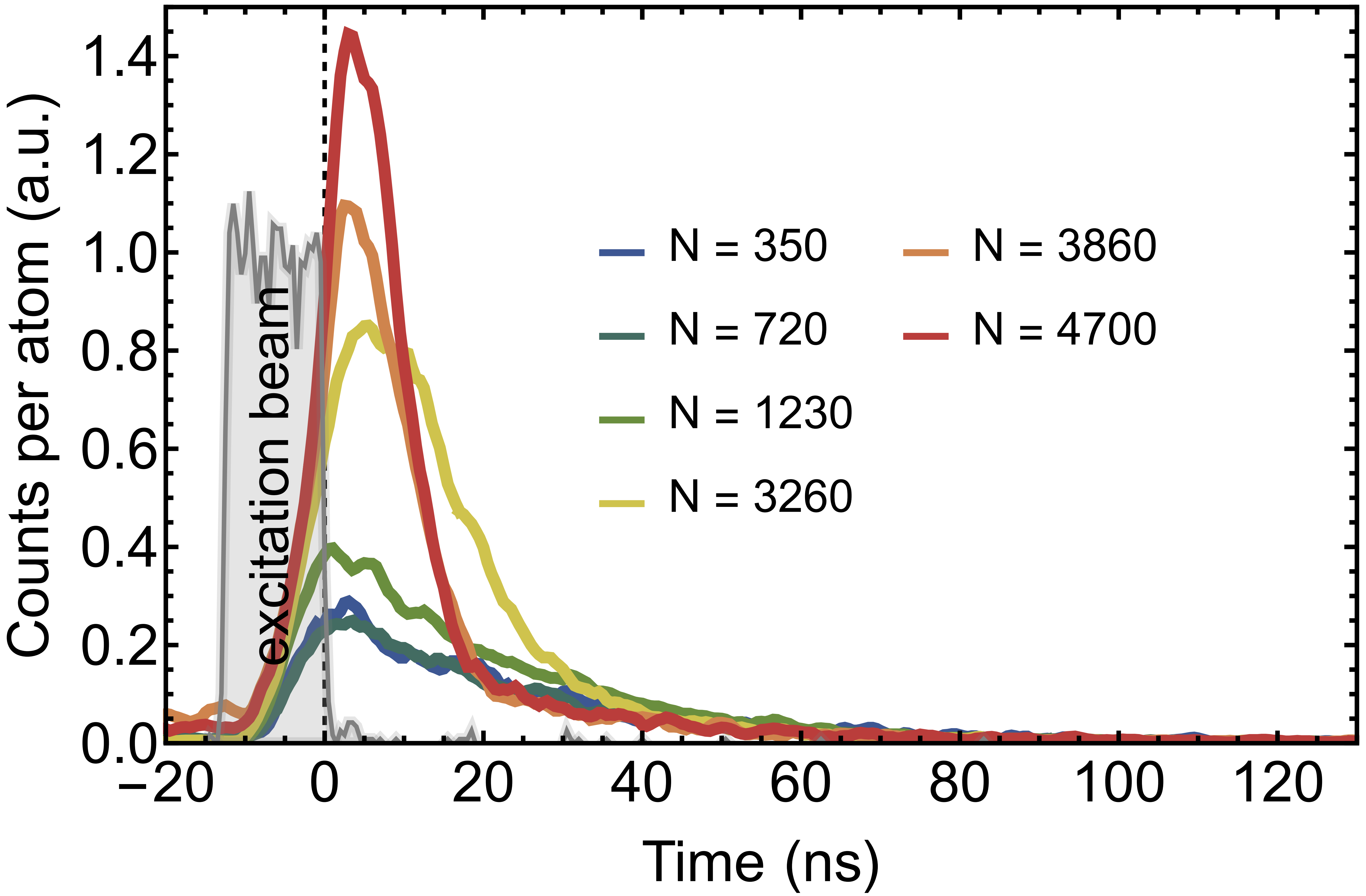

G. Ferioli et al., Phys. Rev. Lett. 127, 243602 (2021)

Dicke superradiance

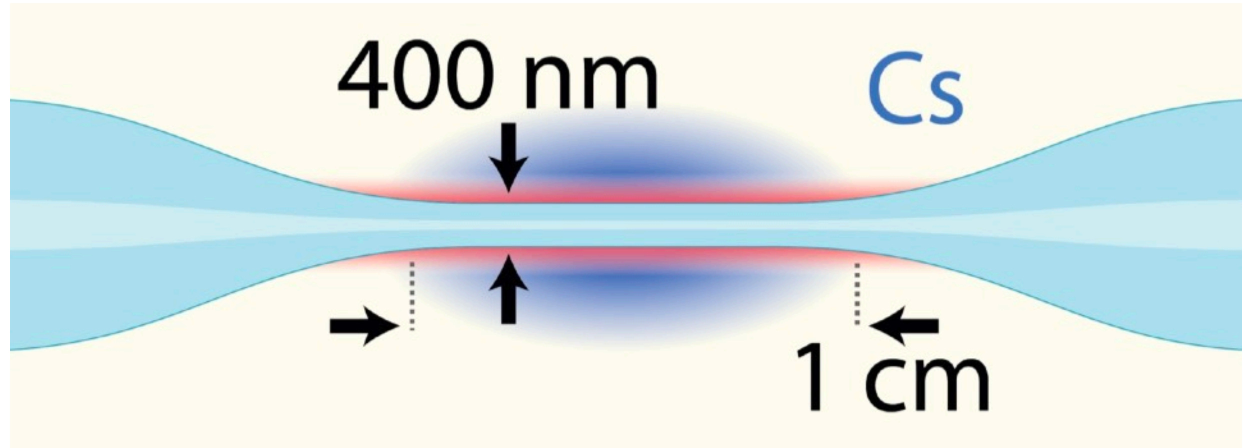

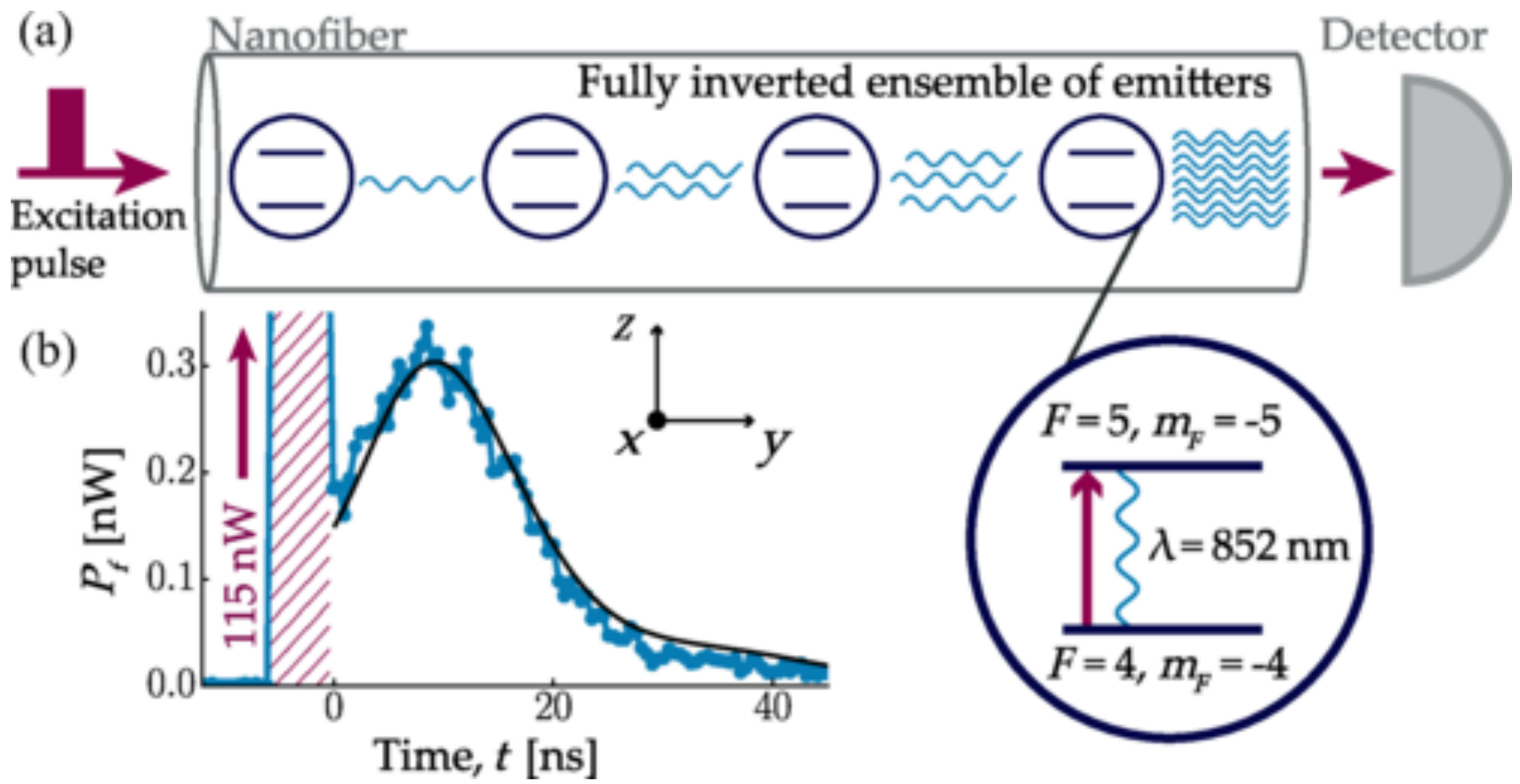

Liedl *et al.*, Phys. Rev. X **14**, 011020 (2024)

Dicke superradiance

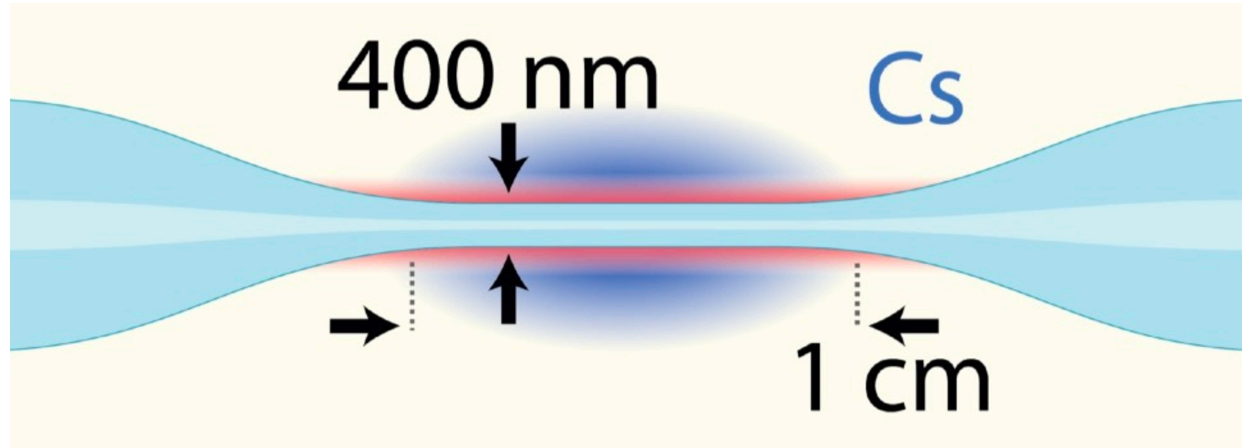

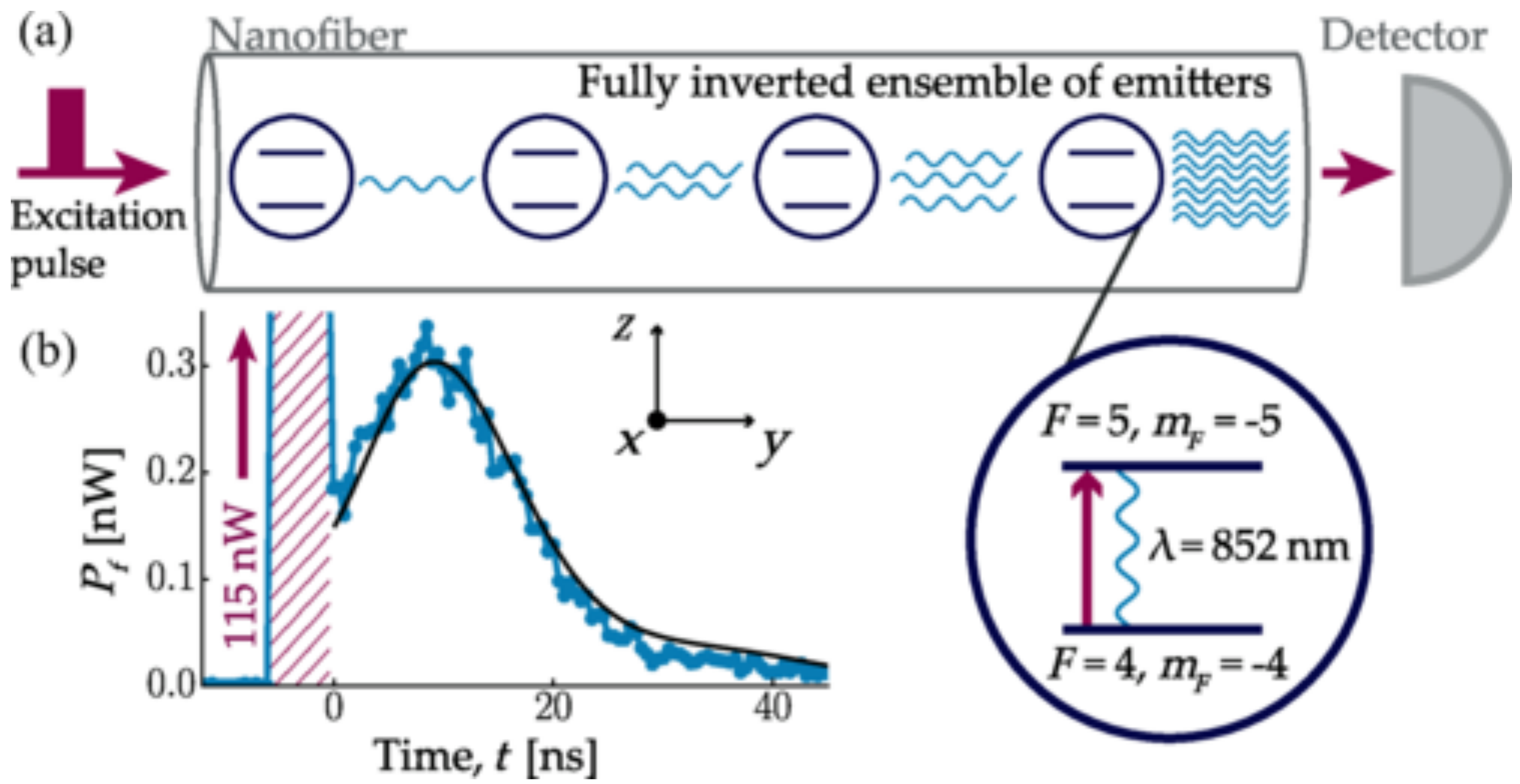

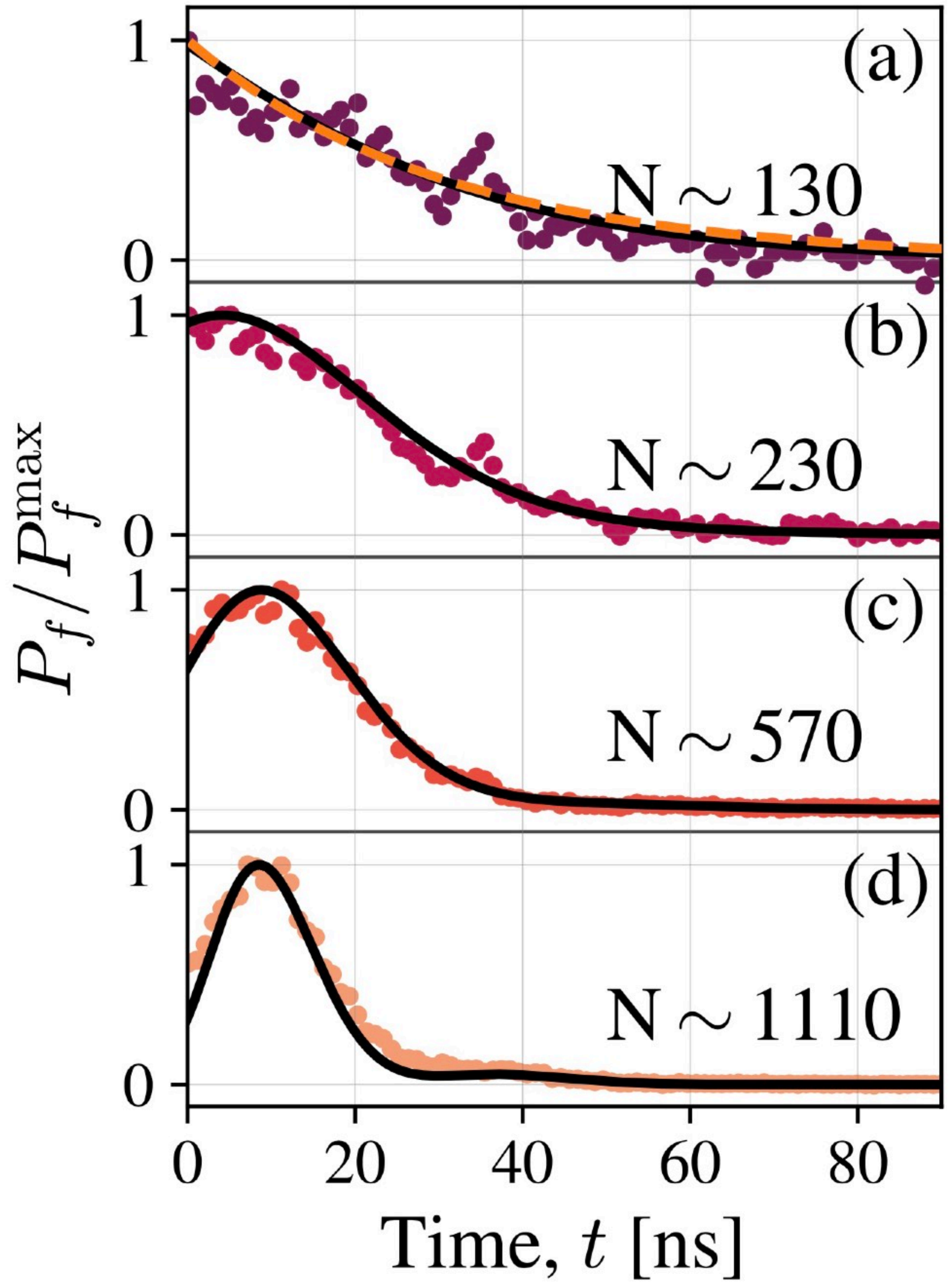

Liedl *et al.*, Phys. Rev. X **14**, 011020 (2024)

Dicke + drive

Dicke symmetric conditions + classical drive

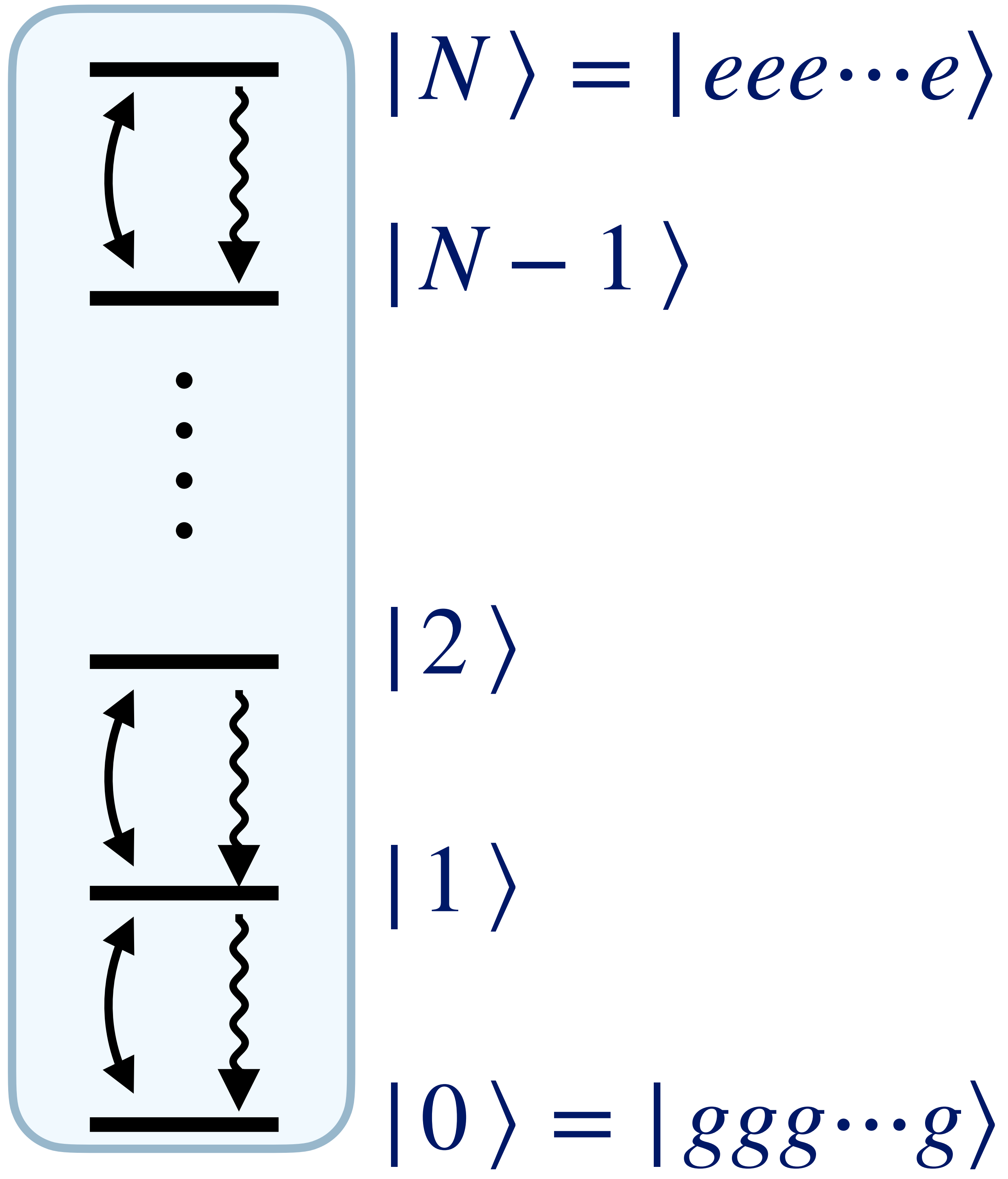

Dicke + drive

Dicke symmetric conditions + classical drive

$$\dot{\hat{\rho}} = \frac{i}{\hbar}\left[\hat{\rho}, \hat{H}\right] + \frac{\Gamma_0}{2}\left(2\hat{S}^-\hat{\rho}\hat{S}^+ - \hat{S}^+\hat{S}^-\hat{\rho} - \hat{\rho}\hat{S}^+\hat{S}^-\right)$$

$$\hat{H} = \frac{\hbar\Omega_D}{2}(\hat{S}^+ + \hat{S}^-)$$

$$\langle n-1 | \hat{S}^- | n \rangle = \sqrt{n(-n+N+1)}$$

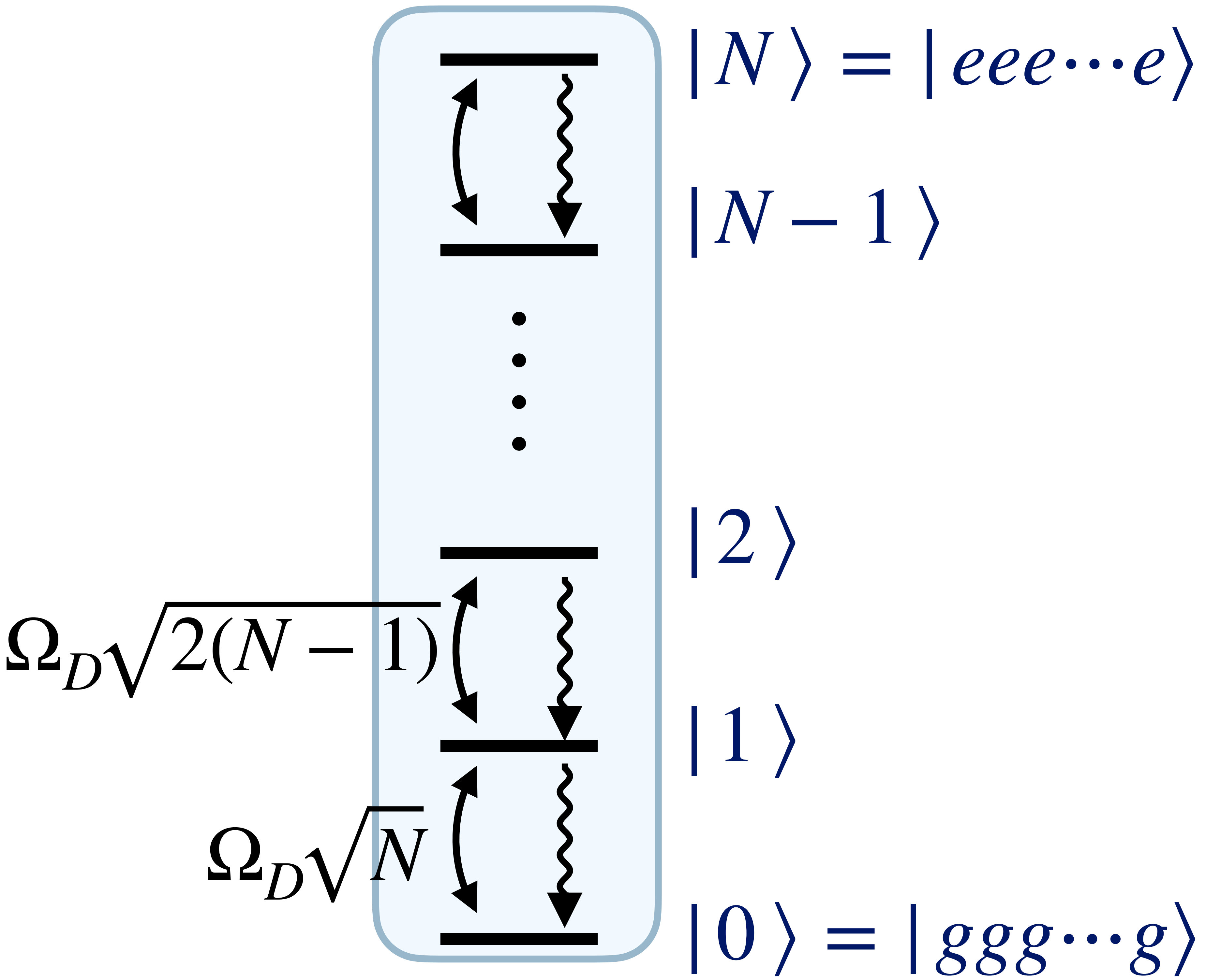

Dicke + drive

$$\dot{\hat{\rho}} = i\frac{\Omega_D}{2}\left(\hat{\rho}\hat{S}^{+} + \hat{\rho}\hat{S}^{-} - \hat{S}^{+}\hat{\rho} - \hat{S}^{-}\hat{\rho}\right) + \frac{\Gamma_0}{2}\left(2\hat{S}^{-}\hat{\rho}\hat{S}^{+} - \hat{S}^{+}\hat{S}^{-}\hat{\rho} - \hat{\rho}\hat{S}^{+}\hat{S}^{-}\right)$$

Dicke + drive

$$\dot{\hat{\rho}} = i\frac{\Omega_D}{2}\left(\hat{\rho}\hat{S}^{+} + \hat{\rho}\hat{S}^{-} - \hat{S}^{+}\hat{\rho} - \hat{S}^{-}\hat{\rho}\right) + \frac{\Gamma_0}{2}\left(2\hat{S}^{-}\hat{\rho}\hat{S}^{+} - \hat{S}^{+}\hat{S}^{-}\hat{\rho} - \hat{\rho}\hat{S}^{+}\hat{S}^{-}\right)$$

Effective Rabi frequency: $\Omega_{\text{eff}} = \Omega_D + i\Gamma_0 \langle \hat{S}^{-} \rangle$

Screening by collective dipole

Dicke + drive

$$\dot{\hat{\rho}} = i\frac{\Omega_D}{2}\left(\hat{\rho}\hat{S}^+ + \hat{\rho}\hat{S}^- - \hat{S}^+\hat{\rho} - \hat{S}^-\hat{\rho}\right) + \frac{\Gamma_0}{2}\left(2\hat{S}^-\hat{\rho}\hat{S}^+ - \hat{S}^+\hat{S}^-\hat{\rho} - \hat{\rho}\hat{S}^+\hat{S}^-\right)$$

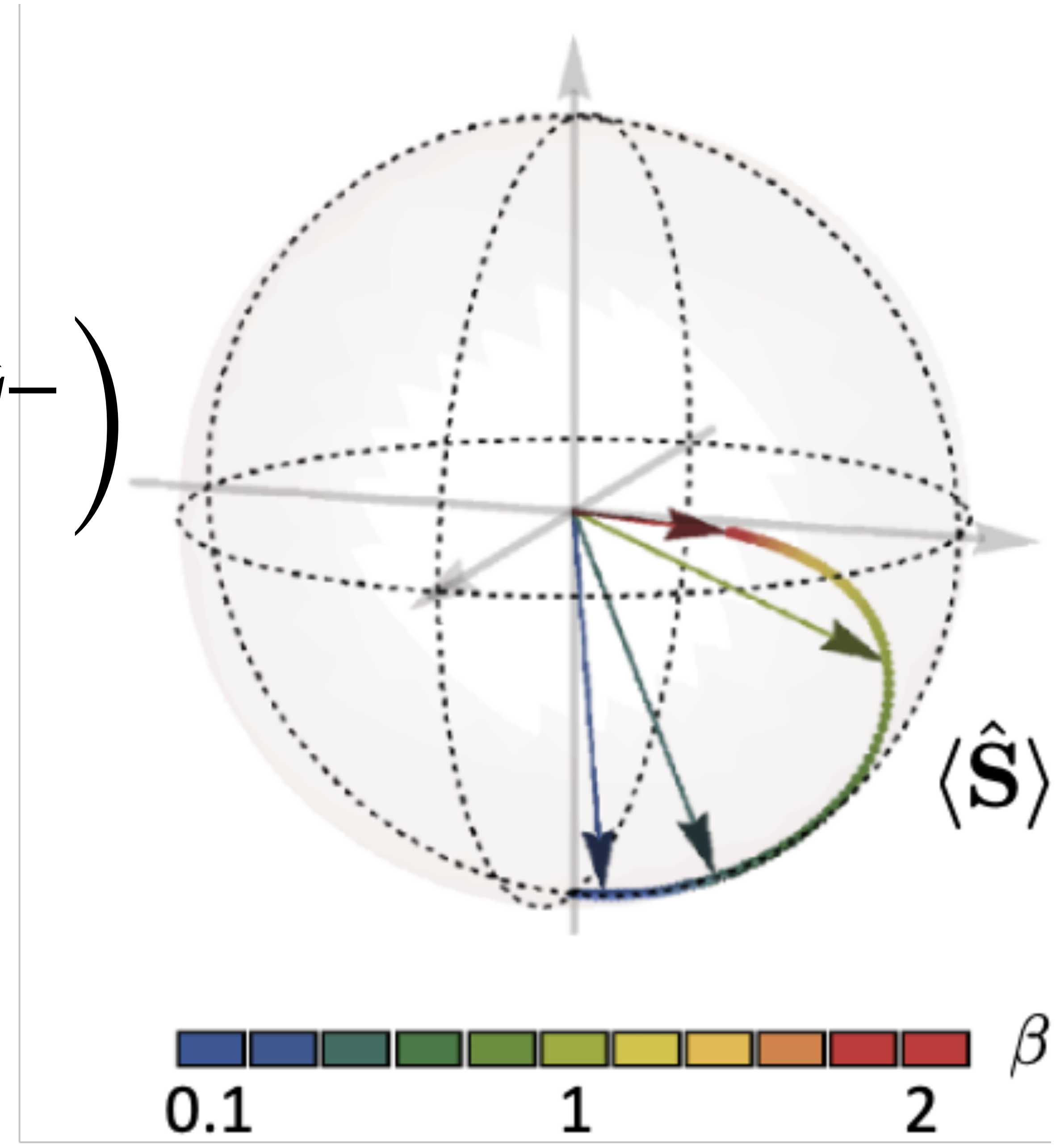

Effective Rabi frequency: $\Omega_{\text{eff}} = \Omega_D + i\Gamma_0 \langle \hat{S}^- \rangle$

Screening by collective dipole

Maximum achievable dipole: $\langle \hat{S}^- \rangle \simeq iN/2$

Recover Rabi oscillations for $\Omega_D > N\Gamma_0/2$

Scaling with $\beta = 2\Omega_D/\Gamma_0 N$

Existence of a non-equilibrium phase transition

D. F. Walls, *J. Phys. B At. Mol. Phys.* **13**, 2001 (1973).

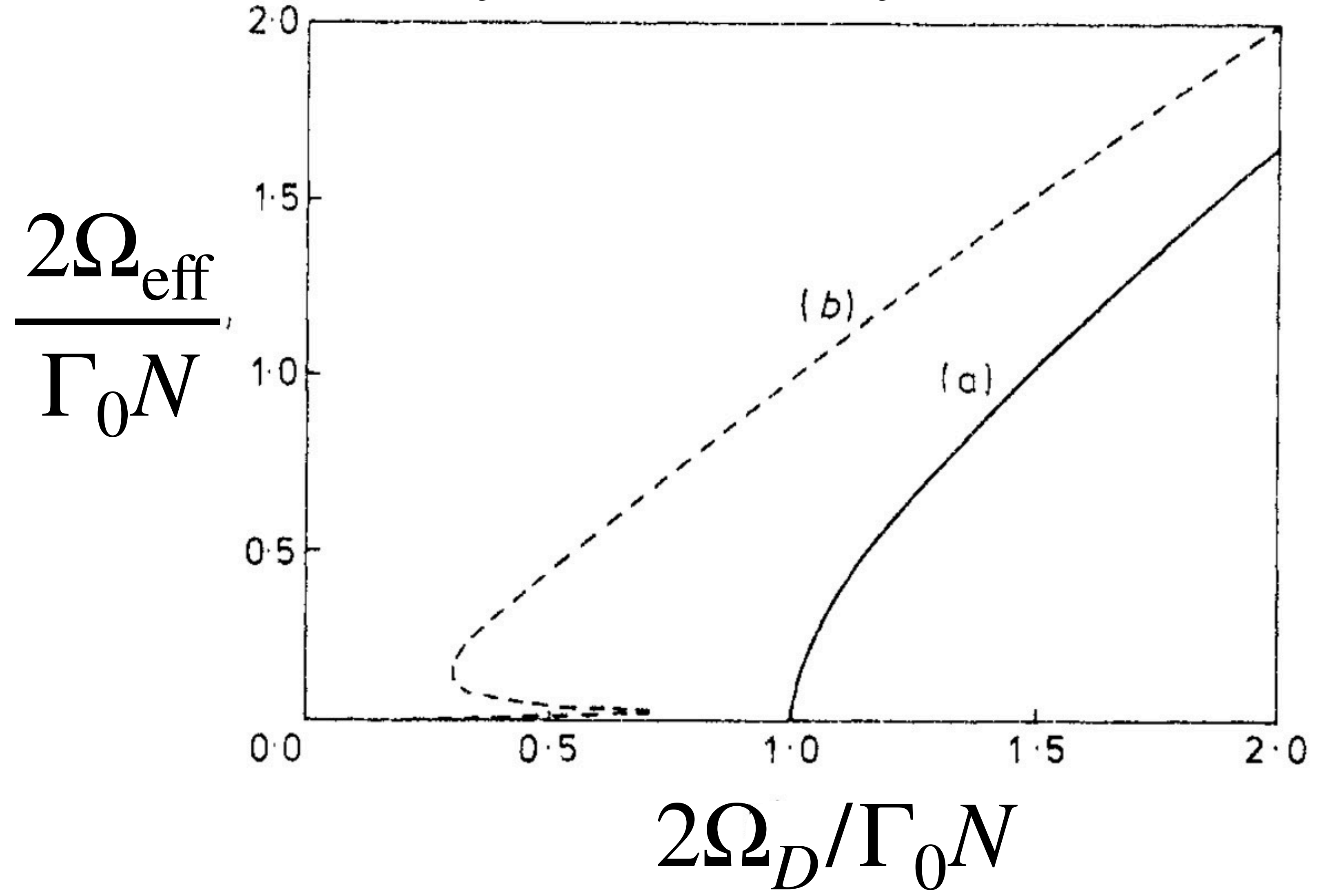

Dicke + drive

Collective spontaneous emission induces squeezing

$$\dot{\hat{\rho}} = i\frac{\Omega_D}{2}\left(\hat{\rho}\hat{S}^{+} + \hat{\rho}\hat{S}^{-} - \hat{S}^{+}\hat{\rho} - \hat{S}^{-}\hat{\rho}\right) + \frac{\Gamma_0}{2}\left(2\hat{S}^{-}\hat{\rho}\hat{S}^{+} - \hat{S}^{+}\hat{S}^{-}\hat{\rho} - \hat{\rho}\hat{S}^{+}\hat{S}^{-}\right)$$

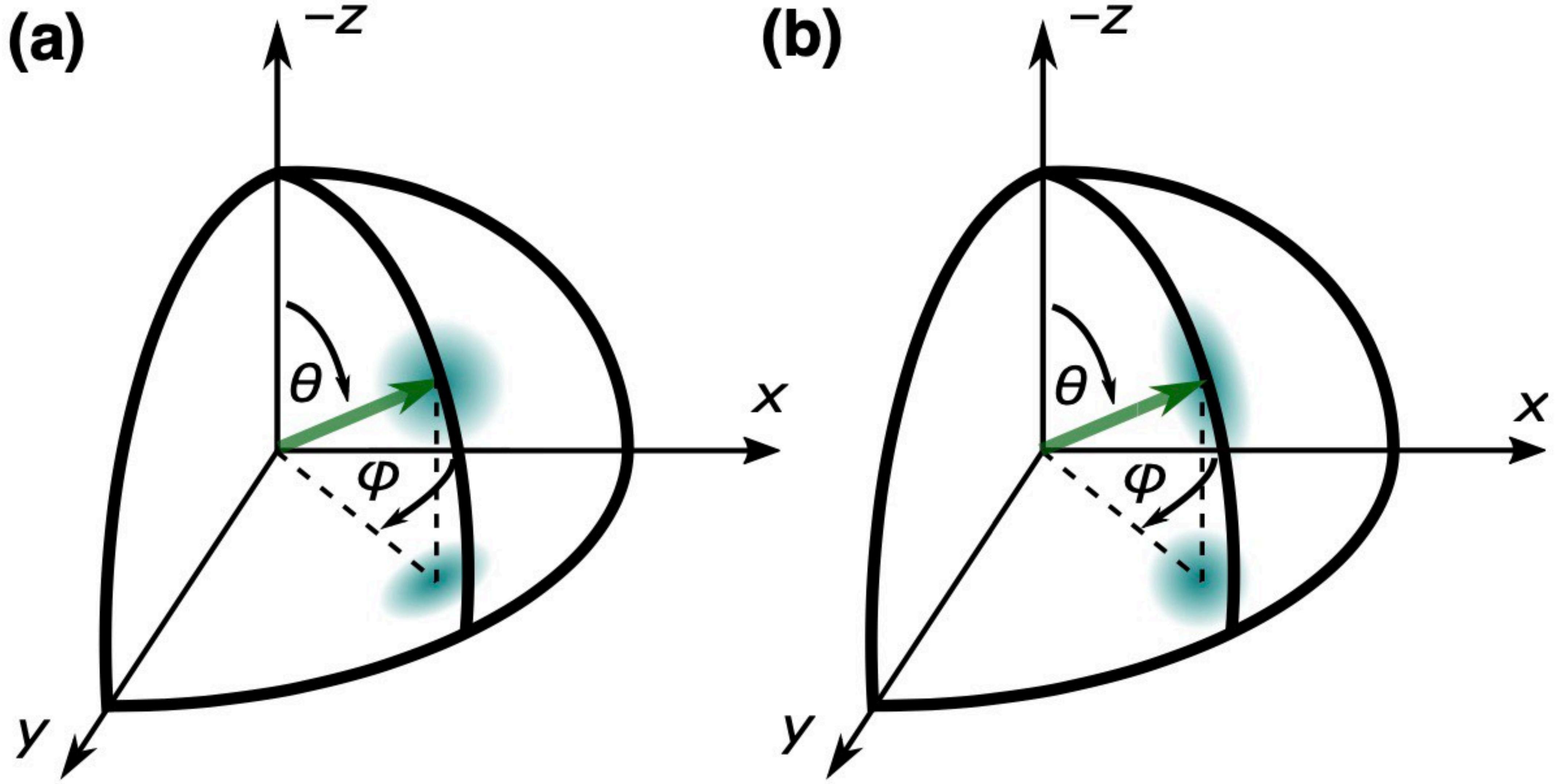

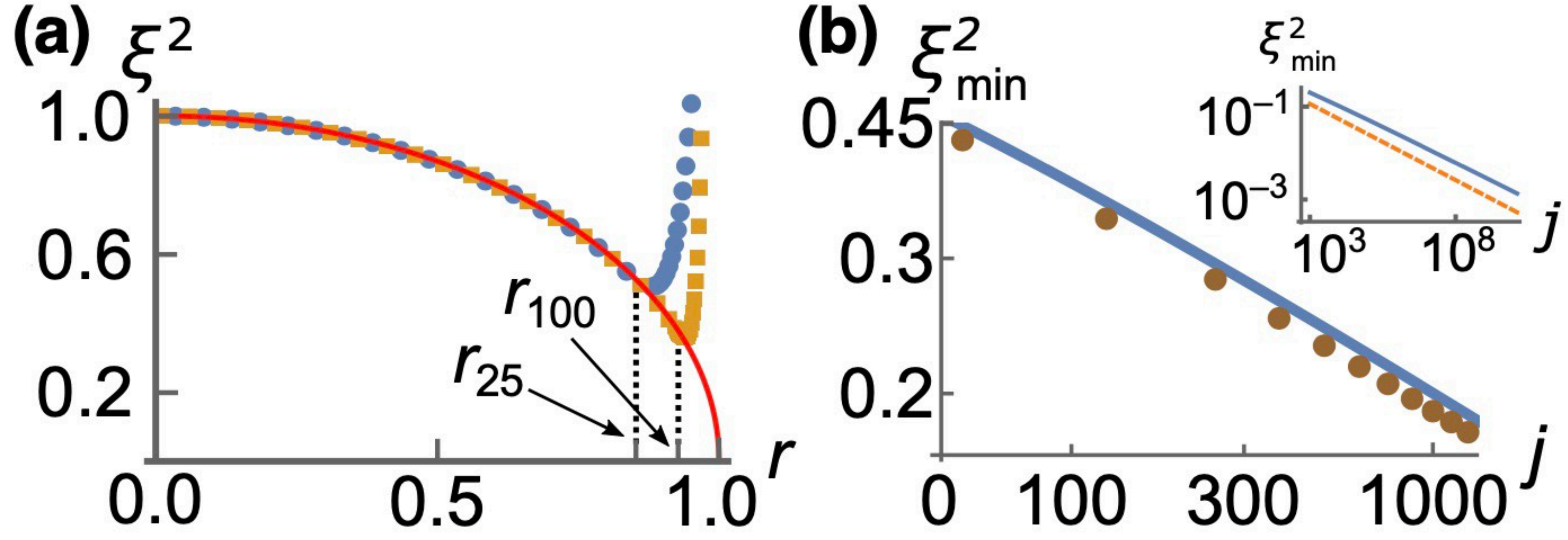

Somech & Shahmoon *PRX Quantum* **5**, 010349 (2024).

The Dicke ladder with drive

In dense microscopic clouds, mean-field dynamics same as Dicke + drive

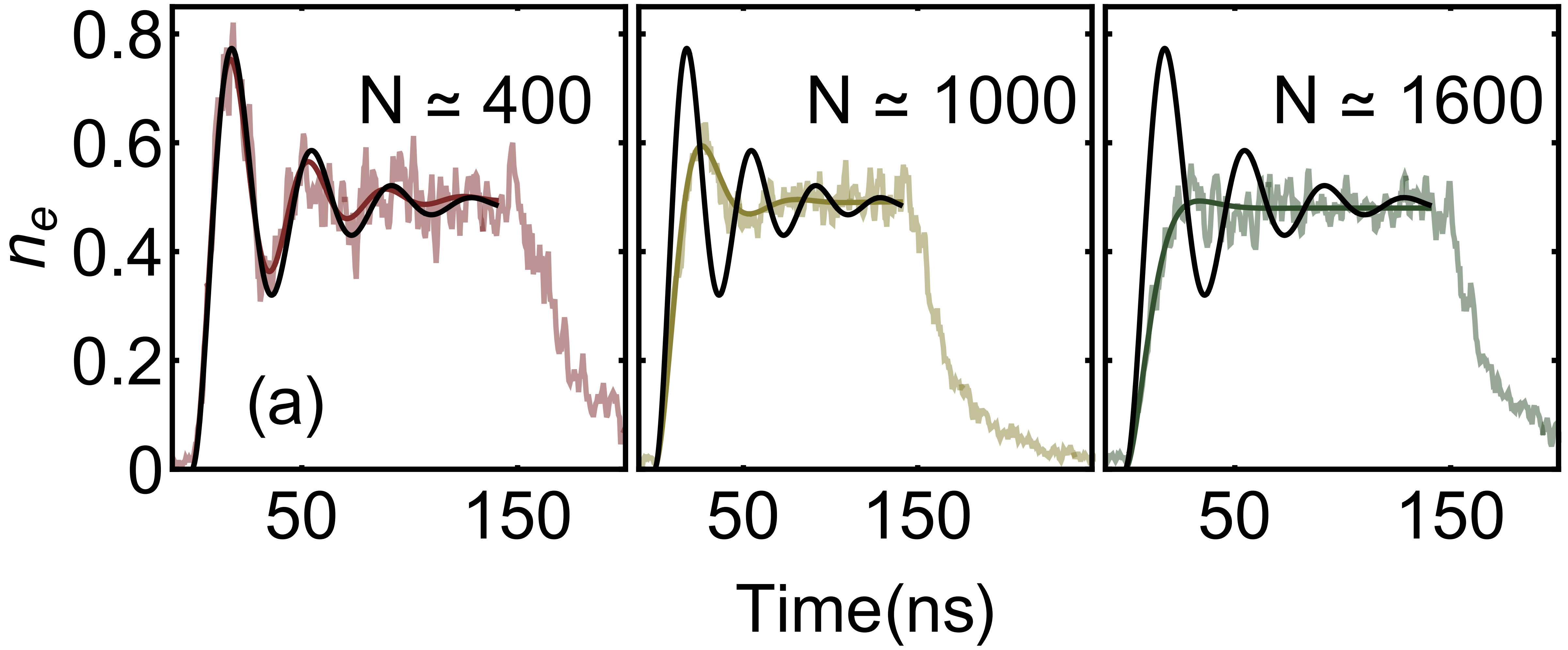

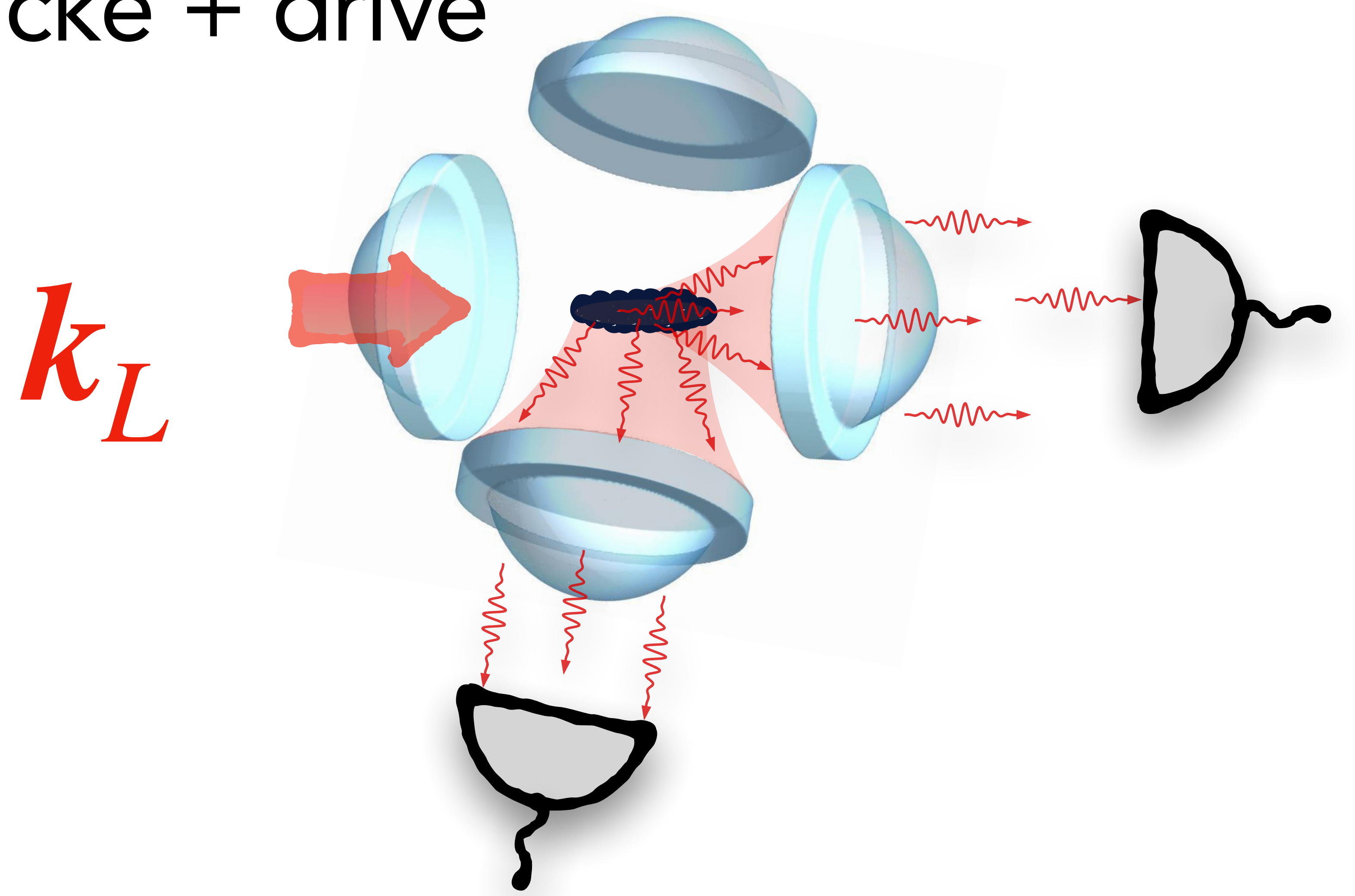

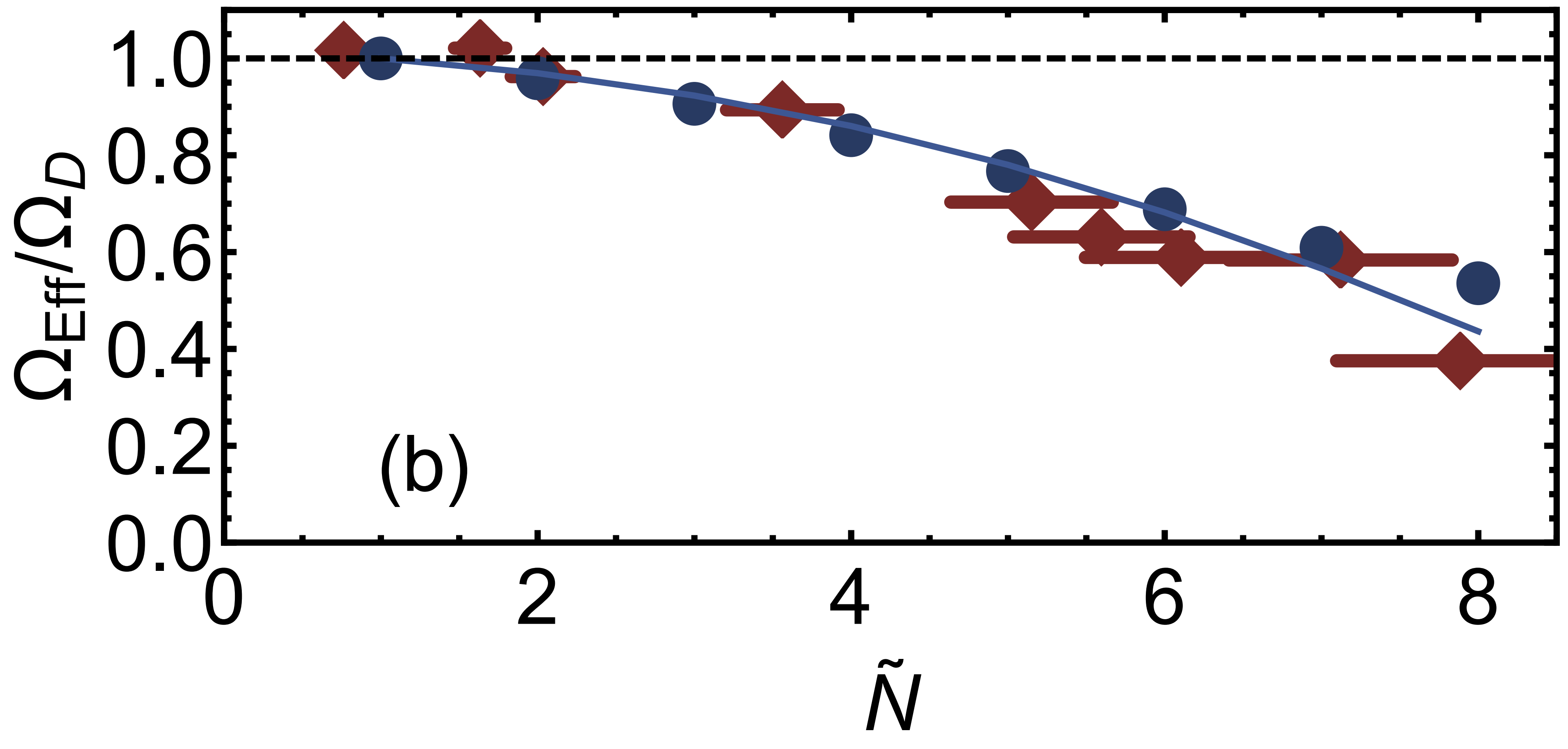

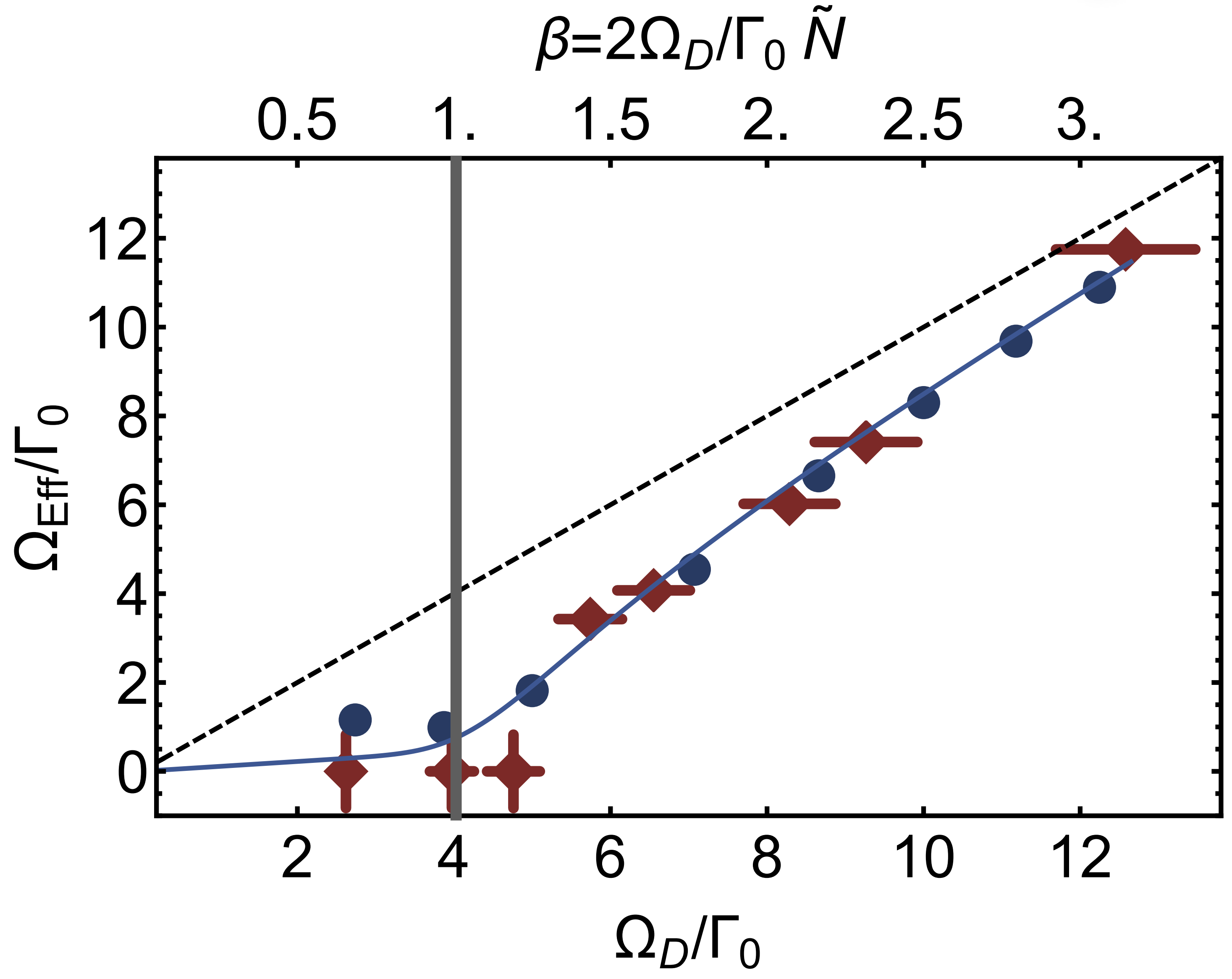

G. Ferioli *et al.*, Nat. Phys. **18**, 1345 (2023)

The Dicke ladder with drive

Realization in a cavity QED system (Sr on the intercombination line)

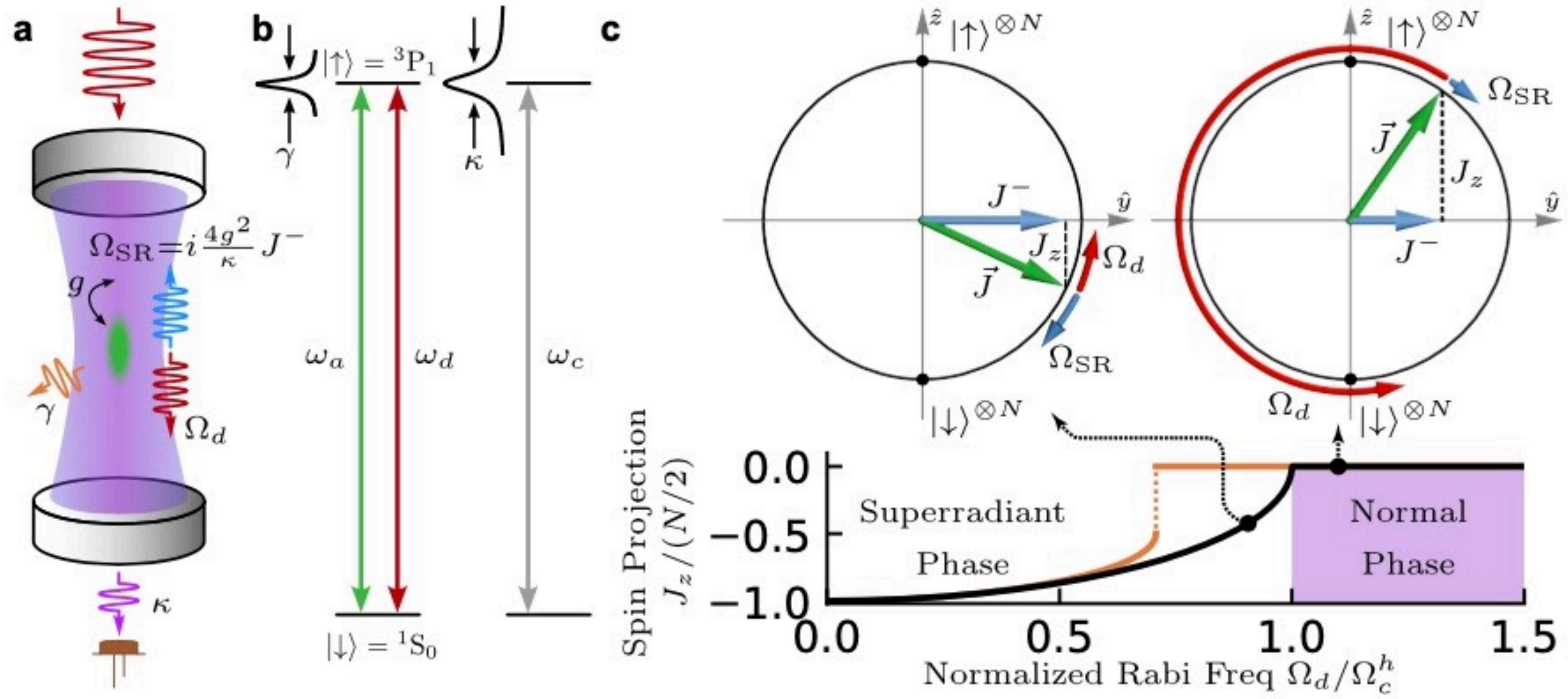

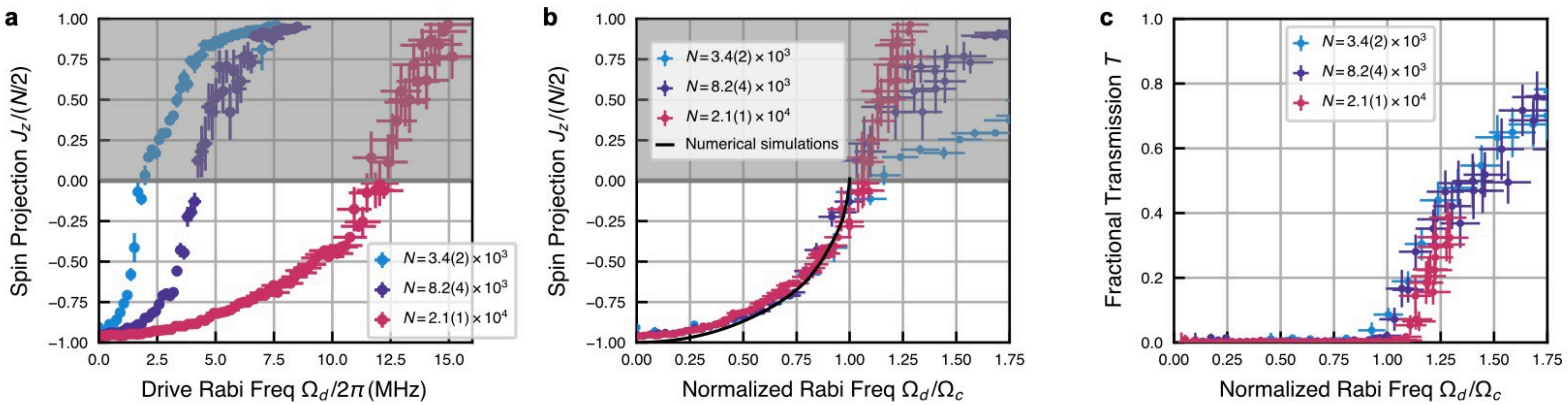

Song *et al.*, arXiv:2408.11086 (2024)

Subradiance

R. H. Dicke, *Phys. Rev.* **93**, 99 (1954).

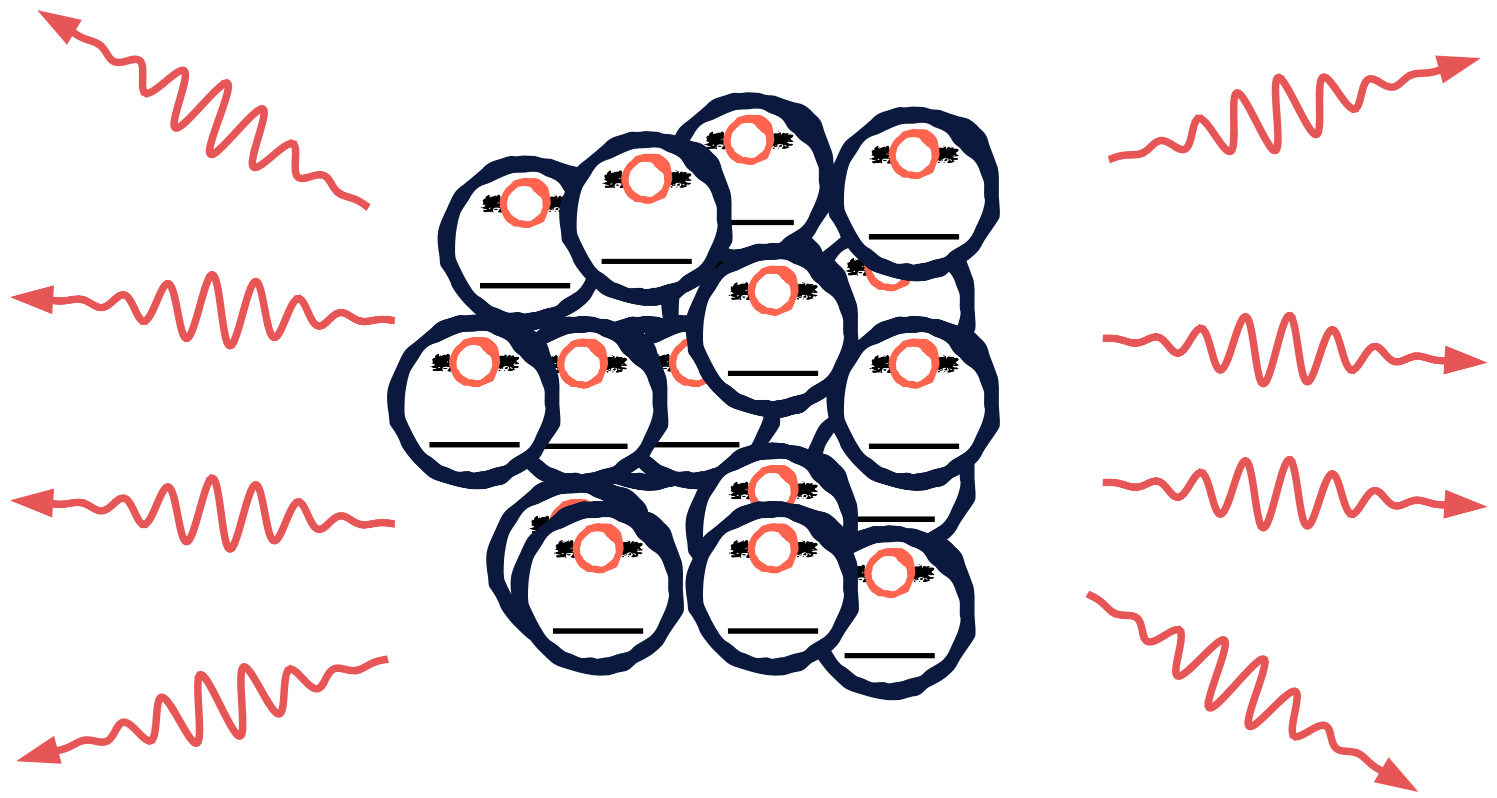

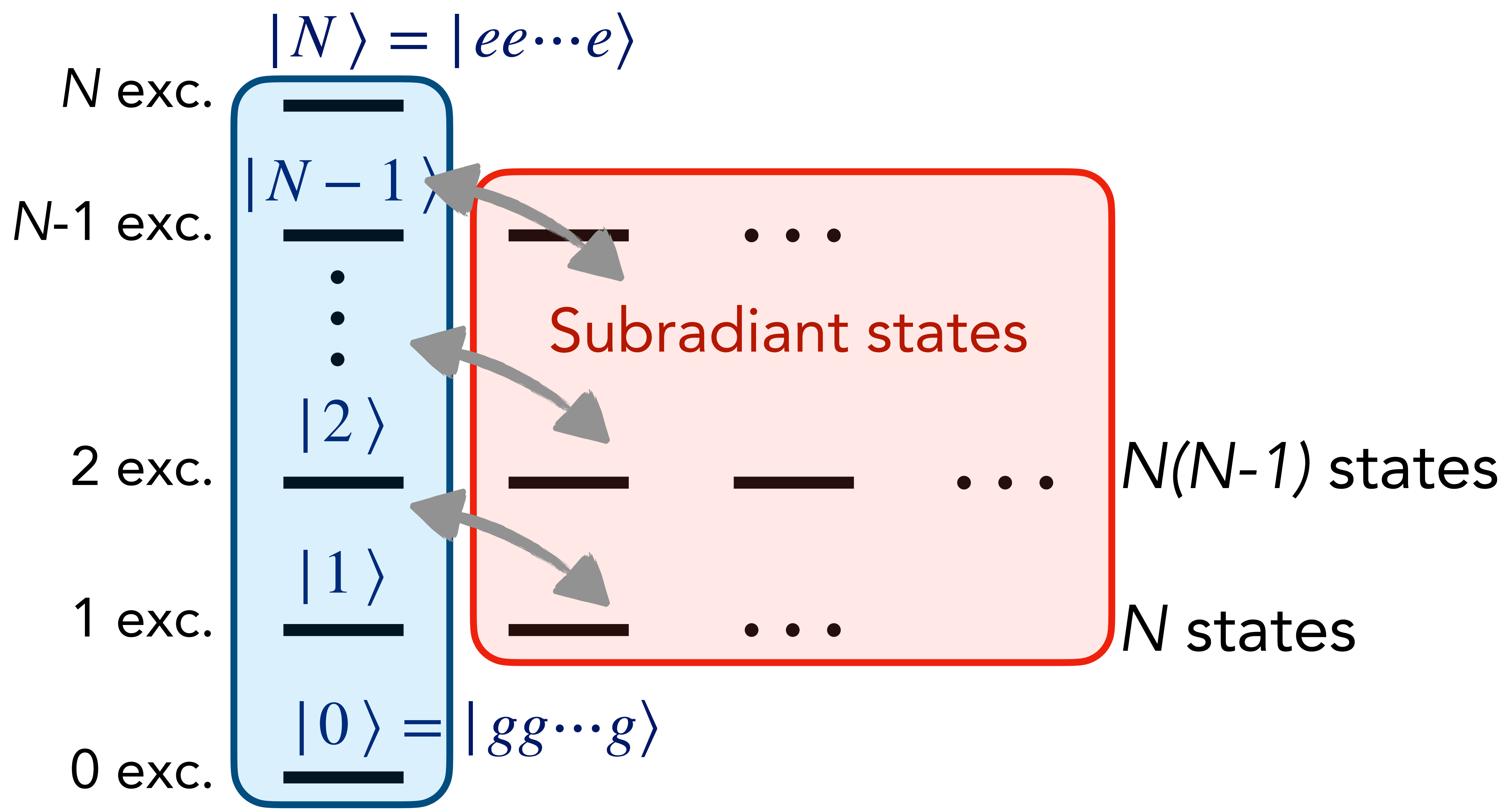

Subradiance

R. H. Dicke, *Phys. Rev.* **93**, 99 (1954).

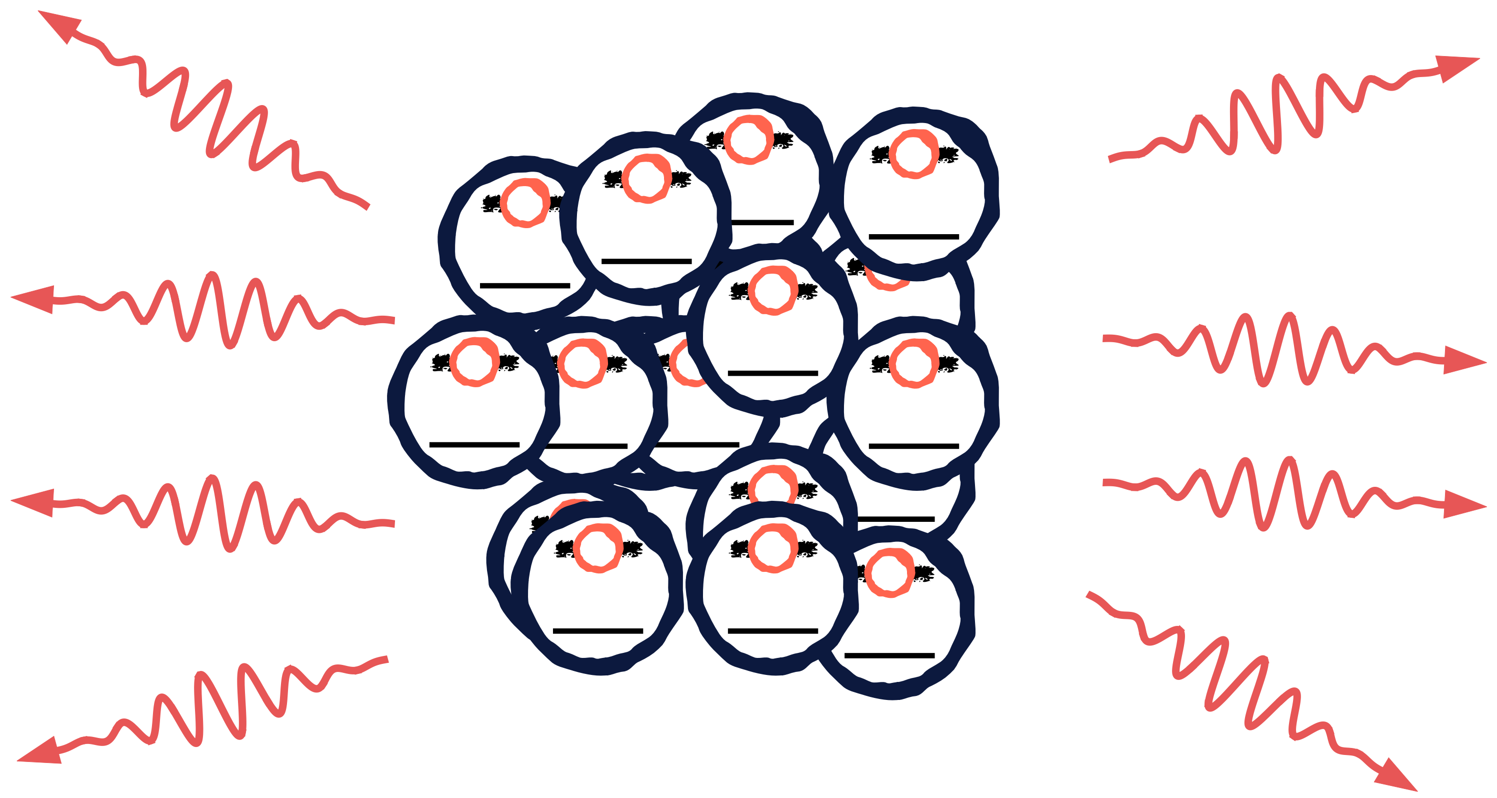

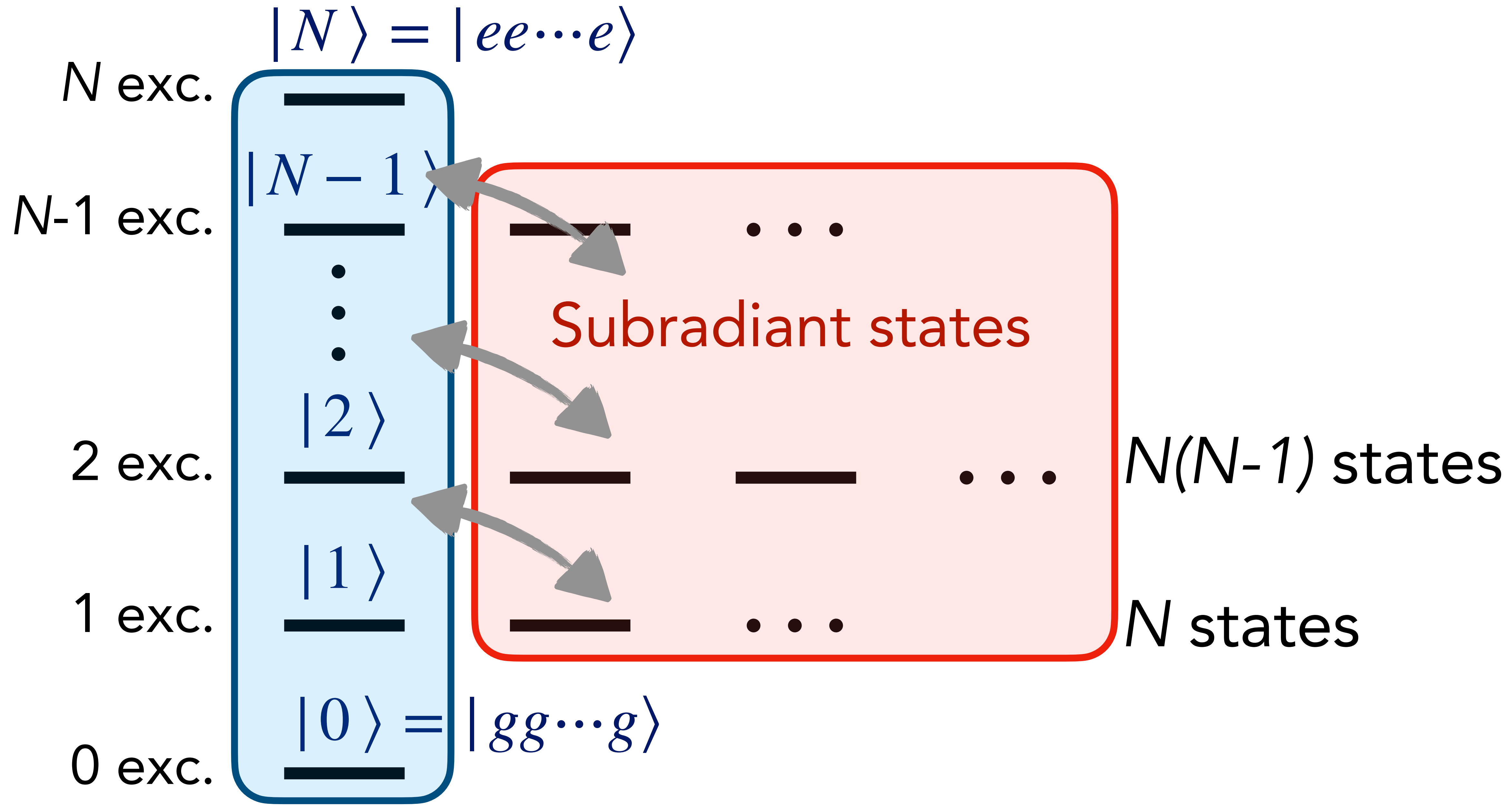

Classical regime

Break Dicke symmetry

Finite-size effects, dipole-dipole interactions : Access to subradiant states

Subradiance

Laser pulse: mostly populates superradiant levels

But long pulse to steady state solution, overlaps with subradiant states

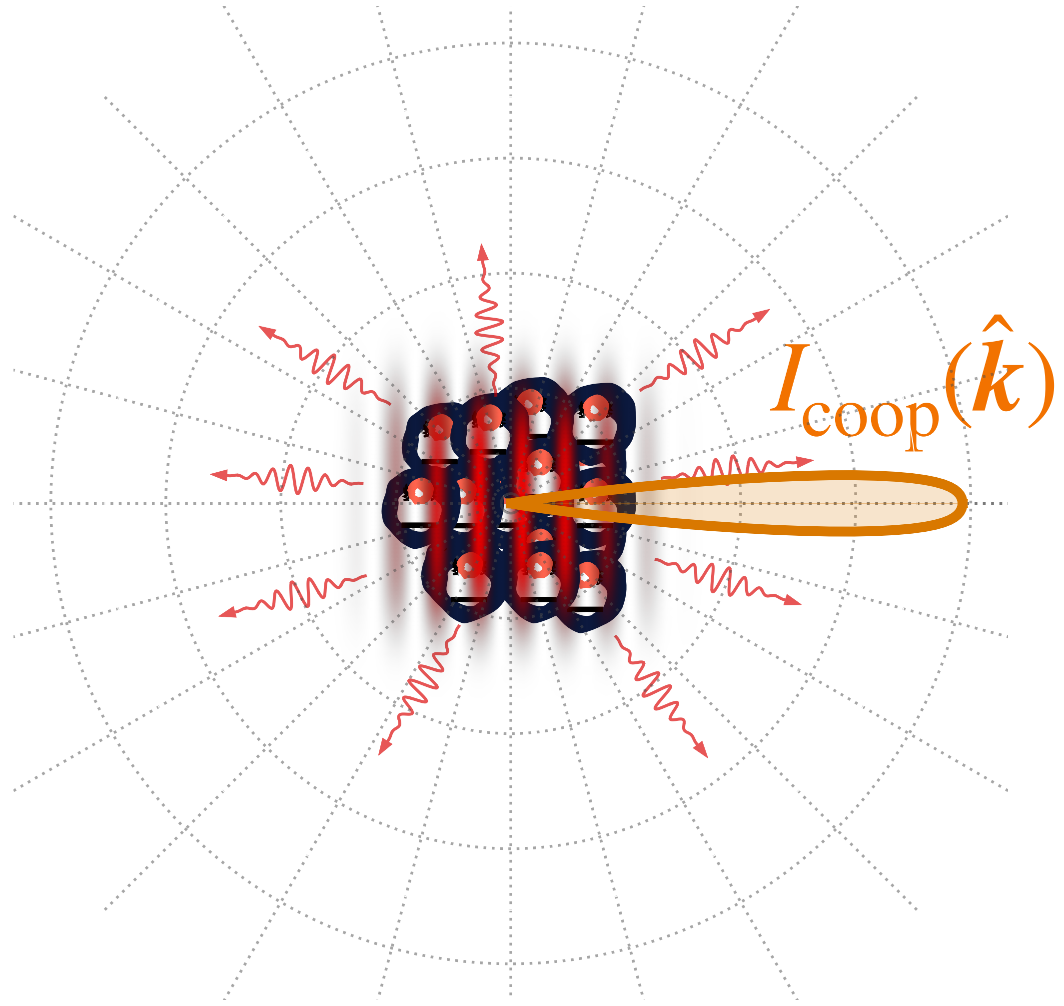

Fast decay of superradiant excitations, followed by slow decay

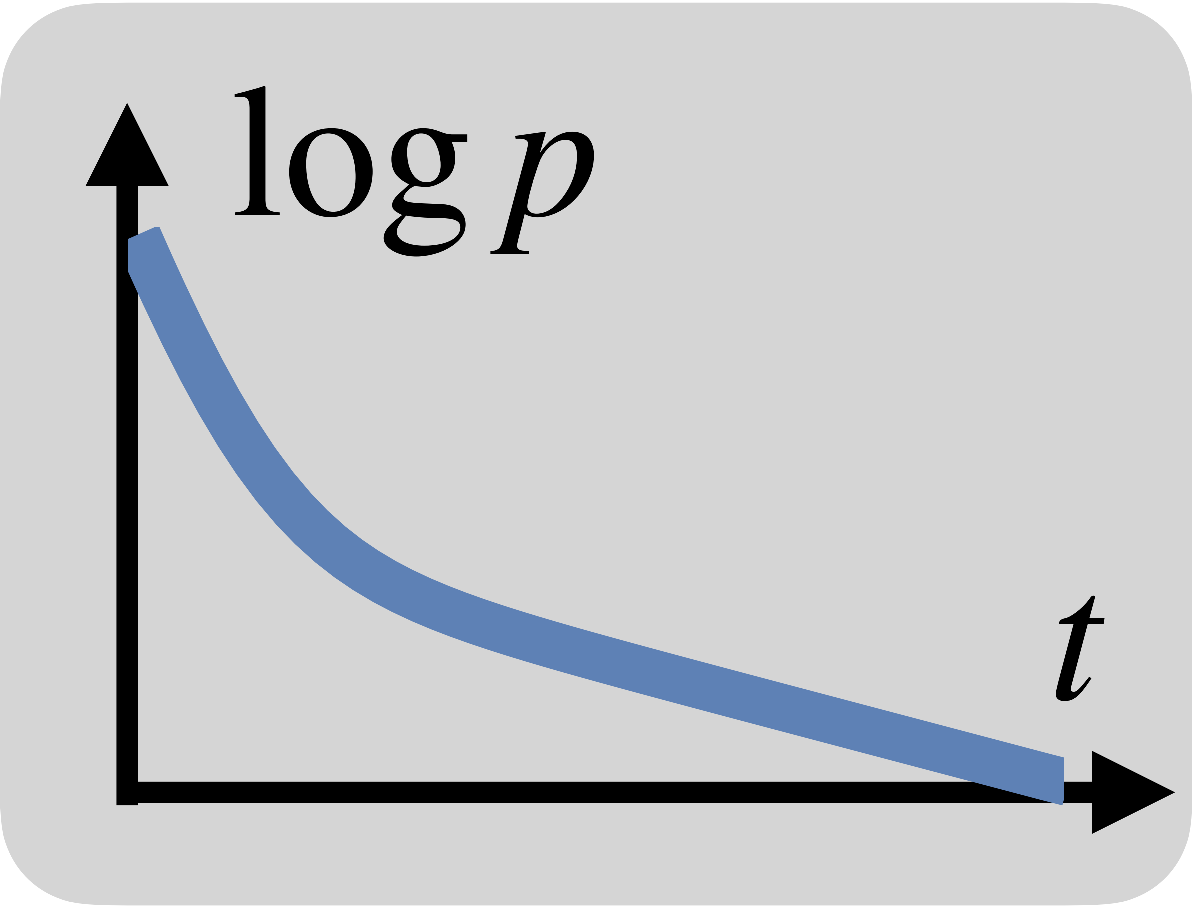

Very few observations

Pavolini *et al.*, *Phys Rev Lett* **54**, 1917 (1985).

2 atoms (ions or dimer)

DeVoe & Brewer *Phys Rev Lett* **76**, 2049 (1996).

Hettich *et al.* *Science* **298**, 385 (2002).

Takasu *et al.*, *Phys Rev Lett* **108**, 173002 (2012).

McGuyer *et al.*, *Nat Phys* **11**, 32–36 (2015).

Subradiance with N atoms

Guerin, Araujo &. Kaiser, *Phys Rev Lett* **116**, 083601 (2016).

Extended samples in MOTs

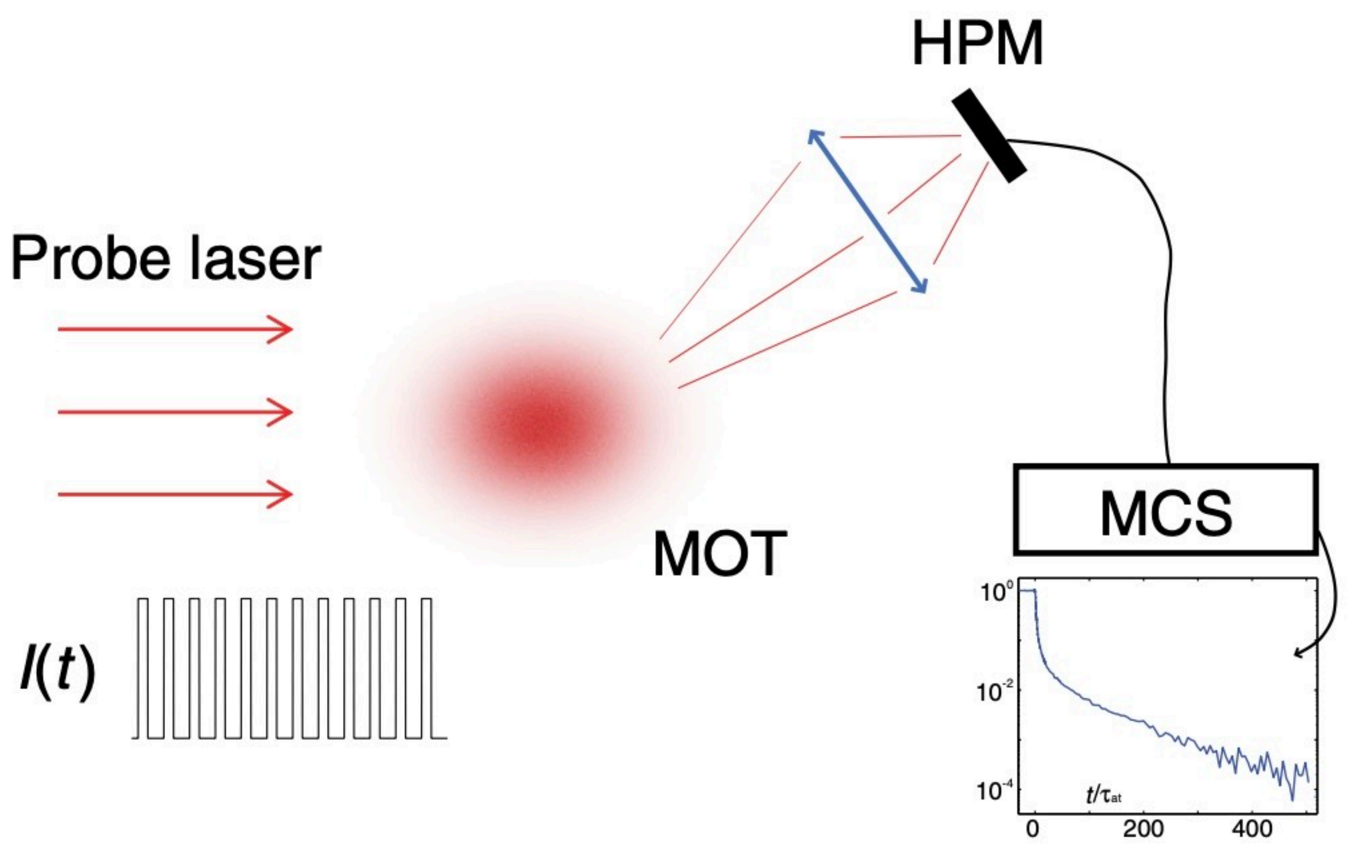

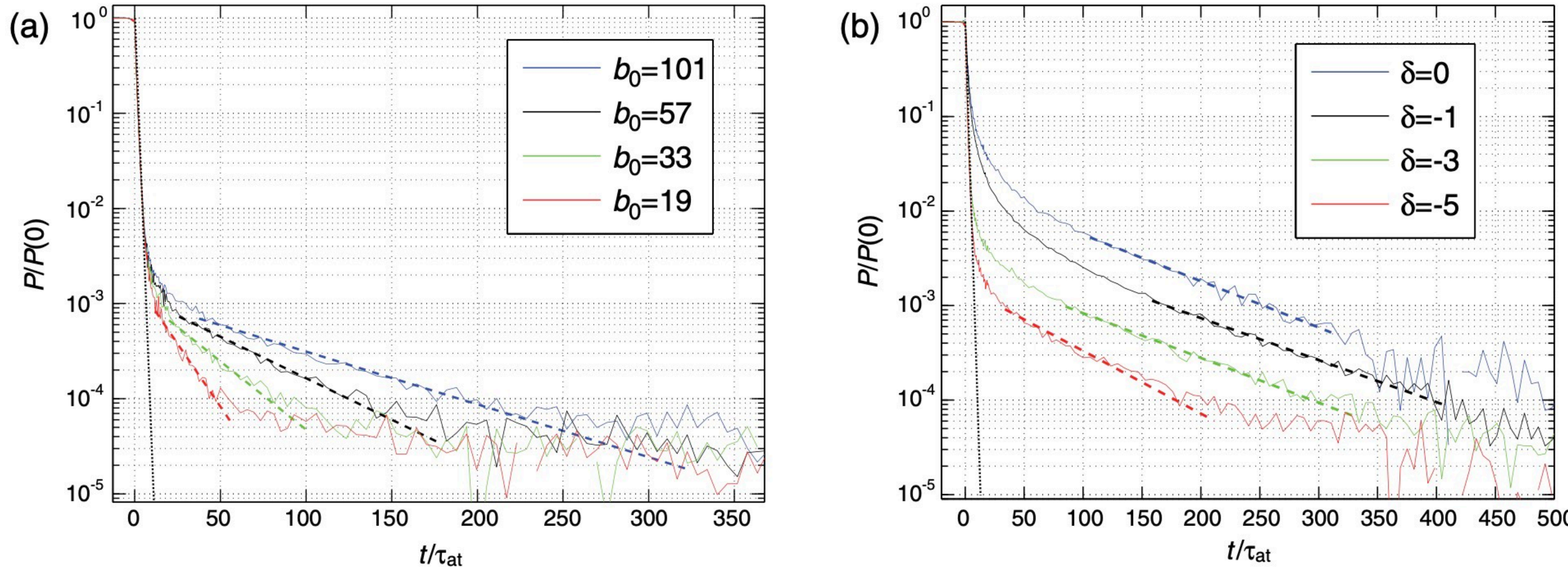

Observed scaling with optical depth

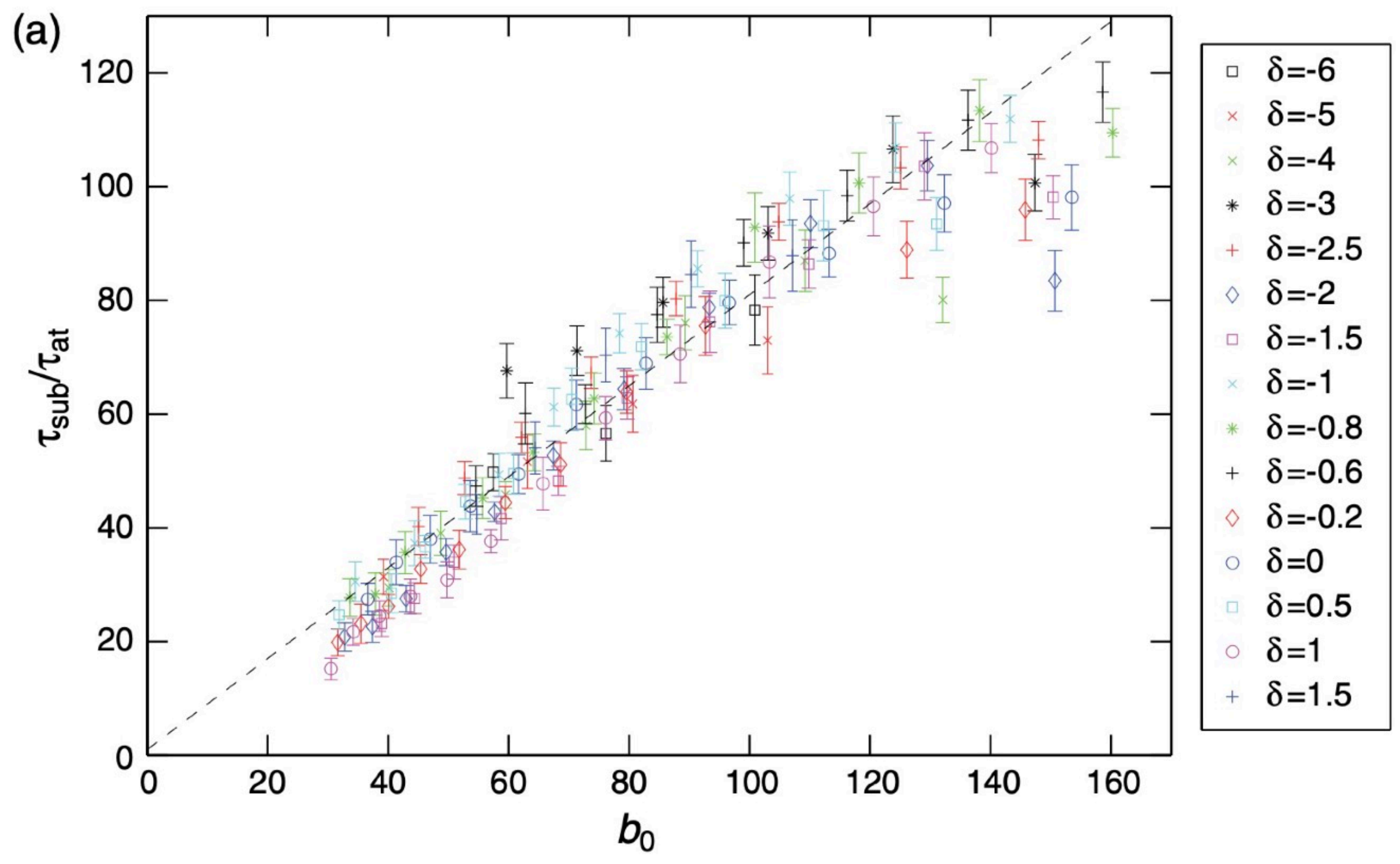

Das, Lemberger & Yavuz *Phys Rev A* **102**, 043708 (2020).

Subradiance in dense samples

Small dense samples ($\sigma_r < \lambda_0$, $\sigma_z \sim 10\lambda_0$)

Low atom number:

Single lifetime exponential decay

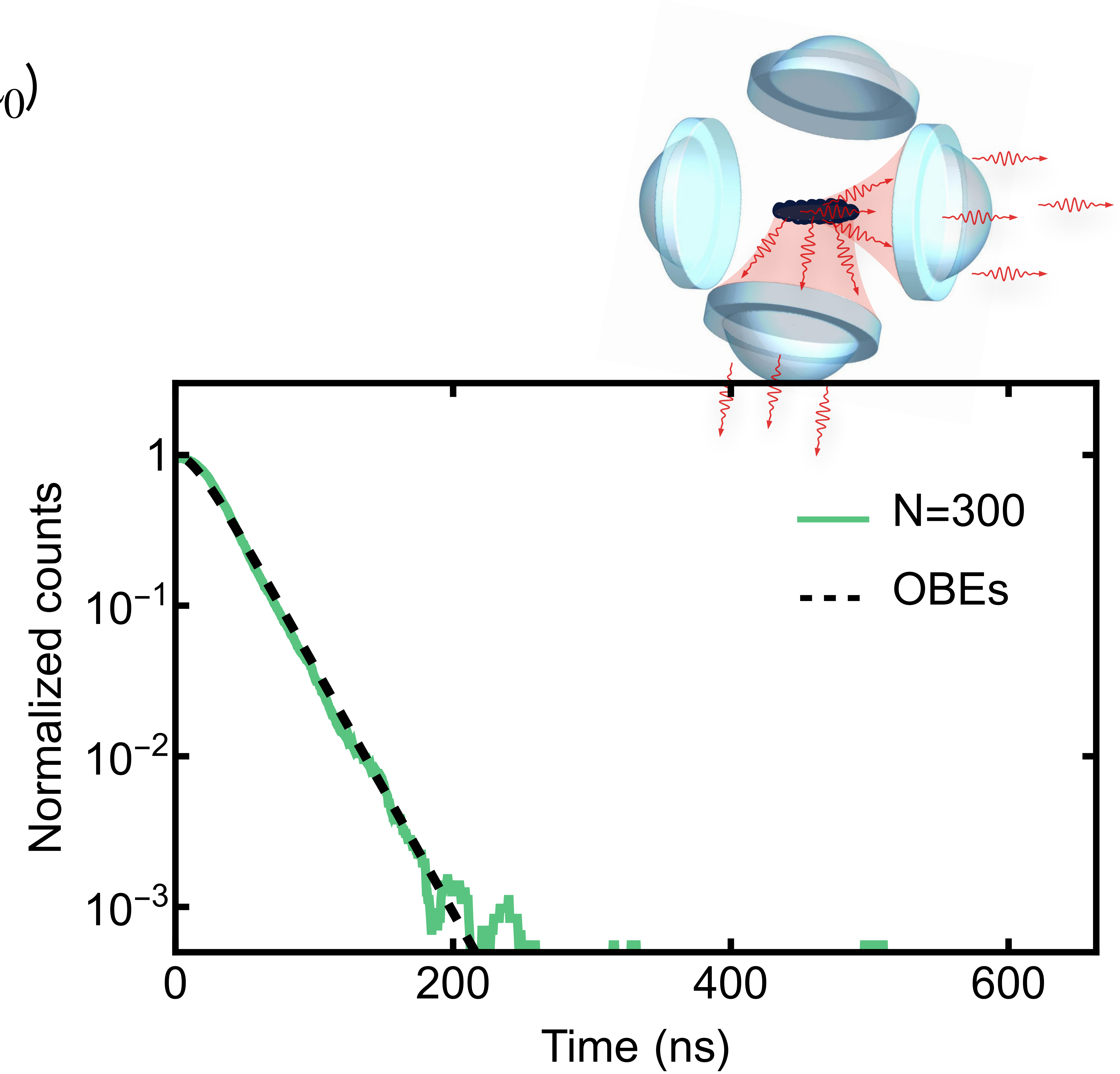

G. Ferioli *et al.*, Phys. Rev. X 11, 021031 (2021).

Subradiance in dense samples

Small dense samples ($\sigma_r < \lambda_0$, $\sigma_z \sim 10\lambda_0$)

Low atom number:

Single lifetime exponential decay

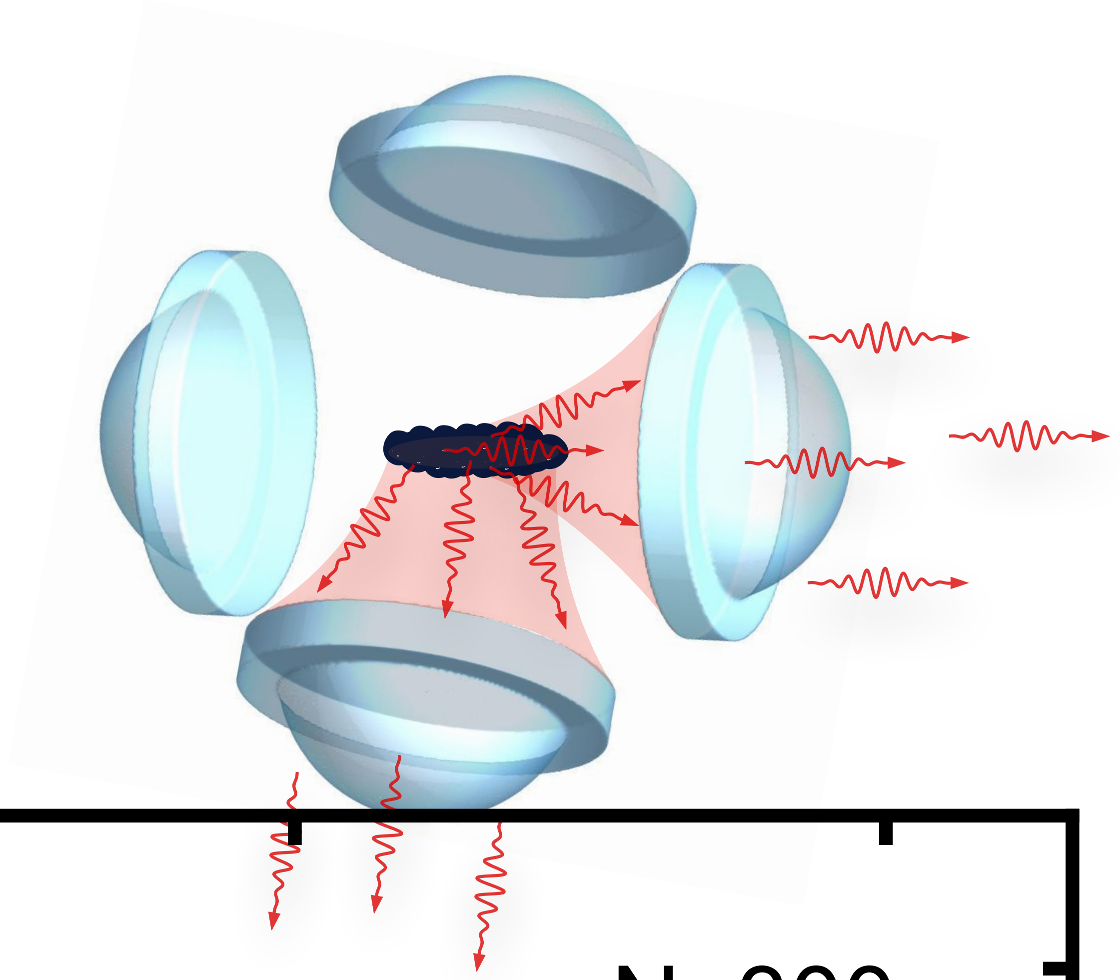

Subradiance

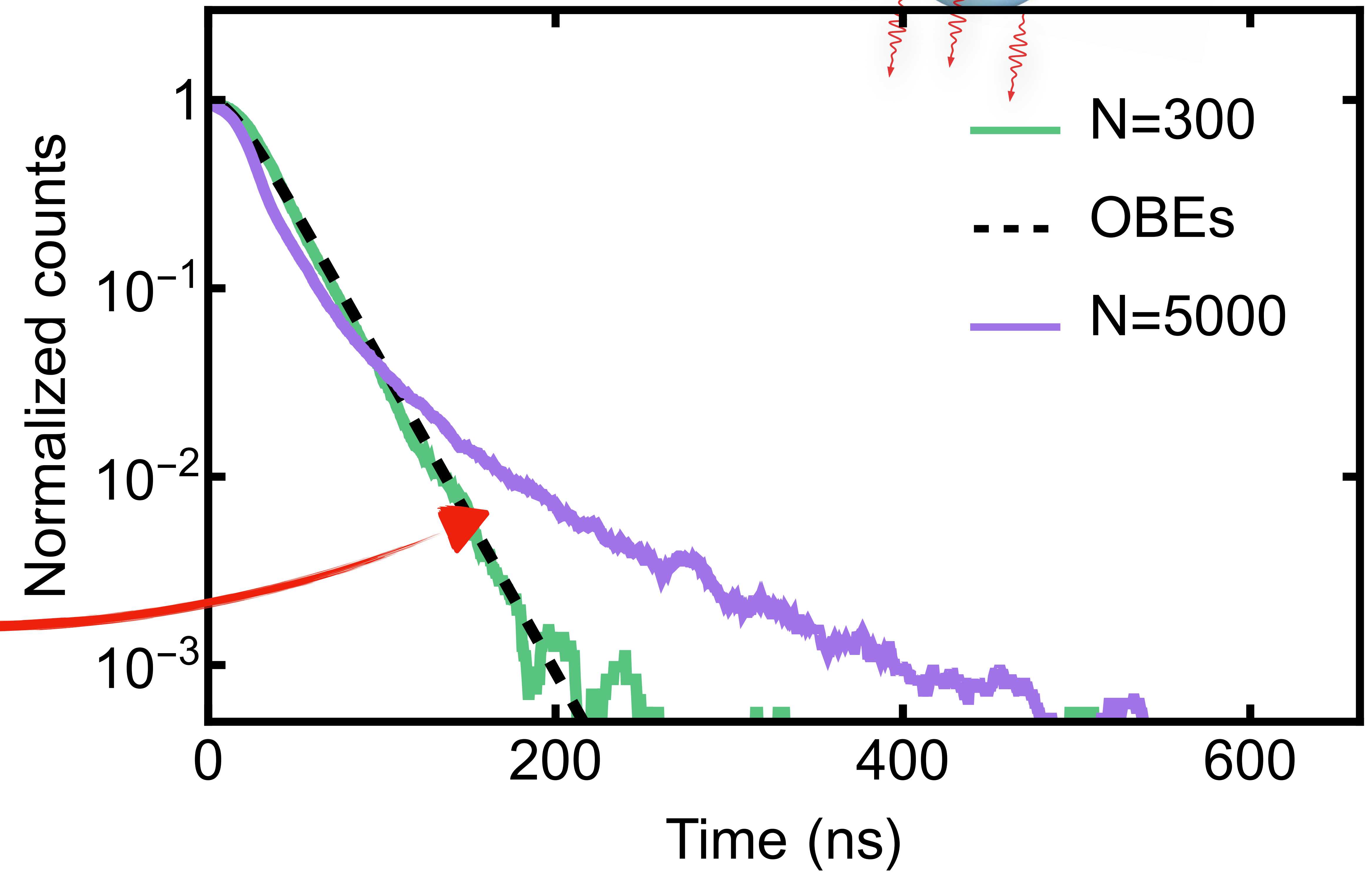

G. Ferioli *et al.*, Phys. Rev. X 11, 021031 (2021).

Storage and release in subradiance

Motivation for subradiance: photon storage

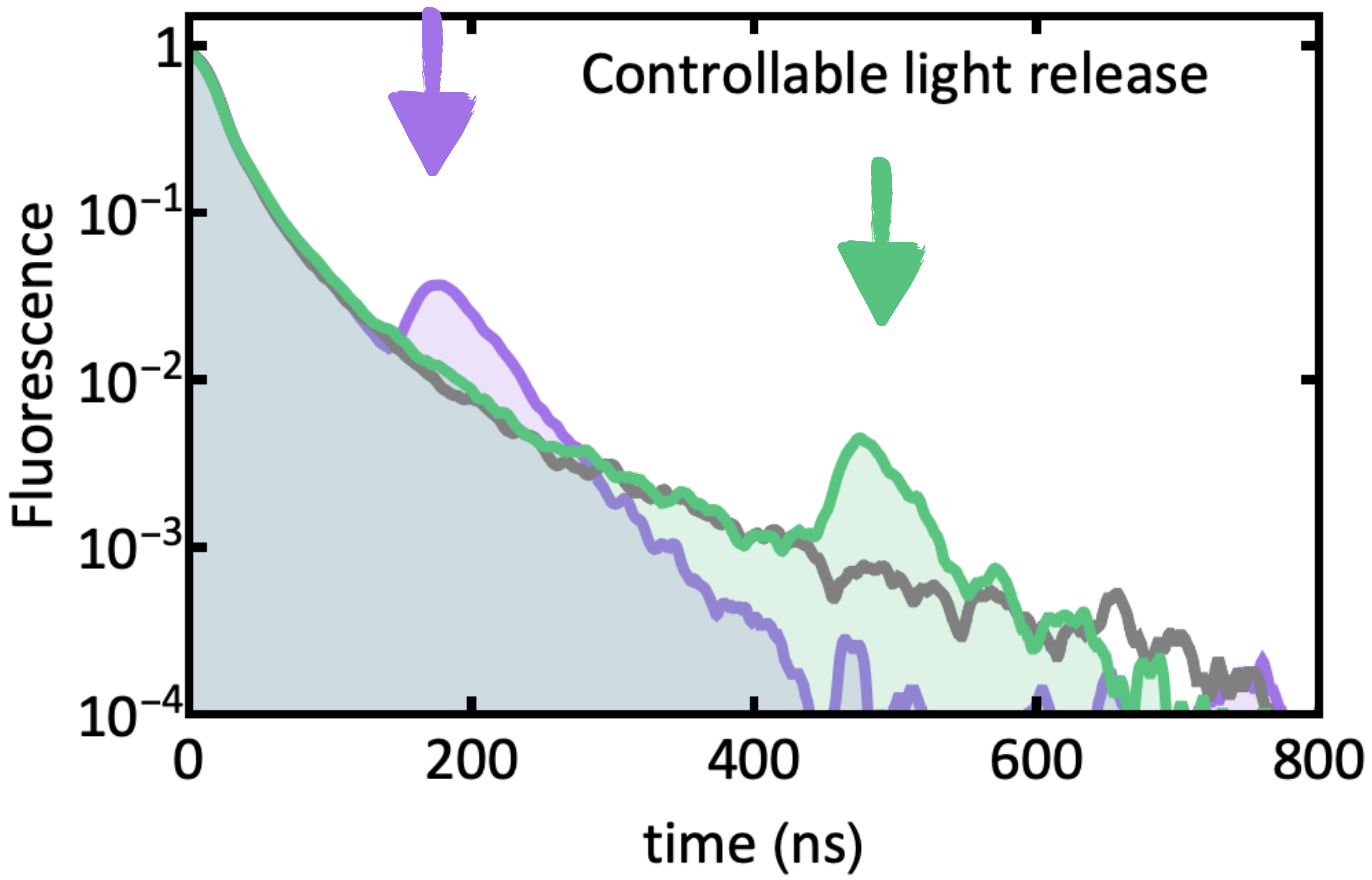

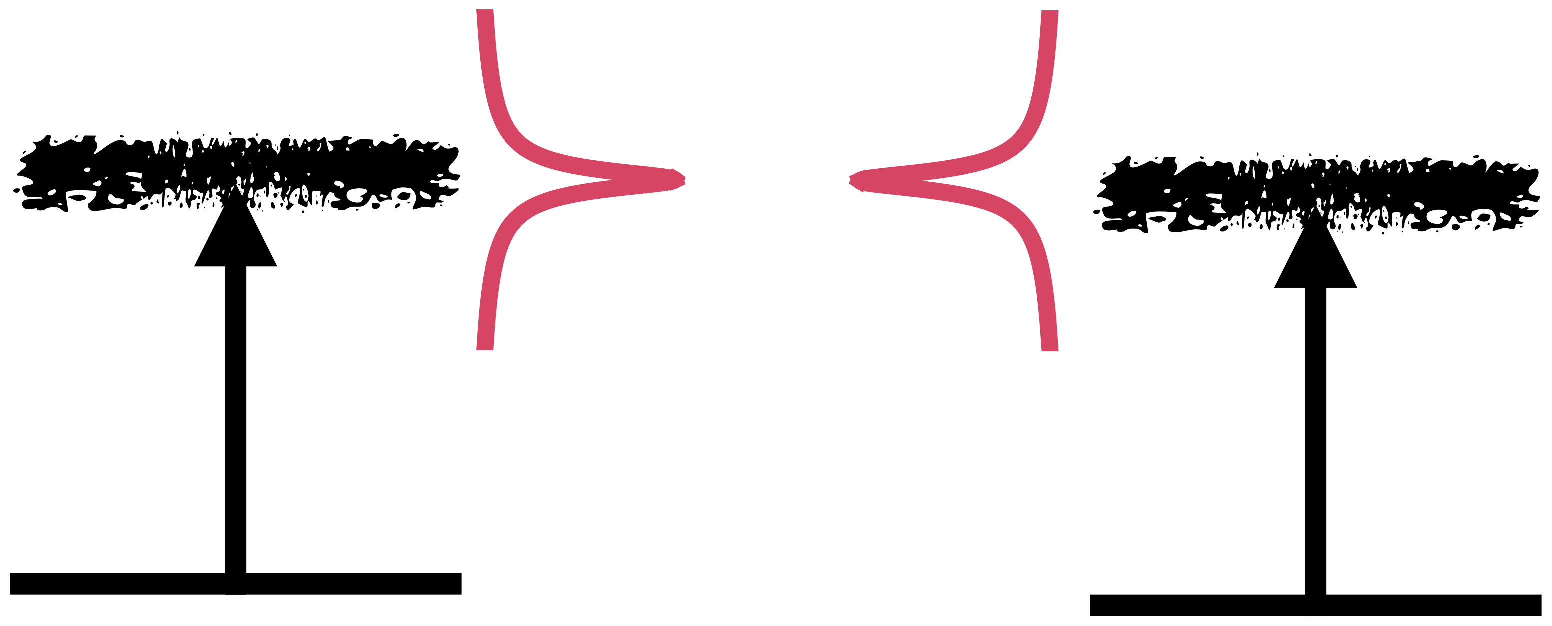

G. Ferioli *et al.*, *Phys. Rev. X* 11, 021031 (2021).

Storage and release in subradiance

Motivation for subradiance: photon storage

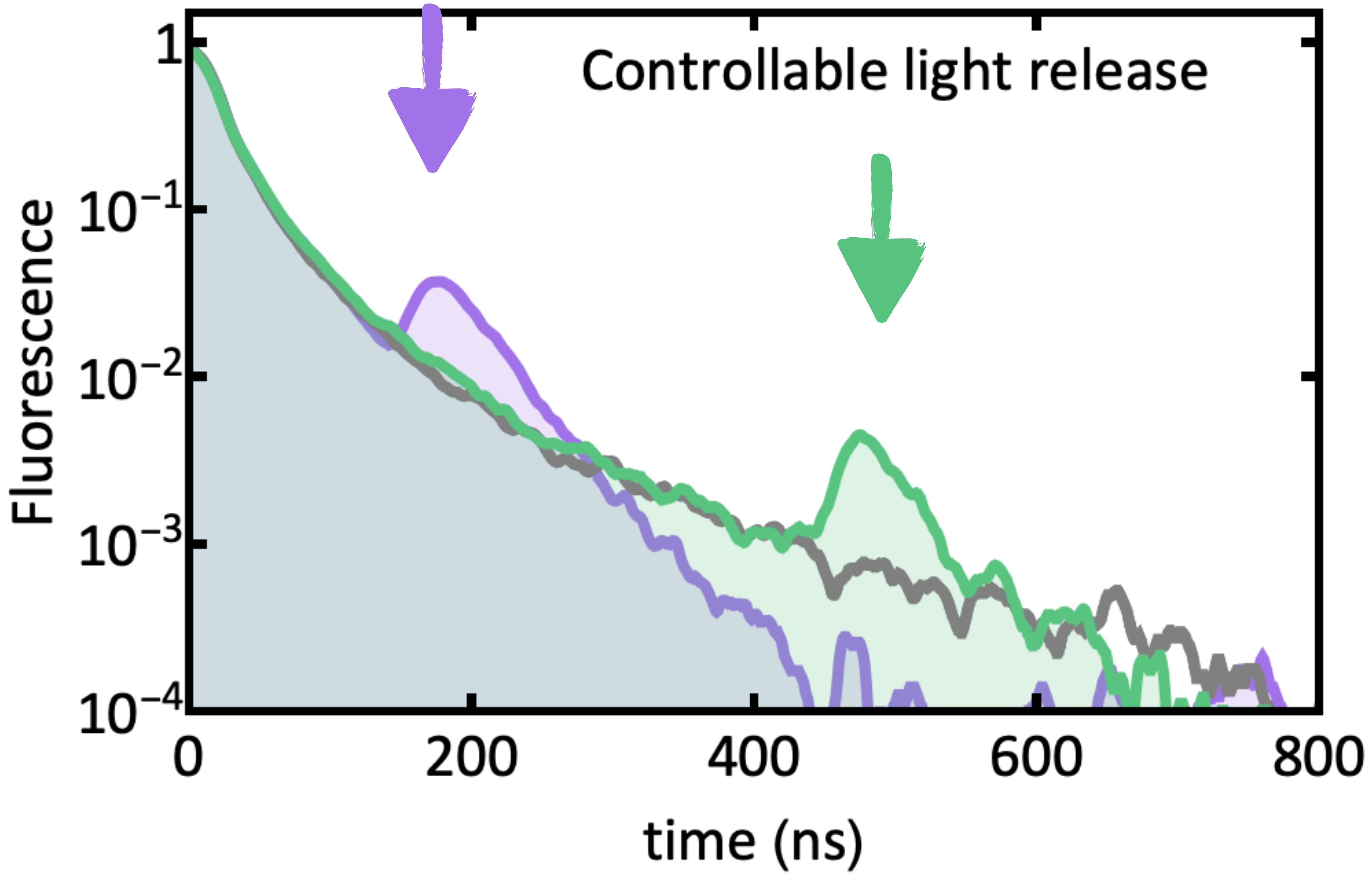

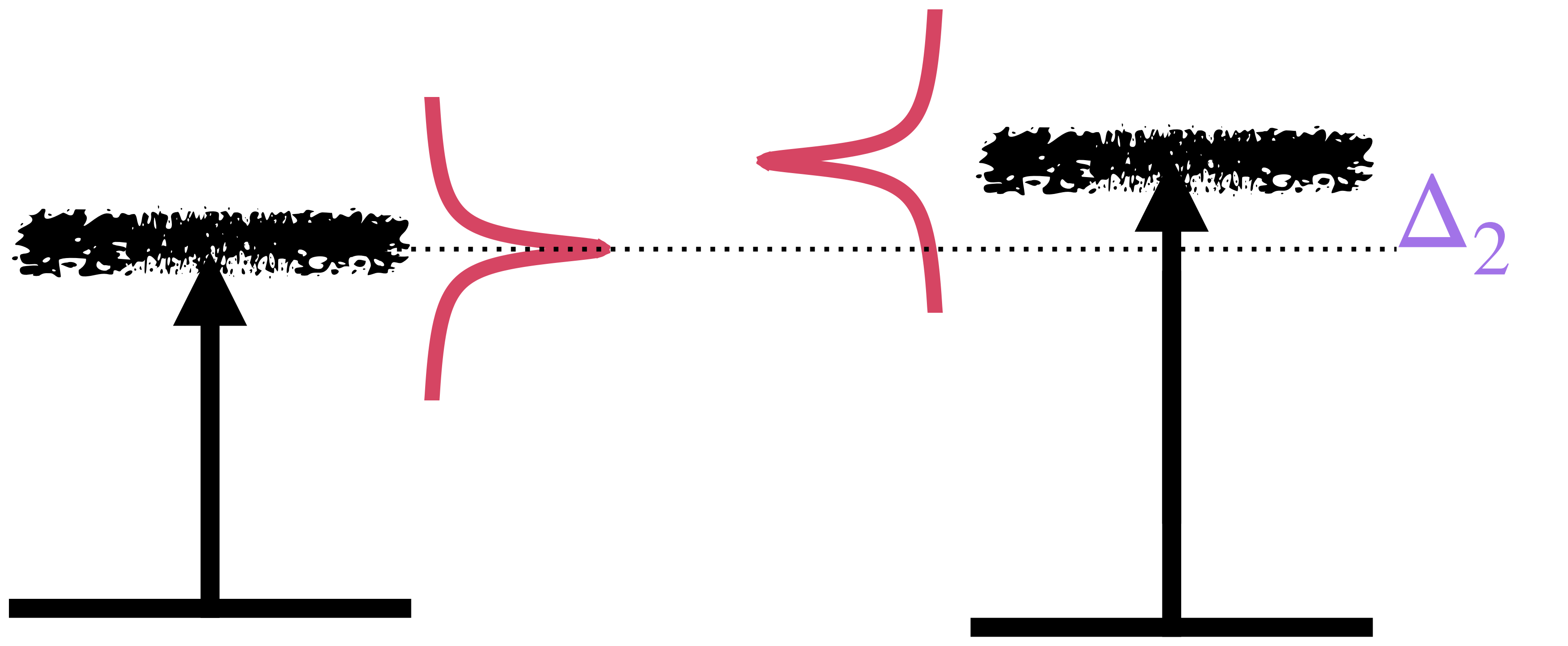

Position-dependent light shift (trap)

Atoms no longer resonant with each other

G. Ferioli *et al.*, *Phys. Rev. X* 11, 021031 (2021).